From Osmolytes to Diabetes: the Impact of Sugars and Sugar Alcohols on the Cystic Fibrosis Pathogen, *Burkholderia multivorans*

Submitted by Carmen Cecile Denman to the University of Exeter as a thesis for the degree of Doctor of Philosophy in Biological Sciences, February 2013

I certify that all material in this thesis which is not my own work has been identified and that no material has previously been submitted and approved for the award of a degree by this or any other University.

(Signature) ……

Acknowledgements

Thank you to family, friends, colleagues, and supervisors for their encouragement, patience and support.

This work was supported by the Cystic Fibrosis Trust and a PhD studentship from the University of Exeter. Thanks to the University of Exeter Sequencing Service; Eshwar Mahenthiralingam (Cardiff University) and Cathy Doherty & John Govan (University of Edinburgh) for provision of isolates and related strain information; Miguel Valvano (Queens' University, Belfast; formerly of University of Western Ontario) for provision of vectors for mutagenesis and complementation.

Table of Contents

List of tables and figures

List of Abbreviations

ASL	Airway surface liquid
Bcc	*Burkholderia cepacia* complex
CF	Cystic fibrosis
CFRD	Cystic fibrosis-related diabetes mellitus
CFU	Colony forming units
CL	Chemiluminescence
EPS	Exopolysaccharide
FEV (1)	Forced expiratory volume in 1 second
LB	Luria-Bertani
MIC	Minimum inhibitory concentration
PBS	Phosphate buffered saline
SCFM	Synthetic cystic fibrosis sputum medium
YEF	Yeast-extract fructose sugar media
YEM	Yeast-extract mannitol sugar media

Published work associated with thesis

Denman CC, Brown AR. Mannitol promotes adherence of an outbreak strain of *Burkholderia multivorans* via an exopolysaccharide-independent mechanism that is associated with upregulation of newly-identified fimbrial and afimbrial adhesins. Microbiology. 2013 Apr;159(Pt 4):771-81. doi: 10.1099/mic.0.064832-0. Epub 2013 Feb 1.

Abstract

The incidence of CF related diabetes is on the rise as patient life expectancy continues to improve. Sugars elevated in diabetics include glucose, fructose, and mannose. These sugars, in addition to mannitol (recently approved as an inhaled osmolyte) are the basis for this study, aimed at assessing the impact these clinically relevant sugars have on virulence in *Burkholderia multivorans*. *B. multivorans* is a member of the *Burkholderia cepacia* complex (Bcc), and is the most frequent cause of Bcc infection in CF patients.

Using an exopolysaccharide-deficient knockout in macrophage and *Galleria mellonella* infection models, biofilm formation, and adhesion assays, this study has identified exopolysaccharide-dependent and -independent phenotypes. Sequencing of *B. multivorans* C1576, a CF outbreak isolate, identified three putative adhesins in clinical isolate C1576 but not present in the sequenced environmental strain ATCC17616. Mannitol promoted adhesion and enhanced expression of these adhesins. This study characterised these adhesins and assessed the distribution within other clinical and environmental isolates of *B. multivorans* and the Bcc.

Additionally, transcriptomic profiling of *B. multivorans* assessed the sugar response and EPS regulation during growth on clinically relevant sugars. Where possible, links were made between phenotypic studies and transcriptome data. *B. multivorans* EPS derived from fructose and mannitol was subjected to composition analysis using mass spectrometry, and assessed for biological activity.

Still relevant to CF related diabetes, the ability of some members of the Bcc to bind insulin was assessed. Results indicated that a minority of strains bound insulin. Furthermore, by using flow cytometry cell sorting and fluorescence microscopy, results also showed only a small number of cells within a given population that bound insulin. In all, this study has added to the knowledge base of *B. multivorans* but more work is needed to fully understand virulence strategies exploited by this CF pathogen.

Chapter 1: General introduction

1.1 Cystic Fibrosis

1.1.1 Epidemiology and distribution

Over 50,000 individuals world-wide are afflicted with Cystic Fibrosis (CF) (81). CF is the most common autosomal recessive heritable disease in Caucasians, though it has also been detected in many ethnic groups. In the U.K., at least 9,000 people are affected with CF, influenced by a relatively isolated population due to ancestry and geography (25,63). The carrier rate for the CFTR mutation that causes CF is one in twenty five people in the U.K (81).

1.1.2 CFTR mutation: disease characteristics and consequences

The underlying genetic cause for CF is mutation of a large gene located on chromosome seven. The gene encodes a protein for an ABC-transporter, which forms chloride-ion channels, the Cystic Fibrosis Transmembrane Conductance Regulator or *CFTR* (100,160,163). More than 1,000 CF-causing CFTR mutations have been identified. Severity of disease is dependent on the type of mutation. The most commonly identified *CFTR* mutation worldwide, found in 70 % of CF patients, is the F508del (a phenylalanine deletion at position 508)(81). Variations of *CFTR* mutations can manifest as protein misreads and total or partial loss of CFTR functionality.

The *CFTR* gene and encoded CFTR protein were structurally and biologically characterised previously (62,147,160). The CFTR protein is normally responsible for regulation of chloride. Defective chloride transport in CF disease manifests itself as negative impacts on sweat, digestive liquids and mucus regulation of sodium and chloride ions across epithelial cells. The leading cause of morbidity and mortality in CF patients is respiratory function decline and failure caused by chronic lung disease, stemming from thick dehydrated mucus obstructing the pulmonary airways and creating an environment hospitable to recurrent and chronic bacterial infection.

Dysfunctional CFTR mis-regulate anion-mediated fluid secretion, resulting in significant sodium ion conductance through channel pores in the cell membrane. This results in thick and dehydrated airway surface liquid (ASL) and mucus, which in turn reduces function of the innate immune system and

hydration of the ASL to enable the body to clear away mucus (81). This creates a naturally inviting environment for respiratory pathogens and opportunistic pathogens to establish infection (82).

The human body is set up with intrinsic barriers to infection; these include the skin, gut, lungs, eyes and nose (224). These built-in barriers prevent pathogens from crossing epithelia and colonising human tissue. Surface epithelia, such as alveolar epithelia lining the human respiratory tract, provide mechanical, chemical and antimicrobial barriers to infection (67,224).Several aspects of mucosal immunity have been linked to the dysfunctional CFTR chloride channels on the apical surface of epithelial cells in CF patients (194). These include the inability to regulate ion flux to sufficiently hydrate the ASL, and altered pH of the lung which can impact on the efficacy of the immune system such as antibodies, anti-oxidants, and proteases (224). These are affected by the inability to hydrate or regulate hydration of the ASL by cilliary movement and chloride channel functionality (148). Several components of the innate immune system response with particular relevance to CF include mucociliary clearance, which in healthy individuals enables grabbing and trapping of bacterial pathogens in the airway mucus while epithelial cilia beat upwards, resulting in movement of mucus and bacteria out of the body (67). Cilliary movement is diminished in CF patients due to the presence of dehydrated mucus (188). In addition to mucociliary clearance, antimicrobial peptides released by epithelial cells can interact and disrupt bacterial membranes (24). Some (but not all) antimicrobial peptides (also found in the ASL) are found to be still functional in the CF environment, but a synergistic effort of antimicrobials, defensins, lysozymes and other components are key for a complete immune response (181). When these and cilliary movement are functioning, they can effectively clear potential pathogens from the respiratory tract (152). In cystic fibrosis patients, fibrosis of the respiratory tract, along with reduced cilliary movement and dehydrated and altered pH of the ASL, leads to a decline in pulmonary health and creates an environment that favours chronic microbial colonisation of airways (177). Respiratory failure due to long-term

microbial respiratory disease is the leading cause of morbidity and mortality in patients with CF (31,63).

Mutated CFTR proteins impact salt absorption in the CF respiratory tract (224). This high salt conductance results in a highly electronegative lumen liquid with high salt content and ceases transport of useful ASL contents, potentially interfering with natural antibiotics, such as antimicrobial peptides, defensins and lysozymes (181,182). This is the basis for the CF high salt hypothesis. The high salt hypothesis states that normal ASL contains low levels of salt as a result of salt absorption in excess of water. Though the airway epithelium is water permeable, salt is retained in thin surface films by a combination of surface tension and impermeant osmolytes. In CF, salt is poorly absorbed resulting in excessively salty ASL that disrupts functionality of mucosal antimicrobial peptides and neutrophil functions (78,226,231). Key features of the high salt model are the lack of a significant shunt for chloride conductance. Of central importance are the CFTR channel role and a switch from isotonic volume absorption to hypertonic salt absorption, and no role for the epithelium sodium channel

The contrasting theory to the high salt hypothesis is the low volume hypothesis (224). Low volume of the ASL liquid could be linked to the chloride ion regulatory role of the CFTR channel. The low volume hypothesis suggests the isotonic fluid absorption in the CF airway is decreased due to low chloride and high sodium transport (103). This depletes the ASL volume and dehydrates the mucus, leading to an infection-prone environment (26). The low volume hypothesis suggests normal ASL has salt levels approximately equal to blood/plasma and would not inhibit innate immune system components (103). In CF, the removal of CFTR inhibition of epithelium sodium channels results in abnormally elevated isotonic fluid absorption which depletes the ASL and reduces mucociliary clearance. Key features of the low volume model are the parallel pathway for chloride ions via shunt pathway(s) and inhibition of epithelium sodium channels via mutated CFTR.

1.2 Cystic fibrosis microbiology

As discussed in the previous section, numerous impaired defences exist within the CF lung that pre-dispose CF patients to infection, making “The microbiology of lung disease in patients with CF is a sub-specialty unto itself” (188). Due to the immune compromised environment in CF lungs they are ideal locations for numerous different opportunistic microbes to establish chronic, debilitating polymicrobial respiratory infections. organisms such as *Haemophilus influenzae* and *Staphylococcus aureus*, infecting patients with CF first (188), followed by the most dominant CF pathogen *Pseudomonas aeruginosa*, acquired later (188). Fungal infections are also more diverse than previously known in CF lung disease, with *Aspergillus fumigatus* and *Candida albicans* (131) most frequently isolated. It has also been established that viruses such as the rhinovirus play a role in the CF respiratory tract (101). Although perhaps not the most frequent cause of CF lung disease, the focus of this thesis are members of the *Burkholderia cepacia* complex, a group of organisms found ubiquitously in the environment but also cause debilitating and unpredictable disease outcomes in CF patients (11,82,108). The polymicrobial nature of the CF respiratory tract means that this list of organisms is only the tip of the iceberg, and for full discussion on the microbial community-based nature of the CF lung, the Sibley *et al.* review is recommended (177).

1.2.1 Treatment options for CF lung disease

Treatments and therapies continue to improve quality and length of life for CF patients. Due to the diminished impaired immune response in the CF lung, frequent courses of antibiotics and respiratory therapies are key aspects of CF respiratory disease treatment. Opportunistic microbial pathogens that colonise CF respiratory tracts are treated with inhaled or intravenous courses of antibiotics. Antibiotics, drugs aimed to restore the ASL, mucolytics to thin mucus and instigate coughing, and/or respiratory therapy are a few of the many treatments for CF disease management. These treatments can aid in reduction of the bacterial load or infection but often do not eradicate the infecting organism completely (136,165). In fact, many CF pathogens are inherently resistant to many antibiotics available, adding to the difficulty in eradicating infection.

1.2.2 CF lung respiratory disease and the Burkholderia cepacia complex

One group of bacterial opportunistic pathogens that are inherently resistant to antibiotics are organisms of the *Burkholderia cepacia* complex (Bcc). Some members of the Bcc are problematic opportunistic bacterial pathogens of the CF lung. The Bcc are a group of at least 17 closely related species (see Table 1.1) for detailed breakdown of species, identification and general characteristics).

Table 1. 1 Taxonomy of members of Burkholderia and members of the Burkholderia cepacia complex (Bcc). Information gathered from recent relevant reviews summarising most up-to-date published information on current *Burkholderia* species relevant to the cystic fibrosis lung disease research undertaken in this thesis.

Species name	Characteristics	Characteristics in CF	Date identified/References
B. cepacia	Environmental	Not highly represented in CF infections	1950,1997 (125,207,214)
B. multivorans	Infrequently isolated from environment	Most frequently isolated from CF patients in most record-keeping countries; patient-to-patient transmission, epidemic strains described	1997 (22,114,125,207)
B. cenocepacia	Commonly found in environment (rhizosphere)	Second most frequent cause of Bcc CF disease; patient-to-patient transmission	1997,2003 (120,125,128,187,207)
B. stabilis	Infrequently isolated from environment, genome stable	Important but not prevalent in CF patients	1997,2000 (125,207,208)
B. vietnamiensis	Commonly found in environment (rhizosphere)	Infrequent infection of CF patients	1995,1997 (114,124,207,207)

B. dolosa	one isolate from environment	Almost exclusively cultured in CF infections;	2001,2004 (22,48,213)
B. ambifaria	Commonly found in environment (rhizosphere)	Infrequent infection of CF patients	2001 (49,125,150)
B. anthina	Environmental and clinical isolates	Infrequent infection of CF patients	2002 (206)
B. pyrrocinia	Environmental and clinical isolates	Infrequent infection of CF patients	2002 (206)
B. ubonensis	Environmental (soil) and clinical isolates	Nosocomial infection	2000,2008 (210,228)
B. latens		Infrequent infection in CF patients, Non –CF infections	2008 (210)
B. difusa	Environment (soil, water)	Infrequent infection in CF patients, Non –CF infections	2008 (210)
B. arboris	Environmental (soil, water, horticulture, industrial contaminant)	Infrequent infection in CF patients, Non –CF infections	2008 (210)
B. seminalis	Environment (Soil, sugar cane, rice,	Infrequent infection in CF patients, Nosocomial	2008 (210)
B. metallica	Few known isolates	Infrequent infection in CF patients	2008 (210)
B. contaminans	Environment (Soil)	Infrequent infection in CF, Non-CF (blood)	2009 (209)

B. lata	Environmen (Soil, flower, river)	Infrequent infection in CF, Non-CF (spinal fluid)	2009 (209)

Bcc infections of CF airways is most commonly associated with chronic infection and a gradual deterioration in lung function, and are consistently identified as an independent risk factor for mortality among CF patients (94,95,118). 4-7 % of patients with CF are infected with a species of the Bcc. *B. cenocepacia* and *B. multivorans* are the most frequently isolated Bcc species associated with CF respiratory infections, together accounting for approximately 70 % of Bcc infections (119). A summary of the significant Bcc infections and their ranking order in frequency of isolation from CF patients is listed in Table 1.2 prevalence of species as presented in recent reviews).

Table 1.2 Bcc infections and the relative importance/frequency of isolation from CF patients. Ranking order of most prevalent Bcc strains known to cause lung disease in CF patients, based on current literature available.

Species	**Prevalence of infection in CF patients**	**Reference**
B. multivorans	Most prevalent Bcc species isolated from CF patients reported in USA/Europe (e.g. ~65% of Bcc cases in U.K.)	(80,119,143)
B. cenocepacia	Second most significant cause of Bcc CF infection (e.g. ~20% of Bcc cases in U.K.)	(80,119)
*B. gladioli***	Primarily a plant pathogen can cause chronic infection in CF patients. ~15 % of USA Bcc CF infections; poor outcome predictor post lung transplant.	As above and (44,157,223)
B.vietnamiensis	~5 % of Bcc CF infections reported in the USA; shown to clear in Bcc co-infection following antibiotic treatment.	(80,119,124)
B. dolosa	Rare CF pathogen; known patient-to-patient spread	(80,116,119)
Other Bcc species	Make up 3 % of recorded Bcc CF infections in USA, another 3 % are unidentified *Burkholderia*.	(77,111)

*Percentage of total referred Bcc cases in CF patients ** Not a member of the Bcc complex but closely related to the Bcc species, an emerging problem especially amongst CF lung transplant patients (REF).

Until recently, *B. cenocepacia* was the most commonly isolated species associated with epidemic spread among CF patients. As a consequence, *B. cenocepacia* has received the most research attention, resulting in the identification of numerous putative virulence determinants (122). However, *B. multivorans* has recently surpassed *B. cenocepacia* in incidence of respiratory infection amongst CF patients in the United States (119) and several other countries (30,50,80,143), but in comparison to *B. cenocepacia*, very little is known about the virulence mechanisms and strategies used by *B. multivorans* within the CF host.

B. multivorans, like *B. cenocepacia*, can also be associated with patient to patient transmission and septic infection (22,222,230), though hospital segregation practice has considerably limited transmissible *B. multivorans* infections (14,222). For the purposes of this study, *B. multivorans* was used throughout as a model organism due to its clinical relevance.

1.3 Cystic fibrosis related diabetes

CF patients now live longer, with the estimated average life span approaching 50 years for infants born in 2000 or after (63). This increased life expectancy has resulted in one-third of the CF population now older than 18 years of age. CF patients are often diagnosed with cystic fibrosis-related diabetes mellitus (CFRD) in their late twenties (151). It is unknown precisely why the onset of diabetes further immune-compromises the patient, but chronic inflammation as a result of long-term infection, such as that in the CF lung, can contribute to insulin deficiency and susceptibility to infection. CFRD patients have an increased risk of infection and pulmonary decline that ultimately leads to drastic respiratory deterioration. CFRD early detection, diagnosis and management with insulin injections is crucial to decrease the contribution of CFRD to morbidity and mortality (7).

The onset of CFRD results in sugars elevated in the diabetic blood, urine (fructose, glucose and mannose) and airways (glucose) (29,98,153). These elevated sugars may effect CF lung microbiology or influence further respiratory decline of patients by contributing to acquisition or strengthening of bacterial infection (98).

The present study provides research contributions to the sparse knowledge that exists concerning links between CF lung microbiology and diabetes, and also adds to understanding the impact clinically relevant sugars have on bacterial behaviour. It is important to understand potential impacts of elevated sugars relevant to CFRD could have on existing polymicrobial lung infections. It is also necessary to understand how insulin administration (aimed at controlling elevated blood sugars) could impact on CF lung disease and thus the overall health of the CFRD patient (113).

1.3.1 Sugars, insulin, and insulin binding by the Bcc

CF and insulin resistance plays an important role in the glucose intolerance of CFRD individuals. There are variable levels of insulin resistance reported in CFRD patients, depending on their overall health stability (105), and researchers report that the bacterial infection within a CFRD patient is influenced considerably by the patients' diabetic state (104,110). Insulin deficiency in CFRD patients could potentially be enhanced by a Bcc infection, due to existing reports that members of the Bcc and *B. pseudomallei* bind human insulin (96,141,227). If indeed members of the Bcc bacteria were able to sequester insulin making it unavailable to the host, there could be consequences for Bcc-infection outcome in CFRD patients. Interestingly, the diabetic state is almost a pre-requisite for *B. pseudomallei* infection, suggesting a link with *Burkholderia* and the immune-compromised diabetic state. The ability of members of the *Burkholderia* to bind insulin appears to be a trait relatively unique to few bacteria species, even separating it from *Pseudomonas*, the genus *Burkholderia* was formerly classified as (141).

The diabetic state involves sugars that are elevated, such as fructose, mannose and glucose in the blood and urine of patients (98,153). Additionally, it

is reported that glucose is elevated in the airways of diabetics (12,29). Onset of CFRD and elevated sugars associated with diabetes in CF patients with Bcc infections could have potential impacts on lung disease. However, any definitive relationship between elevated sugars, CFRD, and the observed overall clinical decline associated with a CFRD diagnosis are poorly characterised, and it is unknown if CFRD or Bcc infection are linked. Onset of CFRD could impact CF lung microbiology and Bcc virulence if elevated airway sugars could induce EPS biosynthesis. Fructose and mannitol, among other sugars, induce copious amounts of EPS to be produced by members of the Bcc. It has been estimated in one study that ~80-90 % of Bcc CF isolates produce EPS (56).

EPS-production is closely linked to unknown nutritional cues. The switch from a non-mucoid to mucoid phenotype, and vice-versa, is not entirely understood but several EPS-related biosynthetic operons are present in the *Burkholderia,* and it is likely the mucoid to non-mucoid transition in chronic infections may be due to different metabolic needs for survival during long-term colonisation (178). It has not been definitively confirmed whether EPS is produced *in vivo*, although attempts have been made to produce definitive evidence for EPS from CF sputum samples (88). EPS production in Bcc CF isolates is inversely related to respiratory decline (233). If EPS were produced *in vivo* it could act as a virulence factor by masking bacterial cell surfaces from neutrophils (51), scavenging reactive oxygen species targeted to kill pathogens (33), increase biofilm formation and resistances to antibiotics (56). Interestingly, an overall slower clinical decline in CF patients has been observed in patients infected with mucoid Bcc isolates (233). Thus, further study is required to fully understand the wide-ranging impact of EPS as a putative virulence mechanism for *B. multivorans*.

1.4 Bcc virulence strategies

1.4.1 Assessing Bcc virulence using plant and animal models of infection

Acquisition of virulence factors by the Bcc, as well as *in vivo* evolution and adaption of the organism during infection, has been described (32,86,130).

One such example is the loss over time of the EPS mucoid phenotype from sequential CF isolates (178,234). Several animal models have been utilised to study bacterial/host interactions and virulence strategies *in vivo* for the Bcc. These include a rat agar bead model of chronic infection (184), the alfalfa seedling infection model (20), a *CFTR* knockout and F508del *CFTR* knockout mice (183), chronic granulomatous (CGD) mouse (57), a CF piglet model (152), the *Danio rerio* zebra fish model (189,203), the soil dwelling nematode *Caenorhabditis elegans* (35), and the greater wax-moth larva *Galleria melonella* (175). The latter was used in the present study to examine the impact of mucoidy on virulence in *G. mellonella* (Chapter 3). These animal models have proven useful for studying Bcc virulence mechanisms *in vivo*. Additionally, tissue culture cell lines with and without CFTR mutations are used to study Bcc host cell interactions (47,192). Macrophage and neutrophil studies, as well as A549 epithelial cells are also used to study host/pathogen interaction, invasion and intracellular survival (32,186). The A549 human lung epithelial and J774.1 mouse macrophage cell line were used in studies presented in Chapter 3 and 5 of this dissertation. A broad overall list of virulence traits in the Bcc are listed in Table 1.3, and further detail given within the following sections of virulence traits particularly relevant to studies in the following chapters.

Table 1.3 briefly outlines the array of virulence factors known to be part of the Bcc virulence armory. As mentioned previously, due it is past dominance *B. cenocepacia* virulence traits have been the best studied and therefore the following table and references are biased for more study having been concentrated on the most dominant CF species.

Table 1.3. Virulence traits in the Bcc. Broad overview with some detail of species regarding virulence strategies employed by members of the Bcc.

Virulence factor	Presence amongst Bcc species	Characteristics	References
Antimicrobial resistance	All species	Natural resistance to many antibiotics and disinfectants	(42,145)

Biofilm formation	All species- but amount and ability can be strain variable	Biofilm formation can be dependent on quorum sensing; provides increased resistance to antibiotics	(34,52,205)
Cable pili, 22-kDa adhesion and other adhesions	*B. cenocepacia*, *B. multivorans*; homologues or other types of adhesins present in other species	Cable pilus required for *B. cenocepacia* full adherence to mucin and epithelial cells; outbreak strain marker.	(61,168,199)
Catalse and SOD	All species		(112)
Cenocepacia island	*B. cenocepacia* island	First pathogenicity island discovered and described in Bcc	(15)
Exopolysaccharide	All species capable of producing EPS – examined in relation to virulence in *B. cepacia*, *B. cenocepacia, B. multiovorans*	Produced by Bcc isolates *in vitro*; induced after passage through murine infection model in *B. cenocepacia*	(39,45,51,55)
Extracellular proteases	*B. cepacia*, *B. cenocepacia*, *B. stabilis*, *B. dolosa*	Zinc metalloprotease required for virulence in *B. cenocepacia* K56-2	(21,53)
Flagella	All species	Polymorphic flagellin subunit; required for cellular invasion but not adherence	(85,202)
Invasion and intraceullar survival	Variable in species tested, can be strain dependent	Some species more invasive than others, some can survival and replicate in macrophages	(99,130)
LPS	All species; serotypable	Unusual lipid-A structure	(217)

	O-antigen variation		
Melanin	*B. cepacia*, *B. cenocepacia*, *B. multivorans*	Scavenges free radicals *in vitro*	(235)
Quorum sensing	*B. cepcia*, *B. stabilis*, *B. multivorans*, *B. cenocepacia*, *B. vietnamiensis*, *B. lata*, *B. dolosa*, *B. pyrocinnia*	All species encode LuxRI system and make AHL compounds; required for full virulence; controls toxins, proteases, lipases, siderophore	(173)
Siderophore production	All species	Four different types produced – ornibactin biosynthesis essential for virulence	(195,218)
Type III secretion system	*B. multivorans*, *B. ambifaria*, absent from *B. cepacia*	Similar inter-species genomic organisiation; required for *B. cenocepacia* virulence in murine infection model	(76,198)
Type VI secretion system	*B. cenocepacia*, *B. multivorans*, *B. cepacia*,*B. vientamiensis*	Involved in cell invasion, transport of type II secretion pathway proteins	(164,167)
Haemolysin	*B. cenocepacia*	Induces degranulation and cell death; haemolytic activity observed in many Bcc species	(21)

1.4.2 Exopolysaccharide – sugars elicit different Bcc phenotypes

Exopolysaccharide (EPS) is a proven virulence factor for *P. aeruginosa* and other bacterial pathogens (190). When grown on certain carbon sources such as fructose and mannitol, Bcc species produce EPS resulting in a mucoid phenotype (17). This mannitol induced mucoid phenotype is observed in 80-90% of Bcc CF isolates (36,234). The most frequently identified Bcc-

synthesised EPS has been characterised, and named cepacian (142). Cepacian is one of several types of EPS known to be synthesised by members of the Bcc (88). Whilst clinical *B. cenocepacia* isolates are frequently non-mucoid as a result of mutations within EPS biosynthetic or regulatory pathways, clinical isolates of *B. multivorans* frequently retain the capacity for EPS production (233).

EPS production by the Bcc has also been associated with bacterial persistence within the lung (51), biofilm formation, resistance to antibiotics (56) and inhibition of neutrophil activity (33). Bcc EPS can further restrict the diffusion of immune cells and antibiotics by blocking interaction with host and bacterial polymers (5,33,36,51). The study included CF Bcc mucoid samples from different countries. One study demonstrated that in over two decades worth of clinical data and a series of Bcc isolates, Bcc conversion from mucoid to non-mucoid phenotype is associated with worsened clinical status (233,234) and persistent infection with poorer clinical outcome (125). If EPS biosynthesis impacted on bacterial overall fitness, it would allow the non-mucoid bacteria in the population to have a competitive advantage for growth and proliferation. EPS production may be metabolically expensive and therefore, selective pressure by inhaled mannitol therapy may select against non-mucoid bacteria.

Structurally similar molecules induce dramatically different phenotypes (Figure 1.1). Although glucose, mannose, fructose and mannitol and are stereochemically similar, these sugars and sugar alcohol induce EPS profiles and support *B. multivorans* growth in different ways. This may indicate that these carbon sources impact on the broader behaviour of the organism in a more complex way than as only a carbon source to support growth and metabolism. Fructose and mannitol induce EPS production (mucoid phenotype), while glucose and mannose do not (non-mucoid phenotype). Media used predominantly for the analysis described in the present study contained 0.2 % (w/v) yeast extract supplemented with 2 % (w/v) sugar as broth or agar. The YEM (mannitol-containing media) is most commonly used to induce the EPS mucoid phenotype in the Bcc, and is almost exclusively used in studies of the impact of mucoidy on the Bcc (17).

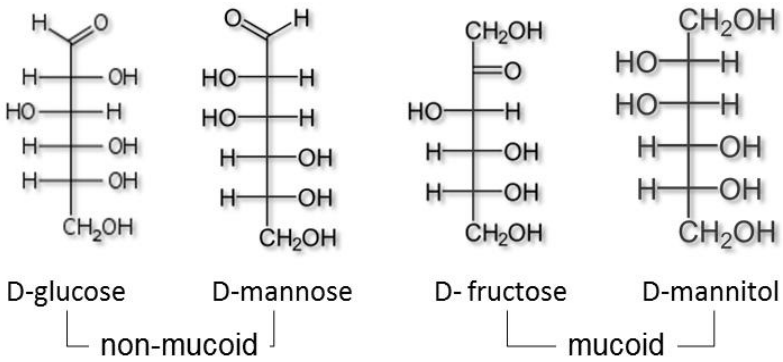

Figure 1.1 Structurally similar sugars result in drastically different phenotypes

Mannose and mannitol are used in the present study for phenotypic characterisation. Chemically similar sugar molecules have different impacts on induction of EPS biosynthesis. Although these sugars are structurally similar, minor differences in stereochemistry lead to drastically different roles in EPS induction.

Recently, the approval of mannitol as an inhaled osmolyte has raised questions; the suggested dosage is 800 mg per day inhaled directly into the lung. Mannitol induces EPS production, and overall, it is still unknown how EPS production impacts on Bcc virulence in the CF lung. Mannitol is a naturally occurring sugar alcohol. In plants, mannitol plays a role in osmoregulation and stress response within cells. In the CF lung, mannitol acts as an osmolyte by drawing liquid towards the epithelial cell layer to rehydrate mucus. The forced expiratory volume per second (FEV_1), is significantly improved in CF patients treated with inhaled mannitol (58). The developers claim sputum microbiology is unaltered over a two week period of treatment with mannitol (23,93). However, it is common practice to exclude CF patients with Bcc infection from clinical trials. This leaves drug developers unaware of effects the drug might have on Bcc infections in the CF lung. Treatment of Bcc infections in CF patients are notoriously difficult to manage, with some infections ranging from acute ‘cepacia syndrome’ to long term infections that can be carried with the patient for a life-time (79,87).

EPS is a putative virulence factor of the Bcc, and a result of bacterial EPS production (induced by mannitol or other sugars) may lead to increased viscosity in the lungs. EPS production by the Bcc in the CF lung could thus lead

to decreased efficacy of respiratory therapy and antibiotic treatments. Recent papers and editorials call for the analysis of the Bcc 'sugar response' (17,83,159), because the impact of mannitol in the CF lung (and other sugars of clinical interest in relation to CFRD) is not understood in relation to Bcc lung disease. The recent EU approval of mannitol means it could be prescribed universally to CF patients, regardless of the patients' lung microbiology profile.

It is necessary to further examine the impact of mannitol and other clinically relevant sugars on EPS production and virulence. The average normal human lung volume is approximately 4.3 litres (54), and the recommended dosage of inhaled mannitol is 400 mg twice daily. If these doses were adhered to, the potential (though not documented or reported in the CF literature) concentration of mannitol would be ~ 1.02 mM. This concentration of mannitol in addition to the CFRD state of elevated sugars in the blood and airways could have deleterious effects by strengthening bacterial infection (29). The dispersal of an aerosol differs depending on the material size and diffusion, and lung volume differs from patient to patient, thus it is difficult to determine actual concentrations of mannitol following inhalation into the CF lung.

1.4.3 Genetic basis for Bcc EPS biosynthesis

EPS is biosynthesised by most members of the Bcc, but the genetic basis and regulation that control EPS production are not fully understood. There are multiple gene clusters that encode EPS production in the Bcc (17,142). The most conserved EPS cluster among the *Burkholderia* is the *bce* cluster. The *bce* cluster located on chromosome 2, is 16.2 kb long and includes 12 different genes (139). Although the *bce* I cluster is presented in Figure 1.2, there is also an identified *bce* cluster II (69). Though the *bce* cluster is well conserved among the *Burkholderia*, the distance between the *bce* I and II cluster, as well as the presence of both, varies from species to species. Interestingly, the greatest distance between *bce* I and II was found in *B. multivorans* ATCC 17616 (69). The *bce* cluster and associated EPS has been one of the most studied virulence factors in the Bcc. Genes within the *bce* cluster encode proteins required for the formation of nucleotide sugar precursors, glycosyltransferases

involved in repeat assembly, and other proteins involved in polymerisation and export of EPS (Figure 1.2).

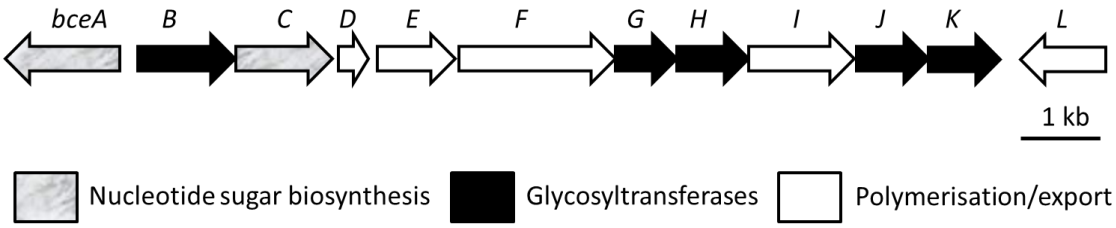

Figure 1.2 The arrangement of the bce I cluster.

The *bce* I EPS gene cluster is conserved amongst Bcc species. The *bceB* glycosyltransferase is assigned to a role involved in repeat unit assembly. This figure based on a figure from Moreira *et al.* (139) and information gathered from burkholderia.com (225).

Within members of the *bce* cluster, *bceB* encodes a glycosyltransferase that initiates the synthesis of cepacian repeat unit (RU) assembly (139). There are also functional equivalents of *bce* and *bceB* in other bacteria (see Videira *et al.* for a detailed list of species and loci (216)). The primary structure of the cepacian repeating unit is a branched acetylated heptasaccharide repeating unit with D -glucose, D -rhamnose, D -mannose, D -galactose, D -glucuronic acid, in a 1:1:1:3:1 ratio (39). This EPS sugar composition is well conserved within cepacian produced by members of the Bcc. Analysis of *B. multivorans* EPS, derived from fructose- and mannitol-induced EPS, is the focus of studies presented in Chapter 6 and 7.

The important role the *bce* gene cluster plays in Bcc EPS biosynthesis is highlighted in the highly transmissible *B. cenocepacia* ET-12 lineage. Members of the ET-12 lineage are predominently non-mucoid. It has been show that this lineage contains an 11 base pair deletion within the *bceB* gene, likely the cause of non-mucoid phenotypes in this transmissible lineage, reputed to favour aggressive infection and can result in septicaemia termed ‘cepacia syndrome’ (17). This is in contrast to *B. multivorans* clinical isolates, which often retain the mucoid phenotype and are linked to more chronic infections.

1.4.4 Adhesion and biofilms

Bcc pathogenesis strategies include adherence using cable pilus structures and fimbriae. Scanning electron microscopy (EM) shows that 60 % of Bcc species express peritricous pili (106). Bacteria use these adhesive structures to attach to host tissues and cells to assist colonisation. After initial colonisation, biofilms develop and are a recognized virulence factor in the Bcc. Biofilms are linked to antibiotic resistant long-term colonisation (95). The most commonly isolated CF Bcc bacteria (*B. multivorans, B. cenocepacia*, and *B. dolosa*) show equal ability to form biofilm, judged by accepted biofilm assays, but there is strain to strain variation in the amount of biofilm formed by differing Bcc species. A major issue with established bacterial adherence through biofilm formation is the effect biofilms have on the host immune inflammatory response, causing mis-regulated long term damage by neutrophil influx. Biofilm formation led by bacterial communication, also known as quorum sensing (QS) ultimately leads to evasion of host response and antibiotic resistance. Biofilm formation has been linked to antibiotic resistance because of decreased metabolic activity (27,212). There has been research interest in ways to improve drug delivery to the CF lung as a means to combat infection and specifically chronic biofilms. Some studies have reported that the non-mucoid phenotype results in enhanced motility but decreased biofilm formation (178), however EPS-attributable phenotypes are not clear cut, and further investigations into the virulence-relevant phenotypes impacted by EPS production will be discussed within the present study. Adhesion and biofilm studies relevant to this dissertation are presented and discussed in Chapters 3 and 5.

1.5 Aims

1. Fully characterise the response of *B. multivorans* to relevant sugars by using phenotypic assays that assess virulence associated phenotypes.
2. Assess the whole genome transcriptional response of *B. multivorans* to clinically relevant sugars.
3. Compare the composition and functional biological activity of *B. multivorans* ATCC 17616 and C1576 fructose-derived EPS compared to mannitol-derived EPS.
4. Investigate insulin binding in the Bcc.

A schematic outlining the approach used to address the thesis aims.

Figure 1.3 Schematic of the approach to research taken to achieve study aims. Three branches of work arise from the main goals of characterising the *B. multivorans* response to clinically relevant sugars and insulin binding; phenotypic analysis, transcriptomic analysis, and assessment of insulin binding using microscopy and flow cytometry studies.

Chapter 2: Materials and Methods

2.1 Bacterial strains

In Table 2.1 are listed the strains used in studies presented in Chapters 3-7. Additional information on the strains used in the insulin binding assays for Chapter 8 can be found in section 2.23, Table 2.4. Details of the strains used in Chapter 5 for Southern hybridisation dot-blot analysis are listed in the appendix, Table 9.5. Table 2.2 provides details of the plasmid constructs and cloning vectors used for mutagenesis and complementation. Primer sequences for the mutagenesis process can be found in Chapter 9, and Appendix Table 9.1 and 9.2.

Table 2.1 Bacterial strains used in this study for Chapters 3-7. Tetracycline resistance TetR, Trimethoprim resistance,TpR

Strain	Relevant characteristics	Source and/or reference
B. multivorans strains		
C1576	CF clinical isolate; Index case of outbreak strain, ST-27	(127)
fim CR	C1576, pGPΩTp::*fim*, Tp^R	This study
hecB CR	C1576, pGPΩTp::*hecB*, Tp^R	This study
hecA *CR*	C1576, pGPΩTp::*hecA*, Tp^R	This study
fim CO	C1576, pGPΩTp:: *fim,* pDA17:: *fim*, Tp^R Tet^R	This study
hecB CO	C1576, pGPΩTp::*hecB*, pDA17::*hecB*, Tp^R Tet^R	This study
C1576 bceB CR	C1576, pGPΩTp::*bceB,* Tp^R	This study
ATCC 17616	Environmental isolate from soil	(127)
ATCC bceB CR	ATCC 17616, pGPΩTp::*bceB,* Tp^R	This study
E. coli strains		
TOP10	*F¯ mcrA Δ(mrr-hsdRMS-mcrBC) Φ80lacZΔM15 ΔlacX74 recA1 araD139*	Invitrogen

	Δ(ara-leu) 7697 galU galK rpsL (Str^R) endA1 nupG λ$^-$	
GT115	*F$^-$ mcrA ∆(mrr-hsdRMS-mcrBC) φ80lacZ∆M15 ∆lacX74 recA1 rspL (StrA) endA1 ∆dcm uidA(∆MluI)::pir-116 ∆sbcC-sbcD*	InvivoGen

Table 2.2 Plasmids constructed specifically for this study. Plasmids constructed for mutagenesis purposes and complementation are described in detail within this table, and when available a reference is made to the original source of the vector.

Plasmid	Relevant characteristics	Source/reference
pGPΩTp	*Ori*$_{R6K}$, ΩTp^R cassette, *mob*$^+$	(71)
pRK2013	*Ori*$_{colE1}$, RK2 derivative, Kan^R, *mob*$^+$*tra*$^+$	(70)
pDA17	*Ori*$_{pBBR1}$,Tet^R, *mob*$^+$, *P$_{dhfr}$*	(72)
pGPΩTp::*hecA*	pGPΩTp; 448 bp internal fragment from C1576 *hecA*	This study
pGPΩTp::*hecB*	pGPΩTp; 444 bp internal fragment from C1576 *hecB*	This study
pGPΩTp::*fim*	pGPΩTp; 426 bp internal fragment from C1576 gene encoding fimbrial usher protein	This study
pDA17::*hecB*	pDA17; 1.8 kb fragment encoding the C1576 HecB-like protein	This study
pDA17::*fim*	pDA17; 2.7 kb fragment encoding the C1576 fimbrial usher protein	This study

2.2 Chemicals, growth media, and culture conditions

2.2.1 General chemical and media purchasing information

Unless otherwise stated, all antibiotics, enzymes, solvents and other chemicals were purchased from Sigma-Aldrich Inc. (Location), growth media from Oxoid (location), amino acids and MOPS from FOREMEDIUM (location), mass spectrometry consumables from Agilent, cell culture media, buffers from

Gibco, cell culture consumables from Nunc and Corning, and RNA consumables from Ambion/ Applied Biosciences.

2.2.2 General culture conditions

Strains were stored at - 80° C in Luria-Bertani (LB) broth with no antibiotics and 16 % (v/v) glycerol. Bacteria were routinely cultured as follows: LB broth cultures inoculated from 3-5 colonies taken from freshly grown agar plates (10 ml volumes in 30 ml culture vessels) were incubated at 37° C with shaking at 250 rpm unless stated otherwise. Strains were incubated for 16-17 hours for RNA extraction protocols, 20 hours for phenotypic assays, and 48 hours for EPS extractions. For routine culture, media were supplemented with trimethoprim (100 µg/ml for Bcc; 50 µg/ml for *E. coli*), tetracycline (100 µg/ml for Bcc; 25 µg/ml for *E. coli*), gentamicin (50 µg/ml for Bcc), or kanamycin (25 µg/ml for *E. coli*) as required (see Tables 2.1, and 2.2).

2.2.3 Growth media

LB broth and agar

LB broth (containing 5 g/litre NaCl – Oxoid) supplemented with 1.5 % (w/v) agar as required.

Sugar media

Sugar media contained 0.2 % (w/v) yeast extract (Oxoid) supplemented with either 2 % (w/v) D-mannitol (for EPS-inducing conditions; YEM media), or 2 % (w/v) D-mannose (for non-EPS-inducing conditions) (166). All strains employed in this study exhibited comparable growth rates within the media used. All sugars used for screening and growth (D-fructose, D-glucose, D-mannose, D-mannitol, D-Adonitol, D-myoinositol, D-Galactose, D-sucrose, D-inulin) were used at 2 % (w/v). Instances where ‘mannitol’ or ‘mannose’ and other sugars are referred to throughout this dissertation, the reader should infer that D-enantiomer forms of the sugars were used. Agar was added to 1.5 % (w/v) as required for sugar agar media.

Motility agar

Swimming agar plates were made as per sugar media but with 0.3 % (w/v) agar, to allow the bacteria to swim through the media.

Synthetic CF sputum medium (SCFM).

SCFM media was prepared as described in Palmer et al. (149) supplemented with either D-mannitol or D-mannose sugars (2 % w/v). Agar was added to 1.5 % (w/v) as required.

SOB broth and agar

SOB broth and agar used for triparental mating was prepared as follows: 2 % (w/v) tryptone, 0.5 % (w/v) yeast extract, 8.5 mM NaCl, and 250 mM KCl. For SOB agar, 1.5 % (w/v) agar was added. The media was sterilised by autoclaving, and once cooled, $MgCl_2$ was added to a final concentration of 10 mM.

Tryptone soya broth (TSB)

Gamma-irradiated TSB powder was purchased from Oxoid and supplemented with 1.5 % (w/v) agar as required.

2.3 Crude DNA extraction

Crude DNA preparations were made as follows: 3-4 colonies from an overnight growth on an appropriate agar plate were re-suspended in 20 µl of alkaline lysis solution (0.25 % SDS, 0.05 N NaOH 92.5 % (v/v) H_2O). The bacteria–lysis solution suspension was heated for 15 minutes at 95° C to lyse the cells, then briefly centrifuged. To this, 180 µl of nuclease-free H_2O was added, the solutions vortexed, and then centrifuged at full speed on a benchtop centrifuge for 5 minutes. Lysates were stored at – 20° C for future use (17).

2.4 Generating crude mutants by insertional inactivation

2.4.1 Construction of vectors

Insertional inactivation to create crude mutants of target genes used the pGPΩTp suicide vector was carried out as described previously (71). In brief, a 400-500 bp PCR product mapping within the target gene was cloned into

pGPΩTp to facilitate homologous recombination and thus insertional inactivation of the target gene. Amplified PCR products and pGPΩTp vector were double digested with *Eco*RI/*Xba*I restriction enzymes (NEB) overnight at 37° C. Digests were separated by gel electrophoresis and the required inserts and plasmid vectors were gel extracted (Qiagen gel extraction kit), and ligated overnight at 16° C with an insert: vector ratio of 1:3 (NEB). For transformations of the vectors into *E. coli* strains, 4 µl of ligation product was used. All primer sequences used for insertional mutagenesis are listed in Chapter 9, Appendix Table 9.1.

Transformants were selected using gentamicin in conjunction with trimethoprim to select for pGPΩTp integrants. Insertional mutants were confirmed by using the pGPΩTp specific RSF1300 primer (71) and appropriate adhesion-specific *Xba*I primer (used for insertional inactivation), additionally RSF1300 was used with a forward checking primer, specific to a region of the gene upstream of the targeted insertional mutagenesis (primer sequences used are available in Appendix Table 9.1).

2.4.2 Conjugation of vectors and validation of resulting insertional mutants

All plasmids (for mutagenesis and complementation) were mobilised into the appropriate *B. multivorans* recipient strain by triparental mating with the helper plasmid, pRK2013 (Table 2.2) (70). Tri-parental mating consisted of 10 ml overnight SOB cultures with or without antibiotics, as appropriate. Cultures were harvested the following day and resuspended in PBS to remove any antibiotics present in the growth media. Mating mixtures were combined in a 1:1:10 helper, donor, recipient ratio, centrifuged, and re-suspended in 2 ml LB broth without antibiotics. 200 µl of the mating mixture was plated without spreading, onto a SOB agar plate and incubated at 37° C agar side up overnight. Growth was then harvested with 1 ml LB broth, and plated onto LB agar supplemented with appropriate antibiotics.

Semi-quantitative RT-PCR was used to validate that insertional inactivation did not cause undue disruption of surrounding gene expression in crude adhesin mutants. Primers were designed internal to genes up and

downstream of the insertional- inactivated targets in adhesin mutants hecA CR, *fim* CR and *hecB* CR. Strains were grown overnight in LB broths supplemented with 100 µg/ml trimethoprim. RNA was extracted using RNA-easy Protect Bacteria Mini Kit (Qiagen) per manufacturer's guidelines, followed by DNAse treatment (1 hour) (Promega). cDNAs were synthesized as described in section 2.16. Samples alongside positive, negative, and non-RT controls were visualised using gel electrophoresis. The sequences of primers for qRT-PCR are available in the Appendix Table 9.3.

2.5 Construction of complemented strains

2.5.1 Construction of complementation vectors

In trans complementation of mutants was achieved using the previously described pDA17 vector (Table 9.2) (72), a broad-host range plasmid that drives constitutive expression of the cloned gene from the *dhfr* promoter. The complete genes that had previously been the target of insertional inactivation, were amplified by PCR, with the sequence for *Nde*I and *Eco*RI restriction enzymes added at the start and stop codon respectively. The product was inserted directly into the pGEM-T Easy Vector System (Promega) and screened using blue/white screening on LB agar supplemented with Ampicillin 100 µg/ml and X-Gal 80 µg /ml. Positive (white) colonies were screened with a primers internal to the gene of interest and either T7 or SP6 primers, specific to the pGEM-T Easy plasmid. PCR-positive clones were sent for sequencing using the T7 or SP6 primers. pGEM-T Easy constructs (Table 2.2) containing *hecB* inserts were double-digested with *Nde*I/*EcoR*I. The *fim* complementation construct in pGEM-T Easy was digested with *Sca*I and *Nde*I/*Eco*RI. The additional ScaI enzyme was included to cut the plasmid backbone enabling separation and visualisation of the insert from the plasmid. Digested insert fragments were separated by gel electrophoresis, excised, purified, and ligated into the vector pDA17 (72) which had been previously digested with NdeI/EcoRI (15° C overnight as described in 2.4.1). Ligations were transformed into *E. coli* Top10 (Invitrogen) cells and plated onto tetracycline 50 µg/ml LB agar plates. pDA17 constructs were mobilised into the appropriate *B. multivorans* recipient

strain by triparental mating with the helper plasmid, pRK2013 (Table 2.2) as described in section 2.4.2 (70). Transformants were selected using gentamicin in conjunction with tetracycline for pDA17 complemented strains. Complemented strains were confirmed by appropriate PCR validation using primers specific to the Tet^R cassette carried on pDA17 (primer sequences listed in Chapter 9 Appendix Table 9.2).

2.5.2 Validation of complemented strain

Transformants described in section 2.5.1 were screened by PCR using internal primers to the adhesin gene. Phenotypic assays were then utilised to confirm the complemented strain had returned to wild-type behaviour.

2.6 Biofilm assay

Biofilm formation was assessed using the 96-well plate and accompanying peg-lid of the MBEC Assay device (Innovotech). Bacteria were harvested from TSB agar and standardized to 10^7 CFU/ml in 10 ml TSB. Wells received either 150 µl of bacterial suspension or an equal volume of un-inoculated tryptone soya broth (TSB). The peg lid was placed on the plate, sealed, and the plate incubated at 37° C with shaking (125 rpm). Following 24 hours incubation, the peg lid was transferred to a fresh 96-well plate containing pre-warmed TSB, and incubated for a further 24 hours (37° C, 125 rpm). The peg lid was transferred to a 96-well plate containing 200 µl 1x PBS per well (PBS tablets: 0.01 mM Na_2PO_4-$7H_2O$, 3 mM KCl, 140 mM NaCl, pH 7.4. Sigma), and incubated at room temperature for 2 minutes to remove loosely-attached bacteria. The peg lid was removed and baked (60° C, 20 minutes). The peg lid was then transferred to a 96-well plate containing 200 µl of 0.1 % (w/v) crystal violet per well, and incubated for 30 minutes at room temperature. The peg lid was washed three times (200 µl of PBS per well) following staining, and the bound crystal violet was subsequently solubilised with 95 % ethanol (30 minutes) prior to measuring absorbance at 570 nm.

2.6.1 Assessing biofilm resistance to tobramycin treatment

Bacteria were harvested from yeast extract sugar media agar (section 2.2.3) and diluted into yeast extract sugar media broths. Biofilms were grown as described in section 2.6 with the following alterations: after the initial 24-hour incubation pegs were washed twice in PBS, then inserted into a fresh 96-well plate containing 200 µl of either 8 µg/ml tobramycin sulphate re-suspended in PBS, or PBS alone (control wells). This plate was then incubated a second time for 24 hours (37° C static). Sessile cells were sonicated (5 minutes) into a fresh 96-well plate filled with fresh 200 µl PBS. CFU/biofilm was determined by viable counts onto LB agar, and percentage survival was calculated relative to untreated biofilms.

2.7 Hydrogen peroxide protection assay

To assess the *in vitro* protection of mannitol to oxidative stress, a method was adapted from Lefebre *et al.* (112) and Katsuwon and Anderson (97). Overnight cultures of *B. multivorans* were grown with shaking at 37° C in mannitol or mannose sugar broths until late stationary phase. Samples were harvested, re-suspended and equalised to an OD_{590} of 1 (equating to approximately 10^9 CFU/ml) in 1x PBS, and then further diluted to 10^8 CFU/ml in LB broth. Samples were treated with 5 mM H_2O_2, and incubated with shaking at 25°C (30 minutes). Control samples were incubated with H_2O in place of H_2O_2. Enumeration of viable CFU was carried out by plating serial dilutions onto LB agar. After 48 hours of incubation, colonies were counted and percentage survival was calculated.

2.8 Swimming motility assay

Bacteria were sub-cultured from LB plates to grow overnight on TSB agar plates at 37° C. Bacteria were harvested from the plates with a sterile plastic loop and standardised to an OD_{590} of 1 in PBS. Cultures were diluted 1:200 in TSB and used to inoculate swimming agar plates (as described in section 2.2.3). A sterile pipette tip was submerged in the 1:200 bacterial suspensions in TSB ~10 mm depth and then inserted into the centre of the agar

plate. Plates were incubated for 48 hours agar side up at 37° C. Motility was quantified at 48 hours by measuring the diameter travelled in mm at the widest point from the base of the plate.

2.9 Mucin adherence assay

Mucin adherence assays were performed as described previously (8), with minor modification. In brief, 50 µl aliquots of 50 µg/ml filter-sterilized porcine mucin protein (Sigma) were applied to wells of a 96-well polystyrene microtitre plate and incubated overnight at 37° C. Bacteria were harvested from LB agar plates (for adhesin mutant experiments) or D-mannitol/D-mannose sugar broths (for mucoidy-related experiments) following overnight incubation, and standardised to 10^9 CFU/ml in PBS. Mucin-coated wells received either 50 µl bacterial suspension, or 50 µl PBS, and were incubated at room temperature for 3 hours, after which wells were washed ten times with 200 µl aliquots of PBS. Bound bacteria were released from mucin with sterile 0.25 % (v/v) Triton X-100 and enumerated by plating appropriate dilutions (in triplicate) onto LB agar. Six wells were processed per strain in each individual experiment.

2.10 Fibronectin adherence assay

To assess the involvement of adhesins in interaction with the host extracellular matrix (ECM) protein fibronectin, the method from Mil-Homens *et al.* (134), was used, substituting TBS buffer for PBS. Wells of a 96-well polystyrene plate were coated with 150 µl of 10 µg/ml fibronectin and incubated overnight at 4° C. Strains were grown on LB agar overnight at 37° C and standardised in PBS to OD_{590} of 1. 150 µl of bacterial suspensions were applied to fibronectin-coated wells, and the plates were briefly centrifuged at 300 x g for 3 minutes. Bacteria were left to adhere at room temperature for 2 hours. Un-bound bacteria were aspirated and wells washed with 200 µl PBS (four times). The plate was baked at 60° C (45 minutes) followed by staining (15 minutes) of adhered cells with 0.1 % (w/v) filter sterilised crystal violet (CV).,Wells were then washed four times with PBS and the stain solubilised in 95 % ethanol (30

minutes) with rocking. The plate was read at 570 nm on a 96-well plate reader. Controls consisted of PBS applied to fibronectin-coated wells.

2.11 Macrophage intracellular survival assay

2.11.1 Culture of J774 macrophages

An adherent mouse macrophage cell line (ATCC® number TIB-67™ (158)), was cultivated per ATCC guidelines, using high glucose Dulbecco's modified eagle medium (DMEM) (SOURCE) with 2 mM L-glutamine and 10 % heat-treated foetal bovine serum (FBS) (Gibco). Cell layers were cultured in 75 ml flasks at 37° C, 95 % air, 5 % CO_2. Media was renewed 2-3 times per week. Growth media was changed prior to harvesting cell layers. Sub-cultivation of the cells was carried out by dislodgment from the flask substrate with a cell scraper and with a sub-cultivation ratio of 1:6. For freezing working stocks of the cell line, cells were suspended in 5 % (v/v) DMSO and DMEM complete growth medium and aliquots made at 10^5 cells per vial. Cells were used in assays between passages three and fifteen before a new working stock of the cell line was used.

2.11.2 Intracellular survival assay

J774 macrophages were cultured as described in section 2.11.1. Bacteria were grown overnight in broths or on plates (yeast extract and sugar or LB) then harvested and equalised to OD_{590} of 1 in PBS. Equalised cultures were then diluted to an MOI 40 (for 4 x 10^6 cells/ml to infect 5 x 10^5 macrophages) in pre-warmed L-15 medium (Gibco). Input inoculum was saved to plate out for viable counts (T = 0 hours). 24-well plates were seeded with 5 x 10^5 J774 macrophages per well and were used within 17 hours (the doubling time of the cell line). Cell monolayers were rinsed twice with pre-warmed PBS to remove traces of DMEM. Wells were overlaid with 1 ml volumes of L-15 with or without bacteria. Plates were incubated statically for 2 hours at 37° C to allow for internalization of bacteria by macrophages. Cells were washed once with 1x PBS and overlaid with L-15 supplemented with 1mg/ml ceftazidime and 500µg/ml kanamycin. Plates were incubated for 2 hours, static, at 37° C. Monolayers were then washed three times with warmed PBS. To lyse

macrophages, 1 ml of 0.1 % (v/v) Triton X-100 was added to all wells prior to serial dilution in PBS for viable counts on LB agar. Plates were incubated at 37° C for 48 hours.

To test the efficacy of antibiotic treatment used in the assay, a killing curve assay was carried out with ceftazidime and kanamycin which resulted in 99.6 % C1576 bacteria killed and 100 % ATCC 17616 killed after 2 hours.

2.12 A549 human lung epithelial cell invasion and adherence assays

2.12.1 A549 culture

A549 human lung epithelial cell line (ATCC® number CCL-185™) (75) was cultured according to the ATCC guidelines. Growth medium was high glucose DMEM with L-glutamine supplemented with 10 % (v/v) heat-treated FBS. Cell layers were cultured in 75 ml flasks and incubated at 37° C, 95 % air, 5 % CO_2. Media was renewed 2-3 times per week. Monolayers were rinsed prior to subcultivation and harvesting with PBS, then 2-3 ml of 0.105 mM trypsin, 0.53 mM EDTA solution was used to release cells from the flask. Cells were sub-cultivated with a ratio of 1:8. Working stocks of the cell line were frozen as described for J77.4 cells (section 2.11.1). Cells were used in assays between passages three and fifteen before a new working stock of the cell line was used.

2.12.2 A549 invasion assay

The method for evaluating bacterial invasion of A549 human lung epithelial cells for this study was based on previous published protocols (32). Plates were seeded as described in 2.11.2. Once seeded, cells were used within the doubling time of 22 hours. Bacteria were grown on LB agar overnight and then standardised to an OD_{590} of 1 and diluted to MOI 50 (for a final concentration of 5 x 10^7 CFU/ml) in pre-warmed L-15 medium. DMEM was removed from A549 monolayers before the addition of 1 ml L-15 bacterial suspension. Bacteria were allowed to invade for 2 hours (37° C static incubation) prior to a PBS wash, followed by antibiotic overlay with 1mg/ml ceftazidime and 500 µg/ml kanamycin.

After 2 hours antibiotics were removed with PBS washing (twice). 200 µl of DMEM with 0.105 mM trypsin/0.53 mM EDTA was added to infected monolayers and incubated at room temperature for five minutes to release the A549 cells from the polystyrene well, followed by 800 µl of 0.25 % (v/v) Triton X-100. Lysates were serially diluted and plated for CFU/ml onto LB agar and incubated for 48 hours. Invasion frequency was calculated as: ((recovered average CFU/ml) /input average CFU/mL) x 100 %.

2.12.3 A549 adherence assay

The method for evaluation of adhered bacteria to human alveolar epithelial cells was adapted from Accord *et al.* (1) and Thomas *et al.* (196). 24-well plates were seeded with 5 x 10^5 A549 cells. Monolayers were rinsed twice with PBS, and blocked with 0.5 % (v/v) filter-sterilised heat-treated FBS for 1 hour to minimise non-specific binding. Bacterial growth was harvested from LB agar, resuspended in PBS and standardised to an OD_{590} of 1, then diluted to 10^7 CFU/ml in L-15 media. The monolayers were rinsed again with PBS and infected at an MOI 20. Bacteria were allowed to adhere for 2 hours before non-adhered cells were removed with an aspirator. Monolayers were then washed five times with PBS. Infected A549 cells were lysed with 0.1 (v/v) % Triton X-100 and lysates were serially diluted and plated onto LB agar and the CFU/ml enumerated. Controls were monolayers overlaid with un-inoculated L-15 media.

2.13 Galleria mellonella infection model

Infection of larvae was guided by the specification as described by Seed and Dennis (175) with minor modifications as described briefly here. Larvae were obtained from LiveFoods U.K. and stored in woodchips at 10° C. A 25 µl 22s gauge gas-tight high performance Hamilton syringe (Cole-Palmer, location), was used to inject 10 µl aliquots of *B. multivorans* at 10^6 CFU/ml into *G. mellonella* via the hindmost proleg. Following injection, larvae were placed in a static incubator in the dark at 37° C. Control larvae were injected with 10 µl of sterile PBS. Per experiment, ten larvae were injected for each strain or growth condition of interest, and larvae were scored as dead or alive at appropriate

time-intervals post infection (p.i). Larvae were considered dead when they displayed no movement in response to touch with a pipette tip. Infection was repeated independently five times (for sugar assay work to assess impact of mucoidy and for adhesin mutants grown from LB agar plates). Input of bacteria was serially diluted in PBS and plated onto LB agar to ensure equal numbers of bacteria were inoculated into the larvae.

2.14 RNA extraction

B. multivorans was cultivated on LB agar growth media from a -80° C glycerol stock, and was subsequently plated onto 0.2 % (w/v) yeast-extract agar supplemented with 2 % (w/v) D-mannitol (standard YEM), 0.25 % (w/v) D-mannitol ('reduced YEM'), 2 % (w/v) D-mannose (YEO), 2 % (w/v) D-fructose (YEF), 2 % (w/v) YE + 2 % (w/v) D-glucose (YEG), or 2 % (w/v) YE + 2 % (w/v) D-mannitol ('non-mucoid YEM').

After approximately 16-17 hours incubation at 37° C, bacteria were harvested from two mannitol and fructose plates, and four mannose and glucose plates. Bacteria harvested from multiple plates were pooled together as single replicates and re-suspended in ice-cold PBS. 2 ml aliquots of bacterial PBS suspension were swiftly pipetted into RNAse-free tubes, chilled in liquid nitrogen, and centrifuged at full speed (4° C) for 5 minutes. The PBS was then decanted, and any remaining media was removed with a pipette. Pellets were immediately frozen in liquid nitrogen and stored at -80° C for up to one week, or processed immediately.

Total RNA extraction was made using the RiboPure kit (Ambion) according to the manufacturers' instructions. The recovered RNA was treated for 1 hour with 10 U of Ambion DNAse, and precipitated with 7.5 mM LiCl (Ambion) to concentrate the RNA before finally being re-suspended in 10 µl of Nuclease-free water. A diluted aliquot of total RNA sample were set aside for nanodrop and RNA quality assessment.

RNA quality was assessed upon electrophoretic separation on the Agilent Bioanalyzer using the RNA 6000 Nano kit (Agilent). Only samples with RNA integrity ratings higher than 7.0 were used for subsequent microarray or RNA-seq analysis.

2.15 Microarray analysis

The custom-made 4 x 44 K microarrays for *B. multivorans* ATCC17616 as well as the protocols used for RNA labelling, hybridisation in the microarray and fluorescence signal scanning were carried out as described for *B. cenocepacia* (170), and were performed in collaboration with Professor Eshwar Mahenthiralingam, Cardiff University. Briefly, 5 µg total RNA from ATCC17616 (see section 2.14) was labeled with the SuperScript Indirect cDNA Labeling System (Invitrogen). 10 µg of total RNA was used per labeling reaction. The amount of random hexamers was doubled to 1 µg per reaction and incubation time increased to 3 hours. Amino-modified first-strand cDNA was coupled with Cy5 dye (GE Healthcare).

For the Cy3-labeled microarray reference sample, genomic DNA of *B. multivorans* ATCC17616 strain was extracted by mechanical disruption using a modified bead-beater protocol (126). 3 ml of an over-night broth culture was harvested, mixed with lysis buffer containing pronase and glass beads, and beat for 10 seconds on the bead-beater. The lysate was incubated at 37º C for 1 hour and mixed with saturated ammonium acetate and chloroform. The mix was centrifuged, the upper aqueous phase removed and the DNA purified by ethanol precipitation. Purified DNA was further treated with RNase.

The genomic DNA was labeled with the BioPrime DNA Labeling System (Invitrogen) at 2 µg genomic DNA per labeling reaction. The dNTP mixture from the kit was replaced with a dNTP mixture containing 1.2 mM each dATP, dGTP and dTTP and 0.6 mM dCTP. 3 µl of Cy3 dCTp stock solution (GE Healthcare) was added per labeling reaction. The reactions were incubated at 37º C for 2

hours and then cleaned with the GFX PCR DNA Purification kit (GE Healthcare).

Microarrays were hybridised according to the Two-Colour Microarray Based Gene Expression Analysis protocol (version 5.5, Feb. 2007, order no. G4140-90050) (Agilent), adjusted for the use of cDNA. The fragmentation step was omitted and instead the hybridisation mix was denatured at 98º C for 3 minutes. Cy5 labeled cDNA was used at 825 ng per sample, and were hybridised against the Cy3 labeled genomic DNA, used at 60 ng per sample. The washing procedure included the use of Stabilizing and Drying Solution (Agilent) to prevent ozone-related degradation of Cy5. All experiments were carried out with three biological replicates per growth condition.

Microarray slides were scanned with a microarray scanner (G2565 BA, Agilent) with the Scan Control software (version A.7.0.3 Feb 2007 (Agilent)) and a scan resolution of 5 µm. The Extended Dynamic Range function, with 100 % and 10 % PMT gain, was enabled. Scanner images were analysed with the Feature Extraction (version 9.5.1 (Agilent)) using the FE protocol GE2_v5_95. Data was then imported into GeneSpring GX (version 7.3.1. (Agilent)) with the Agilent FE data import plug-in switched on to preprocess the data. Normalisation was performed with the Agilent FE saved scenario: First every spot of the signal channel was divided by the control channel. Each chip was then normalised to the 50th percentile of all measurements of that chip followed by normalisation of each gene to its median.

Clustering of samples for quality control and comparisons for statistical analysis were carried out using GeneSpring GX (version 7.3.1). As previously described by Sass *et al.*. (171), probe and intergenic (IG) sequences were evaluated in Gene Spring by removing unreliable features, removal of results with fold changes less than 1.5 in the compared conditions of interest. This was followed by 1-way ANOVA statistical tests for significant p-values < 0.05 with a parametric t-test with 5 % false discovery rate without multiple testing comparison or post-hoc tests.

Further details on microarray data quality control, analysis and fold-change parameters are presented in Chapter 4. Complete GeneSpring microarray data can be found on the Appendix CD.

2.16 Quantitative RT-PCR analyses

Transcript levels from selected genes were assessed via quantitative RT-real time PCR (qPCR). RNA was extracted (RiboPure Bacteria Kit, Ambion) from bacteria grown in synthetic CF sputum media (SCFM) (149) supplemented with either 2 % (w/v) mannitol or 2 % (w/v) mannose. cDNA was synthesized from 4 µg of total RNA (SuperScript III reverse transcriptase, Invitrogen), diluted 1:50 and used as template in qPCR using Platinum SYBR Green qPCR Supermix (Invitrogen) on an Mx3005P QPCR system (Agilent).

Cycling conditions were as follows: 1 cycle of 95°C (10 min), 40 cycles of 95°C (15 seconds) and 55°C (1 minute) with fluorescence measured at the 55°C annealing step. Then, a denaturation melt curve as follows: 95° C (1 minute), with fluorescence measured from 55°C (30 s) to 95°C (30 s). The $2^{(-\Delta\Delta CT)}$ method was used to calculate relative gene expression between the mannitol and mannose growth conditions, normalised to *gapA* expression (121). Primers used for qRT-PCR are listed in Appendix Table 9.3.

2.17 RNA-seq analysis

2.17.1 mRNA enrichment and sample quality assessment

Ten micrograms of total RNA were subjected to two successive rounds of rRNA depletion using MicrobeExpress (Ambion) per the manufacturer guidelines. The precipitation step was lengthened from 1 hour at -20° C to overnight at -80° C. Resulting mRNA was re-suspended in 25 µl TE buffer and frozen at -80° C. An aliquot of mRNA was used for analysis on the Agilent Bioanalyzer (RNA Prokaryote Nano kit series). Depletions were deemed successful when, compared to the original total RNA, the 16s and 23s peaks were eradicated.

2.17.2 Library preparation

RNA-seq analysis libraries were prepared from the resulting mRNA (section 2.17.1) using the TruSeq RNA protocol (Illumina). Samples were ligated to NEXTflex™ DNA adapters for sample differentiation. Amplified libraries were checked using the Agilent Bioanalyzer and concentration was estimated and standardised. Concentration of the pooled (8.1 mM) library was additionally verified using a qRT-PCR standard curve against a library of known concentration. Clustering of samples onto the flow cell was performed by bridge PCR using the Illumina cBot prior to sequencing on an Illumina HiSeq2000 platform.

2.17.3 RNA-seq data analysis

Mapping of resultant reads was to the *B. multivorans* ATCC 17616 reference genome. Subsequent expression analyses was carried out using the CLC Genomics Workbench (CLC bio) to identify differentially-expressed genes (two-group pair-wise comparisons), with statistical analysis performed using Kals' test and with FDR-corrected p- values and post- ests. CLC Genomics Workbench was used with default parameters. Further details on sample comparisons and quality control are described in Chapter 4.

2.18 EPS extraction

The method for EPS extractions was modified from Conway *et al.* (2004) (51). *B. multivorans* was grown on EPS-inducing sugar agar, specifically yeast extract and mannitol or fructose for 48 hours at 37° C. After incubation, agar plates were flooded with 5 ml of 2 % (v/v) phenol in 0.9 % (w/v) NaCl. The slurry was stirred in a glass beaker using a magnetic stir rod at 4° C for five hours at 150 RPM. The slurry was then pipetted into a phenol-safe plastic centrifuge tube with screw-cap lid (Oak Ridge/Nalgene), and spun at 10,000 x g (30 minutes) to separate cells from the EPS supernatant.

Supernatant was transferred to a fresh phenol-safe plastic centrifuge tube with screw-cap lid, and four volumes of ice-cold 95 % ethanol was added, mixed and centrifuged at 9,600 x g (10 minutes). Ethanol was decanted and the remaining loose pellet EPS was dissolved in 10 ml de-ionised H_2O by mixing

with a pipette and sitting at room temperature for 15 minutes. Samples were dialysed against 1 litre of Milli-Q dH_2O at 4° C for 48 hours with water changed twice daily. The dialysis tubing was at a molecular weight cut off of 3500 Daltons.

The dialysed sample was snap frozen in liquid nitrogen, and then freeze-dried for 24-36 hours (or until dry). Dry EPS extracts were stored at -20° C for short term storage, or - 80° C for long-term storage. EPS samples resuspended in water or buffer for use in assays was stored at 4° C (for up to one week) or -20° C.

2.18.1 Confirmation of sugars in EPS samples by the Dubois assay

To verify the presence of sugars within the EPS extracts prior to mass spectrometry, the Dubois test (phenol sulphuric acid) was performed (66). This method uses colorimetric detection for the determination of sugars. Briefly, 2 mg/ml of rhamnose, mannose, galactose, and glucose sugar standards were prepared in water. This standard mix of sugars was serially diluted in water from 2 mg/ml to 80 µg/ml. EPS samples of 1mg/ml were serially diluted in water to 80 µg/ml. 50 µl of EPS sample or standard sugar mix was added to a well of a polystyrene 96-well plate in triplicate, followed by the addition of 150 µl of 98 % (v/v) sulphuric acid, 30 µl of 5 % (w/v) phenol. The plate was incubated for 5 minutes at 90° C in a static water bath, cooled to room temp for 5 minutes, and absorbance measured in a microtitre plate reader at 490 nm.
N.B. The phenol sulphuric acid method is reported to be accurate to +/- 2 %.

2.19 Mass spectrometry analysis of EPS

2.19.1 Acid hydrolysis

Ten milligrams of freeze-dried EPS extracts were re-suspended into HPLC- MS grade H_2O. 5mM heavy labelled (D-[1-^{13}C]) galactose, glucose and mannose sugars were added to samples for standard addition quantification (spiked). Both spiked and un-spiked EPS samples were then acid hydrolysed using 2 M trifluoroacetic acid (TFA). Re-suspended solutions of EPS were mixed 50:50 with acid and baked for 1 hour at 110° C in 1 ml Teflon capped

ReactiVials (Fisher Scientific). Post hydrolysis, the samples were re-suspended in 50 µl HPLC grade H_2O and 25 µl was transferred into glass vials.

2.19.2 Glucose oxidase-treatment of EPS

Glucose and galactose sugars have the same mass, resulting in difficult separation between these two sugars using mass spectrometry. Chemical removal of glucose in a given sample using glucose oxidase and comparison of this treated sample with an untreated sample allowed for quantitative differentiation between the two sugars. Mannose is also of the same mass as glucose and galactose but did not co-elute over the same acquisition time period on the mass spectrometer. The glucose oxidase was re-suspended in sodium acetate buffered to pH 5.1 (0.2 M sodium acetate (Fluka)) in H_2O. The buffer pH was adjusted using glacial acetic acid to a final concentration, 50mM. Freezer stock solutions of glucose oxidase were made at 100 U/ml in 10 % glycerol and acetate buffer. Catalase was added to the reaction (in order to neutralise H_2O_2 , a by-product of the reaction). 1,000 U/ml enzyme stocks of catalase were made up with 10 % glycerol and acetate buffer, then stored at 4° C. The reaction consisted of 2.5 µl of oxidase for 125 µl reaction of EPS and acetate buffer, with 500 U catalase. The reaction was allowed to proceed for a maximum of 15 minutes to prevent any cross-reactivity with galactose.

Precipitation of samples to remove protein was carried out following glucose oxidase treatment using ice-cold acetonitrile in a 1:3 ratio. Samples were gently mixed and centrifuged at 12,000 RPM for 60 minutes (4° C), followed by the removal of the supernatant by pipette. The supernatant volume was reduced by centrifuging in a speed vacuum to ~ 50 µl. Hydrolysed and or glucose oxidase-treated EPS samples were re-suspended in H_2O rather than acetonitrile prior to running on the mass spectrometer. This was due to an observed improvement in chromatography when compared to acetonitrile run samples. Post hydrolysis, samples were re-suspended in 50 µl HPLC grade H_2O and 25 µl was pipetted into glass vials.

2.19.3 Running conditions for Agilent QQQ-ESI-LCMS

Quantitative analysis of EPS composition was performed using an Agilent 6420B triple quadrupole (QQQ) mass spectrometer (Agilent Technologies, Palo Alto, CA, US). The QQQ-ESI-LC mass spectrometer was coupled to a 1200 series Rapid Resolution HPLCsystem. Five microliters of sample extract was loaded onto a Waters X-Bridge Amide HILIC. The flow rate was 0.2 m/min and the column temperature was held at 35 °C for the duration. The following gradient was used: 0 min – 0% B; 17 min – 54 % B; 18 min – 0 %; 9 min post-time. QQQ source conditions were as follows: gas temperature 350 °C, drying gas flow rate 9 L/minute, nebulizer pressure 35 psig, capillary voltage 4 kV. The fragmentor voltage and collision energies were optimized for each compound. Table 2.3 concisely outlines these mass spectrometry method specifications used for detection of rhamnose, glucose, galactose and mannose in *B. multivorans* EPS samples. This method was optimised for hexose sugars, including ^{13}C labelled sugars.

Table 2.3 QQQ HPLC-mass spectrometry conditions for sugar analysis. *The dwell time represents 125 milliseconds the time that the mass spec scans for the sugar of that particular mass (e.g. rhamnose 163.3) before it scans the next mass.

Method	Sugars SIM amide column- 13CHex			
Flow rate (ml/min)	0.3			
Injection volume	5 µl			
Gradient*	0 min	0 % mobile phase B		
	17 min	54 % mobile phase B		
	18 min	0 % mobile phase B		
Stop time	18 min			
Post time	9 min			
Mobile phase A	10 % acetonitrile, 90 % H_2O	0.1 % ammonia		
Mobile phase B	10 % H_2O, 90 % acetonitrile	0.1 % ammonia 5 mM ammonium formate		
Column	Waters X-Bridge Amide HILIC	3.5µm particle size, 2.1x150mm column		
Column temperature	35 °C			
Acquisition type	Selected ion monitoring (SIM)	Glucose, mannose, galactose – 179.1	Polarity- NEG	Dwell time*- 125
		Rhamnose – 163.2	NEG	125
		^{13}C hexoses – 180.1	NEG	125

Further detail on the method development process from EPS extraction to data analysis for EPS composition analysis is described in detail in Chapter 6.

2.20 Iron toxicity assay

The protective effect of EPS against iron toxicity was assessed using a method previously described (68). Overnight mannose-broth cultures of B. multivorans were standardised in PBS and incubated at 30°C in the presence or absence of 2.5 g/liter purified fructose- or mannitol- derived EPS and 50 mM $FeSO_4$. Percentage survival over three hours was calculated by plating serial dilutions of the CFU at T = 0 and hourly time points onto LB agar.

2.21 Desiccation assay

The protective effect of EPS against desiccation was assessed using a method previously described (68). Overnight mannose- broth grown cultures of *B. multivorans* were standardised in PBS, and 10 µl of bacteria suspension was air-dried and incubated (30° C) in the presence or absence of 2.5 g/liter of purified fructose- or mannitol- derived EPS. Viable CFU were determined by rehydration of desiccated wells by the addition of 100 µl PBS. Percentage survival over three hours was calculated by plating serial dilutions of the CFU at T = 0 and daily time points onto LB agar.

2.22 Xanthine/xanthine oxidase generation of reactive oxygen species

The xanthine/xanthine oxidase method can be used for *in vitro* cell-free detection of reactive oxygen species (ROS) was modified from Bylund *et al.* and Simpson *et al.* (33,180). This method uses xanthine as a substrate, and xanthine oxidase, an oxidant, used with isoluminol (4-Aminophthalhydrazide) provided detection of CL. The reaction reagents were added together, pre-incubated at 37° C. Every three minutes CL was measured at 37° C using a TECAN fluorescent plate reader. Reactions were carried out in triplicate wells of a white, clear flat bottom 96-well plate. All reaction constituents were made up on the day in Krebs ringer buffer (KRG) as follows: pH 7.3, NaCl (120 mM); KCl (5 mM);KH_2PO_4 (1.7 mM); Na_2PHO_4 (8.3 mM); D-Glucose (10mM); $CaCl_2$ dihydrate (1mM);$MgCl_2$ (1.5 mM)). Xanthine was stored in a 10 mM stock in 1 M NaOH, wrapped in foil and kept at 4° C for up to three months. The final

concentration of xanthine included in the reaction was 6 mM. XO was used to start ROS production at 12.5 U. Isoluminol was used at a final concentration of 0.8 mM. EPS samples were diluted from 50 mg/ml stocks in deionized Milli-Q water to 1 mg/ml and 0.5 mg/ml. As a reaction control, 80 U/ml superoxide dismutase (SOD) was used. Horse radish peroxidase (HRP) was used in the assay at 4 U/ml in KRG. Reaction components were added to the desired final concentrations in a final volume of 250 µl in the following order: 0.8 mM isoluminol, 1 mg/ml EPS, SOD, or KRG only, 6 mM xanthine, 4 U/ml HRP, 10 minute static incubation (37° C) to equilibrate, 12.5 U xanthine oxidase. CL readings were then taken in 3 minute intervals using the incubation setting at 37° C, on a TECAN fluorescent plate reader (TECAN Infinite 2000 PRO series). Controls were isoluminol in KRG alone, blank wells, and SOD containing wells. Further detail on this method is described in Chapter 7 where results and reaction schematic are presented.

2.23 Insulin binding assay

The ability of a panel of *Burkholderia* strains to bind insulin was assessed with a protocol described previously (141). Table 9.4 in the Appendix lists strains used in the insulin binding studies (detailed in Chapter 8). Briefly, cells were harvested from an LB overnight culture of strains listed in Table 9.4. Cells were centrifuged for 3 minutes at 6,500 x g. Cultures were equalised to 0.7 OD_{590}. Cells were again pelleted, washed in 500 µl 10 mM MOPS (pH 7) and centrifuged again. The pellet was re-suspended in 100 µl MOPS containing FITC-insulin at a final concentration of 1µg/µl. Following 20 minutes incubation at room temperature in the dark, cells were washed three times in 1 ml PBS and re-suspended in 100 µl PBS.

For purposes of fluorescence microscopy, 20 µl of insulin-exposed bacterial culture was added to a microscope slide. The slide was air-dried, heat-fixed, and a cover-slip mounted with Prolong Gold anti-fade mounting medium (Promega).

For 96-well fluorescent plate reader analysis, after the wash steps, insulin-exposed cultures were added directly to wells of a black 96-well plate for

quantitative analysis at FITC-wavelength (530 ± 30 nm) with a TECAN fluorescent plate reader (TECAN Infinite 2000 PRO series).

2.24 Investigation of insulin binding by flow cytometry

The flow cytometer used in the present study was a BD FACS Aria II (Becton Dickenson), 488 nm excitation laser, Size (Forward scatter) detector and Internal Complexity (Side scatter) detector. PBS was used for analysis and sheath fluid sorting of all samples. Samples were analysed using a BD FACS Aria II Fluorescence Activated Cell Sorter (FACS) equipped with a 100 µm sheath fluid nozzle. Particle fluorescence was excited at 488 nm, and fluorescence intensity recorded at 530 ± 30 nm. Particle sorting efficiency was controlled by routinely calibrating with BD FACS Accudrop beads and enabling the 'Sweet Spot' application. These two measures ensured a steady and constant stream of microdroplets through the FACS.

When possible, at least 10,000 events were recorded for each sample and the distribution of the optical properties from each event were used to construct areas of interest or 'gated' populations. FITC-insulin exposed cells were sorted using FACS and re-cultured to isolate and enrich the small subpopulation of insulin binding cells. Isolated bacteria that had bound FITC-insulin after 20 minutes exposure to insulin were then sorted out from at least 10,000 cells according to stringent gating for strong FITC- fluorescence.

After the initial exposure and sort, insulin-bound bright cells were re-grown prior to re-sorting using FACS to assess the stability of the insulin-binding phenotype. Insulin-bound cells were re-grown in either LB broth supplemented with CV (0.01 % (w/v)) and *Burkholderia cepacia* selective supplement, BCSM agar, or LB agar to monitor for growth and contamination. Re-growth between insulin exposure and re-sorting was for 48 hours.

2.25 Persister assay for insulin binding

To quantify insulin binding of Bcc persister cells, a persister cell assay using was used to reveal persister cells after treatment with 100x MIC of

ciprofloxacin or ceftazadime. Bacterial cultures were growth overnight in LB to stationary phase. Optical density was measured at OD_{590} to estimate the number of cells/ml. For stationary phase cultures, the absorbance OD_{590} of 0.2 was approximately 2 x 10^8 CFU/ml. 500 µl of adjusted cultures were mixed with 500 µl antibiotic solutions (with a final cell density of 10^8 CFU/ml per well of a 48-well microtitre plate). Antibiotics used were ceftazidime or ciprofloxacin at 100x MIC and incubated statically at 37° C for exactly 24 hours.

Following incubation, the contents of each well of the 48-well microtitre plate were transferred to microcentrifuge tubes and centrifuged for 4 minutes at maximum speed. The spent LB supernatant was removed using a pipette, and 1 ml fresh LB was used to re-suspend the pellet. At this point aliquots were removed to carry out post-treatment viable counts (t_{24h}) to enable the calculation of persister cell frequency. CFU/ml was determined before, (t_0) and after the antibiotic treatment (t_{24h}). Persister frequency was calculated as (CFU/ml at t_{24}) / (CFU at t_0/2).The input, t_0, is halved in the equation because the culture was initially standardised to 2 x 10^8 CFU/ml and then 500 µl of that standardised culture is mixed with 500 µl of antibiotic, thus halving the dilution to a final cell density of 10^8 CFU/ml. Antibiotic stocks were made up at double strength concentration to account for this dilution.

To continue on and exposure persister cells to insulin, another centrifugation step was done with subsequent re-suspension in 1 ml MOPS. Microscopy of ceftazidime-derived persister cells entailed combining three 1 ml wells (technical replicates from the 48-well plate) prior to insulin exposure. After the insulin exposure and washing steps described in the previous paragraph, 20 µl of washed insulin-exposed cells were pipetted onto a clean microscope slide, air dried, heat-fixed, and mounted with coverslips using Prolong-Gold anti-fade mounting solution (Promega). Cover-slipped slides were then dried in the dark overnight (and kept damp). Coverslips fixed in place with nail varnish the following day. Slides were then analysed on a Zeiss AXIOSTAR epifluorescence upright microscope under FITC and phase-contrast viewing at 100x oil immersion magnification. Slide boxes were stored long-term at -20° C with desiccant.

For FCM analysis of ciprofloxacin-derived persister cells, eight (technical) replicates of 1 ml wells were pooled together for each strain from a 48-well plate. After pooling, the insulin-binding assay and subsequent wash steps were scaled up relative to the increase in volume. Samples were re-suspended in a final volume of 7 ml PBS prior to FCM analysis.

2.26 Statistical analyses

All experiments were performed at least in triplicate, with subsequent statistical analysis by one-way ANOVA and Tukey post-tests (Graphpad Prism 5.0) or followed by other relevant comparisons such as a Dunnetts' test or orthogonal contrasts (IBM SPSS Statistics, v. 20) to determine p-values. Standard error of the mean is represented by error bars. $P < 0.05$ was deemed to be statistically significant. The type of statistical test used, sample size, p-values, and error bars are outlined in each figure legend.

Transcriptomic data was processed using two differing statistical methods. Microarray data were compared and calculated with the 1-way ANOVA test using GeneSpring GX version 7.3.1. (Agilent), whilst the RNA-seq analysis was analysed using CLC Genomics Workbench with a Kals' test and Bonferroni post-test. FDR-corrected p- values were deemed significantly when $P < 0.05$.

2.27 DNA sequencing of B. multivorans C1576 and identification of loci encoding putative adhesins.

Genomic DNA from *B. multivorans* C1576 was extracted using the PureLink Genomic DNA kit (Invitrogen) and sequenced on an Illumina platform following library preparation using the TruSeq DNA protocol (Illumina). Reads were initially mapped to the *B. multivorans* ATCC 17616 reference genome, enabling identification of unmapped reads (sequences present in C1576 but absent from ATCC 17616). These unmapped reads were subjected to both *de novo* assembly and re-mapping to alternative Bcc reference genomes. Mapping

and *de novo* assembly was performed using CLC Genomics Workbench (CLC bio). Loci encoding putative adhesins were located within the mapped/assembled sequence reads by BLASTN analysis, and the identity of the putative adhesins to known sequences was assessed by BLASTN and BLASTP analysis at NCBI and www.burkholderia.com (225).

2.28 Dot-blot hybridisations

Genomic DNA was extracted using the Pure Link Genomic DNA Purification kit (Invitrogen) and was normalised to 85 ng/µl in 0.1 M NaOH. Three microliter aliquots of the resulting DNA were replica-spotted onto Hybond-N+ membranes (GE Healthcare) and air-dried. Membranes were rinsed (4 x SSC, 5 minutes; 0.5 x SSC, 5 minutes) prior to baking (80° C, 2 hours). The PCR DIG probe Synthesis kit (Roche) was used to generate probes specific for the genes encoding the fimbrial usher protein and HecB-like protein, with the probe sequences corresponding to nucleotides 2515-2940 of JX191919 and nucleotides 12641-13084 of JX191920 respectively (see Appendix Table 9.1 for primer sequences). Subsequent pre-hybridisation, hybridisation, washing and detection were performed using the DIG-Easy Hyb, DIG Wash and Block Buffer Set, and CDP-Star (Roche) according to manufacturer's instructio

Chapter 3: Characterisation of exopolysaccharide-dependent and -independent phenotypes in the cystic fibrosis pathogen *B. multivorans*

3.1 Introduction

Organisms of the *Burkholderia cepacia* complex (Bcc) are important pathogens of cystic fibrosis (CF) patients. *B. multivorans* is responsible for the majority of Bcc infections of CF patients in the U.K. Growth of members of the Bcc on numerous sugars and sugar alcohols can induce a dramatic overproduction of exopolysaccharide (EPS), a putative virulence factor. Amongst the most potent inducers of EPS production are mannitol (recently approved in CF patients as an inhaled osmolyte) and fructose (which is reported to be elevated in the blood and urine of diabetic patients (Kawasaki et al. 2002)). Although levels of fructose in the lung have not been reported, it has been shown that glucose is elevated in the airways of diabetics (29). Consequently, if airway concentrations are similarly elevated, the onset of CF-related diabetes (CFRD) or the therapeutic administration of mannitol could potentially promote EPS production within the lungs of Bcc-infected patients.

Whilst an aim of this study was to assess the role of EPS in virulence, the present study also examined the extent to which differences were due to the EPS itself, or the culture conditions used to promote its production. Consequently, the adopted strategy was to create non-mucoid isogenic mutants; specifically, by inactivation of the *bceB* gene (which encodes a glycosyltransferase (216)) in the *B. multivorans* CF outbreak isolate C1576 and the environmental isolate ATCC 17616. C1576 is the index case of a transmissible outbreak of *B. multivorans* from a paediatric CF clinic in the U.K. (222). ATCC 17616 is the annotated genome reference strain for *B. multivorans*, and was originally isolated from the maize rhizosphere. The most commonly produced type of EPS by the Bcc is cepacian. The structure and role of BceB in the cepacian pathway has been previously characterised and described previously (216). The *bce* cluster is highly conserved amongst members of the Bcc, and is found in whole, or part, in nearly all members of the genus *Burkholderia*. As described by Ferreira *et al.*, the proposed pathway leading to the sugar nucleotide precursors for cepacian (the most commonly produced EPS detected to be produced by members of the Bcc involves the BceB priming glycosyltransferase (Priming GT) which plays a role in transfer of

assembled sugar nucleotides onto the repeat unit of polysaccharide prior to transfer across the bacterial outer membrane. The Bce proteins within the cepacian biosynthesis pathway include those involved in nucleotide sugar biosynthesis (BceA, BceC, BceM, BceN, BceT), glycosyltransferase activity (BceB, BceG, BceH, BceJ, BceK, BceR), polymerisation/export functions (BceD, BceE, BceF, BceI, BceQ) and acyltransferase activity (BceO, BceS, BceU). BceP is of unknown function (68). Inactivation of the *bceB* gene in *B. ambifaria* resulted in total loss of mucoidy, and the present study predicted the same would be true in *B. multivorans* (17).

The impact of EPS production on virulence relevant traits in *B. multivorans* was assessed by creating EPS-deficient *bceB* mutants. The use of *bceB* mutants alongside the respective ATCC 17616 and C1576 wild-type strains allowed for detection of EPS-independent and EPS-dependent phenotypes. An EPS-independent phenotype was attributed to the sugar or sugar alcohol used as a carbon source for growth rather than EPS. This differentiation between an EPS-dependent phenotype versus independent is a novel approach in contrast to previous literature reporting effects of mucoidy and the impact of EPS on virulence in wild-type strains only grown with mannitol to induce EPS, without an isogenic non-mucoid isolate to compare back to. The sugar response of *B. multivorans* to mannitol has not previously been characterised in this manner. The representative non-mucoid control used in phenotypic characterisation studies was mannose, which is another sugar elevated in diabetes (relevant to CFRD) (153). The phenotypic studies focused on mannitol (as a model for mucoidy inducing sugars) and mannose (non-mucoid inducing) to assess EPS-independent and EPS-dependent phenotypes.

3.2 Aims

To fully characterise the response of *B. multivorans* to mannitol and mannose by using phenotypic assays with an EPS-deficient mutant to assess phenotypes as EPS-dependent or EPS-independent in the following assays:

- Biofilm formation and antibiotic exposed biofilm survival
- Swimming motility
- Virulence in *Galleria mellonella*
- Macrophage uptake and survival
- Resistance to oxidative stress induced by H_2O_2
- Adhesion to mucin and extracellular matrix proteins
- Invasion of A549 alveolar epithelial cells

3.3 Results

3.3.1 Inactivation of bceB in B. multivorans

B. multivorans possesses several putative EPS biosynthetic gene clusters. The present study focused on the most highly conserved EPS cluster within the Bcc, the *bce* cluster. The present study demonstrates that inactivation of *bceB* (which encodes a glycosyltransferase) eliminated EPS biosynthesis in *B. multivorans* C1576 and ATCC 17616, irrespective of the sugar or sugar alcohol present in the growth media (shown in Figure 3.1, and summarised in Table 3.1). This indicated common pathways for EPS production are utilised in the response of different carbon sources.

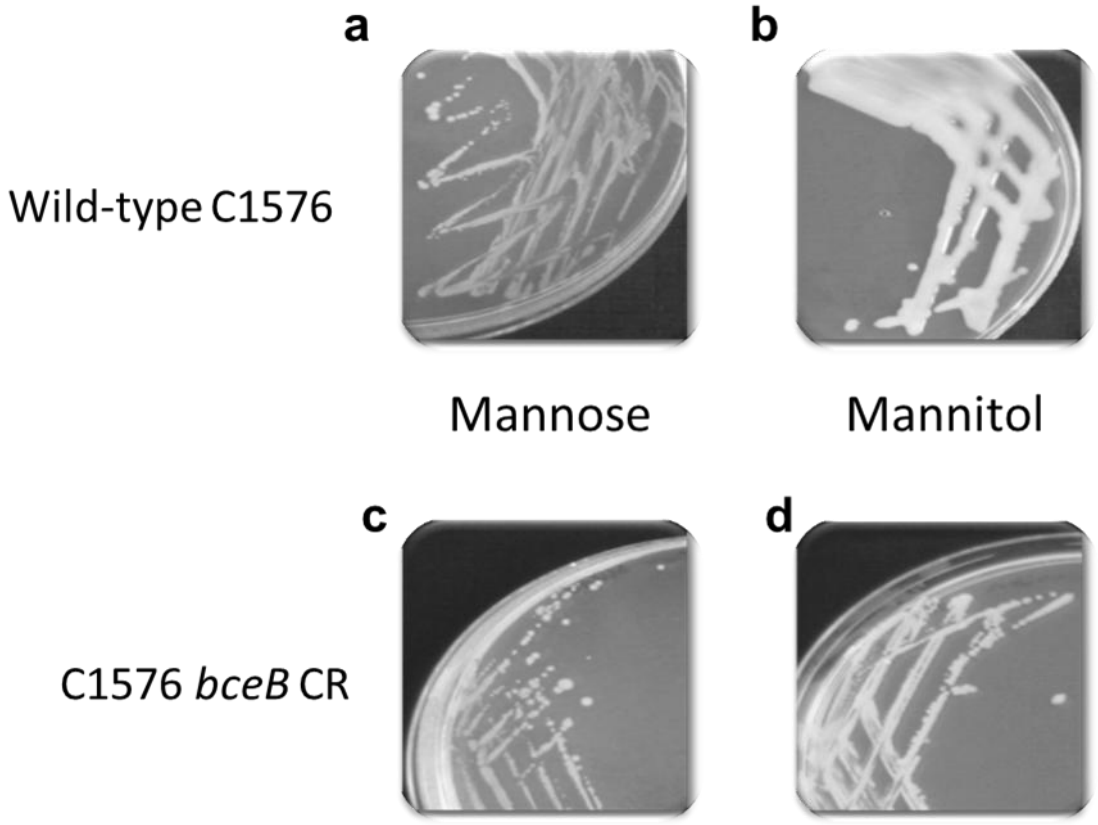

Figure 3.1 B. multivorans C1576 wild-type and EPS-deficient mutant grown on mannitol and mannose. Following 48 hours of growth *B. multivorans* C1576 wild-type and bceB crude (CR) EPS-deficient mutant were assessed for the ability to produce EPS on mannitol and mannose sugar agar plates. The wild-type grown on mannose is non-mucoid (a) whilst the wild-type produces EPS on mannitol (b). The C1576 bceB CR EPS deficient mutant is non-mucoid on both mannose (c) and mannitol (d). Inactivation of *bceB* renders the strain EPS-deficient.

Figure 3.1 highlights the phenotypic differences between mannose and mannitol in the wild-type C1576. The wild-type is non-mucoid on mannose, but produces EPS on mannitol and induces a mucoid phenotype in an observable glossy sheen to the growth on the plate (Figure 3.1(b)). The C1576 *bceB* mutant is non-mucoid on all sugars. These same observations of mucoid/ non-mucoid phenotypes were observed in the *B. multivorans* ATCC 17616 wild-type and *bceB* EPS-deficient mutant. These findings are summarized in Table 3.1.

The purpose of Table 3.1 is aimed to specifically indicate the EPS status of the wild-type and bceB CR C1576 and ATCC 17616 on various carbon sources, and this was done alongside relevant controls. *B. cenocepacia* K56-2 was used as a negative control. It carries an 11 bp deletion within the *bceB* gene and is non-mucoid on all sugars and sugar alcohols. *B. ambifaria* was used as a basis for comparison from the literature (17). All sugars, with the exception of fructose, that induced EPS biosynthesis were sugar alcohols. All sugars and sugar alcohols tested failed to induce EPS production in the C1576 and ATCC 17616 bceB CR mutants, indicating commonality of pathways for EPS biosynthesis regardless of carbon source or strain. This indicates *bceB* plays a broader role in other pathways of EPS biosynthesis rather than solely in the *bce* EPS cluster.

Table 3.1. EPS biosynthesis of Bcc species when grown on sugar media agar supplemented with a variety of sugars and sugar alcohols. The purpose of Table 3.1 is to indicate the EPS status of *B. multivorans* wild-type C1576 and ATCC 17616 and bceB CR mutants on various carbon sources. All strains tested were ranked according to a scale previously described in Bartholdson *et al.* (17). EPS production was scored on a scale from – (no EPS) to +++ (very mucoid). An example of +++ mucoid growth can be seen in Figure 3.1 (b). *B. ambifaria* AMMD and *B. cenocepacia* K56-2 were included as controls. All the sugars used were in the D-enantiomer form.

Species	Strain	Source	Yeast Extract	Glucose	Sucrose	Fructose	Inulin	Glycerol	Mannitol	Glucitol	Ribitol	Inositol	Mannose
B. ambifaria	AMMD	Soil	-	-	++	+++	-	+++	+++	+++	+++	-	-
B. cenocepacia	K56-2	CF	-	-	-	-	-	-	-	-	-	-	-
B. multivorans	C1576	CF	-	-	+	+++	-	+++	+++	+++	+++	+++	-
B. multivorans	C1576 *bceB* CR		-	-	-	-	-	-	-	-	-	-	-
B. multivorans	ATCC 17616	Soil	-	-	+	+++	-	+++	+++	+++	+++	+++	-
B. multivorans	ATCC 17616 *bceB* CR		-	-	-	-	-	-	-	-	-	-	-

3.3.2 Assessing growth and mucoidy of B. multivorans on sugars and sugar alcohols

Having created and confirmed the ATCC 17616 and C1576 *bceB* EPS-deficient mutants, the wild-types and *bceB* mutants were used in growth assays to ensure that the inactivation of *bceB* did not alter the overnight growth optical density compared to the wild-type. This ensured difference in growth did not impact on phenotypes observed in future experiments. The *B. multivorans* wild-type and mutants exhibited comparable growth in all sugars and sugar alcohols tested. 24 hour average OD_{590} was ~1.8 for mannitol and mannose, and lower overnight OD_{590} 0.4-0.6 in glucose and galactose. Neither glucose nor galactose induced EPS synthesis. These sugars were not used of phenotypic studies. Growth in glucose is revisited in Chapter 4 with modified media used for the purposes of transcriptomic studies. For purposes of simplification, the remainder of the studies for virulence relevant phenotypes included mannitol as the model for EPS inducing growth condition, and mannose for non-mucoid growth condition, although fructose and glucose are included in transcriptomic studies reported in Chapter 4. These sugars were chosen not only due to

clinical importance but also because the wild-type and bceB CR mutants growth was comparable in D- mannitol or D-mannose.

3.3.3 Mannitol promotes biofilm formation in an EPS-independent manner.

Having carried out studies that confirmed the *B. multivorans* EPS-deficient knockouts, phenotypes were characterised between the wild-type and *bceB* mutant for assessing the sugar response in phenotypic studies relevant to virulence. The impact of carbon source on biofilm formation in *B. multivorans* was first assessed.

Pellicle formation, or biofilm formed in static conditions, was tested in *B. multivorans* ATCC 17616 and C1576 grown and incubated statically for up to 72 hours at 37° C. Yeast extract media with or without sugars, LBB, or SCFM media with or without sugars, were inoculated and pellicle formation was assessed visually. *B. multivorans* ATCC 17616 formed thicker pellicles spanning the entire air/liquid interface as well as on the sides of the 50 ml Falcon tubes, whilst C1576 formed easily disrupted, thinner pellicles floating across surface of media. This is consistent with ATCC 17616 being a robust biofilm former. This method did not reveal any obvious sugar impacts on pellicle formation. To enable a more robust study of the impact different sugars have on biofilm formation, a quantitative assay was adopted, using the MBEC biofilm device.

The environmental strain *B. multivorans* ATCC 17616 was used for 96-well pegged lid biofilm assays as it is a robust overnight biofilm former. ATCC 17616 wild-type and *bceB* mutant biofilm formation was assessed after 24 hours of growth in mannitol (EPS-inducing) or mannose (non-EPS inducing). *B. multivorans* was grown on sugar yeast extract agar prior to inoculation into 96-well plate biofilm device.

The impact of sugars on biofilm formation was assessed by first preconditioning strains during overnight growth on sugar agar prior to inoculation into sugar broths for 24 hour biofilm formation (Figure 3.2). In these experiments, the wild-type ATCC 17616 formed significantly more biofilm in mannitol than in mannose. The *bceB* mutant also formed significantly more

biofilm in mannitol than in mannose. These results indicate an EPS-independent sugar effect on biofilm formation, with mannitol promoting biofilm formation. Additionally, the *bceB* mutant in mannitol formed more biofilm than the wild-type in mannitol. This indicates more biofilm is formed in the absence of EPS. These findings highlight the wider impact of sugars and EPS production on biofilm formation.

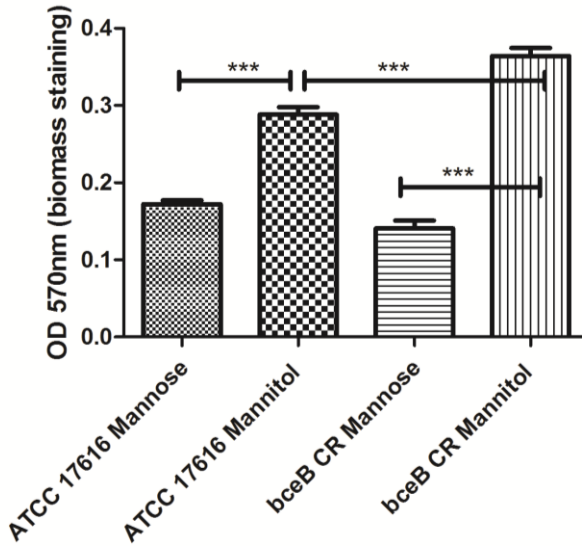

Figure 3.2 B. multivorans ATCC 17616 and bceB CR mutant biofilm formation. Assessment of biofilm formation indicates mannitol enhanced biofilm formation in an EPS-independent manner. The bceB CR mutant in mannitol also formed significantly more biofilm than the wild-type in mannitol. Graph is representative of at least three biological replicates, bars are representative of mean values from 16 wells per growth conditions/strain, and error bars are SEM. *** P< 0.0001. Statistical test used was 1-way ANOVA with post-test.

3.3.4 Mannitol grown biofilms are resistant to tobramycin independent of EPS

The impact of sugar grown biofilms and their resistance to antimicrobial killing was assessed. CF patients are regularly administered antibiotic treatment with inhaled tobramycin for either *Pseudomonas aeruginosa* and/or Bcc infection. Due to the enhanced biofilm formation in mannitol, the potential clinical impact of EPS and biofilm resistance to antibiotic treatment, growth of *B. multivorans* ATCC 17616 in mannitol could alter the efficacy of tobramycin in an EPS-dependent or -independent manner. ATCC 17616 biofilms grown in

mannitol or mannose were exposed to tobramycin at 4x the MIC (8 µg/ml) for 24 hours. This concentration is clinically relevant as it is reported that following inhalation, tobramycin concentrations in the alveolar fluid have been recorded as high as 9.2 µg/ml (16).

The biofilm-covered pegs were harvested and biomass was plated for viable counts. In previous biofilm assays, sugars played an EPS-independent role in ATCC 17616 biofilm formation. Mannitol promoted biofilm formation in an EPS independent manner (Figure 3.2). Mannitol enhanced biofilm survival in the presense of tobramycin in an EPS-independent manner (Figure 3.3). Both wild-type and bceB CR mutant mannose-grown biofilms had a 0.012-0.015 % average survival relative to untreated biofilms, in contrast to the mannitol-grown wild-type (11.4 % average survival) and bceB CR mutant (6.7 % average survival) biofilms.

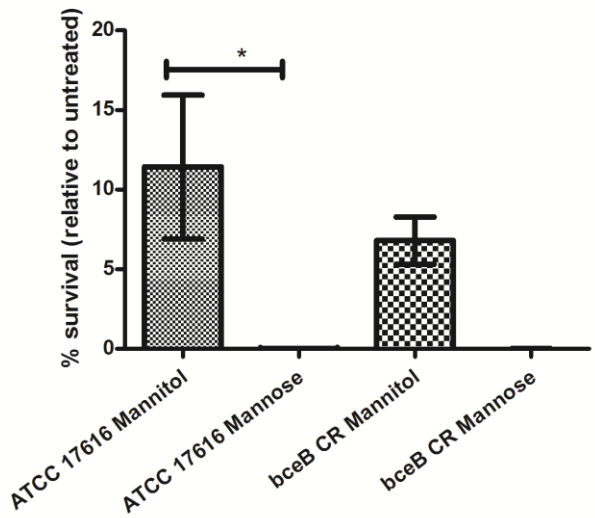

Figure 3.3 B. multivorans ATCC 17616 wild-type biofilms survived tobramycin exposure significantly better than mannose grown. Though there was no significant difference between the bceB CR mutants in mannitol compared to mannose, the similar trend as the wild-type was observed. The graph is representative of three biological replicates, and bars are the median values from three wells (N=3). Error bars are SEM and. * $P<0.05$. Statistical significance was assessed using a 1-way ANOVA and post-test.

The ATCC 17616 wild-type and *bceB* mutant biofilms survived better after formation in mannitol compared to mannose. There was a significant difference between the wild-type in mannitol compared to mannose. Survival of tobramycin treatment is likely EPS-independent, although the mannitol vs. mannose comparisons for the bceB CR mutant was not significant (P = 0.078). These studies highlight the impact of biofilm and sugars on ATCC 17616 antimicrobial killing by the aminoglycoside tobramycin.

3.3.5 Swimming motility is enhanced by mannitol in an EPS-independent manner

The impact of mannose and mannitol on swimming motility was carried out by making swimming media with the same 2 % sugar and 0.2 % yeast extract agar used previously, with 0.3 % (w/v) agarose content. The impact of mannose and mannitol on swimming motility in *B. multivorans* ATCC 17616 and C1576 was assessed. Results show (Figure 3.4) mannitol enhanced motility in both wild-type *B. multivorans* ATCC 17616 and C1576 and for both *bceB* mutants. Differences in motility are an effect of the sugar, rather than EPS.

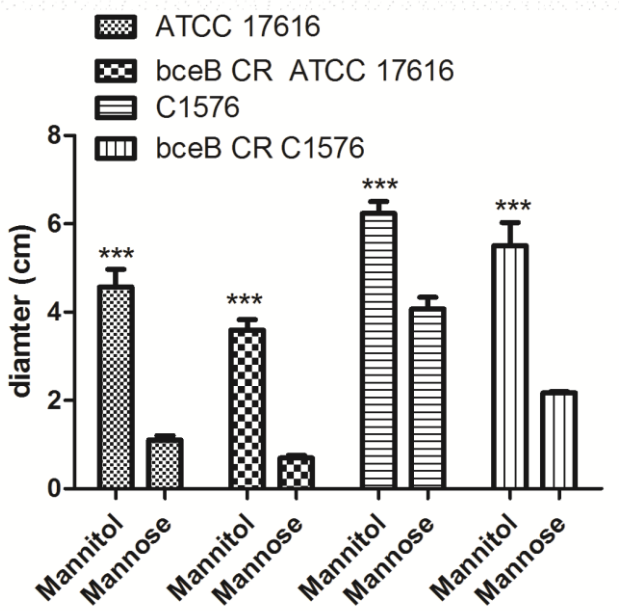

Figure 3.4. The impact of sugars on B. multivorans swimming motility. 0.3 % (w/v) agar supplemented with yeast extract and the sugar was inoculated with a standardised bacterial suspension. Figure shows median diameter measured on swimming agar plates totalling five plates per growth condition and strain (n=5). *** $P < 0.0001$. Asterisks indicate significant increase in motility in mannitol relative to non-mucoid mannose control. 1-way ANOVA and post-test were used to assess statistical significance.

3.3.6 Growth in mannitol attenuated virulence in the Galleria mellonella model of infection

G. mellonella (greater wax moth larvae) model of infection has been well established as a screening system for attenuated virulence studies for a number of bacteria, including the *Burkholderia* (175). *B. multivorans* was grown on sugar agar, standardised in PBS and used to infect larvae at an input of approximately 10^4 CFU. Controls were inoculated with PBS, and of this control group, 100 % survived. Results show C1576 wild-type and *bceB* mutant grown in mucoid grown conditions is attenuated in this model (Figure 3.5). Initially it was hypothesised that since the process of EPS production is metabolically expensive, the wild-type C1576 would be less virulent in the larvae. This was not the case, as both the wild-type and *bceB* mutant both were attenuated in

virulence following growth on mannitol. This indicated *B. multivorans* virulence was EPS-independent and attenuated virulence was not due to reduced fitness of the wild-type.

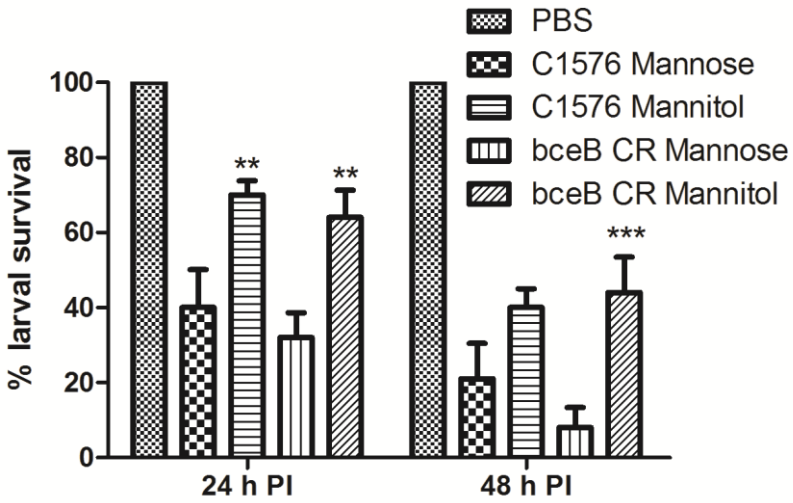

Figure 3.5. Larval survival during B. multivorans infection. Survival of *G. Mellonella* was monitored and recorded at 24 and 48 hours (h) post-infection (PI). Larvae were inoculated with *B. multivorans* C1576 wild-type and bceB mutant grown on mannose or mannitol. Following growth in mannitol, C1576 *bceB* mutant was attenuated in virulence at 24 hours. 100 % of controls survived (inoculated with PBS). Asterisks denote significant attenuation relative to mannose. Bars represent average percentage survival from five separate experiments with 10 larvae each condition. Error bars are SEM. ** $P < 0.005$, *** $P<0.0001$. Statistical significance was assessed by two-way ANOVA analysis followed a post-test.

3.3.7 Impact of sugars on B. multivorans macrophage survival

For this assay, J774.1 murine macrophages were infected (MOI 40) with mannitol or mannose-grown *B. multivorans* C1576. After two hours initial uptake, extracellular bacteria were killed with a two hour ceftazadime and kanamycin treatment. The four hour time point was taken two hours after antibiotic treatment. The 24 hour time point was taken after a separate two hour of antibiotic treatment. Infected monolayers were lysed, serially diluted, and plated for viable counts onto LB agar.

Time points taken were input or 0 hours, 2, 4, and 24 hours. Figure 3.6 shows the percentage of survival relative to input bacteria of the macrophage infection time series representative of several repeats of this macrophage

infection experiment. This study first examined whether any differences in uptake existed between mannitol or mannose growth C1576 wild-type and mutant. There were no significant differences between any of the strains at the 2 hour time-point (Figure 3.6). There was some technical replicate-variation at this 2 hour time point for the wild-type – with one low value being an outlier (0.28 % survival) compared to the other two average percentage survival at 2 hours post-infection (1.25 and 3.78 %). This lower value outlier further suggests more exploration (possibly with fluorescent microscopy) into earlier uptake time points is needed to definitively pinpoint the potential role for EPS in uptake by macrophages. In a separate experiment where only input and 2 post-infection time points were taken with mannitol-grown bacteria, the wild-type in mannitol compared to the bceB CR in mannitol, resulted in a 0.11 % and 0.85 % uptake, respectively, suggesting that EPS did indeed impact on uptake in this instance relative to the mutant in mannitol. Overall, difficulties with reproducibility of this experiment would be greatly improved by using engineered aminoglycoside-sensitive strains, as outlined by Hamad *et al.* (86).

At 4 and 24 hours post infection, (post infection periods considered relevant to intracellular survival and growth), the C1576 wild-type grown in mannitol (EPS-inducing) was significantly different ($P < 0.05$) from all three other samples. Figure 3.6 indicates that all 4 strains grew intracellularly. The C1576 wild-type and bceB CR mutant grown in mannitol appear different in growth rate from 4 to 24 hours compared to the mannose grown strains. There was a 1.2-log increase in growth in both the mannitol-grown wild-type and *bceB* mutant, indicating an EPS-independent ability to replicate and survive within macrophages during these periods. In the mannose-grown wild-type and bceB CR mutant, only a 0.9-1-log increase in growth occurred between 4 and 24 hours post-infection. This suggests that mannitol promoted intracellular growth and survival relative to mannose. This leads to the conclusion that both wild-type and bceB CR strains growth equally well in mannose as in mannitol, hence the inclusion of mannose throughout phenotypic studies presented in this chapter.

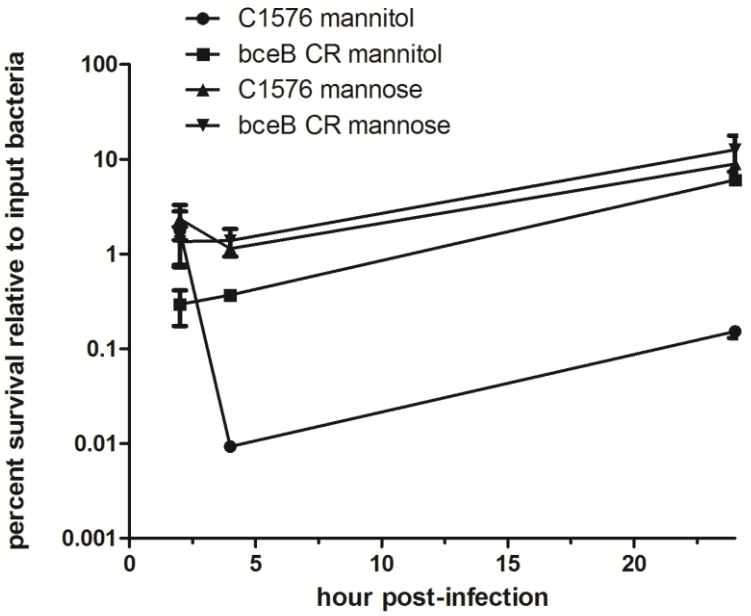

Figure 3.6 Macrophage uptake and survival assay with B. multivorans C1576 wild-type and bceB mutant. C1576 was grown in mannitol or mannose-yeast extract broths, then standardised and used to infect J774.1 murine macrophages. Chart shows representative average percentage survival from three wells per condition. 2, 4 and 24-hour time points were taken. Error bars represent standard error (SEM). Statistical significance (calculated by orthogonal contrasts using SPSS) exists at 4 and-24 hours post infection between the wild-type C1576 grown in mannitol and the three other conditions.

To improve upon the macrophage infection assay, the preference would have been to avoid high concentrations of ceftazadime and kanamycin which are routinely used in the literature for this type of assay. Hamad *et al.* reported a mutagenesis system for *B. cenocepacia* to create gentamicin sensitive mutants by deleting/inactivating a gentamicin efflux pump (86). The same approach was adapted for mutagenesis of *oprA* (gene involved in resistance to aminoglycosides e.g. gentamicin) in *B. multivorans* ATCC 17616 and C1576; however the process was unsuccessful after repeated attempts to obtain gentamicin sensitive mutants. Thus, this experiment was difficult to reproduce. In previous repeats of the macrophage infection assay, mannitol-grown wild-type and bceB CR mutant were relatively equal in uptake at two hours post infection, though on one other previous experiment, the mutant was increased

in uptake 3-fold relative to the wild-type grown in mannose. This initial uptake time point required optimisation. From previous repeats of the macrophage survival assay, at 24 hours post infection the C1576 bceB CR mutant grown in mannitol and mannose had a 9-10 % survival (relative to input), whilst the wild-type C1576 grown in mannitol and mannose had a 1.3-3 % survival (relative to input), respectively. These results contradicted the data presented in Figure 3.6 and again highlight the need for a reproducible system for modelling macrophage infection processes.

During optimisation of MOI for the macrophage survival assay, it was observed that an MOI of 40 resulted in ~ 5 % survival (relative to input) of both wild-type and bceB CR at 24 hours post infection (the only time point taken during optimisation). When the MOI was increased to 100 (an excessive load of bacteria per macrophage), 45 % survival of the mannitol-grown wild-type was observed. However, the mannitol-grown C1576 bceB CR mutant lysates replicated to 300 % relative to the input of bacteria. It is likely in this case that bacteria had been taken up, replicated, and then spread to surrounding cells within the monolayer. The monolayer was not entirely intact at this time point as viewed under bright field microscopy, indicative of bacterial lysis of the macrophages.

3.3.8 Growth in mannitol leads to protection from H_2O_2 induced oxidative stress

A hydrogen peroxide *in vitro* protection assay was used to determine the impact of sugars on protection from H_2O_2 induced stress. As described in the methods chapter, *B. multivorans* C1576 mannitol- or mannose-grown culture were standardised to an OD_{590} of 1 in PBS prior to exposure to 5 mM H_2O_2. Figure 3.7 depicts average percentage survival of *B. multivorans* wild-type and *bceB* mutant following exposure to 5 mM H_2O_2. Mannitol grown C1576 wild-type and *bceB* mutant survived treatment with H_2O_2 better than mannose grown. The C1576 *bceB* mutant grown in mannitol survived significantly less than the wild-type grown in mannitol. This indicates the mechanism for mannitol stress protection acts independent of EPS, although the presence of EPS may still play a role to some extent.

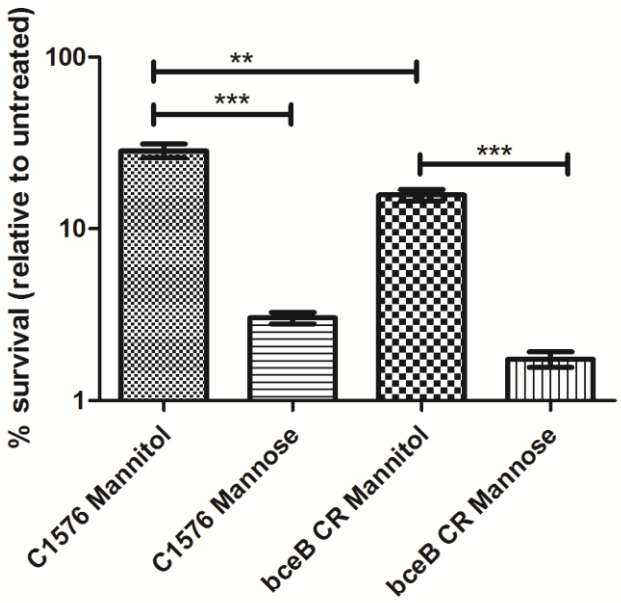

Figure 3.7. B. multivorans C1576 wild-type and bceB mutant grown in mannitol or mannose treated with 5 mM H_2O_2. Mannitol-grown C1576 wild-type and C1576 bceB CR mutant survived oxidative stress significantly better than mannose grown, whilst there still was a significant difference between the wild-type and bceB CR mutant in mannitol, indicating mannitol promotes survival by an EPS-dependent and –independent mechanism. The figure represents the mean of three wells per treatment (n=3). Error bars represent SEM and statistical significance was assessed using a 1-way ANOVA and post-tests. **P <0.005, ***P <0.0001

3.3.9 Invasion of A549 epithelial cells is EPS-independent

It has been shown previously that members of the Bcc are invasive to this cell line (32). Bacteria were grown in mannitol or mannose cultures and used to infect A549 epithelial cell monolayers (MOI 50). After 2 hours, extracellular bacteria were killed with antibiotic treatment. After an additional 2 hours monolayers were lysed using Triton-X 100. Lysates, containing bacteria that had successfully invaded A549 cells and survived antibiotic treatment, were plated for viable counts. Results in Figure 3.8 shows the mannitol-grown C1576 wild-type and *bceB* mutant invade A549 cells significantly better than when grown in mannose. Mannitol promoted invasion of A549 epithelial cells in an EPS- independent manner. Overall, it should be noted that invasion levels are

extremely low, however these results and significant differences were reproducible and thus deemed biologically relevant.

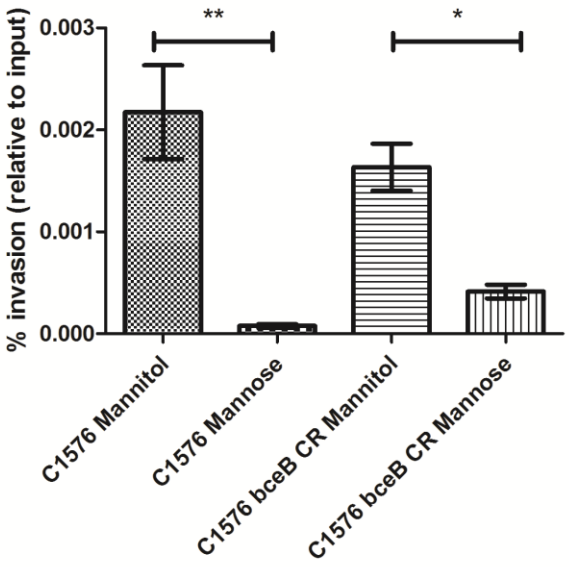

Figure 3.8. The impact of sugars on invasion of A549 lung epithelial cells. A549 lung epithelial cells were infected with mannitol- and mannose-grown *B. multivorans* C1576 (MOI 50). C1576 wild-type and bceB mutant was significantly more invasive when grown in mannitol compared to bacteria grown in mannose, indicating mannitol enhanced invasion was independent of EPS. Representative data from experiment repeated three times, bars are median of three wells (n=3) per strain and growth condition. * $P < 0.05$, ** $P < 0.005$, error bars represent SEM. Statistical significance was assessed using a 1-way ANOVA with post-tests.

3.3.10 Impact of mucoidy and sugars on abiotic adhesion is strain variable

3.3.10.1 The impact of EPS and sugars on adhesion to extracellular matrix proteins

The impact of mucoidy and sugars on the ability of *B. multivorans* to adhere to three different types of extracellular matrix (ECM) proteins was assessed, by coating the wells of polystyrene plate with fibronectin, laminin, or collagen (type II). After allowing bacteria to adhere to coated wells for two hours, no differences were detected in the crystal violet reading (as assessed by reading absorbance at 570 nm) between mannitol or mannose grown C1576 wild-type or *bceB* mutant (data not shown). These adhesion experiments were

optimised and repeated at least four times; no significant differences were observed.

3.3.10.2 The impact of EPS and sugars on adhesion to mucin

Next, the impact of mucoidy on adhesion to the glycoprotein mucin was assessed. Mucins are abundant in the mucus and CF respiratory tract and presence of mucin proteins are elevated in the lung during periods of pulmonary exacerbation. *B. multivorans* ATCC 17616 and C1576 *bceB* mutants were grown in mannitol or mannose. Cultures were standardised prior to application for three hours to mucin coated wells in a polystyrene plate. Wells were then washed 10x in PBS and protein/bacteria released from wells with Triton-X 100. Serial dilution of lysates onto LB agar allowed for calculation of viable CFU. The input and three hours post adhesion were used to calculate percentage adhesion.

In the mucin adhesion assay, *B. multivorans* ATCC 17616 adhesion was EPS-dependent. The wild-type in mannitol adhered significantly more than the wild-type in mannose and the mannitol grown *bceB* mutant (Figure 3.9(a)). Mannitol grown C1576 wild-type and *bceB* mutant (Figure 3.9 (b)) adhered significantly better than wild-type grown in mannose. This indicates C1576 adhesion to mucin is EPS-independent and that there is strain variation in mannitol promoted mucin adhesion, with mannitol having a broader positive effect on adhesion.

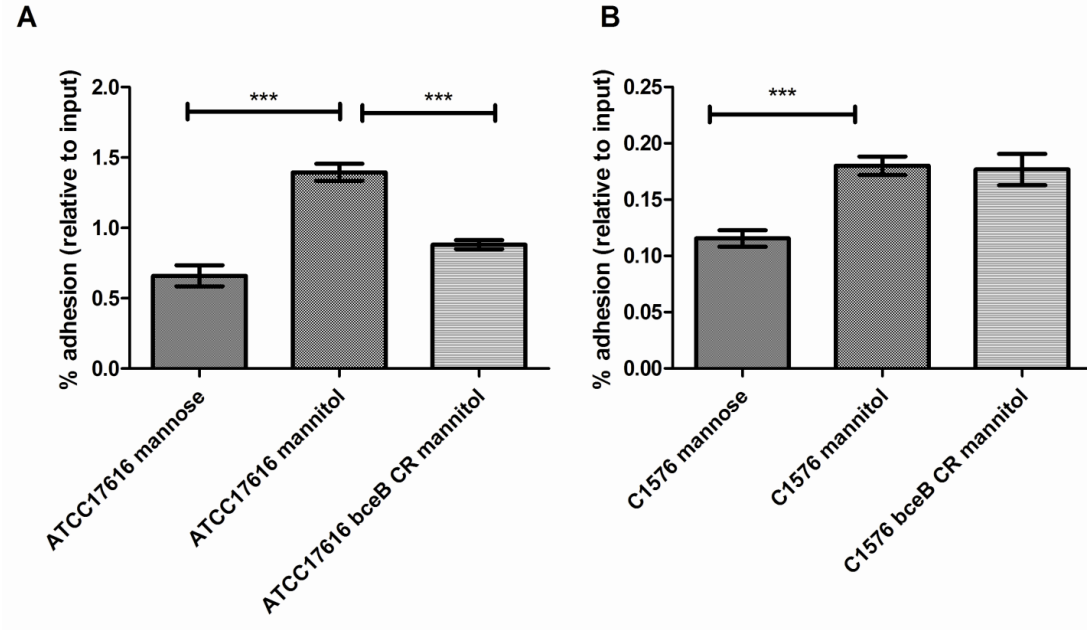

Figure 3.9. The role of EPS in promoting the adherence of B. multivorans to mucin is strain-dependent. Bacteria were grown overnight in mannitol or mannose-containing media, prior to adhesion to mucin-coated wells for 3 h. Following washing, adhered bacteria were enumerated by viable counts. Data correspond to mean of three independent experiments, each in triplicate. Error bars indicate SEM. *** $P < 0.0001$. (a) Adhesion of wild-type *B. multivorans* ATCC 17616 and the corresponding EPS-deficient *bceB* mutant. The enhanced adhesion of wild-type observed in the presence of mannitol is abolished in the bceB mutant, indicating it to be EPS-dependent. (b) Adhesion of *B. multivorans* C1576 and the corresponding EPS-deficient *bceB* mutant. The enhanced adhesion of wild-type in presence of mannitol is retained in the *bceB* mutant, indicating it to be EPS-independent.

These mucin adhesion results, and additional experiments where the characterisation of novel adhesins identified in *B. multivorans* C1576, will be described further in Chapter 5. Data shown in Figure 3.9 here, is re-presented in Chapter 5 as a means to re-iterate rationale for the sequencing and characterisation study.

3.4 Discussion

B. multivorans is now the most frequently isolated member of the Bcc in CF patients, however relatively little is known about the virulence and the role of EPS in this species. Results from the present study suggest EPS-dependent and EPS-independent phenotypes are apparent following growth on mannitol. This study focused on mannitol and mannose as models for other

mucoid (EPS-inducing) and non-mucoid (non EPS-inducing) sugars. To determine the actual impact of EPS production and growth mannitol had on the phenotypic behaviour of *B. multivorans*, an EPS-deficient mutant was made by insertional inactivation of the *bceB* gene, which encodes a glycosyltransferase within the *bce* EPS cluster. Virulence-related phenotypes assessed within this chapter were altered following growth in the presence of mannitol compared to mannose, and these phenotypes were largely EPS-independent. Throughout these experiments, the differentiation between EPS-dependent and -independent phenotypes was distinguished by using the *bceB* mutant.

Cumulatively, the phenotypic assays used to study *B. multivorans* in the present study showed the influence clinically relevant sugars have on virulence-related strategies and phenotypic behaviour of this opportunistic pathogen. The assessment of phenotypes, which were the focus of this study, would not have been attributable to EPS (EPS-dependent) or broader sugar effect (EPS-independent) without the inclusion of the *bceB* non-mucoid mutants. An EPS-deficient mutant has not previously been used to assess Bcc phenotypes and the association with mucoidy and EPS production, and therefore it is possible that previous studies outlining the impact of mucoidy on behaviour of the organisms have not taken into full account the broader impact the sugar plays on phenotypes such as motility and stress survival.

The present study demonstrated that inactivation of *bceB* eliminated EPS biosynthesis irrespective of the sugar or sugar alcohol present. This indicated that EPS pathways must be common in their response to different sugars, thus confirming the crucial role of the *bceB* gene and its protein product in biosynthesis of EPS in *B. multivorans*. In phenotypic studies, growth on mannitol enhanced motility, increased biofilm formation and invasion of A549 epithelial cells, and attenuated virulence in the *G. mellonella* insect model of infection. Crucially, these same observations were made in the wild-type and in the non-mucoid *bceB* mutant, indicating that these phenotypes are EPS-independent.

The present study found growth on mannitol (and to some degree EPS) promoted invasiveness to A549 epithelial cells. It was previously reported that *B. multivorans* and *B. cenocepacia* are invasive to A549 epithelial cells, and that lipase activity is linked to the ability to invade (140). In other cell lines, literatures suggested the production of EPS by the Bcc could functionally mask uptake and recognition by immune cells; however the present study observed no differences were observed between the C1576 mannitol-grown wild-type (mucoid) or *bceB* non-mucoid mutant at 2 hours post infection. At 4 and 24 hours post infection, it was observed that both strains in mannose and mannitol were able to survive and replicate in macrophages. At both 4 and 24 hours, the wild-type C1576 grown in mannitol was significantly different than the other samples.

Admittedly, due to difficulties in reproducibility and the intrinsically resistant nature of *Burkholderia* requiring high concentrations of antibiotics (to kill extracellular bacteria), it would be best for future experiments to utilise aminoglycoside-sensitive strains, created by a clean deletion of gentamicin-specific efflux pump genes (as described by Hamad *et al.* for *B. cenocepacia* (86)). The use of gentamicin-sensitive strains in conjunction with fluorescent confocal microscopy would be an ideal combination to further elucidate the role EPS in macrophage uptake and survival in *B. multivorans*. In the present study, attempts were made to generate gentamicin-sensitive *B. multivorans* strains, but this proved unsuccessful. It is possible that *B. multivorans* compensated for the deletion of one gentamicin efflux pump by activating others. Using confocal microscopy, it has been observed that members of the Bcc can survive and multiply in vesicles within macrophages for extended periods of time. These specialised vesicles have been termed *Burkholderia cepacia* containing vesicles (BcCV's) and were quantifiable using fluorescent confocal microscopy (109). Recent studies have reported *B. multivorans* co-localisation with lysozymes in BcCV's during 2-6 hours post-macrophage infection, though there was strain variation observed (172). A study including both microscopy and aminoglycoside-sensitive mutants could elucidate the mechanism of mannose- or mannitol-grown *B. multivorans* survival within macrophages at varying time

points, and confirm the significant difference at 4 and 24 hours between wild-type mannitol-grown (EPS-inducing growth condition) from other samples.

Since it is possible there are other gentamicin efflux pumps able to compensate for the loss in *B. multivorans,* it may require more than one gentamicin efflux pump clean deletion to create a gentamicin sensitive strain. Additionally, full assembly of the C1576 genome would also be of benefit for creating a gentamicin-sensitive CF isolate.

Abiotic adhesion to mucin was EPS-independent in the CF clinical isolate C1576. This EPS-independent adhesion could allow for a competitive advantage during pulmonary exacerbations in the CF lung, during which time mucin levels are elevated. The adhesion of the environmental strain ATCC 17616 was EPS-dependent, perhaps owing to its environmental lifestyle, where EPS is reported to play a role in adhesion and initial colonisation for many plant symbionts and pathogens (68). The EPS-independent adhesion of C1576 indicated variance between these two isolates from different sources. This variance was further explored by sequencing the CF isolate C1576. Subsequent analysis of the *de novo* assembled sequence and results on the study of novel adhesins identified and characterised are presented and discussed in Chapter 5. Furthermore, studies used to assess whether growth on different sugars and sugar alcohols influenced the transcriptional profiles of *B. multivorans*, and analysis of the EPS composition and biological activity following growth on mannitol and fructose are described and discussed in Chapters 4, 6 and 7, respectively.

Mannitol is a sugar alcohol formed by the reduction of mannose or fructose. It is involved in the bacterial catabolism pathway, where it serves as a source of fermentable sugar (191). The inhaled administration of the recommended 800 mg a day of mannitol as an osmolyte for CF patients or the use of mannitol-coated antibiotics (2,3) could impact the phenotypic behaviour of the organism. The clinical trials reported during development of inhaled mannitol have shown two weeks of treatment does not alter bacterial diversity or bacterial load. It is possible that administration of mannitol could put selective

pressure within the lung to select for loss of EPS production, potentially leading to a mucoid to non-mucoid transition and more aggressive infection. However, many of the phenotypes observed in *B. multivorans* wild-type and mutant were not dependent on the production of EPS but rather an effect of mannitol itself. The present study examined the impact of growth in mannitol and mannose on *B. multivorans* biofilms, and the impact of sugars on biofilm eradication by tobramycin, an aminoglycoside antibiotic. Findings showed mannitol promoted biofilm formation and survival against antimicrobial killing in an EPS-independent manner. Tobramycin is prescribed for the treatment of Bcc and *P. aeruginosa* CF respiratory infections, therefore the potential for EPS or mannitol to protect biofilms from eradication by antibiotic treatment is clinically relevant. Biofilms are implicated in chronic recurrent infections and are made of dormant cells and highly antibiotic resistant persister cells. It has been reported that mannitol enabled the eradication of bacterial persisters by aminoglycosides (6). Mannitol was used to activate *E. coli* persister cells prior to treatment with gentamicin, streptomycin, and kanamycin. This combination resulted in reduced persister cell survival and halted the spread of *E. coli* in the murine model of infection. The quinolones and β-lactam classes of antibiotics were not enhanced in bactericidal killing against isolated *E.coli* persister cells by mannitol, suggested mannitol specifically potentiated persister cell killing for aminoglycosides only. Allison *et al.* suggest the addition of mannitol or other metabolites could increase bactericidal effects of antibiotics against biofilms and persister cells, thereby improving eradication of chronic and recurrent infections (6). Based on these findings, it might be expected that growth in mannitol might enhance biofilm eradication by tobramycin through its actions on persister cells; however the present study found the opposite effect of enhanced biofilm survival following tobramycin exposure. The present study used mature biofilms grown on polystyrene pegs, which likely contained a more realistic mix of cell types, and therefore is more clinically relevant than an isolated population of persister cells.

Elevated sugars due to administration of inhaled mannitol, or glucose, (which is known to be elevated in diabetic airways (29)) could influence

phenotypic behaviour by increasing available carbon source in the airways, or by inducing EPS production. It seems prudent to monitor the impact of mannitol administration or the onset of CFRD on the microbiology and behaviour of the organism within the context of CF lung disease and CFRD management. This could be done by using YEM growth media to monitor for loss of mucoidy and link EPS with disease progression. An indication of whether the organisms had switched between a mucoid or non-mucoid phenotype over a period of colonisation could guide treatment options and predictability of infection outcome, although both host and bacterial factors would play roles. The administration of mannitol could promote the mucoid to non-mucoid transition by placing selective pressure on the metabolically expensive EPS biosynthesis process. Silva *et al.* showed that a non-mucoid *B. multivorans* isolate survived long-term nutrient deprivation better than a mucoid isolate, thus suggesting mucoidy could be a disadvantage to chronic infection where nutrient deprivation and stresses are encountered. The study also suggested that in the mucoid and non-mucoid CF isolate pair, taken 13 years apart, bacterial fitness had changed to survive in the CF lung by supressing EPS production ability and varying other phenotypic traits (178). This brings into question whether monitoring clinical isolates on YEM alone is enough for monitoring the broader potential for clinical impact of mannitol administration on the CF lung. It may be conducive to use the 96-well biofilm assay to assess if mannitol administration enhanced antibiotic resistance during or after the course of treatment.

The data from the present study suggest a role for mannitol in stress protection of *B. multivorans*. The evidence related to biofilm formation and antibiotic resistance, oxidative stress survival, as well as a role for motility are in agreement that mannitol benefits the organism, triggering phenotypic changes relevant to stress survival and virulence. The importance and role of EPS in the clinical lifestyle of *B. multivorans* and other members of the Bcc has been a topic of discussion in the literature. Zlosnik and colleagues suggested that a mucoid strain could be associated with a strain that favours a chronic attenuated infection (234). EPS-dependent and independent traits outlined in the present study could be linked to survival in the CF lung, where interactions

with phagocytes, community lifestyle within biofilms, and exposure to antibiotics and other stresses, are common.

Taken together, these data indicated inhaled mannitol could have potentially deleterious effects on the CF lung harbouring a *B. multivorans* infection. Sugars and sugar alcohols altered the behaviour of the organism and induced putative stress resistance and virulence-related phenotypic changes linked to persistence and chronic infection. Careful consideration when prescribing mannitol and watchfulness for any changes in bacterial phenotypes during and after mannitol treatment would aide guidance of treatment options and prediction of infection outcome.

3.5 Conclusions

1. The *bce* gene cluster plays a pivotal role in EPS biosynthesis in *B. multivorans*. Inactivation of *bceB* resulted in total loss of mucoidy on all sugars and sugar alcohols tested, which suggests commonality of EPS biosynthesis pathways.

2. There exists a wider role for mannitol in the behaviour and response of *B. multivorans* based on results from virulence related *in vitro* and *in vivo* phenotypic studies. The *bceB* isogenic mutant used in assays alongside wild-type EPS-producing strains allowed assignment of phenotypes as EPS-dependent or EPS-independent.

Chapter 4: Transcriptomic profiling of the *B. multivorans* sugar response

4.1 Introduction

To date, few gene expression studies have examined *B. multivorans*, and transcriptional profiling of the response to clinically relevant sugars and the determination of the molecular basis for EPS biosynthesis has not been performed. The present study used transcriptional profiling by two different methods, microarray and RNA-seq, to determine the *B. multivorans* whole genome sugar response to clinically relevant sugars fructose, mannitol (both EPS-inducing), mannose and glucose (non-EPS inducing). The present study describes the impact of clinically relevant sugars on mucoidy and gene expression of both an environmental *B. multivorans* isolate (ATCC 17616) and a CF isolate (C1576) in EPS and non-EPS inducing sugars.

Literature suggests a role for mucoidy in stress protection pertinent to chronic infection. A study by Silva *et al.* indicated motility, chemotaxis, biofilm formation, nitrogen metabolism; antibiotic resistance, membrane proteins, and secretion genes were altered in the transcriptome profile comparison of a *B. multivorans* clonal non-mucoid and mucoid isolates (178). Determining an organism's transcriptional response to growth on different clinically relevant sugars would reveal the underlying process of EPS biosynthesis and allow for interpretation of *B. multivorans* behaviour relevant to potential ramifications in the CF lung. The current study adopted a well-rounded approach to assess the nutritional cues for EPS and *B. multivorans* gene expression changes in response to clinically relevant sugars fructose, mannitol, mannose and glucose.

4.2 Aims

1. Use transcriptomic profiling methods (microarrays and RNA-seq), to examine the whole genome regulation of *B. multivorans* following growth on fructose, mannose, glucose, and mannitol. Identify commonalities with previously published transcriptome studies of Bcc and mucoidy and relate findings to Chapter 3 phenotypic studies.

2. Study EPS induced by differeing sugars/nutritional cues and the transcriptional response that results in EPS production in order to define the genetic basis for EPS production.

4.3 Results

4.3.1 Growth media used to investigate nutritional cues of EPS induction

Prior to selecting growth conditions for use in transcriptomic studies, the mucoidy of *B. multivorans* in a variety of nutritional conditions was assessed. It is well established that YEM induces mucoidy in the Bcc, but the molecular basis and genetic controls of EPS induction by mannitol or YEM or any specific nutritional cue is not known. Therefore the present study examined EPS induction in defined media with and without mannitol, as well as by modifying standard YEM by altering mannitol or yeast extract concentrations.

N-minimal media with 2 % (w/v) mannitol failed to support EPS production in *B. multivorans* even after 48 hours of growth. Synthetic Cystic Fibrosis sputum Media (SCFM) + 2 % (w/v) mannitol did induce EPS production of both *B. multivorans* ATCC 17616 and C1676 (Table 4.1).The impact of concentration of YE in the media whilst maintaining the sugar present at 2 % (w/v) was next assessed based on previous observations with N-minimal media that something in addition to mannitol was required for EPS-induction. Increasing the YE content of YEM from 0.2 % to 2 % (w/v) rendered *B. multivorans* non-mucoid. Thus this suggested there must be a nutritional deprivation or concentration gradient requirement to induce EPS biosynthesis. The impact of changing concentration of the EPS-induction sugar mannitol was assessed. The sugar agar YE concentration was held constant (0.2 % (w/v)), and mannitol concentration varied from 0.25 %-2 % (w/v). At 0.25 % (w/v) mannitol, *B. multivorans* still produced EPS produced, therefore, for ATCC 17616 microarrays the lower reduced 0.25 % (w/v) mannitol (reduced YEM) was used and compared to the standard YEM media. This comparison was used to identify any dose-dependent whole genome responses to mannitol.

As previously highlighted in Chapter 3, D-glucose and D-galactose did not support robust growth in *B. multivorans* when used to supplement 0.2 (w/v) YE. When the YE was increased in the media to 2 % (w/v) with 2 % (w/v) D-glucose growth was robust. The comparison between this D-glucose containing media (YEG) and non-mucoid YEM is the only comparison made with D-glucose where

the only difference in the media is the sugar. Genes differentially expressed were in response to glucose or mannitol rather than EPS production.

Table 4.1. B. multivorans growth on different media alters mucoidy. *B. multivorans* ATCC 17616 and C1576 mucoidy was scored as '+' if EPS was visibly produced, and '-' if non-mucoid. YE, yeast extract. SCFM, synthetic cystic fibrosis media (made as described by Palmer et al.). *No observed growth defect in glucose (YEG).

Media	YE conc. (% w/v)	Sugar conc. (% w/v)	Mucoidy
YE/SUGAR MEDIA			
Non-mucoid YEM	2	2	-
Reduced YEM	0.2	0.25	+
YEG*	2	2	-
YEM	0.2	2	+
YEF	0.2	2	+
YEO	0.2	2	-
OTHER MEDIA			
N-minimal + Mannitol	n/a	2	-
SCFM* + Mannitol	n/a	2	+

*Palmer *et al.* (149)

Thus, growth media chosen for transcriptional profiling based on these studies of the nutritional cues for EPS production included, for microarray growth conditions, EPS-inducing D-fructose (YEF) and two concentrations of mannitol (0.25 % (w/v) 'reduced YEM') and standard YEM. The non-mucoid control used in the microarray studies was mannose (YEO). Cardiff University collaborators had designed an Agilent custom ATCC 17616 4 x 44K microarray platform, which restricted use to the environmental ATCC 17616 isolate.

The use of the clinical isolate without a fully annotated reference genome was possible using RNA-seq. Growth conditions for *B. multivorans* C1576 RNA-seq analysis included two mannitol-containing growth media: standard YEM and non-mucoid YEM. YEO, and YEG, were also included.

These different growth conditions enabled comparisons and whole genome expression analysis of the *B. multivorans* sugar response. Comparisons were made between growth conditions that were altered in only sugar content. Though it would seem more clinically relevant to utilised SCFM media with or without the clinically relevant sugars in this study, the aim was to fundamentally assess the underlying transcriptional controls of EPS production to assess the whole genome response to clinically relevant sugars. Thus, the growth media commonly used to induce EPS (YEM) and variation of this media was adopted for transcriptional profiling (Table 4.1).

4.3.2 Transcriptional profiling sample quality control

Quality control of data obtained from the microarray study was assessed using GeneSpring GX software version 7.3.1, by Dr. Andrea Sass (formerly of Cardiff University, presently of University of Ghent). *B. multivorans* ATCC 17616 microarray replicate samples were clustered for similarity (Figure 4.1). The mucoid fructose and mannitol samples clustered together, and mannose and the lower percentage of mannitol are separate in the tree hierarchy. This analysis, and raw data processing, expression analysis and statistical tests were generated by GeneSpring software. Lists of significantly differentially expressed genes were analysed using Microsoft Excel.

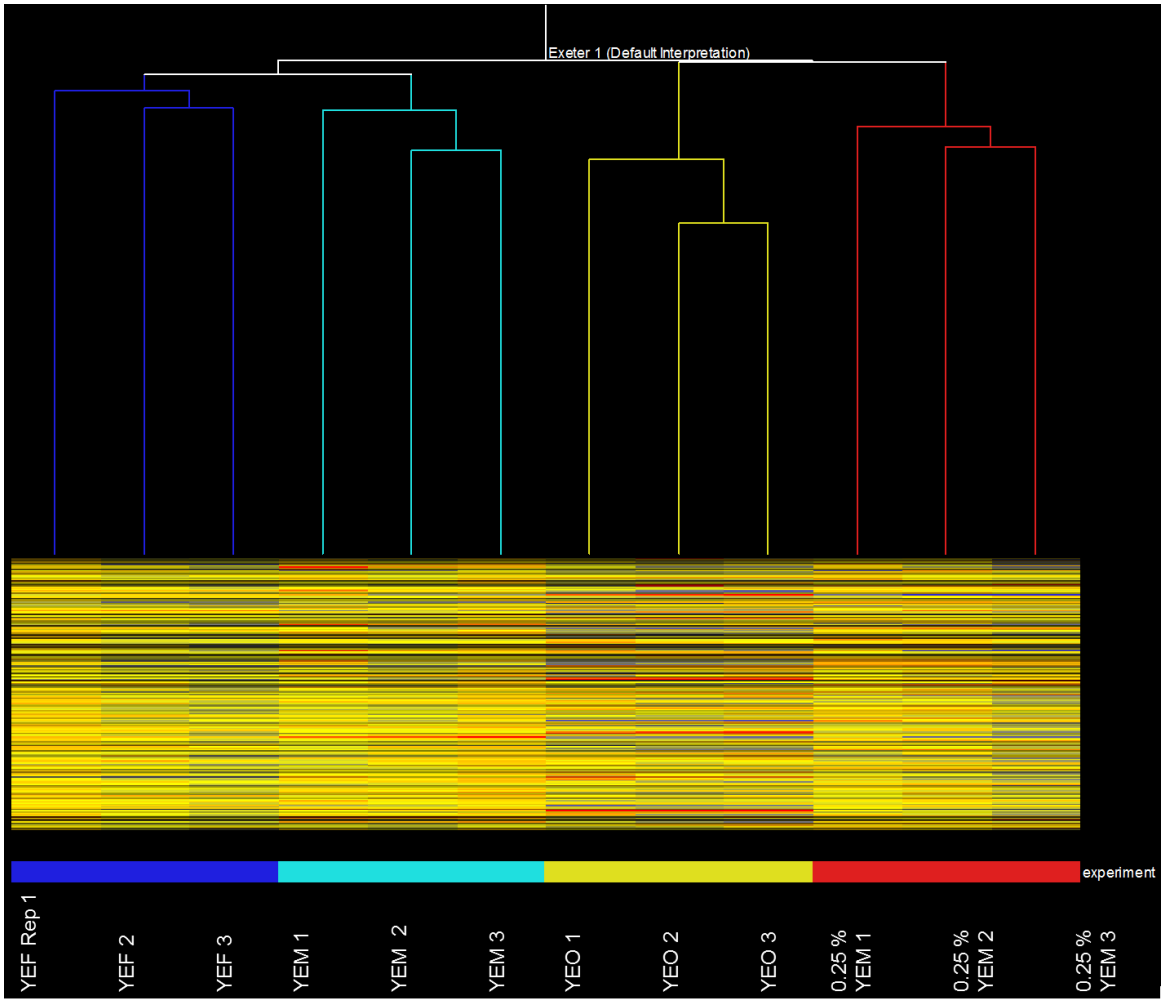

Figure 4.1. B. multivorans ATCC 17616 microarray biological replicates. The samples clustered together by growth conditions, with mucoid conditions D-fructose (YEF) and the higher concentration of D-mannitol (YEM) more closely related on the tree than reduced YEM and D-mannose (YEO). Clustering was based on sample and default settings on GeneSpring GX software version 7.3.1 expression analysis software.

All microarray data, fold changes and p-values of gene lists can be found in the Appendix CD. Microarray differentially expressed genes with a less than 1.5-fold-change were excluded from statistical analysis. Data significance was achieved by 1-way ANOVA analysis. Intergenic (IG) regions were excluded in the microarray gene expression analysis.

In Figure 4.2, hierarchical clustering of RNA-seq samples is shown. During quality control of RNA-seq data, it become clear through principal component analysis using a projection scatter plots, as well as RPKM values, that only 2/3

biological replicates per condition should be carried forward for further analysis. Reasons for these dissimilarities between the remaining biological replicates have not been identified, but outliers were excluded to prevent skewing of data. Thus, two biological replicates per growth condition were used for statistical analysis and data presented in following discussion are based on four pair-wise sample comparisons. The YEM, YEG and non-mucoid YEM growth conditions clustered on a branch separate from the YEO samples, but pairs of samples from different growth conditions were still distinct. RNA-seq data was analysed with CLC Genomics Workbench expression analysis software (CLC bio). Each pairwise comparison was followed by statistical testing using Kals' test and post-tests with FDR-adjusted p-values. The ATCC 17616 reference genome was used to map C1576 RNA-seq reads. Future research will also include mapping RNA-seq reads to the *B. multivorans* CGD1 reference genome, and further assessing the C1576 transcriptional response with a larger sample size.

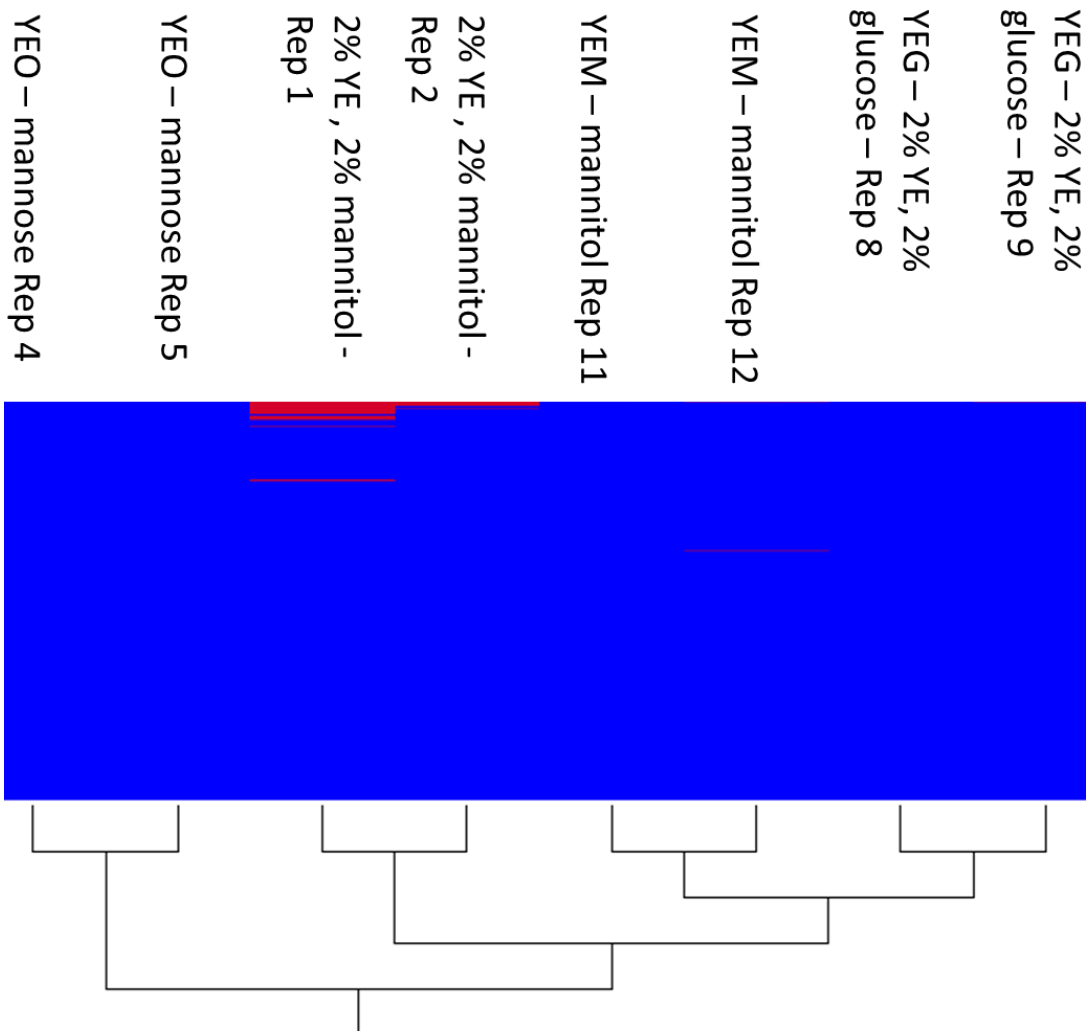

Figure 4.2. B. multivorans C1576 RNA-seq biological replicates. Hierarchical cluster generated by CLC Genomics workbench (CLC bio) for sample quality control prior to expression analysis. Non-mucoid growth conditions: YEO, non-mucoid YEM and YEG. Mucoid condition: YEM. Two biological replicates (Rep) per sample and pair-wise comparisons were carried forward for statistical analysis.

Genes in the RNA-seq data not significantly differentially regulated were not included in any further analysis. Significantly regulated genes common to all pairwise comparison from biological replicates were identified and used for data analysis. Complete gene lists of significant differentially expressed genes and raw data from the RNA-seq study are included in the Appendix CD.

4.3.3 Transcriptome distribution of global differential gene expression

The number of genes differentially transcribed in *B. multivorans* ATCC 17616 and C1576 from the transcriptome studies are listed in Table 4.2.

Table 4.2 B. multivorans global gene expression in response to growth on different sugars. *B. multivorans* ATCC 17616 and C1576 differentially expressed genes but there were overall fewer genes differentially expressed in C1576 likely due to the variability between samples. Two biological replicates per growth condition were used for RNA-seq analysis. 'vs.' indicates genes differentially regulated in the first growth condition relative to the second.

***B. multivorans* growth condition**	**Number of genes significantly altered in gene expression**		
	Upregulated	**Downregulated**	**Total**
ATCC 17616 Microarray			
YEM vs. YEO	825	647	1472
Reduced YEM vs. YEO	886	738	1624
YEF vs. YEO	804	792	1596
Common genes mucoid vs. YEO	386	420	806
C1576 RNA-seq			
YEM vs. YEO	86	36	122
YEG vs. non-mucoid YEM	8	266	274
YEM vs. non-mucoid YEM	68	436	504

In order to define the impacts of clinically relevant sugars on gene expression in mucoid (EPS-inducing) and non-mucoid growth conditions, transcriptional profiling was performed in growth conditions outlined in Table 4.2. Overall, the three mucoid growth conditions used for ATCC 17616 microarray, there were 386 commonly upregulated genes and 420 commonly down regulated genes. There were a much greater number of differentially expressed genes in the microarray dataset than in the RNA-seq data set. This is likely due to the variance between RNA-seq samples forcing the use of only two biological replicates per growth condition and thus fewer genes were deemed statistically significant. In the RNA-seq analysis, there were 86 upregulated genes in YEM vs. YEO, and 36 downregulated. Appendix Table 9.6 lists common genes to C1576 YEM vs. YEO, and all three ATCC 17616 mucoid

conditions vs. YEO. The conditions resulted in 39 differentially expressed genes. Of these 39 genes, only three showed differential regulation between strains (being upregulated in C1576 and downregulated in ATCC 17616), indicating minimal strain variation during growth in mucoid-growth conditions.

4.3.4 B. multivorans global gene expression of EPS biosynthetic genes

Due to the mucoid *B. multivorans* phenotype during growth on mannitol and fructose, it was predicted that EPS genes such as the *bce* cluster, would be upregulated in *B. multivorans* strains following growth on EPS-inducing sugars. As expected, in the YEM vs. YEO C1576 RNA-seq data set, 6 *bce* EPS cluster genes were highly upregulated in YEM relative to YEO. Several *bce* genes in YEM relative to non-mucoid YEM comparison were upregulated as expected (Table 9.7). C1576 RNA-seq data from the YEM relative to YEO growth condition was validated by quantitative real-time PCR (qRT-PCR) and showed a 193-fold upregulation in *bceB*. It is clear from this data that the *bce* cluster is involved in C1576 mannitol-induced EPS production. In contrast, microarray results indicated key EPS cluster genes in ATCC 17616 YEM and YEF relative to non-mucoid YEO were not upregulated (although many genes in the *bce* cluster were expressed) (Appendix Table 9.8). ATCC 17616, like C1576, was visibly mucoid during growth on reduced YEM, standard YEM, and YEF agar plates. Results from, Chapter 3 indicated ATCC 17616 and C1576 require *bceB* for the production of EPS on all sugars tested, indicating a common pathway connecting Bcc EPS biosynthesis. Results from this study showed no upregulation of known EPS genes was observed in ATCC 17616, including the *bce* cluster. Thus, EPS production in ATCC 17616 is not via upregulation of the *bce* or *wcb* EPS clusters. The downregulation of *bceB* ATCC 17616 microarray results was validated using qRT-PCR. Results showed ATCC 17616 in YEM (relative to YEO) downregulated *bceB* 14-fold.

There were several genes of EPS clusters first identified in *B. cenocepacia*, which have orthologs in *B. multivorans* ATCC 17616 that could be responsible at least in part for EPS production. Nine different genes related to these alternative EPS clusters were upregulated in ATCC 1716 YEM vs. YEO growth conditions, and eight were upregulated in YEF vs. YEO comparison. Of

those upregulated genes from the two growth conditions, seven were commonly upregulated in mannitol and fructose. Their putative roles included peptidoglycan glycosyltransferase activity, transcriptional regulators, and ABC transporters. In ATCC 17616 mucoid YEF and YEM relative to YEO both Bmul_4113 (a putative polyphosphate kinase) and Bmul_4390 (a Crp/FNA family transcriptional regulator) were downregulated. In contrast, both genes were upregulated in C1576 (Table 9.7), thus showing the same trend as the *bce* cluster in which ATCC 17616 varies from C1576 in genes used for EPS production. Of note is the general expression, but not differential expression, of the *bce* cluster in ATCC 17616. Therefore the cluster could still play a role in EPS production, as evidenced by the ATCC 17616 *bceB* mutant being non-mucoid on all sugars (refer to Chapter 3 Results).

In the ATCC 17616 15 different *bce* cluster genes were upregulated in YEF relative to YEM comparison. This was interesting, because neither the YEF nor YEM vs. YEO comparisons individually upregulated *bce* genes (as discussed above). This suggested these EPS-inducing sugars are not equal in their impact on EPS gene expression. Due to differences between different EPS-inducing carbon sources, and the fact that Bcc studies exclusively use mannitol to induce EPS biosynthesis, the potential for differences between *B. multivorans* ATCC 17616 and C1576 fructose-or mannitol-derived EPS composition and biological activity are assessed as part of this dissertation. Results from those studies are presented and discussed in Chapters 6 and 7, respectively.

4.3.5 Genes involved in cell wall integrity and permeability

Cell wall integrity and permeability are important for maintaining bacterial survival and success in the host environment, as well as the allowance for secretion systems for the export of virulence proteins and adhesive structures. The reduction in outer membrane proteins is an important adaption to maintain the impermeability of the outer membrane and improve antibiotic resistance in Gram-negative bacteria (10).

Differential expression of outer-membrane protein coding genes in the *B. multivorans* ATCC 17616 and C1576 are listed in the Appendix Table 9.9 and 9.10, respectively. Porin genes differentially expressed in ATCC 17616 mannitol and fructose vs. YEO were generally downregulated. This overall decreased expression in ATCC 17616 outer-membrane protein-encoding genes is suggestive of a less permeable outer membrane structure in EPS-inducing growth conditions, which could indicate an antibiotic resistant adaption. If grown in YEM, which results in downregulation of eight different porin- encoding genes in ATCC 17616, this could explain the enhanced resistance to tobramycin observed for mannitol-grown ATCC 17616 biofilms previously discussed in Chapter 3. In contrast to the *B. multivorans* ATCC 17616 microarray study, whilst three porin-encoding genes showed differential expression in C1576 under YEG relative to non-mucoid YEM, none were differentially expressed in YEM relative to YEO, suggesting strain-to-strain variation.

4.3.6 Differential regulation of transcription and signal transduction genes

Aside from the potential for EPS-producing strains differing in their membrane integrity, altering the carbon source for growth also altered the expression of large numbers of transcriptional regulators in the ATCC 17616 microarray and RNA-seq data sets, suggesting a major rewiring of *B. multivorans* transcriptional networks as part of the whole-genome response to different sugars contained in the growth media. Of keen interest to this study was to identify regulators highly enhanced in expression in all mucoid growth conditions relative to non-mucoid.

The ATCC 17616 transcriptional regulators enhanced in expression are listed in Appendix Tables 9.11 and those differentially expressed in growth conditions of interest for C1576 in Table 9.12. These tables are not all-inclusive- they list the most upregulated or common transcriptional regulators genes from growth conditions of interest. Two LysR family of transcriptional regulators, (Bmul_2557 and Bmul_5074), an AraC transcriptional regulator (Bmul_3782), and the TetR transcriptional regulator (Bmul_4689) were commonly regulated in

all the mucoid vs. YEO ATCC 17616 microarray data sets. In the C1576 RNA-seq data, although not significant in all pairwise comparisons (and thus not included in Table 9.11), it was noted that Bmul_2557 was enhanced in expression in 2/4 YEM vs. Non-mucoid YEM pair-wise comparisons, suggesting this regulator could be linked to mannitol-based induction of EPS, although further validation is required. Had time allowed, these regulators enhanced in expression common to both strains' transcriptome profiling data would have been pursued using molecular mutagenesis techniques. Currently, without knowing the targets of these regulators, it is difficult speculate what impact their differential regulation has on the behaviour of the organism.

Of note, concerning motility is the upregulation in ATCC 17616 YEM vs. YEO of the flagella transcriptional activators *flhC*, *flhD*, and *flgM*. This is detailed as part of the flagella assembly pathway in Figure 4.5.

4.3.7 B. multivorans differential expression of motility genes

Transcriptomic profiling revealed altered gene expression related to motility and chemotaxis in EPS-inducing conditions in the two *B. multivorans* isolates. Phenotypic studies showed mannitol-enhanced motility in wild-type ATCC 17616 and C1576 and the corresponding non-mucoid *bceB* mutants (Chapter 3, Figure 3.6). This mannitol-enhanced motility was EPS-independent thus the impact on motility was due to effects of mannitol. The ATCC 17616 microarray data, motility genes were upregulated in mucoid growth conditions relative to YEO (Figure 4.3 (a), and Appendix Table 9.13). This observation correlated with phenotypic studies from Chapter three which showed mannitol enhanced motility relative to mannose. Figure 4.3 (b) shows that fructose enhanced motility, but not to the same extent as mannitol. In accordance with the phenotypic study, the microarray data showed YEF vs. YEO upregulated fewer motility related genes compared to the YEM vs. YEO (Appendix, Table 9.12). In the reduced YEM vs. YEO fewer motility-related genes were upregulated compared to YEM, suggesting that mannitol-enhanced motility is dependent on the concentration of mannitol. Bmul_0162 (*motA*) and its

enhanced expression in the ATCC 17616 microarrays was validated by qRT-PCR - *motA* was upregulated 8-fold in YEM vs. YEO and 4-fold in YEF relative to non-mucoid YEO.

(a)

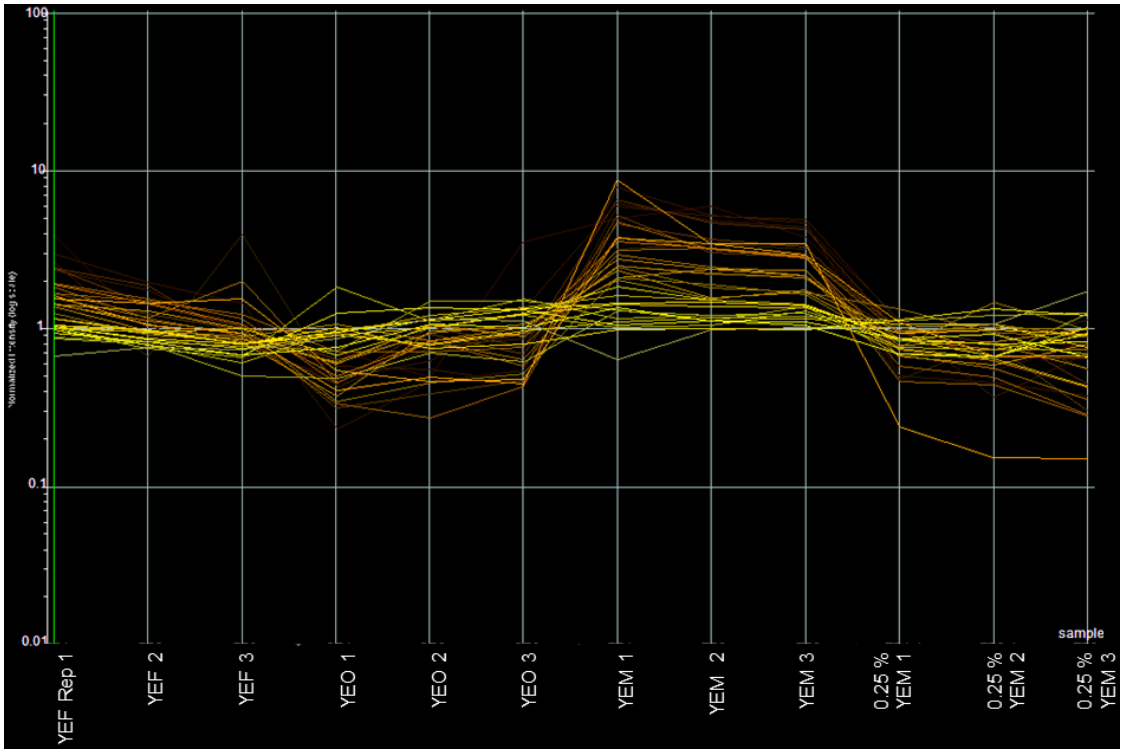

Figure 4.3 (a). Differences between carbon sources in enhancement of motility. GeneSpring display shows on the x-axis, sample/growth conditions, relative to (log) intensity normalised expression of *B. multivorans* ATCC 17616 flagella-related genes significantly differentially expressed in the microarray data set (36 selected genes in total). Most upregulated flagella genes were in YEM, corroborated by phenotypic studies and qRT-PCR. Values above one are upregulated, below one are downregulated.

(b)

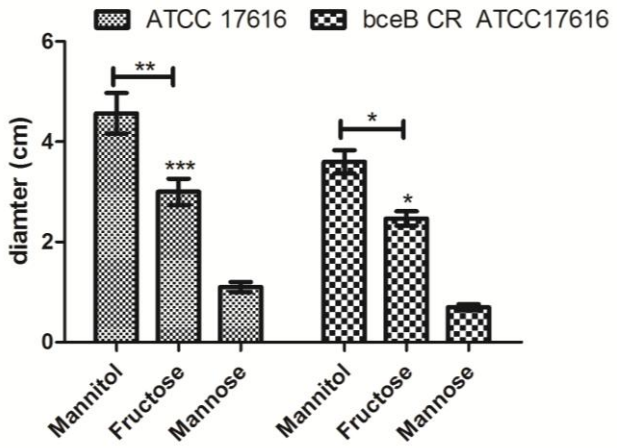

Figure 4.3 (b). Phenotypic study corroborates significant mannitol enhanced motility more than motility enhanced in fructose. This same data set presented in Chapter 3 (without the fructose motility data), which showed significant differences between mannitol and mannose in both the wild-type and bceB CR mutant. Asterisks with bars indicate mannitol enhanced motility relative to fructose, and asterisks alone are significant upregulation of motility in fructose relative to mannose.

Chemotaxis genes were altered in the *B. multivorans* ATCC 17616 data set that are involved in the pathway leading on to flagella biosynthesis. Figure 4.4 shows in green chemotaxis genes upregulated in ATCC 17616 YEF vs. YEO, but *cheW*, *cheZ* and *MotA/B* were also upregulated in YEM relative to YEO. *MotA/B* were downregulated in the C1576 YEG relative to non-mucoid YEM comparison.

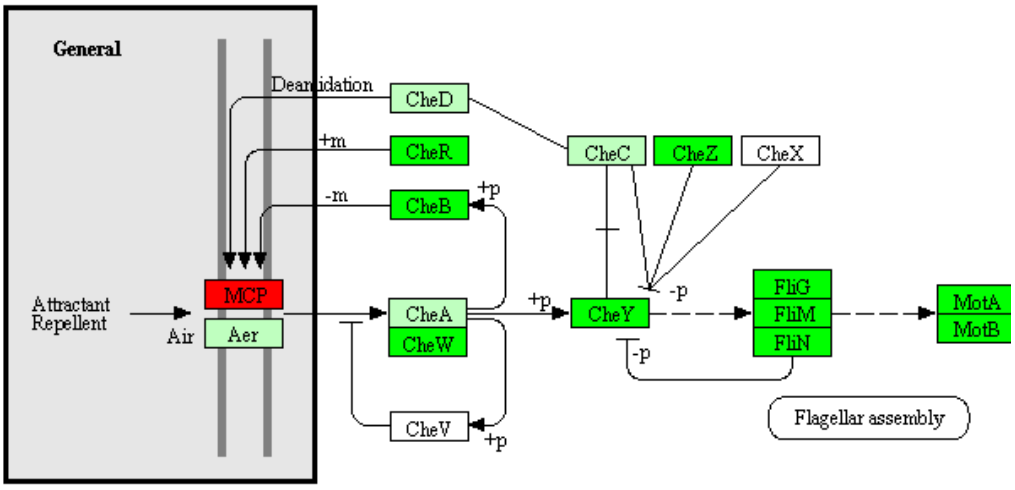

Figure 4.4 B. multivorans genes involved in bacterial chemotaxis. This pathway leads on to flagella biosynthesis which is summarised in Figure 4.5. In the *B. multivorans* ATCC 17616 YEF vs. YEO data set, red boxes show genes downregulated; dark green boxes indicate upregulation, light green boxes indicate organism specific pathways but lack of differential expression, and white boxes show genes with no orthologue in *B. multivorans* but are involved in the pathway in other organisms. This figure was made using KEGG Mapper Search&Color pathway. Reference organism selected *was B. multivorans* ATCC 17616 (JGI).

Figure 4.5 summarises the flagella assembly pathway and the differentially expressed genes in YEF relative to YEO growth conditions from the transcriptome profiling of ATCC 17616. Although YEF vs. YEO differentially regulate genes are shown, there were many similarities between the two mucoid growth conditions and their upregulation of motility genes.

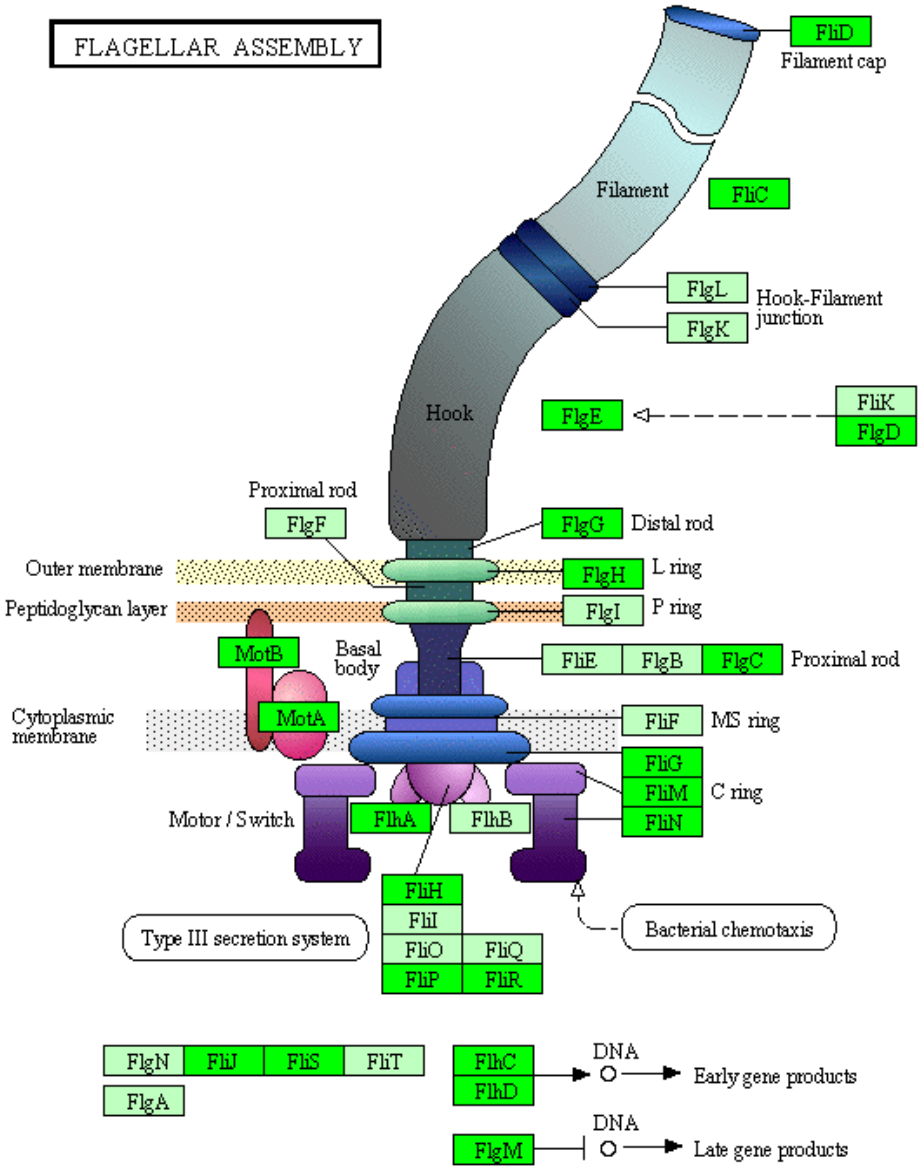

Figure 4.5. B. multivorans ATCC 17616 flagella assembly pathway. Dark green boxes indicate a gene is upregulated in ATCC 17616 YEM vs. YEO data sets, whilst light green boxes indicate no significant differential expression. The majority of these genes were also upregulated in YEF vs. YEO. This figure was made using KEGG Mapper Search&Color pathway. Reference organism selected was *B. multivorans* ATCC 17616 (JGI). See Appendix Table 9.13 and 9.14 for further details of ATCC 17616 and C1576 differentially regulated flagella-related genes and fold changes.

Mannitol- and fructose-enhanced motility in ATCC 17616 and C1576 wild-type and *bceB* CR mutants was shown in phenotypic studies. This data indicated C1576 was more motile in mannitol than ATCC 17616, indicating strain

variation. However, flagella synthesis and regulator genes were not observed in the C1576 YEM vs. YEO RNA-seq significantly expressed genes, though there were some genes relating to flagella biosynthesis and chemotaxis differentially regulated in YEM vs. non-mucoid YEM (Table 9.14). This highlights the need for further transcriptional analysis of C1576, which was hampered by variation between replicates and resulted in only two replicates per growth condition. Cases where variation between the two strains is observed over an entire pathway and contradicts phenotypic data, highlights it would be worth reassessing the C1576 transcriptional response to validate these observations.

4.3.8 Differential expression of genes related nitrogen metabolism

Differential expression of nitrogen metabolism during growth on EPS-inducing and non-inducing sugars could indicate alternative energy pathways or anaerobic metabolism is being utilised (178). Appendix Tables 9.15 and 9.16 present genes pertinent to nitrogen metabolism and assimilation from the ATCC 17616 microarray and C1576 RNA-seq data, respectively. In the ATCC 17616 YEF vs. YEO microarray data, nitrate reductase-encoding genes *narG* and *narH* were upregulated, along with decreased expression of several nitrate ABC transporters. Genes connected to nitrogen metabolism are likely connected to anaerobic metabolism by reduction of nitrate and upregulation of genes such as these have been linked to *B. pseudomallei* survival within macrophages and *B. multivorans* adaption to the CF lung (43,178). Two genes related to nitrogen metabolism were also identified in the C1576 RNA-seq data; these genes were linked to metabolism and secondary metabolite biosynthesis.

4.3.9 B. multivorans secretion genes differentially expressed following growth on different sugars

The C1576 RNA-seq YEG vs. non-mucoid YEM comparison resulted in a group of secretion genes decreased in expression, suggesting protein export and secretion via the Sec pathway was altered during growth on different

carbon sources. Figure 4.6 summarises the roles of these genes in protein secretion and export (details in Appendix Table 9.17).

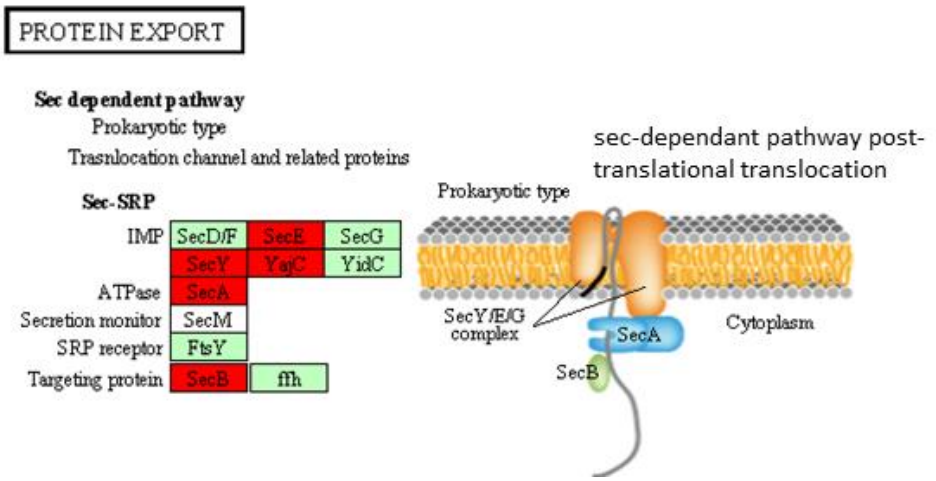

Figure 4.6 B. multivorans C1576 secretion genes. YEG vs. non-mucoid YEM growth conditions from the C1576 RNA-seq data resulted in decreased expression of genes related to the Sec protein export pathway. Light green boxes were not differentially expressed in the C1576 data set, while red boxes indicate gene was decreased in expression, and white boxes are genes in pathway without orthologues in *B. multivorans*. This figure was made using KEGG Mapper Search&Color pathway. Reference organism selected was *B. multivorans* ATCC 17616 (JGI). See Appendix Table 9.17 and 9.18 for further details of C1576 and ATCC 17616 differentially regulated secretion-related genes and accompanying fold changes.

Whilst there were secretion-related genes altered in expression in the ATCC 17616 microarray data set, (Appendix Table 9.18), including the upregulation of two different Vrg family Type VI secretion genes in the YEM and YEF relative to YEO comparisons, no distinct single secretion pathway was altered as was observed in C1576. It has been shown in *B. pseudomallei* that type six secretion genes are upregulated during macrophage infection (43). This indicates growth on different EPS-inducing sugars does not significantly alter protein secretion and export in ATCC 17616 for the conditions profiled in the present study.

4.3.10 Expression of antibiotic resistance-related genes

In the RNA-seq C1576 data, no differentially expressed antibiotic-resistance-related genes were observed in growth conditions of interest. In the ATCC 17616 microarray study, YEF and YEM relative to YEO comparisons resulted in five antibiotic resistance-related genes commonly regulated these EPS-inducing conditions (Appendix Table 9.19). The ATCC 17616 YEF vs. YEO resulted in three β-lactamase domain-containing proteins enhanced in expression. The reduced YEM growth condition (not listed in table) did not differ significantly in the regulation of antibiotic resistance-related genes relative to standard YEM, indicating no strong correlation between antibiotic resistance-related genes and mannitol dosage. General trends appear to be focused on the downregulation of RND efflux systems and several ABC transporters linked to antibiotic transport mechanisms in these mucoid conditions. In all, YEM conditions resulted in the downregulated of 15 different antibiotic-resistance genes, while the YEF growth condition 13 different resistance genes (all relative to non-mucoid control YEO). Of the seven RND efflux pump proteins downregulated, six were downregulated. The importance of RND efflux transporters has been discussed in a transcriptome analysis of *B. cenocepacia*, which showed a role for these pumps was much wider than just drug resistance, but also influenced biofilms formation and other traits relevant to pathogenesis (19).

4.3.11 B. multivorans differential expression of metabolism-related genes

It would be expected that different carbon sources used for growth and stimulation of EPS-production could elicit central carbohydrate metabolism pathways, as possibly differential impacts on metabolism and other secondary metabolism processes. In the ATCC 17616 mucoid growth conditions relative to YEO data sets, genes encoding products involved in fructose and mannose metabolism and the pentose phosphate pathway were found to be differentially expressed (Table 9.20). However, there were differences between mucoid growth conditions. ATCC 17616 upregulated fructose/mannose/pentose phosphate metabolism and synthesis pathways in YEF relative to YEO but not

in the YEM relative to YEO. In the ATCC 17616 reduced YEM relative to YEO data set are a plethora of glutathione metabolism-related genes (linked to nitrogen assimilation and metabolism) which could indicate reduction of the main carbon source mannitol results in altered metabolic pathways seeking alternative energy sources due to decreased carbon availability.

In the ATCC 17616 YEF relative to YEO comparison is a cluster of upregulated succinate dehydrogenase/fumarate reductase activity. These genes, *sdhC*, *sdhD* and *sdhB* are involved in oxidative phosphorylation and metabolic processes related to the TCA cycle (based on KEGG pathway predictions) and these genes encode proteins closely associated in a complex with flavo proteins and iron containing proteins involved in electron transport and oxidative phosphorylation. This indicates fructose metabolism impacted the organism differently than mannitol, as these genes were differentially regulated in the YEF relative to YEO comparison, but absent in the YEM relative to YEO comparison.

Another upregulated gene of note in the YEF relative to YEO data (but absent in the YEM vs. YEO comparison) is the gene encoding *cstA*, a peptide transporter shown to be induced by carbon starvation and the global regulator *csrA* in *E. coli* (65,174). Again, it is interesting this gene was enhanced in expression in the YEF conditions relative to YEO but not in YEM relative to YEO.

In the C1576 RNA-seq data set genes involved in monosaccharide transport were downregulated – including several ABC transporters involved in polyol and monosaccharide transport, most notably in the YEG vs. non-mucoid YEM where genes differentially expressed then will represent the organisms' specific response to glucose or mannitol rather than EPS or nutrient deprivation (Appendix Table 9.21). Of note are the group of genes *rbsA*, *rbsB*, and *rbsC* all decreased in expression in YEG relative to non-mucoid YEM; in *Haemophilus influenzae* these genes have been linked to quorum signal uptake, mature biofilms formation, and are linked to chemotaxis (9). Another group of genes downregulated in the YEG vs. non-mucoid YEM data encoding binding-protein

dependent inner membrane transport system are Bmul_2428, Bmul_2429 and Bmul_2430. These three genes appear to be part of an operon involved in transport and orthologues in *B. mallei* are annotated as encoding maltose-binding and transporting proteins.

4.3.12 Mucoid growth conditions and differential expression of genes related to adhesion

Transcriptomic data was assessed for any adhesin-related gene expression to add to the Chapter 3 observations of mucin adhesion variation between the two *B. multivorans* strains in this study. Phenotypic studies had previously shown EPS-dependent adhesion in the environmental isolate ATCC 17616. In the ATCC 17616 microarray data, downregulation of a fimbrial biogenesis usher protein was observed in YEM vs. YEO (Table 9.22). In all mucoid vs. non-mucoid *B. multivorans* ATCC 17616 and C1576 data is the gene Bmul_3709, encoding a haemolysin-type calcium-binding region protein that has been well-characterised in other members of the Bcc as a 22kDa adhesin (*adhA*) associated with a cable pilus required for *B. cenocepacia* binding and transmigration across epithelial cells and linked to persistence (77,201). The calcium-binding region contained in *adhA* has been linked to other secreted proteins involved in protein re-folding after transport across the cell membrane and has been reported to facilitate protease activity in *P. aeruginosa* and to binding of erythrocytes by *E.coli* (18,123). Bmul_3709 has orthologues in 13 other *Burkholderia* species, according to genomes available on burkholderia.com, and 82 % homologous at the amino acid level to *B. cenocepacia* J2315 BCAM2143 (or *bapA*, synonym for *adhA*). Although the role of this *bapA*/*adhA* adhesin is well-characterised in *B. cenocepacia*, confirmation is needed to determine and describe what role this highly upregulated gene in mannitol may play in *B. multivorans* and virulence. As *adhA* is the most highly upregulated gene common to the mucoid vs. non-mucoid data sets, and is most upregulated in C1576 YEM vs. YEO (Table 9.23) it would be of interest to study through mutagenesis the role of this adhesin in *B. multivorans* virulence.

In the RNA-seq data set, adhesins were enhanced in expression in the CF isolate C1576, which correlated with the phenotypic study which showed mucin adhesion was enhanced by mannitol in this isolate independent of EPS production. This mannitol enhanced EPS-independent adhesion in C1576 spurred the whole genome sequencing of C1576 and the RNA-seq analysis to define the transcriptional response of this isolate in relation to virulence associated genes. Due to the fact that the adhesins identified in C1576 were not present in ATCC 17616, the reference genomes of *B. multivorans* CGD1 (a clinical chronic granulomatous disease isolate) and *B. ambifaria* MC0-4 were used to identify these adhesins from the RNA-seq data where. Specifically genes encoding fimbrial and filamentous haemagglutinin-related genes were assessed, and more detail on these adhesins and their mannitol enhanced expression in C1576 is presented and discussed in Chapter 5. Briefly, the gene expression profiles from YEM vs. YEO growth conditions indicate mannitol upregulated entire adhesin-related loci (Appendix Table 9.23).

4.3.1 Mucoid growth conditions and differential expression of genes related to oxidative stress survival

Superoxide dismutase (SOD) proteins are involved in protection against reactive oxygen species and oxidative stress. Genes coding for SOD proteins were differentially expressed in the *B. multivorans* ATCC 17616 transcriptome profiling (Table 9.22). Specifically, genes encoding two different SOD encoding genes were equally upregulated in all three mucoid conditions of the ATCC 17616 data relative to YEO. Production of peroxidases, SOD, and catalases are bacterial tools for dealing with reactive oxygen species/oxidative stress. Use of these tools has been confirmed for all species of the Bcc (112). In the phenotypic studies presented in Chapter 3, EPS-independent mannitol-enhanced survival to hydrogen peroxide exposure was observed in C1576 and *bceB* CR mutant following their growth in mannitol (or mannose) containing broths. However, the wild-type EPS producing C1576 also still survived hydrogen peroxide treatment better than the bceB CR mutant in mannitol, indicating some protection may be due to EPS. Though no differentially expressed SOD-encoding genes were detected in C1576 RNA-seq growth

conditions, in the ATCC 17616 microarray data the two upregulated SOD-encoding genes indicate mucoid-inducing sugars could contribute to enhanced oxidative stress survival in ATCC 17616. Future studies would be advantageous to confirm this using an *in vitro* oxidative stress assay with *B. multivorans* in order to validate this observation for ATCC 17616.

4.4 Discussion

The growth of Bcc on numerous sugars and sugar alcohols is known to induce dramatic overproduction of EPS, a putative virulence factor linked to immune response evasion and chronic or persistent disease. The therapeutic administration of mannitol, or the onset of CFRD and associated elevated sugars, may promote EPS production within the lungs of Bcc-infected patients or have wider unknown consequences on the bacterial cell (and thus course of infection). Growth on minimal media where mannitol is the only carbon source does not result in EPS production, indicating some additional component(s) in the media, besides mannitol, trigger EPS biosynthesis. Studies presented in Chapter 3 showed mannitol dramatically altered motility, biofilm formation, survival of H_2O_2 oxidative stress, and other virulence-related phenotypes. Crucially, these same observations were made in both the wild-type *B. multivorans* C1576 and in an isogenic non-mucoid mutant. These studies highlighted a wider transcriptional response to mannitol that impacts directly on virulence traits.

Using *B. multivorans* ATCC 17616 (an environmental isolate) and C1576, a CF outbreak isolate, the aim of this project was to employ microarray and RNA-seq to define (at a transcriptional level) how sugars like mannitol and fructose promote EPS production, and how clinically relevant sugars influence the global gene expression of *B. multivorans*. Results from transcriptional profiling of ATCC 17616 showed the environmental isolate did not upregulate *bce* or *wcb* EPS biosynthetic gene clusters in mucoid growth conditions, but did upregulate parts of other less-studied EPS clusters. Of interest was the comparison between the two mucoid conditions, YEF vs. YEM, which resulted in upregulation of numerous genes in the *bce* cluster relative to YEM, indicating

differences exist between these sugars. It has been reported that ATCC 17616 produces the most common type of Bcc EPS, cepacian (68), whilst C1576 is reported to produces a mix of polysaccharides besides cepacian (88). Thus, although *bce* is linked to cepacian biosynthesis, cepacian could be made via other uncharacterised polysaccharide biosynthesis pathways, or pathways for other types of polysaccharide biosynthesis could be redundant and contribute towards EPS biosynthesis regulation. In ATCC 17616, the *bce* cluster was expressed, but not upregulated in YEM or YEF relative to YEO. From previous studies in Chapter 3 it is known that *bceB* disruption abolished EPS production in ATCC 17616 and C1576, thus the *bce* cluster is involved in ATCC 17616 EPS biosynthesis, but it must not be the only gene cluster involved. This suggests a master regulator involved in EPS biosynthesis and other stress responses that could be linked or activated by mannitol and EPS-inducing sugars. In contrast, C1576 did upregulate the *bce* cluster in YEM relative to YEO. This indicates a potential strain difference in how *B. multivorans* responds to mannitol at a transcriptomic level. There were other observed strain variations in phenotypic studies such as adhesion to mucin and swimming motility. Additionally, three novel adhesins identified in the genome of C1576 but absent from the ATCC 17616 genome were found to be specifically upregulated by mannitol (these adhesins are the subject of the following Chapter 5 and paper published in the journal Microbiology (61)). These strain variations clearly indicated that transcriptome analysis of the C1576 response to mannitol is essential to understand the basis for EPS synthesis in this organism, and the wider impact of mannitol on virulence.

The present study used the comparison of transcriptome profiles from ATCC 17616 microarrays with RNA-seq data from C1576 to reveal some commonalities that may lead to identification of the EPS regulators (and genes) involved. Many transcriptional regulators were differentially expressed in the transcriptional profiles of ATCC 17616 and C1576, indicating the influence different sugars and EPS induction have on the major rewiring of cellular processes. The upregulated transcriptional regulators in mucoid growth conditions are potential candidates for future study and could be linked to

transcriptional control of whole organisms stress responses and/or EPS biosynthesis.

B. multivorans ATCC 17616 and C1576 were altered in global gene expression related to motility, EPS-related genes, secretion and outer membrane proteins, nitrogen metabolism and other genes involved in stress resistance, and antibiotic resistance. Some differences between strains both grown in YEM relative to YEO were observed as well as some mannitol dose-dependent differences in ATCC 17616 (specifically related to motility). Fructose and mannitol-grown ATCC 17616 in most instances resulted in commonly regulated genes increased or decreased in fold-change to the same extent. Antibiotic resistance genes abundantly differentially expressed in ATCC 17616 YEF vs. YEO and the YEM vs. YEO, indicate the carbon source and mucoidy impacts on the antibiotic resistance systems in this organism; similar antibiotic resistance genes were absent from differentially expressed genes in C1576 RNA-seq data. Efflux transporters such as the RND (resistance nodulation resistance division) super family of efflux pumps have been shown to influence not only antibiotic resistance profiles of *B. cenocepacia* but wider virulence relevant attributes such as biofilm formation (19).

The instances of strain variability between the C1576 and ATCC 17616 could be down to the variability in the RNA-seq data, and the resulting small number of genes identified as being differentially expressed in various growth conditions of interest and thus fewer genes reached statistical significance for further analysis. Of the pathways identified as altered in different ATCC 17616 following growth on different sugars, many were not altered in corresponding C1576 data sets. In light of the variability between replicates this does not necessarily mean that those genes were not altered in C1576, but rather significance of those genes was lost. Additional transcriptomic studies of C1576 in response to mannitol is required to elucidate to what extent differences between these *B. multivorans* strains is accurate.

A publication by Silva *et al.* compared the transcriptomes of *B. multivorans* clonal CF isolates (one mucoid, one non-mucoid). They observed many similar

alterations in gene expression as in the present study of *B. multivorans* transcriptome comparisons of mucoid vs. non-mucoid growth conditions. A summary of some of the striking similarities between the Silva *et al.* data set and data from the ATCC 17616 and C1576 transcriptome profiles can be found in Appendix Table 9.24, with the Silva *et al.* data presented with mucoid vs. non-mucoid isolate. Genes that overlapped between the two studies reveal the potential significance between mannitol induction of genes related to nitrogen metabolism, secretion, and motility. Silva and colleagues observed an overall increase in transcripts of genes encoding for nitrogen metabolism indicating reduced metabolic needs in the non-mucoid isolate as an adaption to chronic infection relative to the mucoid, initial isolate (178). Silva and co-authors suggested due to the lack of EPS biosynthesis of their non-mucoid clonal isolate, metabolic pathways were altered, and loss of the ability to produce EPS, and reduced in motility-related gene expression were additional means of adapting to the CF lung environment. From personal communications with the authors of the Silva *et al.* study (138), they found no mutations within known EPS biosynthetic genes to explain the appearance of the non-mucoid isolate. Although there could be a mutation in a yet unidentified EPS gene that could explain EPS-deficiency of this isolate, it is also suggestive of a mutation in a global regulator controlling EPS or stress response in general (of which EPS is included). The overlap of differentially expressed gene networks and pathways identified in the present study and the Silva *et al.* study suggests the regulator controlling EPS is also involved with regulation of several other pathways relevant to stress response, survival or adaption. The transcriptional regulator Bmul_2557 was upregulated in the Silva *et al.* data mucoid vs. non-mucoid isolate, and in both ATCC 17616 YEF and YEM growth conditions relative to YEO. Additionally, though not significant in all pairwise comparisons, Bmul_2557 was also upregulated in YEM vs. non-mucoid YEM C1576 RNA-seq data – indicating it is EPS specific not an upregulation in response to just mannitol. This transcriptional regulator and several other potential candidates could be missing links to elucidating EPS regulation in the Bcc.

What effect alterations in gene expression induced by mannitol and EPS biosynthesis have on *B. multivorans* in the CF lung are unknown. The recommended dose of inhaled mannitol is 800 mg per day. In a normal human lung, with an average volume of 4.3 litres, this dosage would be equivalent to ~1.02 mM of mannitol per day directly into the airways. This concentration is likely an underestimate for mannitol distribution in a CF lung which is obstructed with inflammation, mucous and bacterial biofilm. Localised concentration of mannitol thus could be significantly higher than the estimated amount for a healthy lung. Media used to study mucoidy in the Bcc YEM in the present study (109.9 mM mannitol) and reduced YEM (13.7 mM mannitol), appear to be high relative to the estimated 1.02 mM within 4.3 litre lung. However, in the ATCC 17616 microarray studies where two different concentrations of mannitol were used to induce EPS, the comparison of the standard YEM and reduced YEM relative to YEO suggested some differences but mainly similarities between the two mannitol doses. The reduced YEM condition resulted in upregulated genes linked to nitrogen metabolism, likely due to reduced carbon source availability, however the lower dosage of mannitol still upregulated flagella related genes and the transcriptional regulator Bmul_2557. Though motility related genes were not as highly upregulated in the reduced YEM compared to standard YEM, a large number of genes encoding proteins involved in flagella assembly and chemotaxis were observed, as well as several genes involved in antibiotic resistance (namely common β-lactamase containing proteins), type six secretion genes, SOD production, and iron uptake and transport.

Beyond EPS and transcriptional regulators, growth on mannitol and fructose altered expression of secretion-related genes, antibiotic resistance genes, and outer membrane proteins. The Silva *et al.* data showed nine type VI secretion genes with increased expression in their mucoid vs. non-mucoid data set (178), of which *bcsJ* was upregulated in mucoid conditions in ATCC 17616. Altered gene expression in virulence-related genes could have potential links with phenotypic assays, such as the attenuated virulence of mannitol-grown *B. multivorans* C1576 in the insect model *G. mellonella*, or the mannitol enhanced invasion of A549 human lung epithelial cells. *B. multivorans* can flourish in

different niche environments, from the soil to the CF lung. In order to accomplish this diverse life-style, it must evolve, acquire and be successful against the onslaught of immune response, oxygen variability, oxidative stress, physical clearance, and frequent long-term high antibiotic exposure at high concentrations. Currently the effects of EPS production *in vivo* and the role for mucoidy and its impact (positive or negative) on virulence in the CF lung are unknown. The present dissertation highlights the potential effects of mannitol treatment and elevation of clinically relevant sugars on the whole-organismal behaviour of *B. multivorans*. Findings of the numerous impacts of mannitol on phenotypes and gene expression relevant to virulence suggest further exploration of alternative osmolyte would be advisable. Researchers are however looking into another sugar alcohol, xylitol, as an osmolyte (229). However, based on the present study observations that *B. multivorans* gene expression is altered beyond EPS biosynthesis induced by different sugars, the same could be true for other sugar alcohols and carbon sources not included in the present study. The sugars chosen for the present study were used due to their present clinical relevance to CF treatment and due to elevation in CFRD.

The present study contributes to sparse knowledge about mucoidy and virulence in *B. multivorans*. For the first time, sugars besides mannitol have been used to induce EPS for gene expression studies. Defining the role of mucoidy and virulence in *B. multivorans* is crucial for understanding the basis for EPS biosynthesis. Overall, improved understanding of the impact of carbon source on mucoidy and virulence could highlight reasons for the unpredictability of infection attributed to Bcc CF lung infection, as the majority of *B. multivorans* clinical isolates often maintain the ability to produce EPS. By investigating two isolates under mucoid and non-mucoid growth conditions, the identification of the whole organism response to EPS-inducing clinically relevant sugars was possible. Overall, for both isolates, different sugars had a much broader influence on whole genome gene regulation rather than solely influencing EPS biosynthesis-related transcription.

4.5 Conclusions

1. Growth on minimal media where mannitol is the only carbon source does not result in EPS production, indicating some additional component(s) in the media, besides mannitol, trigger EPS biosynthesis.
2. ATCC 17616 did not differentially regulate known EPS genes of the *bce* cluster in mucoid growth conditions. In contrast, C1576 did differentially express EPS genes involved in the *bce* cluster in mucoid versus non-mucoid growth conditions.
3. Growth on different sugars resulted in differential expression of genes involved in antibiotic resistance, motility, chemotaxis, and metabolism.
4. Transcriptional regulators highly upregulated in mucoid growth conditions are potential candidates for future study and could be linked to transcriptional control of EPS production.

Chapter 5: Identification and characterisation of novel adhesins in a *B. multivorans* CF outbreak isolate

5.1 Introduction

When grown on certain carbon sources (most notably mannitol), Bcc species produce exopolysaccharide (EPS), resulting in a mucoid phenotype (17). EPS production by the Bcc has been associated with bacterial persistence within the lung (51), biofilm formation (56) and inhibition of neutrophil activity (33), whilst it has recently been proposed that an inverse correlation exists between the quantity of EPS production by Bcc organisms and the rate of decline in CF lung function (233). Bcc EPS production induced by mannitol has gained clinical relevance following the approval of a dried-powder preparation of mannitol for use as an inhaled osmolyte in CF patients. Whilst mannitol therapy clearly improves CF lung function (23,59,93,193), the potential impact on *Burkholderia* organisms within the lung is unknown.

In the present study, the role played by mannitol and the associated mucoid phenotype in bacterial adherence was investigated. As reported previously in Chapter 3, mannitol promoted *B. multivorans* adherence in a strain-dependent manner which differed in the way EPS contributed to adhesion to mucin. The present study reports the genome sequencing of a CF outbreak strain *B. multivorans* C1576. Sequencing enabled the identification of two *B. multivorans*-specific adhesin loci. Specific adhesins have not previously been described in *B. multivorans*. These fimbrial and afimbrial loci, which contribute to biofilm formation and mucin adherence, appear specific to *B. multivorans* and show enhanced expression in the presence of mannitol. These observations provide new insight into *B. multivorans* biology and highlight the potential microbiological impact of inhaled mannitol therapy in CF patients.

5.2 Aims

Examine the EPS-independent adhesion phenotype in CF outbreak-isolate C1576 using the following approaches:

a. Whole genome sequencing to identify putative adhesins
b. Insertional mutagenesis of identified adhesins
c. Characterise adhesins in phenotypic assays
d. Assess distribution of adhesins amongst a panel of clinical and environmental Bcc isolates.

5.3 Results

5.3.1 The contribution of EPS to adhesion is strain-dependent in B. multivorans

In the Bcc, disruption of the gene encoding the BceB glycosyltransferase eliminates EPS biosynthesis when bacteria were grown on mannitol (17). Consequently, to enable EPS-dependent and EPS-independent effects of mannitol to be determined, as outlined in Chapter 3, two representative strains of *B. multivorans* were inactivated for *bceB* - the environmental isolate *B. multivorans* ATCC 17616 and the CF isolate *B. multivorans* C1576. The C1576 CF isolate is the index case of an outbreak within a paediatric CF unit in Glasgow (UK) (222), and has previously been designated as sequence type (ST)-27 by multi-locus sequence typing (MLST). The phenotypes of the resulting non-mucoid mutants were characterised extensively and described within Chapter 3. Disruption of *bceB* in the two *B. multivorans* strains resulted in a complete loss of EPS production, as judged by visual scoring of mucoidy and quantitative analyses (dry weight and sugar content) of EPS extractions from wild-type and *bceB* mutants following growth on YEM media (data not shown). Disruption of *bceB* did not impact on the growth of strains under any culture conditions tested.

Wild-type and *bceB* mutants of each strain were cultured in the presence of either mannitol (EPS-inducing) or mannose (non-inducing) prior to quantifying adherence to mucin. As shown in Figure 5.1 (same data presented in previous Chapter 3) mannitol promoted adherence of both wild-type isolates relative to the mannose, non-mucoid control. As shown in Fig. 5.1, within the context of the mucin adhesion *in vitro* assay, the environmental ATCC 17616 strain adhered considerably better to mucin than the clinical isolate C1576. However, irrespective of their basal level of adherence, mannitol promoted adherence of both strains to mucin (orthogonal contrast, ATCC 17616: $P < 0.0005$; C1576: $P < 0.0005$).

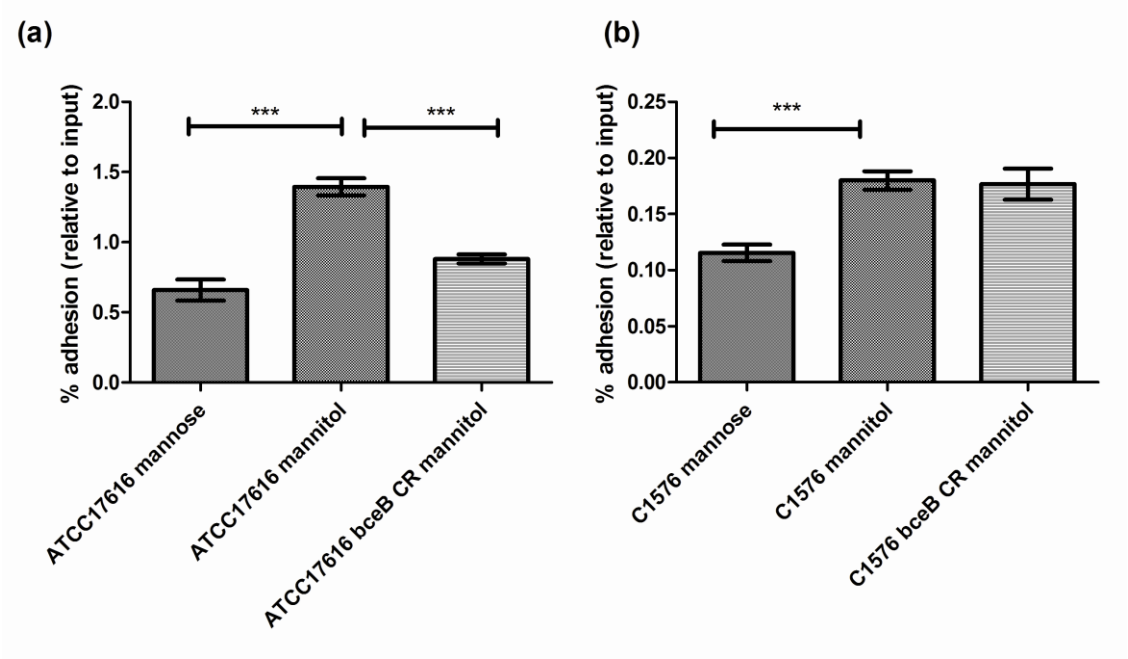

Figure 5.1 B. multivorans strains ATCC 17616 and C1576 (wild-type and bceB mutant of each) adhesin to mucin. Strains were grown overnight in either mannitol-containing media (YEM) or mannose-containing media, prior to assessing adherence to mucin-coated wells. The ATCC 17616 adhered significantly better to mucin than the C1576 (note the differing scales on the y-axes). However, irrespective of this difference, growth in mannitol promoted the adherence of both strains (relative to growth in mannose). Disruption of the *bceB* gene in ATCC 17616 abolished the enhanced adherence observed following growth in mannitol, indicating it to be EPS-dependent (a). In contrast, inactivation of *bceB* in C1576 did not affect the enhanced adherence, indicating it to be EPS-independent (b). Data correspond to mean of three independent experiments, each in triplicate. Error bars indicate SEM. *** $P < 0.0005$.

Mannose was chosen as a non-EPS-inducing control as the growth dynamics of the mannitol- and mannose-grown bacteria were comparable. Mannose has been suggested to act as an anti-adhesive for certain bacterial species, reducing adherence to epithelial cells (1). However, it has previously been reported that mannose does not block mucin-binding by *Pseudomonas* (*Burkholderia*) *cepacia* (168). Consistent with this, mucin adherence of *B. multivorans* C1576 was not reduced by pre-treatment with mannose (Figure 5.2), suggesting that the differential adherence observed between the mannitol- and mannose-grown cultures is due to mannitol promoting adherence, rather than mannose reducing adherence.

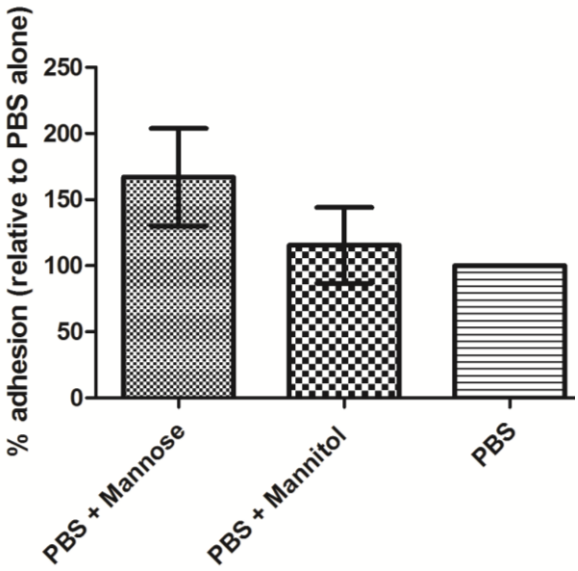

Figure 5.2. Mucin adhesion assay carried out following pre-treatment of mannitol-grown bacteria with mannose. *B. multivorans* C1576 was grown overnight in mannitol and yeast extract (YEM) broth, then cells were washed and harvested, and re-suspended in PBS. Then, mannose (PBS + Mannose) or mannitol (PBS + Mannitol) was added to a final concentration of 2 % (w/v), the same concentration in YEM or mannose-containing sugar media. The control was PBS alone (PBS) added to a standardised culture. Bars represent percentage adhesion relative to the PBS control, average of three wells (n=3) per treatment. Error bars represent SEM.

Whilst mannitol promoted adherence of both isolates to mucin, comparison of the wild-type and EPS-deficient *bceB* mutants revealed differing roles for EPS. Inactivation of *bceB* in ATCC 17616 blocked this enhanced adherence (Figure 5.1(a)), indicating that it was EPS-dependent. In contrast, the enhanced adherence of C1576 was still evident following inactivation of *bceB* (Figure 5.1(b)), indicating that it was independent of EPS status. These observations led us to investigate the genome of C1576 in an attempt to identify strain-specific adhesins that may account for this strain-to-strain variation in adherence phenotype.

5.3.2 Identification of loci encoding putative fimbrial and afimbrial adhesins in B. multivorans C1576.

Illumina genome sequencing of isolate C1576 with subsequent mapping to the ATCC 17616 reference genome allowed us to identify sequences present

within C1576 that were absent from ATCC 17616. Analysis of these unmapped reads resulted in the identification of two distinct loci encoding putative fimbrial and afimbrial adhesins (Fig. 5.3). The sequences of these loci have been deposited in GenBank under the accession numbers JX191919 (fimbrial) and JX191920 (afimbrial).

The putative fimbriae-encoding locus is predicted to encode three putative fimbrial proteins, a FimC chaperone protein and a fimbrial usher protein. The nucleotide sequence of the locus is >99 % identical to an equivalent fimbriae-encoding locus present in *B. multivorans* CGD1, a recently-sequenced isolate from a chronic granulomatous disease (CGD) patient (211). In CGD1, the locus is formed by genes BURMUCGD1_3349 to BURMUCGD1_3353. The organisation of the locus is identical in the two isolates, and amino acid identity between the corresponding encoded proteins is 99-100 %. A similar locus with the same gene organisation is observed in two other sequenced CGD *B. multivorans* isolates (CGD2 and CGD2M), although the percentage amino acid identity of the encoded proteins compared to those of C1576 is lower (average 83 %). Outside of *B. multivorans*, the predicted fimbrial proteins of *B. multivorans* C1576 typically exhibit 35-55 % amino acid identity with proteins encoded by comparable loci in other sequenced *Burkholderia* or non-*Burkholderia* species.

The locus encoding the putative afimbrial adhesin of *B. multivorans* C1576 is depicted in Fig. 5.3 (b). Based on sequence similarity to representative proteins (Appendix Figures 9.1 & 9.2), the locus is predicted to encode components of a two-partner secretion (TPS) pathway responsible for the secretion of an adhesin of the filamentous haemagglutinin (FHA) family. The locus encodes two putative TpsA proteins (264 kDa and 68 kDa respectively) that belong to the FHA-family of outer membrane proteins, although only the larger of these two proteins has a mass consistent with the large exoproteins of the TpsA (*hecA*-like) family. The locus is also predicted to encode a single protein of the TpsB family that likely facilitates secretion of the FHA family adhesin(s). Phylogenetic analysis confirms relatedness of this protein to known TpsB transporter proteins, particularly the HecB protein of *Erwinia chrysanthemi*

(102,162) (Figure. 9.3). Consequently, the present study proposes that the TpsB family protein of *B. multivorans* C1576 is a HecB-like protein. Consistent with this, comparable phylogenetic analysis of the 264 kDa TpsA family protein of *B. multivorans* C1576 shows relatedness to the HecA protein of *Erwinia chrysanthemi* (Fig. 9.4 in the Appendix), although the phylogenetic distances are greater than that observed between the corresponding TpsB proteins. Immediately downstream of the *hecB*-like gene is a gene encoding a putative PpiC-type peptidyl-prolyl cis-trans isomerase (PPIase) protein, predicted to localise to the cytoplasmic membrane. It is conceivable that this PPIase plays a role in the secretion of the FHA family protein, as has been described for a periplasmic PPIase of *Bordetella pertussis* (89).

Analyses of available *Burkholderia* genomes reveals that the closest FHA-related adhesins to that of *B. multivorans* C1576 are found in the environmental isolate *B. ambifaria* MC40-6 (approximately 83 % amino acid identity between corresponding proteins) and *B. phymatum* STM815 (approximately 65 % amino acid identity between corresponding proteins). Amino acid identity to related proteins of non-*Burkholderia* species (including the prototypic FHA/FhaC of *Bordetella pertussis* and the HecA/HecB of *Erwinia chrysanthemi*) is approximately 28-30 %.

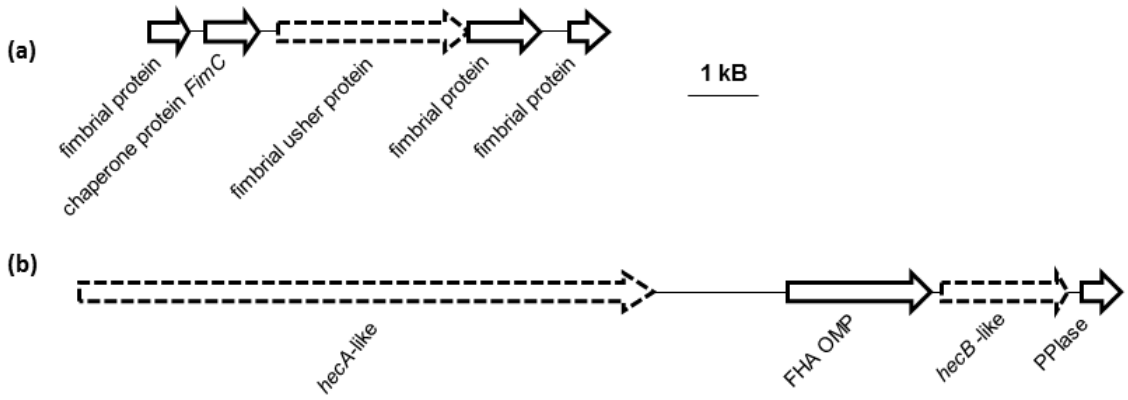

Figure 5.3. The fimbrial and putative FHA loci identified within B. multivorans C1576. Dashed outline denotes genes targeted by insertional inactivation. FHA OMP, Filamentous haemagglutinin outer membrane protein; PPIase, PpiC-type peptidyl-prolyl cis-trans isomerase. (a) The C1576 fimbrial locus encodes five fimbrial proteins relating to fimbrial chaperone and assembly. (b)The C1576 putative FHA-like locus encodes a putative HecA/HecB two-partner secretion (TPS) system, predicted to facilitate the secretion of the HecA-like encoded filamentous haemagglutinin.

5.3.3 The loci encoding putative adhesins of B. multivorans C1576 differ in strain distribution.

The analysis of available genome sequences referred to above suggested that the two loci were not widely distributed within the Bcc and wider *Burkholderia* genus. Using dot-blot hybridization, the distribution of each locus was assessed (based on the presence or absence of a representative gene for each) within a wider panel of *Burkholderia* isolates, with a particular focus on clinical *B. multivorans* isolates (Table 5.1).

Table 5.1. Distribution of the the putative HecA-like, HecB-like and fim adhesins amongst clinical and environmental B. multivorans isolates. Isolates are sub-divided into ST-27 and non-ST-27 ('other'). None of the adhesins were detected in non-*B. multivorans* isolates. Southern hybridisation dot-blot analysis was carried out using DIG-labelled PCR probes for each adhesin.

	Clinical		Environ.
	ST-27	Other	
hecA	26/26	4/57	0/6
hecB	26/26	5/57	0/6
fim	26/26	47/57	3/6

A representative image of the dot-blot analysis for a panel of *B. multivorans* isolates is shown in Figure 5.4.

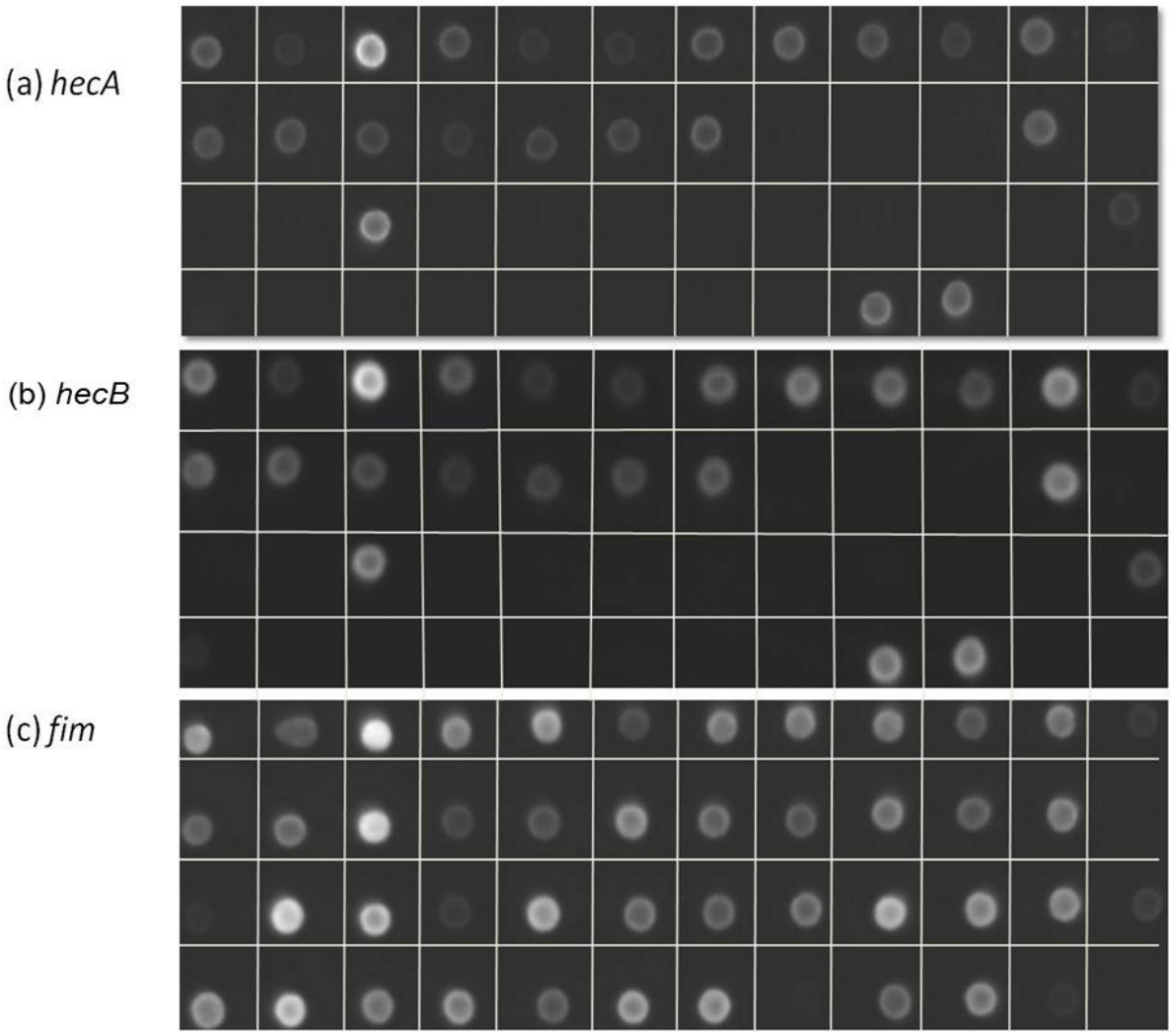

Figure 5.4. Dot-blot hybridisation of genomic DNA from B. multivorans clinical and environmental strain panel. Adhesins were detected with DIG-labelled probes in a panel of clinical and environmental *B. multivorans* isolates. DIG-labelled adhesin-specific probes and genomic DNA from *B. multivorans* and Bcc isolates were hybridised and blocked using ROCHE Southern Hybridisation buffers, and visualised using CDP-Star chemiluminescence substrate. As can be seen based on this representative image, more strains contained the fimbrial usher adhesin than the two afimbrial hecA-like and hecB-like adhesins.

Genomic DNA was isolated from a total of 97 Bcc isolates, comprising 83 clinical *B. multivorans* isolates (including 26 representatives of strain ST-27), six environmental *B. multivorans* isolates, and representatives of other Bcc species (for strain details, see Appendix, Table 9.5).

Genomic DNA from the assembled strain panel was probed for the presence of genes encoding the putative fimbrial usher and the HecB-like

proteins. Based on the presence of these representative genes, results (summarised in Table 5.1, and detailed in Table 9.5) reveal that the locus encoding the putative fimbrial proteins is widely distributed amongst both clinical and environmental *B. multivorans* isolates, being observed in 76/89 isolates tested. In contrast, the locus encoding the FHA-family adhesin is more restricted in distribution, being limited to clinical isolates and particularly the ST-27 outbreak strain (occurring in 100 % of ST-27 isolates, compared to < 9 % of non-ST-27 isolates). None of the non- *B. multivorans* isolates within the strain panel harboured either gene.

5.3.4 The fimbrial and FHA-family adhesins of B. multivorans C1576 contribute to adherence and biofilm formation.

Next, the present study sought to evaluate the role of these putative adhesins in adherence and biofilm formation. Individual mutants were generated by insertional inactivation of the genes encoding the putative HecA-like, HecB-like and fimbrial usher proteins (resulting in strains and vector constructs hecA CR, hecB CR and fim CR respectively, Chapter 2 Table 2.1, Table 2.2). Both the *hecB*-like and fim crude mutants were complemented *in trans* using the pDA17 constitutive expression vector. The hecA CR mutant was not complemented due to the large size of the gene (> 8 kb). However, RT-PCR analysis of hecA CR mutant confirmed that the expression of downstream genes was maintained following *hecA* inactivation. Additionally, RT-PCR analysis confirmed that genes flanking all of the inactivated genes within each of the mutants were still expressed (data not shown, primers used for RT-PCR can be found in Appendix Table 9.3).

To evaluate the role of the adhesins in abiotic adherence, the ability of the strains to adhere to mucin and to the extracellular matrix protein fibronectin was assessed. None of the mutants exhibited a significant reduction in fibronectin binding ($P > 0.05$, data not shown).

In contrast, adhesin mutants were significantly reduced in their adherence to mucin relative to the wild-type strain ($P < 0.0005$; Fig. 5.5(a)). Appropriate complementation of two of the mutants (*fim* CO and *hecB* CO)

partially restored mucin adherence ($P < 0.05$ relative to the corresponding mutant strain), albeit not to wild-type levels (Figure. 5.5 (a)). This partial complementation has been observed previously with the pDA17 vector, including in a recent study of an adhesin-like gene of *B. cenocepacia* (134), and this could reflect sub-optimal gene dosage from the complementation vector.

Next assessed was adherence to the A549 human lung epithelial cell line. As shown in Figure 5.5(b), the fim, hecA and hecB crude mutants showed significantly reduced adherence to A549 cells relative to wild-type. In contrast to the mucin and fibronectin adherence assays, complementation of the *fim* and *hecB* mutants failed to restore adherence to A549 cells. It is conceivable that overexpression of these adhesins from the complementation vector masked other cell-surface components that play an important role in the adhesion of *B. multivorans* to epithelial cells.

Next, the ability of all strains to form biofilm was assessed using the MBEC biofilm assay device (Innovotech). As shown in Figure. 5.5 (c), all three mutant strains (fim CR, hecA CR and hecB CR) exhibited significantly impaired biofilm formation relative to wildtype C1576 ($P < 0.0005$), indicating that both adhesins are important for biofilm formation. Appropriate complementation of both mutants fully restored biofilm formation (Figure. 5.5(c)).

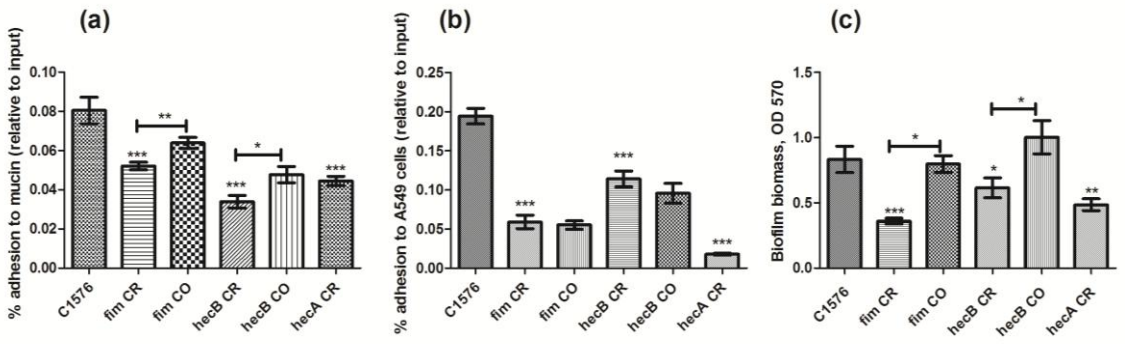

Figure 5.5. Adhesins of B. multivorans C1576 contribute to biotic and abiotic adherence and biofilm formation. Wild-type *B. multivorans* C1576, the fim, hecA and hecB CR insertional mutants and complemented strains were assessed for adherence and biofilm formation. Graphs show representative data from at least three independent experiments. Asterisks alone indicate statistical significance relative to wild-type C1576, whilst asterisks with bracket bar directly beneath compare the adhesin mutant (CR) to the corresponding complemented strain (CO). * $P < 0.05$, ** $P < 0.005$, *** $P < 0.0001$ as assessed by orthogonal contrast and 1-way ANOVA with Tukey post-test. Error bars represent SEM. (a) Mucin adherence assay showed all adhesin mutants significantly impaired in adherence to mucin. Complementation of fim and hecB mutants only partially-restored adherence. Results are expressed as percentage adhesion relative to input. (b) Adherence to A549 epithelial cells. All mutants were significantly impaired in their adherence to A549 cells. Complementation failed to restore adhesion. Results are expressed as percentage adhesion relative to input. (c) All mutants show reduced biofilm formation relative to wild-type, with fim and hecB complementation fully restoring biofilm formation.

Finally, to investigate the role of these adhesins during infection, all strains were assessed within the *G. mellonella* infection model, a model that has been used previously to investigate the role of *Burkholderia* adhesins (134). Neither mutant exhibited altered larval killing compared to wild-type C1576, with all strains killing 100 % of larvae within 72 hours at an inoculum of approximately 10^4 CFU (data not shown). Larvae injected with PBS exhibited 100 % survival for the duration of the experiment. Therefore, individually, the putative fimbrial usher protein or the HecA- and HecB-like proteins are not required for full virulence in the *G. mellonella* model.

5.3.5 Mannitol promotes expression of both adhesin loci, enhancing adherence of C1576

As had been previously shown, growth of C1576 in mannitol promoted adherence to mucin in an EPS-independent manner (Fig. 5.1). Having identified adhesins within C1576, their expression in the presence of mannitol was also assessed. As part of the wider on-going study of the genome-wide transcriptional response of *B. multivorans* to mannitol (discussed in depth in the previous chapter, Chapter 4), RNA-seq analysis on the Illumina platform was performed. Analysis of this transcriptome dataset reveals that growth in mannitol promotes expression of both loci encoding the putative fimbrial and afimbrial adhesins (Fig. 5.6). This is particularly the case for the putative fimbriae-encoding locus, every gene of which is significantly upregulated by growth in mannitol. All genes of the putative fimbriae-encoding locus were significantly upregulated following growth in YEM, with 2.5- to 13-fold increases in expression relative to that observed in mannose-grown cultures. Upregulation of the locus encoding the putative FHA-family adhesins was also observed, albeit to a lesser extent (1.5- to 2-fold). Of those, only the genes encoding the putative 68 kDa FHA-like protein (FHA OMP 2) and HecB-like protein were deemed to be significantly upregulated.

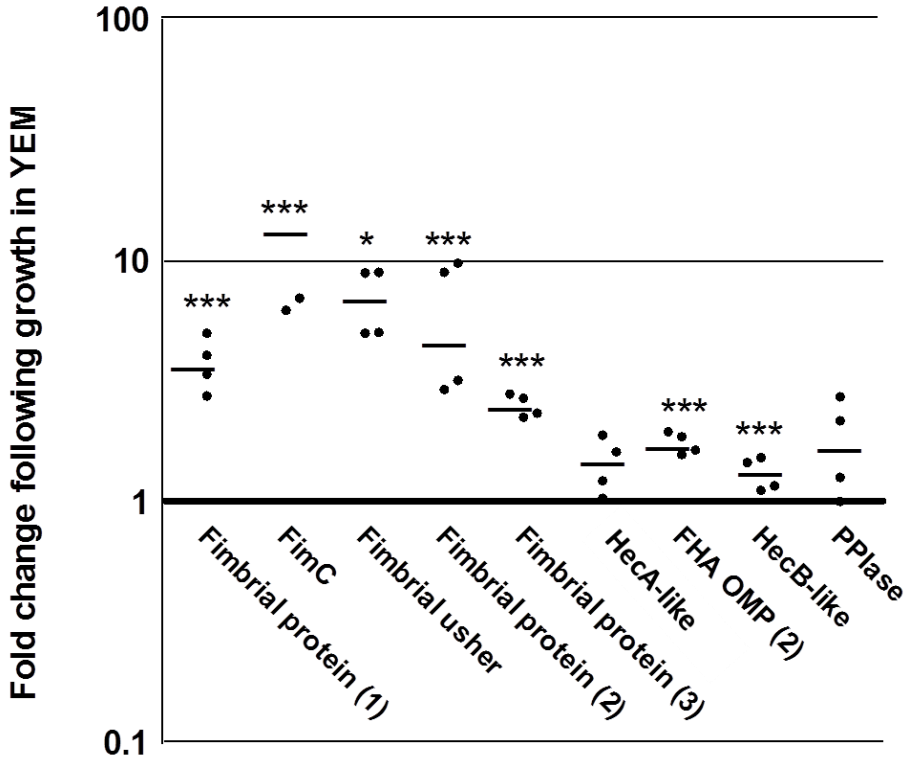

Figure 5.6 RNA-seq analysis reveals elevated expression of both putative adhesin-encoding loci following growth in mannitol. The relative expression of the genes of the putative adhesin-encoding loci of *B. multivorans* C1576 was assessed by RNA-seq. The graph shows the fold change in gene expression observed following growth in the mannitol-containing YEM media, relative to the expression level observed in equivalent mannose-containing media. For each gene, data are depicted in two ways: (1) The horizontal bar indicates the fold change that was calculated from the combined analysis of the two biological replicates per condition; (2) the variance in the fold change for each gene is shown by the individual data points (filled circles) that each represent analysis of the biological replicates individually (i.e. a single pairwise mannitol-vs.-mannose comparison). The fold change of the *fimC* gene could not be calculated for two of the four pairwise comparisons as one of the mannose-grown samples had an RPKM value of 0. Asterisks denote FDR-adjusted P-values (* $P < 0.05$, *** $P < 0.0005$), and relate to the combined analysis of the biological replicates.

Having shown this upregulation of adhesins in response to mannitol, it was next determined to what extent the individual adhesins contributed to the mannitol-promoted adherence phenotype shown in Figure 5.1 (b). The wild-type and adhesin mutants were cultured in mannose or mannitol-supplemented broth prior to the mucin adherence assay. Relative to wild-type, both *fim* CR and *hecB* CR mutants showed impaired mucin adherence following growth in mannose-containing media ($P < 0.05$), consistent with the results presented in

Figure 5.5 (a), and consistent with a general defect in adherence following inactivation of either adhesin. Despite this lower basal level of adherence, the adherence of the *fim* CR strain was still elevated 5- to 6-fold following growth in mannitol ($P < 0.0005$). This is consistent with observations of the wild-type, and suggests that the putative fimbrial adhesin does not play a significant role in the enhanced mucin adherence that is induced by mannitol. In contrast, the adherence of the hecA CR and hecB CR strain was not enhanced following growth in mannitol ($P > 0.05$), indicating that the putative FHA-family adhesin loci contributes to the mannitol-induced mucin adherence. Whilst it is the fimbrial locus that is most significantly elevated following growth in mannitol (Figure 5.6), it is the locus encoding the putative FHA-family adhesin that appears to be a key determinant of the enhanced adherence. Although perhaps unexpected, this may reflect the fact that the *hecB* gene is predicted to encode the transporter for the FHA adhesin rather than the adhesin itself, and thus *hecB* expression is not a reliable indicator for the amount of mature adhesin on the cell surface.

5.4 Discussion

In this study two distinct adhesin loci were described in *B. multivorans* that each played a role in adherence and biofilm formation. These loci varied in their strain distribution; the fimbrial locus was widely distributed in clinical and environmental *B. multivorans* isolates, whilst the FHA locus was restricted to clinical *B. multivorans* isolates, and was particularly associated with those of the ST-27 outbreak strain. Strikingly, mannitol, recently approved as an inhaled osmolyte therapy for CF patients, up-regulated both loci and promoted bacterial adherence.

Whilst adhesins have been described in other Bcc and within the wider *Burkholderia* genus (13,134,201), the present study represents the first characterisation of fimbrial and FHA adhesins within Bcc, and the first characterisation of any adhesins within *B. multivorans*. FHA adhesins of *B. pseudomallei* play a role in adhesion to human epithelial cells (179), consistent

with our observations in *B. multivorans*. Whilst fimbrial and FHA adhesins are common within *Burkholderia*, there is considerable diversity between adhesins of different species, as evidenced by the present study in which amino acid identity to comparable adhesins in other *Burkholderia* species was typically 35-55 %. Such sequence variation profoundly alters adhesin binding specificities and affinities, impacting on host tropism and capacity for virulence (90,185). *Burkholderia* species are an extremely versatile group of organisms that includes human, animal and plant pathogens. The role played by species-specific adhesins in conferring such diverse host adaptations remains to be elucidated.

In contrast to the widely-distributed fimbrial locus, it is striking that the FHA-like locus reported in the present study was found only in clinical isolates, although further environmental isolates need to be studied to test this association more rigorously. The low number of environmental *B. multivorans* included in the assembled strain panel reflect the infrequent isolation of this species from the natural environment (14). Furthermore, all but two of the FHA-positive clinical isolates (detailed in the Appendix, Table 9.5) belong to sequence types associated with patient-to-patient transmission, notably ST-27, ST-25 and ST-179 (14). Putative transmissibility factors have been identified in other Bcc species (46), and whilst their predictive value has been questioned (80), our observations justify further studies to investigate the strength of the association of the FHA-encoding locus with transmissible strains, and its potential as a marker for transmissibility amongst clinical *B. multivorans*.

The rationale for this study of adhesins within the *B. multivorans* ST-27 strain stemmed from our observations that whilst mannitol promoted bacterial adherence to mucin, the role played by EPS was strain-dependent. The present study emphasises the difficulty in establishing the role of EPS in virulence, as the growth conditions commonly used to induce and study EPS (the mannitol-containing media, YEM) clearly illicit a response within the bacterium that is wider than the EPS biosynthetic pathway. Consequently, attempts to identify the role of EPS through phenotypic observations of whole organisms risk being skewed by the wider non-EPS response to mannitol, potentially resulting in

phenotypic traits being wrongly assigned to the mucoid phenotype. The present approach undertaken in this study (comparison of wild-type and isogenic EPS-deficient mutant formulated in Chapter 3) is better-suited for defining phenotypes truly associated with EPS production. The strain-dependent role of EPS in promoting bacterial adherence highlights the multi-factorial aspect of Bcc virulence, and the fact that the contribution of individual virulence determinants within any given strain is influenced by the presence or absence of other complementary factors. One consequence of this is that the biological significance of the documented mucoid to non-mucoid transition frequently observed amongst Bcc CF isolates (234) will be heavily strain-dependent.

Whilst the ability to utilise mannitol as a carbon and energy source is common amongst both Bcc and *Pseudomonas aeruginosa* (the dominant CF pathogen), it was considered unlikely that inhaled mannitol therapy would significantly affect bacterial burden in the lung (161), and this appears to have been borne out by subsequent clinical trials (93,193). However, the fact mannitol promotes EPS, together with our observations that mannitol promotes expression of adhesins that contribute to adherence and biofilm formation, indicate that administration of mannitol is likely to have profound phenotypic consequences on Bcc within the lung, even if bacterial burden is unaltered. Whilst inhaled mannitol therapy clearly improves lung function (3,23,59), it would appear prudent to monitor the microbiology status of CF patients receiving mannitol, particularly those infected with Bcc.

In summary, this study has identified and characterised *B. multivorans*-specific fimbrial and FHA-like adhesins, confirming their role in biotic and abiotic adherence, and biofilm formation. In so doing, this study has highlighted the strain-to-strain variation in EPS contribution to Bcc virulence, and the difficulty in assigning phenotypic traits to EPS due to the wider response of Bcc to mannitol. Previous studies (described in Chapter 4) aimed to define the genome-wide response to mannitol and identify global regulators that may be responsible. From those studies, candidate transcriptional regulators were identified and though not within the scope of this present study, would be

interesting candidates for mutagenesis and characterisation in order to define Bcc EPS regulation.

Overall, the impact of mannitol on the Bcc is unequivocal, and close monitoring of Bcc-infected patients receiving inhaled mannitol therapy would appear prudent. The broader impacts of sugars relevant to diabetes and mannitol on the phenotypic and gene expression behaviour of the organism require careful consideration when considering the appropriate treatment and disease management options for CF patients.

5.5 Conclusion

1. Fimbrial and afimbrial adhesins in *B. multivorans* contribute to biotic and abiotic adherence and biofilm formation.

2. The distribution of the FHA-like afimbrial adhesins was restricted to clinical *B. multivorans* isolates.

3. C1576 growth on mannitol upregulates both adhesin loci and thus mannitol as an inhaled osmolyte has potential impacts directly on virulence of this organisms in the CF lung.

Chapter 6: Composition analysis of mannitol- and fructose-derived exopolysaccharide produced by *B. multivorans*

6.1 Introduction

Bcc mucoid isolates are linked to chronic persistent infection and inhibited clearance in the mouse chronic lung infection model (51). Although EPS production is still debated to occur *in vivo*, the impact of mucoidy on the progression of Bcc infection has been interpreted across a panel of 100 clinical isolates paired with detailed clinical data, revealing a potential link in mucoid strains favouring persistent rather than acute infection (233). In previous chapters of the present dissertation, the varied impacts of EPS production and the EPS-inducing sugar mannitol on virulence relevant phenotypes (Chapter 3 and 5) and gene expression (Chapter 4) were discussed. Findings from these previous studies indicated phenotypic or gene expression profiles were altered following growth on yeast extract sugar agars containing fructose, mannose, glucose, and mannitol. These sugars are of interest due to clinical relevance (mannitol is an approved inhaled osmolyte in CF patients; glucose, fructose and mannose are elevated in diabetics urine and blood). Mannitol and fructose induce a mucoid, EPS-producing phenotype in *B. multivorans.* Although levels of fructose in the lung have not been reported, it has been shown that glucose is elevated in the airways of diabetics (29). The structure and biological activity of Bcc EPS derived from mannitol has been studied and characterised to some extent; however no studies have included fructose, or any other sugars that induce EPS synthesis. One study suggested up to ~ 80 % of CF isolates produce EPS (139). Production of EPS by members of the Bcc has been shown to use the *bce* EPS biosynthetic gene cluster; this gene cluster was the focus of Chapter 3, assessing the impact of mucoid on virulence-relevant *B. multivorans* phenotypes. The present study characterised the EPS composition from mannitol- and fructose-induced *B. multivorans* EPS. In the following Chapter 7, the biological activity of fructose-and mannitol-derived EPS will be examined. Some studies have reported the dominant type of EPS made by the Bcc is cepacian, and other types of EPS. Interestingly, though the *bce* operon is required for EPS biosynthesis and is linked to cepacian production, a mixture of up to five polysaccharides have been identified from mannitol-induced EPS-producing Bcc isolates (88). The inclusion of fructose as well as mannitol in the

following EPS composition studies aimed to further understanding of the biological role of carbon source and the impact of different EPS-inducing sugars may have on *B. multivorans* EPS composition. This knowledge would forward understanding of the role EPS production and carbon utilisation plays within the host. The main aim of the present study was to assess whether *B. multivorans* ATCC 17616 (environmental isolate) and C1576 (clinical isolate) EPS composition differed following growth on fructose and mannitol.

6.2 Aims

1. Develop and refine EPS sample extraction and preparation to enable mass spectrometry analysis.

2. Optimise sugar detection and analysis methods using QQQ-LCMS

3. Assess the impact of carbon source used for growth on *B. multivorans* EPS composition, specifically EPS induced following *B. multivorans* ATCC 17616 and C1576 growth on fructose and mannitol.

6.3 Results

6.3.1 Standards for EPS mass spectrometry analysis

The repeating unit structure of the exopolysaccharide cepacian has been the focus of previous studies in the literature. Analysis of Bcc EPS including methylation, sugar analysis, chromatography hydrolysis, mass spectrometry, and NMR studies aimed at identifying the structure, acetylation state, and repeating unit of cepacian induced following growth in mannitol (37,39,107). The repeating unit (RU) was determined first in structure and further characterised as the building block for cepacian (37-39,107,117). Cepacian consists mainly of a highly branded heptasaccharide-RU. The oligosaccharide structure of the biological RU of cepacian was previously elucidated using *B. pyrrocinia* BTS7 (39). The cepacian RU contains D-glucose, D-galactose, D-mannose, and D-rhamnose in a ratio of 1:1:3:1 (38). These four sugars were chosen as standards to assess EPS composition of *B. multivorans* ATCC 17616 and C1576 grown on fructose and mannitol.

A mix of four sugars was prepared to form a standard sugar mix. Each sugar was combined at equal concentrations and then serially diluted to be used to create a standard curve. Concentrations used were: 10 mM, 0.1 mM, 0.5 mM, 0.025 mM, 0.0125 mM. Individual standards of each sugar were run at 10 mM and were included on each QQQ-LCMS run for EPS composition analysis, along with the sugar standard mix (at five concentrations) and EPS samples. Figure 6.1 shows the chromatogram of the standard mix of the sugars in the order at which they eluted. The mass spectrometer used was the 6410 enhanced sensitivity triple quadrupole (QQQ) (Agilent Technologies). The QQQ was linked to an Agilent 1200 series HPLC stack for online LC-MS. Serial dilutions of the sugar mixes were included in every QQQ-LCMS run in order to obtain standard curves (for sample concentration calculation) and monitor sensitivity and calibration of the mass spectrometer. Figure 6.1 shows fructose and fucose in the standard mix, but these sugars were not included in further analysis as they were not detected in the *B. multivorans* EPS samples after preliminary analysis (data not shown). Of note is the overlap of glucose and galactose peaks (and to some extent mannose) at the same acquisition time

and mass. This issue was problematic during early data analysis and method optimisation and is discussed in following results sections.

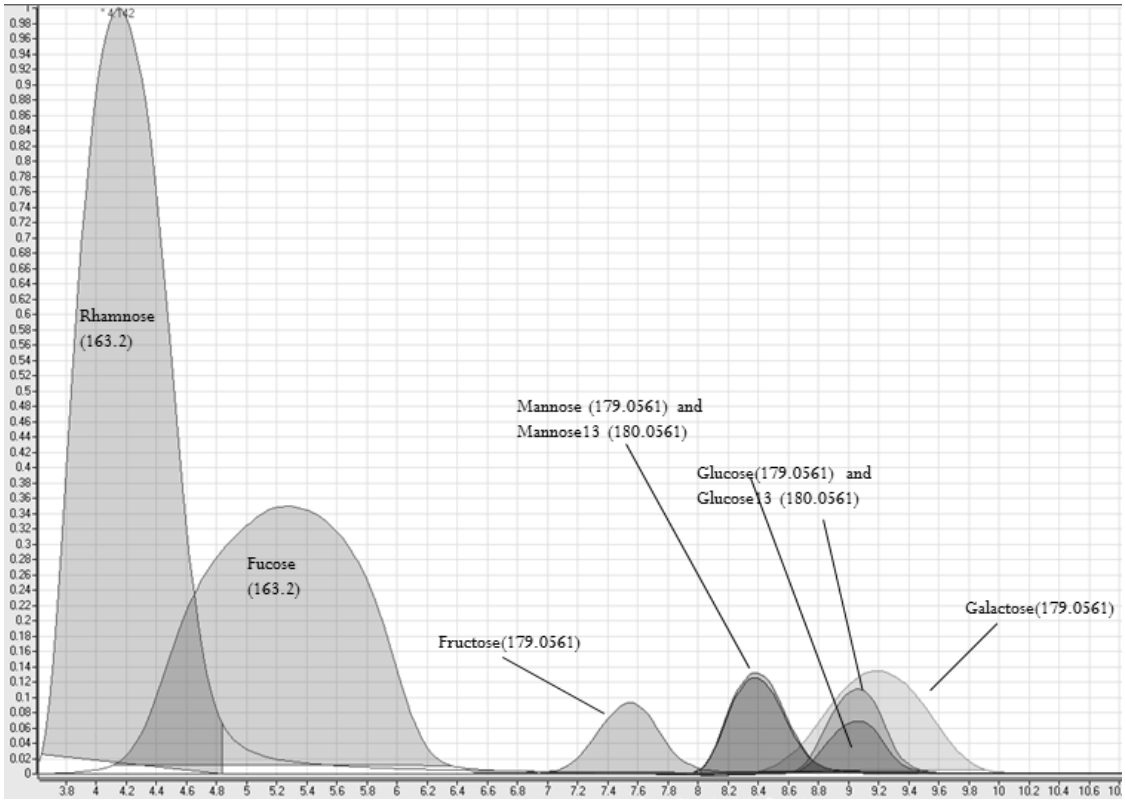

Figure 6.1. Chromatogram of the sugar standard mix. Sugars shown on axes indicate elute in ion counts (y-axis) vs. acquisition (or retention) time (x-axis). Retention time indicates length (in minutes) of time compound spent on the HILIC column prior to detection relative to the other sugars. Fructose and fucose were easily detectable, as was rhamnose. The mass-to-charge ratio (m/z) of each sugar is included in parentheses next to the sugar name. Mannose, glucose, galactose, 13Mannose and 13Glucose were included to demonstrate the m/z difference of 1 in the 13C labelling of one carbon in each of those sugars.

6.3.2 Verification of sugar content in B. multivorans EPS extracts

Once the sugar standards were selected and identified at individual masses and acquisition times, EPS from *B. multivorans* could be extracted following 48 hours of ATCC 17616 and C1576 growth on mannitol or fructose sugar agar. To confirm sugars were present within EPS extracts, the Dubois test (phenol sulphuric acid) was performed. This method uses a colorimetric detection for the determination of sugars and is used to determine the

concentration of individual sugars making up polysaccharides (66). Results from the Dubois assay showed that sugars were present at low concentrations. Thus a highly concentrated sample amount was chosen for mass spectrometry analysis. Ten milligrams (± 0.5 mg) of crude EPS extract for each sample was found to be a reliable quantity for mass spectrometry analysis. The methods for further sample preparation were next optimised.

6.3.3 Optimisation of internal sugar standards

Due to the co-elution of sugars of the same mass (glucose, galactose, and mannose), heavy labelled ^{13}C sugars were used for direct quantification via standard addition at a final concentration of 0.05 mM. Internal standards (re-suspended in HPLC grade water) were added and 10 mg EPS was re-suspended to a final volume of 50 µl. The ^{13}C sugars were added into EPS samples and are detected at a different mass than the accompanying unlabelled sugar, so amounts can be quantified easier between these sugars of the same mass.

6.3.4 Acid hydrolysis of EPS extracts

Analysis of the constituent monosaccharides of the EPS was carried out by hydrolysis. Acid hydrolysis optimisation involved extensive trials using different reaction conditions. Temperature, length of hydrolysis, and type of acid were optimised to achieve a completely hydrolysed sample at a determinable concentration without extensive charring. EPS samples with and without the heavy labelled sugars were hydrolysed in 2 M trifluoroacetic (TFA) acid or glacial acetic acid (17 M) in screw cap glass universal tubes at 100, 120, or 165 °C for 1, 2, 3, or 4 hours. These acid hydrolysis trials were carried out on mannitol-derived C1576 EPS. In the end, the decision was made to use the stronger, TFA acid at 2 M (as was previously reported in the literature (51)) as the acetic acid did not completely or as effectively hydrolyse the polysaccharide samples, observed as groupings of steep chromatogram peaks at high retention times that did not align with any standards used. Also, the length reported in literature for a 2 M TFA acid hydrolysis for 2 hours was shortened to 1 hour, as there was less apparent charring but still complete hydrolysis at the 1 hour time

point. Literature sources reported using the higher 165 °C temperature; based on previous Ph.D. research work in the lab of Professor N. Smirnoff (221), the temperature was decreased slightly to 110° C, which still proved effective with a 1 hour hydrolysis of the polysaccharide constituents. Finally, during the hydrolysis step, an issue arose with evaporation of the sample which resulted in low concentration of sugars in early mass spectrometry results. A switch from glass universals during acid hydrolysis to air-tight Teflon capped-Reacti-vials was made to avoid the issue of sample loss during acid treatment. These steps to optimise the acid hydrolysis process of sample preparation greatly improved the amount of sugars detected by mass spectrometry making detection and analysis robust. Following acid hydrolysis, the sample was snap frozen, freeze dried, and re-suspended in 50 µl HPLC-grade H_2O (original starting material was 10 mg ± 0.5 mg freeze-dried EPS).

6.3.5 Glucose oxidase treatment of EPS extracts

Finally, for each type of EPS sample, the separation of glucose and galactose for quantitation was difficult, even with standard addition of heavy labelled sugars in each sample. For each mannitol- and fructose-derived EPS sample from *B. multivorans* ATCC 17616 and C1576, there were three sample preparations: (i) acid hydrolysed, (ii) acid hydrolysed with ^{13}C labelled sugar (for standard addition quantitation), and (iii) acid hydrolysed glucose oxidase-treated ^{13}C labelled (spiked for standard addition). The glucose oxidase treatment selectively destroyed glucose using glucose oxidase, catalase, followed by an acetonitrile precipitation to remove protein. By creating these three types of samples for each *B. multivorans* EPS extract the different sugars even of the same mass were detectable as separate entities. An attempt at also using the galactose oxidase enzyme was carried out; however reaction conditions were not optimised further once the glucose oxidase destruction was proven successful (Figure 6.2). EPS extracts with and without glucose-oxidase treatment and EPS samples with or without standard addition of ^{13}C labelled sugars, allowed for quantified concentration by comparing the difference between the individual sugar peaks in chromatograms.

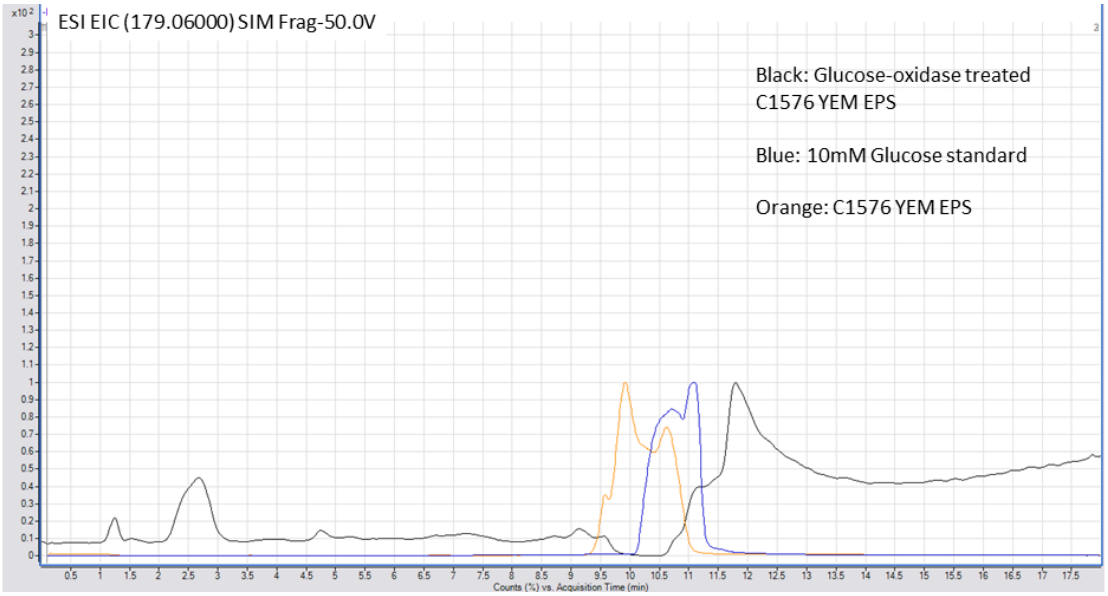

Figure 6.2. Destruction of a glucose by glucose oxidase. 10 mM glucose shown in blue line is a standard. *B. multivorans* C1576 mannitol-derived EPS was treated with glucose oxidase (black line), or was not treated by glucose oxidase (orange). Graph axes show counts vs. acquisition time. The mass-to-charge ratio (m/z) of each sugar is 179.06. The glucose-oxidase treated sample shows no peak where the glucose standard lies.

6.3.6 QQQ-LCMS method

The triple quadrupole (QQQ) MS was used for the task of performing targeted analysis for mannose, galactose, glucose and rhamnose. The HPLC and MS source parameters were previously optimised for hexoses and other sugars based on work carried out in sugar analysis by Dr. Hannah Florance and Dr. Mike Page (University of Exeter). Raw data was processed using MassHunter Qualitative and Quantitative software (Agilent). Data obtained from mass spectrometry runs were analysed in Microsoft Excel spread sheets for quantitative, standard peak addition and standard curve analysis. 1-way ANOVA statistical analyses and post-tests were then applied to identify if there were significant differences in EPS composition of samples from different carbon sources and different strains. The mobile phase buffers used for QQQ-LCMS analyses were optimised to improve chromatography and resolution. Mobile phase A was 90 % LCMS grade acetonitrile and 10 % H_2O, with 0.1 % ammonia. Mobile phase B contained 10 % LCMS-grade acetonitrile and 90 %

LCMS grade H_2O with 0.1% ammonia and 5 mM ammonium formate. Ammonium formate improved chromatography but decreased sensitivity; ammonia balanced this out by improving the sensitivity of detection.

6.3.7 Data processing

Following QQQ-LCMS runs, raw data was analysed with MassHunter software (Agilent) and the software was used to calculate peak areas for the sugars of interest in EPS samples. This analysis was limited to detection of glucose, mannose, galactose and rhamnose by mass. Concentrations of sugars were estimated based on the standard curve for each individual sugar taken from the mixed sugar standard chromatograms. ^{13}C –internal standard (spiked) samples were used to directly calculate sugar composition relative to the un-spiked samples by:

$$\text{Signal Spike} = \text{Signal Spiked} - \text{Signal Sample}$$

Then the instrument response was calculated per unit of measure (mM)

$$\text{Instrument Response } (nmol^{-1}) = \text{Signal}_{\text{Spike}} / \text{Conc}_{\text{Spiked}}$$

Followed by calculation of concentration by dividing the sample signal by the instrument response, or

$$\text{Conc}_{\text{Sample}} = \text{Signal}_{\text{Sample}} / \text{Response } (nmol^{-1})$$

The dilution factor was accounted for in the sample by

$$\text{Final Conc}_{\text{Sample Ext}} = \text{Conc}_{\text{Sample Extract}} * \text{Dilution factor}$$

Where

$$\text{Conc}_{\text{Sample Extract}} = (\text{Conc}_{\text{Sample}} / 5\ \mu l) \times 50\ \mu l$$

Then concentration of sample in dry weight material from extract was determined by

$$\text{nmol per g} = (\text{Final Conc}_{\text{Sample Ext}} * 1000/10\ mg)$$

These equations were built into an Excel worksheet where retention times, injection volumes, peak areas (manually selected from data files using the Agilent workstation MassHunter software) and amount of starting material were input into the spread sheet and automatically calculated to minimise errors in calculations from one experiment to another.

6.3.8 B. multivorans EPS composition analysis

Detection of individual sugars was successful after extensive optimisation of sample preparation. Figures 6.3 and 6.4 represent at least three combined biological replicates from different EPS sample extractions of mannitol- and fructose-derived EPS. These EPS samples were subjected to the same processes of extraction, sample hydrolysis and/or standard addition. Figure 6.3 shows EPS composition profiles of *B. multivorans* ATCC 17616, the environmental isolate (Figure 6.3 (a, b)), and C1576, the CF outbreak-isolate (Figure 6.3 (c, d)). Based on the reports that state ATCC 17616 produces only cepacian, and C1576 a mixture of different EPS types, the ratios of sugar composition were compared to known cepacian sugar ratios. As previously stated, the cepacian RU (based on analysis of *B. pyrrocinia* EPS) contained rhamnose, mannose, glucose and galactose in a ratio of 1:3:1:1. ATCC 17616 is reported to produce only cepacian; a comparison of ATCC 17616 mannitol-derived EPS with cepacian reveals altered rhamnose, mannose, and galactose average (EPS molar ratio of 2:5:1:3 of rhamnose, mannose, glucose, and galactose). Differences between the ATCC 17616 EPS from YEM and cepacian could be due to the technical variation in the mass spectrometer. The ratios of individual replicates were pooled (n= 4 run on the same mass spectrometer but on different days) and error could have been introduced by sample variation from differing mass spectrometry runs. The content of ATCC 17616 YEM glucose and galactose was significantly different (1:3 ratio), whereas the cepacian glucose to galactose ratio is 1:1.

The ATCC 17616 fructose-derived EPS had a rhamnose, mannose, glucose and galactose profile of 3:2:1:4. Clearly, these ratios are again different from cepacian, possibly due to technical variation but also potentially due to

fructose altering the EPS profile of ATCC 17616. Although the mannitol and fructose molar ratio comparison is not significantly different between strains or carbon-sources, this could be due to technical variability between mass spectrometry runs (see Table 6.1) rather than actual lack of significant differences. One EPS sample was run on different days (in order to assess the technical variability from day-to-day use of the mass spectrometer). This did result in different concentrations of sugar measured. The sample C1576 YEM EPS extract actual sugar concentrations are shown in Table 6.1, but similar observations were made for all other EPS samples. Table 6.1 shows clear technical variation and inconsistencies from one sample run (1^{st} run, 2^{nd} run) for some sugars on the QQQ-LCMS. The most obvious variability lies in quantification of glucose and galactose are the two sugars most clearly drastically different from one mass spectrometry analysis to another. Although the average molar ratio of C1576 YEM between rhamnose and galactose is significant, as is the glucose and galactose content comparison (Figure 6.3), these significant differences were not present in the C1576 fructose-derived EPS. Compared to cepacian, C1576 YEM contains more galactose but less mannose than cepacian, by the rhamnose, mannose, glucose, galactose ratio of 1:2:1:5 (C1576 fructose-derived EPS was also different from cepacian – with ratio for the same sugars estimated as 3:2:2:3). Though the differences between cepacian and C1576 samples would be interesting due to the fact that C1576 is known to produce multiples types of polysaccharide, results are not reproducible from one run on the mass spectrometer to another so differences cannot be confidently assigned to carbon source or strain variation.

Table 6.1. Technical variability in sugar analysis method. A *B. multivorans* C1576 EPS composition profile is shown. The same EPS extract sample from mannitol grown C1576 was run under the same mass spectrometry conditions, on two different days. Rhamnose concentration did not vary, but mannose, galactose and glucose concentrations did. 1st, 1st run; 2nd, 2nd run.

	Sugar concentration (mM)							
B. multivorans	**Rhamnose**		**Mannose**		**Galactose**		**Glucose**	
Strain/EPS	**1^{st}**	**2^{nd}**	**1^{st}**	**2^{nd}**	**1^{st}**	**2^{nd}**	**1^{st}**	**2^{nd}**

C1576 mannitol	0.041	0.042	0.001	0.006	0.007	0.018	1.050	0.110

Although there could have been some minor biological variability, the methods used for Bcc growth and EPS extraction are well established in the literature for studying Bcc EPS. The present study only utilised one mass spectrometry technique to study EPS composition. Other research groups specialised to work in polymer and carbohydrate chemistry interrogate composition, acetylation status, and structure of EPS samples, and therefore a more comprehensive approach using a variety of techniques would be useful for future research, which should be focused on developing a more specific method for sugar composition and develop a way to differentiate sugars of the same mass (glucose, mannose, galactose) by more reliable means. In Figure 6.4, the EPS of both *B. multivorans* strains is compared from both carbon sources. There appear to be potential differences between ATCC 17616 and C1576, and between strains grown on the same sugars, but there were no significant differences of comparisons between individual sugars. The data presented in Figure 6.4 is the same molar ratios presented in Figure 6.3, only combined and compared in different ways. One key point to remember is the large error bars from the composition analysis of *B. multivorans* EPS was the technical issues with reproducibility. Therefore it is difficult to draw conclusions until further studies are undertaken as the impacts of different EPS-inducing sugars on *B. multivorans* EPS composition.

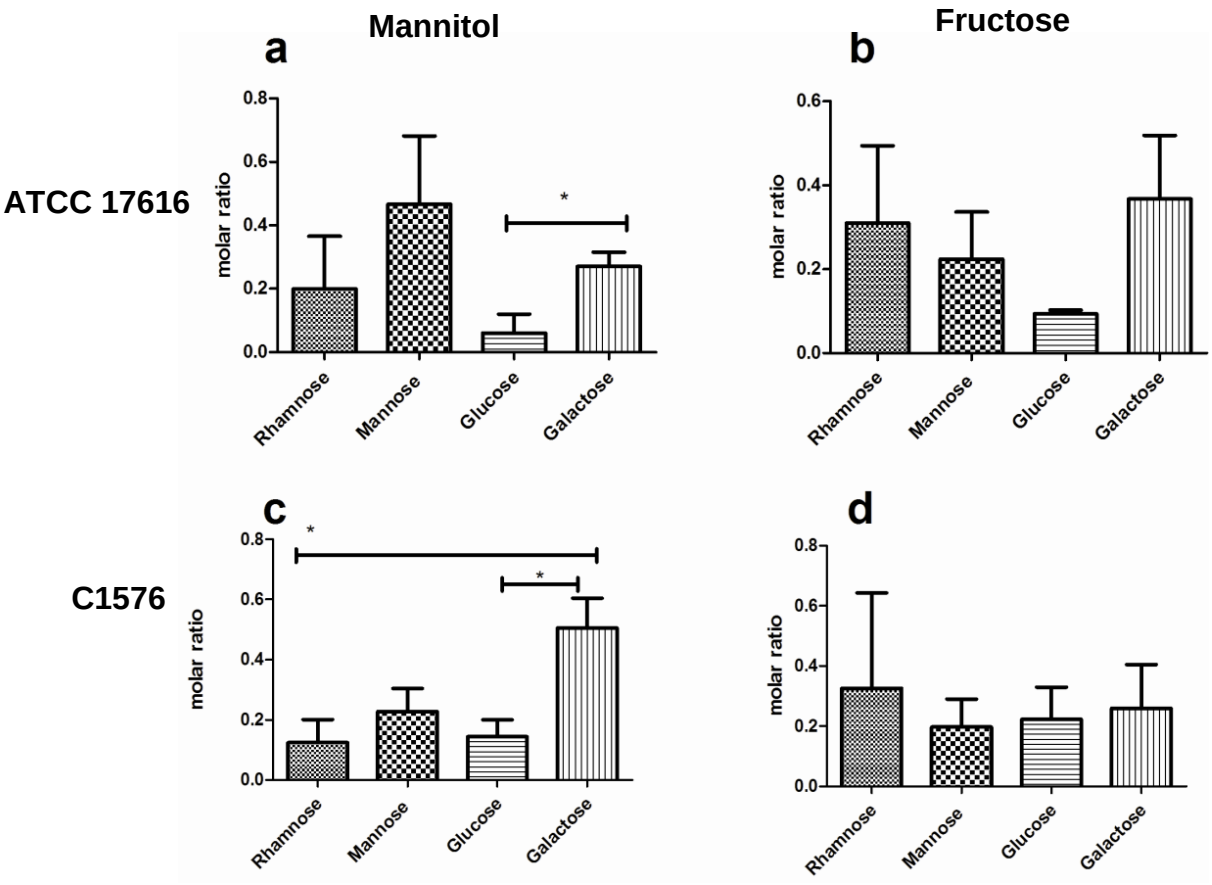

Figure 6.3. Composition of B. multivorans EPS profiles. Fructose- and mannitol-derived EPS profiles from *B. multivorans* ATCC17616 and C1576. ATCC17616 EPS derived from mannitol (a) contains significantly less glucose than galactose and in the fructose derived EPS from the same strain; this same difference exists (b) but is not statistically significant. C1576 EPS derived from mannitol contains significantly more galactose that glucose or rhamnose (c) whilst these differences are not observed in the fructose derived EPS from the same isolate (d). * $P < 0.05$, 1-way ANOVA analysis.

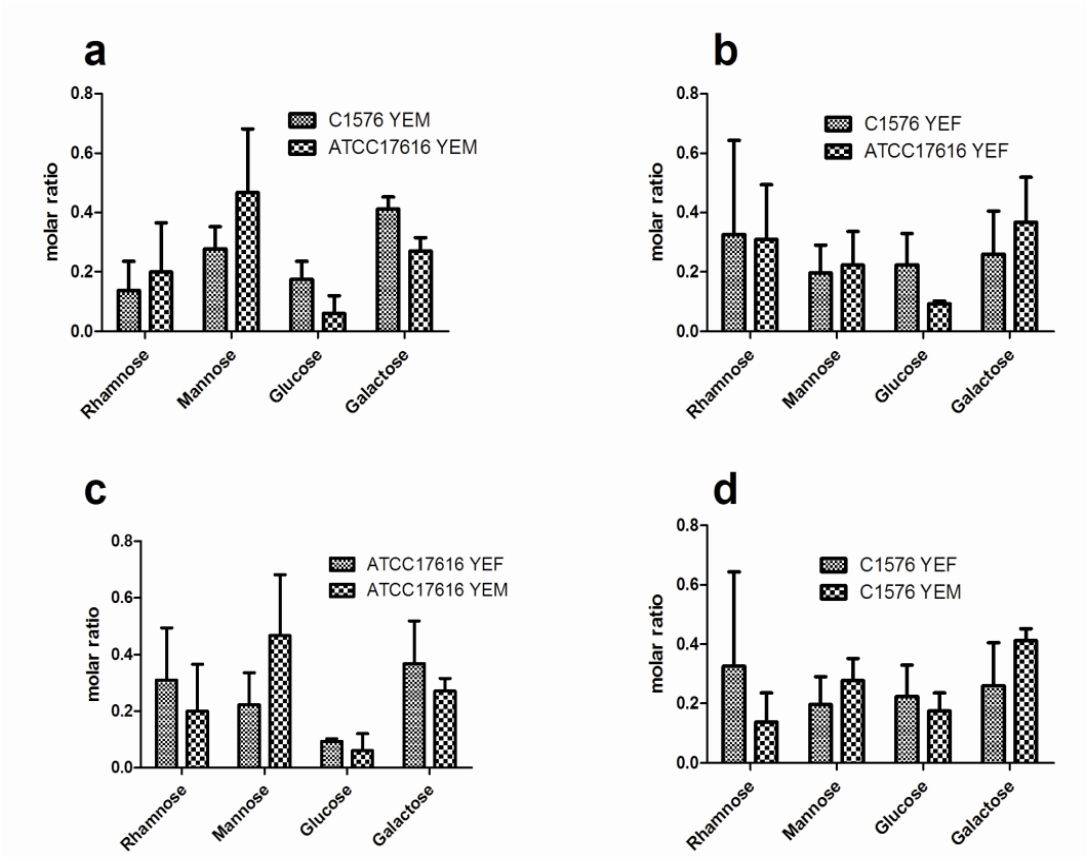

Figure 6.4. Relative comparisons between mannitol-and fructose-derived B. multivorans EPS. EPS profiles compared between *B. multivorans* ATCC 17616 and C1576. Molar ratios were calculated, and no statistical differences between EPS derived were observed, likely due to large variation between replicates, as indicated by SEM error bars. Data shown are mean values of 3-4 biological replicates.

6.4 Discussion

Previous chapters of the present dissertation have discussed the wide-reaching impact of carbon source on the phenotypic and transcriptomic behaviour of *B. multivorans*. The present chapter aimed to assess the impact of carbon source on the actual composition of EPS. Chapter 7 will focus on the impact different carbon sources have on the biological activity of EPS. *B. multivorans* C1576 grown on mannitol produces a mixed polysaccharide based on previous reports. Knowledge of the composition of polysaccharides is useful for understanding EPS properties, tailoring polymers with desired characteristics, and providing insight into potential antigenic interactions or

properties (88). EPS production has been detected in numerous clinical and environmental Bcc isolates following growth with mannitol (68,88,142). Results from mass spectrometry-based analysis of C1576 EPS derived from fructose versus mannitol indicates that the sugar ratios do not differ significantly depending on carbon source used for growth or strain type.

Concerning the impact different sugars and EPS induction have on phenotypic behaviour (see previous Chapters 3 and 5) and gene expression profiles (see previous Chapters 4 and 5) growth on mannitol, fructose, glucose and mannose altered phenotypic behaviour and gene-expression with regards to virulence-relevant traits. These results were largely EPS-independent, even though mannitol and fructose both induce EPS production in *B. multivorans* wild-type ATCC 17616 and C1576. Thus, though the present study could not conclude definitely whether different sugars impact EPS composition, the body of work presented in this dissertation still suggests altering the carbon source used to induce EPS production broadly influences the behaviour of the whole organism.

Future study, beyond the scope of this dissertation, could assess incorporation of mannitol and fructose during growth and EPS production in *B. multivorans* through the use of radio-labelled ^{13}C sugars as growth substrates. This would assess whether *B. multivorans* uses an EPS-inducing sugar in carbohydrate metabolism or solely as a means to induce EPS production. Future work is required to improve current EPS compositional analysis and define structural alterations different carbon sources may have on EPS. This could involve NMR analysis of EPS for structural analysis. Improved mass spectrometry analysis to enable sugar composition content would seem prudent, as the methods and equipment applied to the present study was not a reliable technology for assessing EPS composition. It was also not a good method for determining if different types of polysaccharides were present in the different EPS extracts. One direct way of assessing if ATCC 17616 takes and converts mannitol to mannose preferentially would be to grow ATCC 17616 on growth media with ^{13}C mannitol. By detection of different sugar fractions, the presence of ^{13}C labelled break down products such as mannose, or other

labelled sugars, would indicate mannitol is broken down during metabolism, rather than acting solely as a signal of EPS production. Since *Burkholderia* breakdown mannitol into mannose, detection of ^{13}C labelled mannose of fructose (products of *B. multivorans* mannitol and fructose sugar metabolism), it could be inferred that if C1576 and ATCC 17616 contain different ratios of these ^{13}C labelled breakdown products, the two strains metabolise or utilise mannitol differently and may therefore produce EPS differently.

Fructose and mannitol both induce EPS production in the Bcc. Though cepacian is the most commonly isolated EPS, some strains produce more than one type of polysaccharide. It may be beneficial for an environmental organism or clinical isolate to produce different types or switching EPS to allow for adherence modification depending on environment, surface properties, or stress. Further study on EPS induction and biosynthesis, and importance of carbon source on the structure and function of EPS are required to better understand the biological significance and impacts of mannitol, fructose, and other EPS inducing sugars, on the Bcc.

6.5 Conclusions

1. *B. multivorans* ATCC 17616 and C1576 EPS derived from fructose or mannitol did not significantly differ in glucose, rhamnose, galactose, or mannose composition using the methods utilised in this study.

2. Future research should utilise more reliable and technically reproducible means to quantify composition of EPS.

Chapter 7: Differences in biological activity between fructose- and mannitol-derived *B. multivorans* exopolysaccharide

7.1 Introduction

The present study furthers work from previous chapters concerning EPS and the influences of different sugars on *B. multivorans* phenotypic behaviour, gene expression, and EPS composition. Mannitol and fructose are sugars that induce the biosynthesis of EPS members of the Bcc. Mannitol was recently approved as an inhaled osmolyte in CF patients, and fructose has been reported to be elevated in diabetics. Levels of fructose in the lung have not been reported, but glucose is elevated in the airways of diabetics (29). As a virulence factor, EPS may be a protective barrier against immune system detection, and aide in establishing mature, architecturally sound, biofilms that are difficult to eradicate in the CF lung (51,56). Environmental Bcc could utilise EPS as a means of attachment during initial colonisation and close association with plant roots for nitrogen fixation purposes (69).

EPS can act as barrier against metal toxicity. Iron is elevated in CF sputum (84), lavage fluid, and lung tissues (74). Bcc EPS is protective against desiccation and iron toxicity (but not zinc) (69). Bcc EPS protection from drying could result in persistence in the home or hospital environment, thus providing a source for environmental acquisition. A significant part of the innate immune response is neutrophil influx to the CF lung are toxic reactive oxygen species (ROS), which are highly bactericidal. Bcc mannitol-derived EPS is protective against ROS (33). However, all knowledge of the Bcc EPS and the impact of mucoidy have stemmed from analysis of biological activity, composition and structure of EPS derived solely from growth on mannitol. Fructose or any other EPS-inducing sugars have not previously been included in these studies.

This study provides evidence for carbon source specific biological activity, indicating for the first time that growth in either fructose or mannitol alters *B. multivorans* EPS biological activity. EPS protection could be related to stress resistance pertinent to the environmental and opportunistic lifestyle of *B. multivorans*.

7.2 Aims

1. This study aimed to assess *B. multivorans* biological activity of fructose- and mannitol-derived EPS through iron toxicity and desiccation survival assays.

2. The ability of mannitol- and fructose-derived EPS to scavenge ROS was also assessed.

7.3 Results

7.3.1 EPS protection from iron toxicity stress is strain- and carbon source - dependent.

The protective effect of EPS against toxic levels of iron (Fe^{2+}) was assessed. EPS was extracted from mannitol or fructose grown *B. multivorans* ATCC 17616 and C1576, using the methods described previously (Methods section 2.20). *B. multivorans* ATCC 17616 and C1576 were grown overnight in mannose broths. *B. multivorans* was then challenged with toxic levels of Fe^{2+} at a concentration of 50 mM ferrous sulphate, in the presence or absence of EPS.

Results showed that following iron ion stress with ferrous sulphate, neither fructose- nor mannitol derived EPS significantly protected ATCC 17616 from Fe^{2+} toxicity (Figure 7.1(a), at 1 hour and 3 hour time points. In contrast, C1576 incubated with mannitol-derived EPS was protected from Fe^{2+} toxicity compared to the no- EPS control (C1576 mannose) at the 1 hour time point (Figure 7.1(b).

Carbon source-dependent protection of C1576 fructose-derived EPS and mannitol-derived EPS was compared. The C1576 mannitol-derived EPS was significantly protective against iron toxicity. Fructose-derived EPS was not protective. C1576 fructose-derived EPS was not protective compared to the no-EPS control C1576 Mannose, and significantly reduced in survival compared to the mannitol-derived (YEM) EPS. Therefore, *B. multivorans* EPS confers resistance to iron toxicity protection in a carbon source- and strain-dependent and manner.

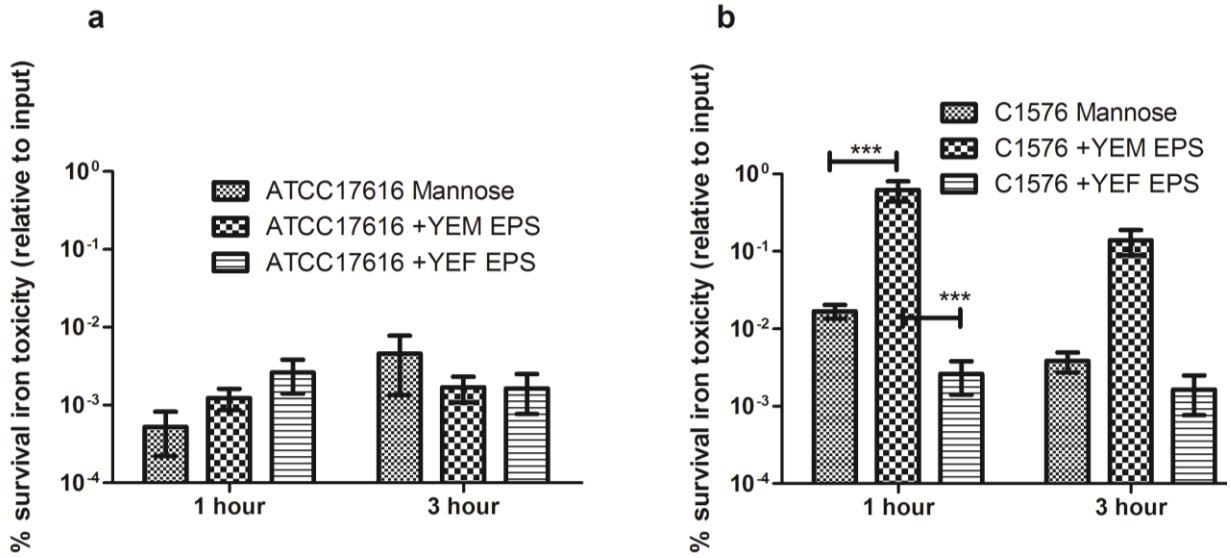

Figure 7.1. EPS protection of B. multivorans to 50 mM of iron stress. YEM, mannitol-derived EPS; YEF, fructose-derived EPS. Graph shows (a) 1 hour and 3 hour time points representing percentage survival relative to input of *B. multivorans* ATCC 17616 (b) 1 and 3 hour time point representing percentage survival relative to input of *B. multivorans* C1576. N=3 wells per condition. Statistical significance was assessed with 1-way ANOVA analysis and Tukey- post-test (*** $P < 0.0001$).

Although the C1576 three hour time points appears significant when comparing C1576 Mannose to the YEM (Figure 7.1 (b)) they are not. Additionally, there are statistical significances between strains, with the C1576 no-EPS control survival the iron exposure significantly better after 1 hour than the ATCC 17616 no-EPS control ($P< 0.001$ ***) and the C1576 mannitol-derived EPS conferring resistance to iron toxicity significantly better than the ATCC 17616 mannitol-derived EPS (which was not protective at all to the ATCC 17616 no-EPS control).

7.3.2 Effect of EPS on desiccation survival is strain - and - carbon source dependent

The effect of EPS on protection from desiccation was assessed. *B. multivorans* ATCC 17616 and C1576 were grown overnight in mannose. Then, with or without the addition of fructose- or mannitol-derived EPS, samples aliquots were added to wells of a polystyrene 96-well plate, air dried, and then

kept at 30° C for several days of desiccation. Viable counts were taken by rehydrating wells with sterile PBS and plating serial dilutions onto LB agar.

After three days of desiccation, fructose-derived EPS from the environmental isolate ATCC 17616 was significantly protective against desiccation compared to the mannitol-derived EPS and the no-EPS control (ATCC 17616 Mannose) shown in Figure 7.2 (a); an asterisk above the YEF EPS sample indicates significant relative to the no-EPS mannose control. ATCC 17616 mannitol-derived EPS was not protective at all relative to the no-EPS control, and thus significantly reduced in survival relative to the fructose-derived EPS (significant at days two and three, signified by the bar between the two samples). Desiccation survival drops between day one and day two for all groups in Figure 7.2 (a).

Both fructose- and mannitol-derived EPS protected C1576 after one day of desiccation, although not significant statistically (Figure 7.2 (b)). Following an overall drop in viability on day two, the mannitol-derived EPS resulted in significantly better C1576 survival that with fructose-derived or no-EPS samples. At three days of desiccation, some growth of the surviving viable cells brought percentage survival level in all three conditions after three days desiccation. This suggests C1576 in all conditions was able to survive desiccation better than the ATCC 17616 no-EPS and YEM EPS samples.

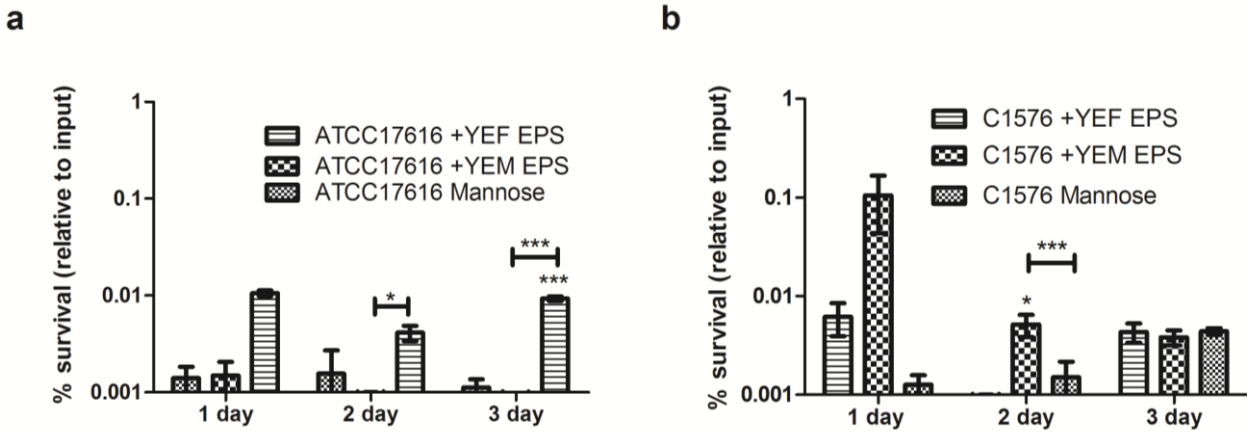

Figure 7.2. Effect of EPS against desiccation. Graphs show EPS derived from mannitol and fructose grown *B. multivorans* ATCC 17616 (a) and C1576 (b) in desiccation assay. Bars represent the percentage survival relative to input after 1, 2 and 3 days. YEM = mannitol-derived EPS, YEF = fructose-derived EPS. N=3, Asterisks with bars below indicate comparison between two conditions. Asterisks without a bar represent significant difference relative to mannose no-EPs control. Statistical significance assessed using 1-way ANOVA and Tukey post-test (P <0.05 *, P< 0.001 ***).

Contamination was monitored over the three day desiccation time points by re-hydrating un-inoculated and plating onto LB agar. Still, it is clear a higher number of cells were recovered after several days in desiccation exposure for both strains. It is possible that EPS shielded surviving cells and these survivors replicated, as the temperature of incubation during the desiccation assay (30° C) supports growth in most members of the Bcc. EPS could lock in moisture and protect cells from drying out, leaving them potentially still metabolically active during desiccation. Interestingly, after two days of desiccation, both mannitol- and fructose-derived EPS from the clinical isolate C1576 survived significantly better than ATCC 17616 with both types of EPS (*P< 0.001* ***, *, respectively).

7.3.3 B. multivorans ATCC 17616 EPS, but not C1576 EPS, scavenges ROS

The xanthine/xanthine oxidase and peroxidase cell free system was used for the generation of ROS. Chemiluminescence (CL) detection with isoluminol was utilised to measure hydroxyl radical generation. CL was measured in a fluorescent plate reader, and EPS (added to reactions to intercept the hydroxyl

radical reaction with isoluminol) or SOD (catalyses superoxides to hydrogen peroxide and oxygen rather than hydroxyl radicals). The reaction scheme is summarised in Figure 7.3.

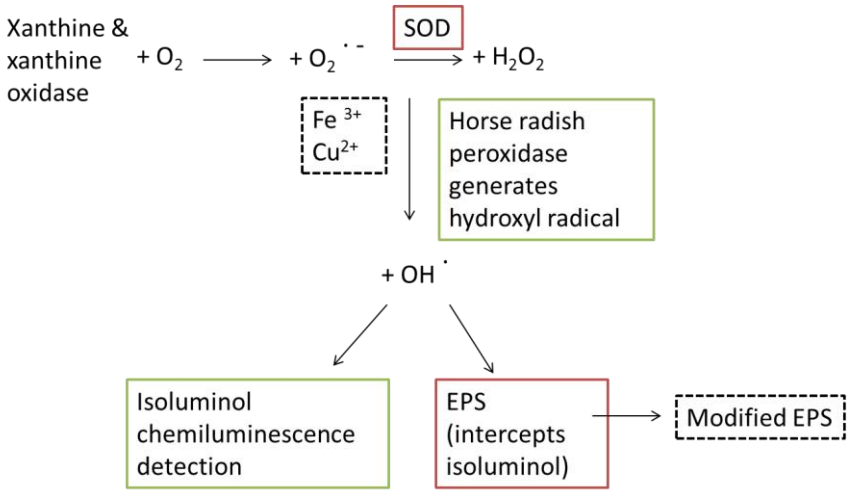

Figure 7.3. Chemical generation of ROS and hydroxyl radical generation with detection by isoluminol. Xanthine and xanthine oxidase react with molecular oxygen to give reactive oxygen species (ROS). The peroxidase was added (green box, horse radish peroxidase) to generate hydroxyl radicals; some of the ROS transitions to hydrogen peroxide. The enzyme SOD (red box) favours the ROS shift to generation of hydrogen peroxide and oxygen rather than hydroxyl radicals. Isoluminol detects the hydroxyl radicals generated in this system, and if EPS is added (red box), this detection is intercepted. Once the EPS and hydroxyl radicals have interacted, the polysaccharide is modified further (dashed black box, not assessed in this assay were what modification were incurred by the EPS). The chemiluminescence signal was collected using a fluorescent plate reader. Iron, copper, and other transition metals (not included in the assay for the present study – dashed black box) can scavenge ROS and prevent reactive oxygen from interacting with the peroxidant and becoming hydroxyl radicals.

In the presence of molecular oxygen, xanthine/xanthine oxidase converts to oxygen radicals, which then are converted in the presence of a peroxidase to hydroxyl radicals, which can be scavenged by polysaccharides. Isoluminol detects hydroxyl radicals and generates CL, indicative of the presence of ROS (specifically hydroxyl radicals). Superoxide dismutases (SOD) catalyse the dismutation of superoxides into oxygen and hydrogen peroxide. This same *in*

vitro ROS system was previously reported in a study that showed mannitol-derived EPS from *B. cenocepacia* quenched ROS production (33).

This study assessed the ability of EPS from *B. multivorans* grown on mannitol and fructose, to quench ROS production in the xanthine/xanthine oxidase system. CL generation allowed for the quantification of the EPS intercepting the isoluminol CL reaction with hydroxyl radicals. This percentage interception of CL ROS detection was calculated with the following equation: % interception of CL response by EPS or SOD = ((normal activity – SOD/EPS CL response)/normal activity)*100, where 'normal activity' was the no-EPS control, and intercepted CL response was by either the SOD or *B. multivorans* EPS intercepting the hydroxyl radicals from detection by isoluminol. Figure 7.4 shows the xanthine/xanthine oxidase CL reaction for three different conditions. Each graph shows the superoxide dismutase (SOD), which inhibits hydroxyl radical production, and the no-EPS control where ROS are generated and peroxidated to hydroxyl radicals and fully detected by isoluminol. C1576 fructose EPS (Figure 7.4(a)) and mannitol EPS (Figure 7.4(b)) intercepted or scavenged nearly 100 % of the hydroxyl radicals, judged by the CL signal response near 0. The EPS concentration used for reaction inhibition was 1 mg/ml. The same trend was observed for C1576 EPS at 0.5 mg/ml EPS concentration (data not shown).

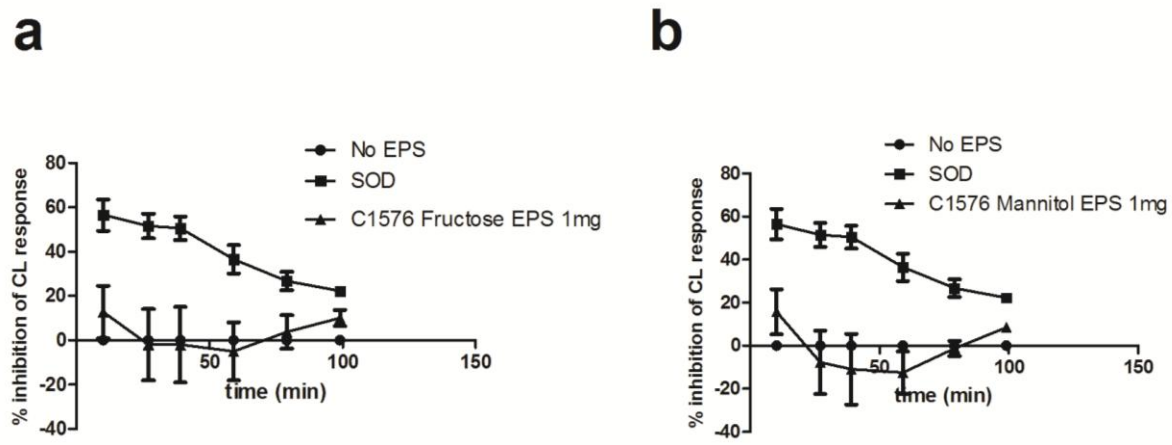

Figure 7.4. In vitro production of ROS and EPS. Graph shows percentage inhibition of CL response. C1576 EPS intercepted the CL response from isoluminol detection of ROS by scavenging hydroxyl radicals. Fructose- and mannitol-derived EPS was used at 1 mg/ml EPS, reaction conditions (a-b). SOD used as control for prevention of hydroxyl radical generation. N=4 wells per reactions condition.

Figure 7.5 depicts the same controls as used in Figure 7.4, with the negative control SOD and no-EPS control intercepting (or not) the % CL response. Figure 7.5 shows % CL response in the presence of ATCC 17616 fructose- and mannitol-derived EPS (Figure 7.5 (a-b)). The same trend was observed for 0.5 mg/ml EPS (data not shown).

Although there were no significant differences between the ability of mannitol-or fructose-derived EPS to scavenge ROS, there is observed strain variation in ability to scavenge ROS. C1576 EPS did not scavenge ROS but ATCC 17616 EPS did. ATCC 17616 fructose-derived EPS scavenged hydroxyl radicals and thus quenched the CL response relative to C1576 fructose-derived EPS in this system ($P = 0.031$). ATCC 17616 mannitol-derived EPS scavenged ROS significantly better in this system compared to C1576 mannitol EPS ($P = 0.0073$). No carbon-source specific differences in biological activity were observed in this assay.

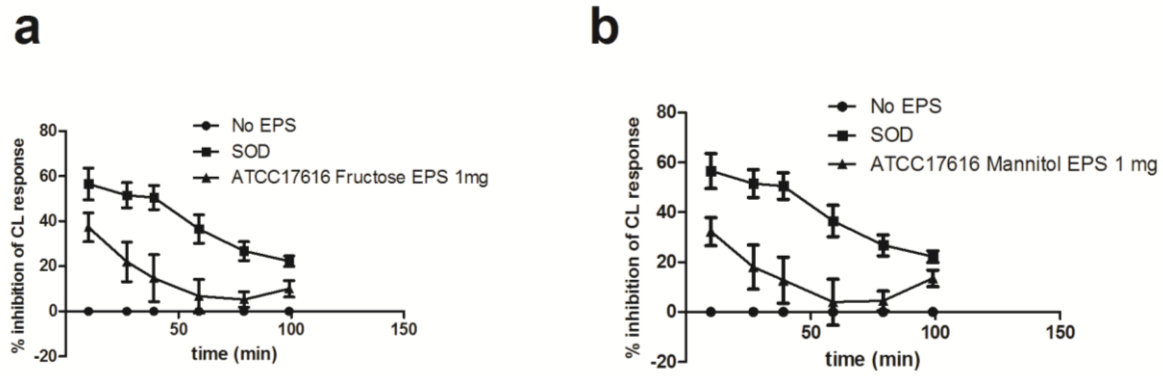

Figure 7.5. In vitro production of ROS and EPS. Graph shows percentage inhibition of CL response. 1 mg fructose- and mannitol-derived ATCC 17616 EPS intercepted the CL detection of hydroxyl radical production (a, b). SOD was used as control for reaction. N=4 wells per reactions condition.

7.3.4 Summary of strain and carbon source variation in biological activity

The carbon source and strain influence the biological activity of *B. multivorans* EPS, depending on the type of assay used to assess biological activity. Subtle alterations in EPS composition, due to growth on different carbon sources could change polysaccharide structure and environmental interactions. No studies to date have compared the biological of activity of Bcc EPS from any other carbon source besides mannitol. Table 7.1 summarises the protective effect of EPS in stress conditions, namely iron toxicity, desiccation, and exposure to ROS.

Table 7.1. Biological activity of EPS summarised for B. multivorans strains ATCC 1616 and C1576. In the table, 'Yes' or 'No' indicates EPS does or does not play a role in protection from iron stress, desiccation, or EPS does/does not scavenge ROS in the xanthine oxidase assay.

***B. multivorans* EPS**	**Iron ion stress**	**Desiccation**	**Scavenges ROS**
ATCC 17616 Fructose	No	Yes	Yes
ATCC 17616 Mannitol	No	No	Yes
C1576 Fructose	No	No	No
C1576 Mannitol	Yes	Yes	No

Overall, different strains produce EPSs with differing biological activities. This study compared the biological activity of EPS isolate from two different *B. multivorans* isolates from drastically different origins (soil, CF lung). Not only was there strain –to-strain differences in EPS iron toxicity, desiccation protection and ROS scavenging, but also variation in protection dependent on carbon-source from which the EPS was derived. Survival of desiccation was dependent on the carbon source used to induce EPS biosynthesis for both strains; however, C1576 survived desiccation better with the addition of mannitol-derived EPS, whilst ATCC 17616 survived desiccation following the addition of fructose-derived EPS. Previous studies had shown that mannitol-induced Bcc EPS scavenged ROS, thus it is interesting that C1576 mannitol-induced EPS did not scavenge ROS whilst both ATCC 17616 mannitol-and fructose-derived EPS did.

7.4 Discussion

EPS produced by members of the Bcc is a putative virulence factor and may play roles in host adhesion, signalling, and could act as a physical barrier from toxic substances or stresses (69). It is important to understand the roles EPS may play in the CF host, because studies have shown mucoidy could be indicative of chronic infection; thus EPS could influence bacterial stress resistance and infection outcome in CF patients (233).

Treatment of the CF lung with inhaled mannitol could potentially trigger EPS production *in vivo*. Although fructose induces EPS biosynthesis and is elevated in the blood and urine of diabetics, there is no existing evidence (to the authors' knowledge) that fructose is elevated in air way tissues (as glucose is reported to be (29)). However, fructose induced EPS was included as a means to compare the impact of carbon source on EPS biological activity, in addition to the fact that it is one of several sugars elevated in diabetics.

The three *in vitro* experiments in the present study highlight the biological activity of EPS produced by a *B. multivorans* CF isolate and environmental isolate. Ferreira *et al.* showed *B. cepacia* EPS was not protective to drying or iron ion stress, whilst EPS from *B. multivorans* and *B. xenovorans* was protective from these stresses (69). Bylund *et al.* showed *B. cenocepacia* mannitol-derived EPS, as had been shown for alginate from *P. aeruginosa*, could scavenge ROS (33,180). This study used the same assay as reported in Bylund *et al.*, but used *B. multivorans* fructose-and mannitol-derived EPS.

The present study first assessed the effect of EPS in protection against iron toxicity. Metal concentrations are elevated during pulmonary exacerbations and following lung transplantation (84,155). Ghio *et al.* reported that bronchoalveolar lavage (BAL) fluid from CF patients contains elevated levels of iron, ferritin, transferrin, heme and haemoglobin, thus indicating iron haemostasis is disrupted in the CF lung (74). Iron concentrations used in the present study were higher than levels reported during exacerbation or after lung transplant in CF patients, but if EPS were protective against high concentrations of iron toxicity, it is likely that EPS would protect *B. multivorans* from lower concentrations of iron comparable to elevated levels in the CF lung. Evidence for elevated iron and iron containing proteins is linked to hemosiderin-laden macrophages, reported to be elevated in patients following lung transplantation, and alveolar macrophages are highly practiced at iron uptake (133). It is assumed that macrophages containing iron intracellularly transport metals that can accumulate in the lower respiratory tract following lung transplant or exacerbation. Overall, regardless of the presence of respiratory disease there is

a cycle, and burden, of iron in the lower respiratory tract (200). Although normal levels of iron are required for bacterial survival, a surplus could lead to toxicity.

B. multivorans environmental survival and resistance to disinfectants could be a reservoir for infection, especially if EPS were protective against elements found in disinfectants. Research has been done into the inclusion of various metals and nanoparticles in hospital surfaces, fabrics, cleaning solutions, and antimicrobial treatments to prevent bacterial infection in plants (73,129,146,169). Copper surfaces, for instance, have been shown to kill *Staphyloccocus haemolyticus* via membrane damage (169); if *B. multivorans* were protected by EPS against iron, perhaps if exposed to a copper antimicrobial surface it may also survive. More research is required to assess the protective effect of EPS against other metal stresses. ATCC 17616 the environmental isolate was not protected by killing due to iron toxicity, regardless of whether the EPS was mannitol- or fructose-derived. However, the CF isolate was able to survive iron toxicity better than the no-EPS control when mannitol-derived EPS was added prior to iron toxicity exposure. The C1576 isolate is the index case of a transmissible outbreak of *B. multivorans* in a paediatric CF clinical outbreak (222).

It may be interesting to note that in the transcriptomic analysis of *B. multivorans* sugar response (discussed in Chapter 4), *B. multivorans* C1576 grown in mucoid-inducing YEM relative to non-mucoid growth conditions showed 16 significantly upregulated gene related to iron and other metal containing proteins involved in post-translational modification, and iron-uptake regulators involved in inorganic ion transport. This could indicate that mannitol present in the lung induces iron uptake but could at the same time offer protection from metal toxicity. In the present study, mannitol-derived EPS protected C1576 from iron stress significantly better than YEF-derived EPS and significantly better than mannose-grown (no-EPS) C1576 alone.

In addition to stress survival from environmental metal toxicity, the ability to survive periods of desiccation would be advantageous to an environmental and opportunistic pathogen such as *B. multivorans*. There is the possibility that patients could acquire *B. multivorans* through the same environmental reservoir.

For example, C1576 enhanced environmental survival due to resistance to metal toxicity or desiccation survival could have contributed to the acquisition from the clinical environment. Several reports have been published that identify multiple patients in a specific area that acquired the same strain of *B. multivorans* at the same time (22,125,135,176,222). If bacteria could survive outside the host for several days, the hospital environment could be a mode of transmission, if surfaces and equipment were not thoroughly disinfected or sterilised. Overall however, the mode of transmission for *B. multivorans* is still unknown, and environmental and clinical isolates are often indistinguishable, thus it is largely assumed source of acquisition is from the natural environment (14). EPS protection from desiccation could contribute to environmental survival in the hospital or a manufacturing environment. The process of desiccation occurs in three phases (as outlined by Vriezen *et al.* (220)). The first phase of desiccation (i) involves drying of cells and slowing of the metabolic processes. Secondly, (ii) the storage phase marked by decline of cell viability, and thirdly, (iii) the rehydration phase or the return to viability. On scale with the time line used for the desiccation assay used in the present study, phase one (i) drying of cells would occur during Day 1 where cells were harvested, and dried, then incubated for multiple days. Phase two (ii) the storage phase, would be comparable to the Day 2 and 3 time points of the present study. Ferreira *et al.* suggested that due to the hygroscopic properties of cepacian, it retains moisture, thus retarding the loss of cell viability during the second phase (ii). This would account for the results of the present study, and correlates with findings from Ferreira *et al.* where mannitol-derived EPS protected Bcc strains from desiccation. Interestingly, their study showed no viable counts survived in any of the three species included in their study when no EPS added following three days of desiccation. However, the present study recovered viable cells after three days of desiccation (though only a small percentage, even in the presence of EPS, relative to input). The rate of desiccation is greatly dependent on the presence of salts, moisture and humidity, temperature, and other factors from the surrounding environment (220).

The transmissibility and environmental reservoirs of *B. multivorans* may be influenced by the ability to survive desiccation. Drabick *et al.* demonstrated strain-to-strain variation between survival on different types of surfaces; the greatest survival on PVC plastic being members of the Bcc (64). It has been suggested that subtle differences in environmental survival may be difficult to detect *in vitro* assays because usually only one stress at a time is applied (154), however survival to desiccation is an obvious attribute which would favour environmental persistence and potential reservoir for infection for *B. multivorans*, and based on results from the present study, *B. multivorans* EPS derived from growth on fructose significantly protected from desiccation the environmental isolate ATCC 17616, but not the CF isolate C1576. Mannitol-derived EPS was not protective for ATCC 17616 but protected C1576 from desiccation.

Differences bet**w**een the results of iron and desiccation assays in the present study and Ferreira *et al.*, both of which used *B. multivorans* ATCC 17616, could be due to a number of factors. Firstly, the fact that different growth medias were used prior to EPS extractions; the present study and previous chapters of this thesis have described the impact of different growth media on EPS biological activity, transcriptomic, and phenotypic response of *B. multivorans.* In the *Rhizobia*, Gram-negative nitrogen fixing bacteria produce EPS in culture that is influenced by carbon source. Different carbon sources resulted in different *Rhizobia* EPS composition (92). Additionally, the present study always incubated the *B. multivorans* with the strain specific EPS for the iron and desiccation assays (e.g. ATCC 17616-derived EPS was added to ATCC 17616 and C1576-derived EPS was incubated with C1576). The Ferreira *et al.* study incubated *B. multivorans* ATCC 17616 with cepacian isolated from clinical isolate *B. cepacia* IST408. Therefore Ferreira *et al.* could not analyse strain-dependent EPS effects on stress survival, or the potential for a mixture of polysaccharides, as reportedly produced by C1576 (88), to be included.
In addition to protection from metal toxicity and desiccation, additional environmental stressors such as oxidative stress and reactive oxygen species could be modulated by the biological activity of EPS. Bylund *et al.* studied *B.*

cenocepacia mannitol-derived EPS and found the EPS inhibited neutrophil chemotaxis and scavenged ROS in the xanthine/xanthine oxidase system (33). The present study utilised the same *in vitro* system for generating ROS in order to determine the ability of fructose- or mannitol-derived *B. multivorans* EPS to neutralise or scavenge ROS. The ability to do so could enable pathogens to evade the host immune response to infection, such as avoiding phagocytosis and antimicrobial killing. During chronic inflammation in the CF lung, *B. multivorans* would be exposed to toxic ROS compounds. Elevated iron in the respiratory tissues and other elevated metal concentrations could potentially support the increased generation of ROS, leading to not only an environment with elevated metal concentrations, but also oxidative stressors. These two components have been suggested as a mechanism for inflammatory response in respiratory diseases such as CF and chronic lung disease (155). The primary immune response in the CF lung is an influx of neutrophils. These cells are potent effector cells of the innate immune response that inundate the CF lung. The neutrophil influx in the lung, with end products of H_2O_2 and ROS, could favour the mucoid phenotype if EPS is protective against these components *in vivo*. Mannitol itself is described as a classical example of a hydroxyl radical scavenger (180). Mannitol was used at 100 mM to inhibit the CL response (96 % inhibition) in a cell free system of generating free radicals (180). Inhibition of the CL response with mannitol was dose dependent, and at 0.1 mM did not inhibit the free radical generation/CL response at all. Interestingly, as shown in the schematic depicting the xanthine/xanthine oxidase reaction, transition metals copper and iron both can prevent superoxides from being peroxidated into hydroxyl radicals (180), suggesting that if EPS contained any such trace metals, EPS scavenging could be influenced by the metals contained in the EPS extracts rather than the polysaccharide scavenging hydroxyl radicals itself. In the present study EPS was checked for protein and DNA content, but not metal content, although Bcc-produced cepacian has not been reported, to the authors' knowledge, to contain metals.

The inhaled administration of 800 mg of mannitol for rehydration od the CF lung could have several affects in protecting bacteria in the CF lung .This

concentration of mannitol could not only act as a scavenger of ROS in its own right, but also, by inducing EPS production in *B. multivorans* and other members of the Bcc, mannitol could trigger other mechanisms for ROS scavenging. Based on the xanthine oxidase system, the present study showed *B. multivorans* EPS could scavenge ROS when grown on mannitol and fructose, but this observation was strain-dependent. Based on previous reports that mannitol-derived Bcc EPS could scavenge ROS, it is interesting that clinical isolate C1576 mannitol- and fructose-derived EPS did not scavenge ROS, whilst both EPSs scavenged ROS from ATCC 17616. In its natural environment, rhizosphere isolate ATCC 17616 could require resistance to metal toxicity, desiccation and oxidative stress to enable continued close association with the plant host. If, as mentioned previously, either of the *B. multivorans* metals had EPS that contained metal, the presence of the metal in the polysaccharide could scavenge ROS more efficiently than an EPS that did not, thus a potential explanation of strain-variation.

Fructose- and mannitol-induced EPS is of interest to the present study not only due to the sugars' ability to induce EPS biosynthesis in *B. multivorans*, but also due to *B. multivorans* transcriptomic response to sugars. In Chapter 4 of this dissertation, differences in the gene expression response following growth on fructose and mannitol were compared in the environmental isolate ATCC 17616. Those findings suggested that in fructose, relative to mannitol (YEF vs. YEM), ATCC 17616 upregulated 194 genes including genes related to motility and chemotaxis, EPS biosynthesis, and several different phospholipases and transcriptional regulators. Among the 86 significantly down-regulated genes in fructose relative to mannitol were genes related to amino acid metabolism, succinate dehydrogenases, β-lactamases, ferric iron uptake mechanisms, hopanoid biosynthesis, pilli, type III secretion. The present study of EPS biological activity and these differences in transcriptomic response to the different sugars indicates that although both sugars induce a similar mucoid phenotype, phenotypic behaviour, gene expression, and biological activity of the EPS is dependent on the carbon source.

Evidence for EPS and stress resistance from this study indicate growth on mannitol and fructose could influence *B. multivorans* survival in the CF lung and the environment by altering the EPS biological activity. These studies indicate that the biological activity of EPS can vary depending on the culture conditions used to induce its production. It is not known what factors induce EPS production *in vivo* or in the natural environment, but the present study highlights EPS biological function in stress survival-related assays can be strain- and carbon source-dependent.

7.5 Conclusions

1. *B. multivorans* ATCC 17616 was not protected from iron stress by fructose- or mannitol-derived EPS. *B. multivorans* C1576 was protected from iron toxicity exposure by mannitol-derived EPS. This indicates strain-variation and carbon source variation in EPS protection.

2. EPS derived from fructose was protective of ATCC 17616 during desiccation; however mannitol-derived EPS protected C1576 from desiccation. This indicates protection from desiccation is strain dependent.

3. EPS derived from mannitol and fructose grown ATCC 17616 scavenged ROS, whilst neither C1576 mannitol- nor fructose- derived EPS scavenged ROS, indicating strain variation in ROS scavenging, but not carbon source derived variation.

Chapter 8: Insulin binding by members of the *Burkholderia cepacia* complex

8.1 Introduction

Insulin is an anabolic signalling molecule with the primary function to regulate glucose uptake from the circulatory system in mammals. Insulin deficiency, glucose intolerance, or impaired sensitivity to insulin can lead to the development of diabetes, a serious cause of decline in health of CF patients (28). Cystic Fibrosis Related Diabetes (CFRD) (137) is now the most common comorbidity in patients with CF, occurring in 15-30 % of CF patients over 30 years of age (7). CFRD is designated as a separate entity representing both type 1 and type 2 diabetes traits (232). Diabetes results in increased glucose, mannose and fructose levels in the urine and blood stream (98,153) and glucose elevated in airway tissues (29). It is well established that patients with diabetes mellitus alone are immune-compromised and therefore more prone to infection (4,7). The response of *B. multivorans* to certain sugars of clinical relevance was addressed in previous chapters of this dissertation. The focus of the present study was to assess the relevance of the onset of diabetes (which further immune compromises patients) and potential impacts of interactions between members of the Bcc and insulin. It is known that some members of *Burkholderia* bind insulin. *B. pseudomallei* possesses specific high affinity binding for human insulin (227) and this affinity appears to be influenced by insulin levels (96). *B. cepacia* was reported as able to bind insulin, potentially due to acid phosphatase activity (96). A consistent pattern of patients presenting melioidosis (of which the causative agent is *B. pseudomallei*) were diabetics (40,156,227). Ultimately, although known to bind insulin, the impact of that binding on the progression of infection in *B. pseudomallei* and members of the Bcc is unknown. Observations of insulin binding by *B. pseudomallei* and members of the Bcc prompted further study of additional members of the Bcc (96,141,227).

8.2 Aims

1. Determine the ability of members of the Bcc to bind insulin.

2. If Bcc members do bind insulin, is insulin binding consistent across the whole population, and can insulin binding be enriched for?

3. Assess whether Bcc insulin binding correlates with a ceftazidime- or ciprofloxacin-derived persister cell phenotype.

8.3 Results

8.3.1 Screening for insulin binding in the Bcc

Firstly, the ability of members of the Bcc to bind insulin was assessed based on the methods described by Kanai *et al.* and Nisr *et al.* (96,141). Both methods involved the use of FITC-labelled insulin (197).The Kanai *et al.* protocol reported an insulin binding method that had used an ATCC strain of *Pseudomonas aeruginosa* as a negative control which allowed a basis of comparison to insulin binding strains. Unfortunately, the *B. (Pseudomonas) cepacia* insulin binding strains used in the Kanai *et al.* study were not obtainable, although efforts were made to obtain the original strains from the authors or strain collections in order to have a positive control. The Kanai *et al.* method fixed agar-grown bacterial cells, 'stained' them with insulin, incubated for 45 minutes at 37° C, and visualised insulin binding by fluorescent microscopy.

During the course of the present study, Nisr *et al.* published a method that provided an improved, more descriptive and quantitative protocol for insulin binding. The method included a more detailed microscopy method and quantitation of insulin binding using fluorescent plate reader technology. Nisr *et al.* reported just three of the 45 microorganisms screened in their study bound insulin: CF isolates of *B. multivorans, B. cenocepacia*, and *Aeromonas salmonicida* (a fish pathogen). The method involved using MOPS buffer during insulin exposure, followed by centrifugation and washing steps with PBS. Insulin exposure was at room temperature, and cells were not fixed to slides with acetone prior to insulin exposure as in the Kanai *et al.* protocol. Rather than using acetone for fixing insulin-exposed cells, the Nisr *et al.* method used air drying and brief heat fixation. The Nisr *et al.* method was adopted for insulin binding plate reader assays and adapted for use in flow cytometry and persister cell assays. Using fluorescent microscopy (Figure 8.1), the FITC-insulin levels indicative of insulin-bound bacteria were significantly higher compared to levels of auto fluorescence or background fluorescence for positive insulin binding strains. Representative images for *B. cenocepacia* and *B. multivorans* are depicted in Figure 8.1 (cells bound to insulin were visualised under GFP

fluorescence). Bright field images of *B. cenocepacia* and *B. multivorans* and GFP show binding to FITC- labelled insulin is localised to bacterial cells (Figure 8.1). Crucially, images show that not all cells in the field of view have bound to insulin. This observation was consistent and reproducible; a minority of cells out of the whole population bind insulin. Variation in the intensity of staining of individual cells may be attributable to (i) the method of fixation, (ii) different planes of focus, (iii) different levels of insulin binding saturation, or (iv), the possibility that some of the labelled insulin may have entered cells.

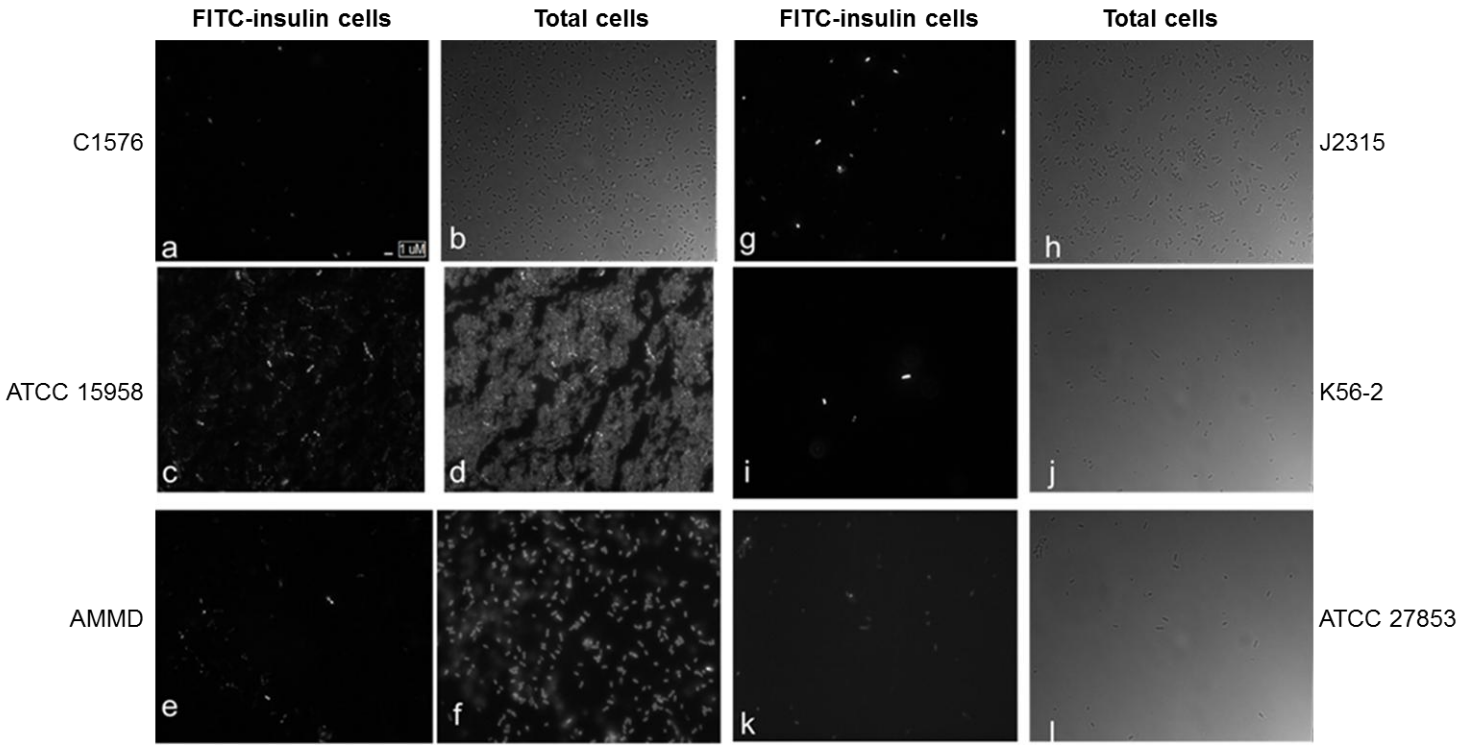

Figure 8.1. Insulin binding visualised by fluorescent microscopy. Insulin binding was visualised at 100 x oil magnification on a Zeiss AXIOSTAR epifluorescence upright microscope. (a-b) *B. multivorans* C1576 FITC (a) and brightfield (b); (c-d) *B. pyrrocinia* ATCC 15958 FITC (c) and phase contrast (d); (e-f) *B. ambifaria* AMMD FITC (e) and phase contrast (f); (g-h) *B. cenocepacia* J2315 FITC (g) and bright field (h); (i-j) *B. cenocepacia* K56-2 FITC (i) and bright field (j); (k-l) *P. aeruginosa* ATCC 27853 FITC (k) and bright field (l). *P. aeruginosa* ATCC 27853 was a negative control (fluorescence in the FITC channel not above auto fluorescence). Cells were exposed to 1 µg/ml insulin.

8.3.2 Screening for insulin binding quantitatively

Initially, a fluorescent plate-reader assay was developed based on the Kanai *et al.* protocol; however, results showed low levels of insulin binding in a number of organisms screened (data not shown) contrary to previously obtained microscopy results, suggesting the Kanai *et al*. protocol was not optimal for quantitative insulin binding studies. A fluorescent plate reader assay based on the Nisr *et al.* protocol was adopted. The 96-well plate assay allowed for quantitation of FITC-insulin binding based on fluorescence of numerous samples at once. Time trials to assess optimal incubation time for insulin exposure using the plate reader indicated no significant difference between 5, 10, and 15 minute incubations for either *B. multivorans* ATCC 17616, C1576, or *B. cenocepacia* K56-2 (data not shown). Nisr *et al.* noted positive insulin binding in *B. multivorans* and *B. cenocepacia* after 5 minutes of incubation with insulin. After exposure to insulin, all strains had significantly enhanced fluorescence relative to the negative *P. aeruginosa* control (Figure 8.2). There were no significant differences between the insulin-binding strains.

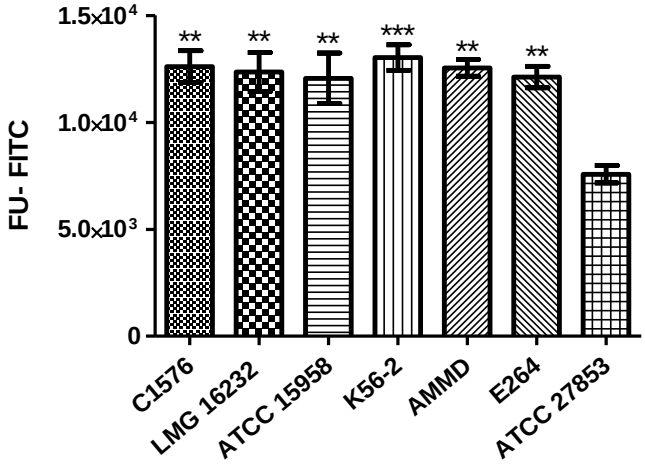

Figure 8.2. Quantitation of insulin binding after insulin exposure. Graph shows *B. multivorans* C1576*, B. vietnamiensis* LMG 16232, *B. cepacia* ATCC 15958, *B. cenocepacia* K56-2, *B. ambifaria* AMMD, *B. thailandensis* E264, following exposure to 1 μg/ml FITC-insulin. Asterisks represent significance relative to negative insulin binding strain *P. aeruginosa* ATCC 27853. ** $P < 0.005$, *** $P < 0.0001$. Statistical significance was determined using a 1-way ANOVA and post-tests. Bars represent the mean from three individual wells.

In this study, a panel of bacterial strains were assessed for insulin binding. Table 8.1 lists the bacterial strains screened for insulin binding, including four isolates of *P. aeruginosa*, one *B. thailandensis* strain, and 16 Bcc strains. Table 8.1 also indicates whether strains were assessed using the Kanai *et al.* or Nisr *et al.* insulin binding methods, or both, and whether the strain was positive (+), ambiguous (?), or negative (-) for insulin binding ability. These observations were made using both fluorescent microscopy and plate reader quantitative assays. The majority of ambiguous (?) binding strains were positive by microscopy but negative by the plate reader assay. Although the plate reader was quantitative, these strains which differed between the two methods were marked as ambiguous should be reassessed with flow cytometry. None of the four *P. aeruginosa* isolates bound insulin, and 10 of the 16 *Burkholderia* strains assessed bound insulin. The strains listed in bold were assessed for insulin binding using the more recently developed Nisr *et al.* insulin binding protocol. Strains not in bold were only assessed with the Kanai *et al.* method and this

should be taken into account – if time had permitted these strains would have been included in quantitative insulin binding protocols. Although background fluorescence was higher in the Kanai *et al.* microscope slides, individually bright insulin bound cells were still clearly visible. *B. multivorans* C1576 and ATCC 17616, *B. cenocepacia* K56-2, *B. ambifaria* AMMD, and the *P. aeruginosa* negative control from Kanai *et al.* were studied using both methods. Although background fluorescence was higher with the Kanai *et al.* method and cells could also be assessed on the microscope, individual bright cells amidst the general population of insulin-binding strains were still visible. Given more time, these strains classed as ambiguous would be re-assessed for insulin binding using plate reader assays. Strains that were very clearly not insulin binding (-) or very clearly insulin-binding (+) were exclusively assigned these phenotypes.

Table 8.1. Insulin binding in a panel of bacterial strains. Insulin binding was assessed in a panel of 20 bacterial strains. '+' indicates positive insulin binding phenotype; '–'indicates lack of insulin binding, '?' indicates ambiguous insulin binding due to results between microscopy and plate reader. Bold script indicates Nisr *et al.* protocol used rather than Kanai *et al.* method. *Asterisks denote strain was assessed with both insulin binding protocols. ** Asterisks indicate this sample was negative by plate reader but positive via microscopy.

Species	Strain ID	Insulin binding
B. ambifaria	AMMD	+
B. anthina	W92	-
B. cenocepacia	**J2315**	**+**
B. cenocepacia	**MC0-3**	**+**
*B. cenocepacia***	ATCC 17765	?
B. cenocepacia*	**K56-2**	**+**
*B. cepacia***	ATCC 17759	?
B. cepacia	ATCC 25416	-
*B. dolosa***	E12	?
B. multivorans*	**C1576**	**+**
B. multivorans*	**ATCC 17616**	**+**
B. pyrrocinia	**ATCC 15958**	**+**
B. stabilis	C7322	+
B. stabilis	LMG 14294	-
B. thailandensis*	**E264**	**+**
B. vietnamiensis	PC 259	+
B. vietnamiensis	**LMG 16232**	**+**
P. aeruginosa	PA01	-
*P. aeruginosa***	H129	?
P. aeruginosa	C3425	-
P. aeruginosa*	**ATCC 27853**	**-**

8.3.3 Insulin binding quantified by flow cytometry

Leading on from confirmed observations of insulin binding in the Bcc, further assessment of the insulin binding was carried out using flow cytometry (FCM). A small population amongst the general population of *B. cenocepacia* J2315 cells bind insulin (Figure 8.1(g)). J2315 insulin-bound cells were clearly distinguishable by fluorescent microscopy. FCM and Fluorescence Activated Cell Sorting (FACS) were used to quantify and isolate J2315 insulin-bound populations from the total population. FACS-sorted J2315 cells were confirmed

as FITC-insulin-bound by microscopy, indicating the sorting process successfully isolated FITC insulin-bound cells (Figure 8.3).

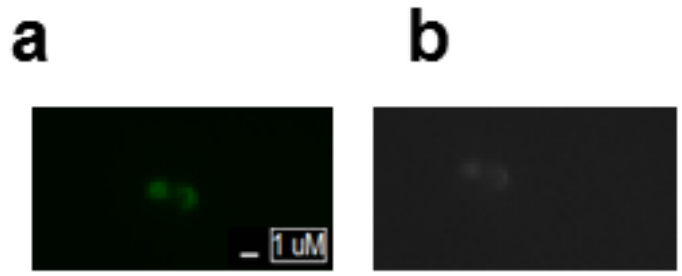

Figure 8.3. FACS sorted B. cenocepacia J21315 after insulin exposure. Confirmation by 100x oil immersion fluorescence microscopy of (a) FITC-bound insulin *B. cenocepacia* J2315 cells and (b) phase contrast image after insulin-bound cells were isolated by FACS.

Following the successful isolation of insulin-bound *B. cenocepacia* J2315 by FACS (Figure 8.3), the same sorted insulin-bound cells were re-cultured for 48 hours using either selective agar or selective broth (as described in Chapter 2 Methods section 2.24). *B. cenocepacia* J2315 is a slow growing strain. Due to the potential stress on cells during the sorting process, J2315 was not readily culturable, hence the 48 hour growth period between sorting rounds. J2315 cells were harvested and re-exposed to insulin, followed by additional rounds of FACS analysis to quantify insulin binding to determine if the insulin binding subpopulation could be enriched. In total, three rounds of sorting were carried out for this assay. Between re-growth and subsequent FACS analyses, potential contamination was prevented by aseptically cleaning the FACS system. Contamination was monitored for every 24 hours by sampling and plating each J2315 culture onto LB agar.

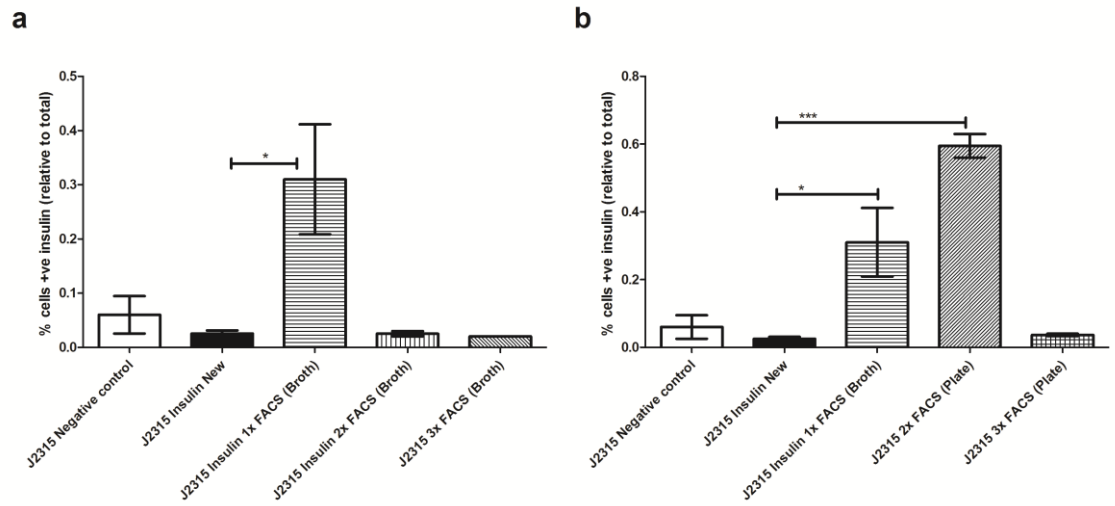

Figure 8.4. FACS analysis results following isolation of FITC-insulin bound J2315. FACS analysis of FITC-bound-insulin *B. cenocepacia* J2315, with subsequent culturing and FACS analysis three separate times (1x, 2x, 3x). J2315 negative control was not exposed to insulin and was made from a fresh overnight culture. N=3. (a) LB broth or (b) BCSM selective agar with selective supplements was used for culturing. *P<0.05, ***P<0.0001. Statistical significance was assessed by using a 1-way ANOVA and post-tests. Bars are representative median values from three biological replicates.

Figure 8.4 depicts results of insulin bound cells re-cultured from broths (a) or plates (b). Controls used were J2315 not exposed to insulin (J2315 Negative control) from a fresh overnight broth for each sort. J2315 Insulin NEW (fresh overnight broth, exposed to insulin) was an insulin exposed control to compare back to for insulin binding enrichment. Overall, differences are apparent, but they are not consistent between the FACS analyses. The observation that is consistent is J2315 is not enriched for insulin binding after repeated isolation and culturing, and overall the percentage of insulin-bound cells remained very low, consistently less than 1 %.

Following repeated attempts of this experiment, the conclusion still held that a small percentage of the total population of cells bound insulin. Despite apparent increases in binding after a second round of sorting Figure 8.4(b), (on previous page), shows significant difference in the twice-sorted plate and broth grown cultures, relative to the NEW J2315. In these conditions, insulin-binding cells were not enriched for following FACS isolation. Therefore, insulin binding was not a stable phenotype that could be enriched for by repeated sorting and

culture, and this suggested insulin binding cells were phenotypically distinct from the general cell population.

8.3.4 Persister cells and insulin binding

Insulin binding potentially could encompass phenotypically distinct variants, reminiscent of persister cells. Persister cells are genetically identical but phenotypically different dormant non-dividing cells within a given population that can be revealed after exposure to high concentrations of antibiotics. *B. cenocepacia* and *B. multivorans* were used in persister cell assays in this study, using clinically relevant antibiotics ceftazidime and ciprofloxacin.

8.3.4.1 Ceftazidime-derived persister cells and microscopy

In this study, *B. cenocepacia* and *B. multivorans* were exposed to 100x MIC of ceftazidime for 24 hours, which resulted in a 99.8 % loss of culturable cells for J2315, ATCC 17616, and K56-2. The persister cells were then exposed to insulin. Ceftazidime, a member of the cephalosporin class of antibiotics, was chosen as it is a clinically relevant antibiotic which is widely used in persister assays; it can be administered in conjunction with tobramycin to treat CF patients with Bcc infections. Fluorescent microscopy was used to distinguish insulin-bound untreated and persister cells as distinct from the total population.

Fluorescent microscopy revealed the 100x the minimum inhibitory concentration (MIC) ceftazidime treated *B. cenocepacia* and *B. multivorans* resulted in cells that were elongated, a phenotype previously reported in other Gram- negative bacteria (41,219).

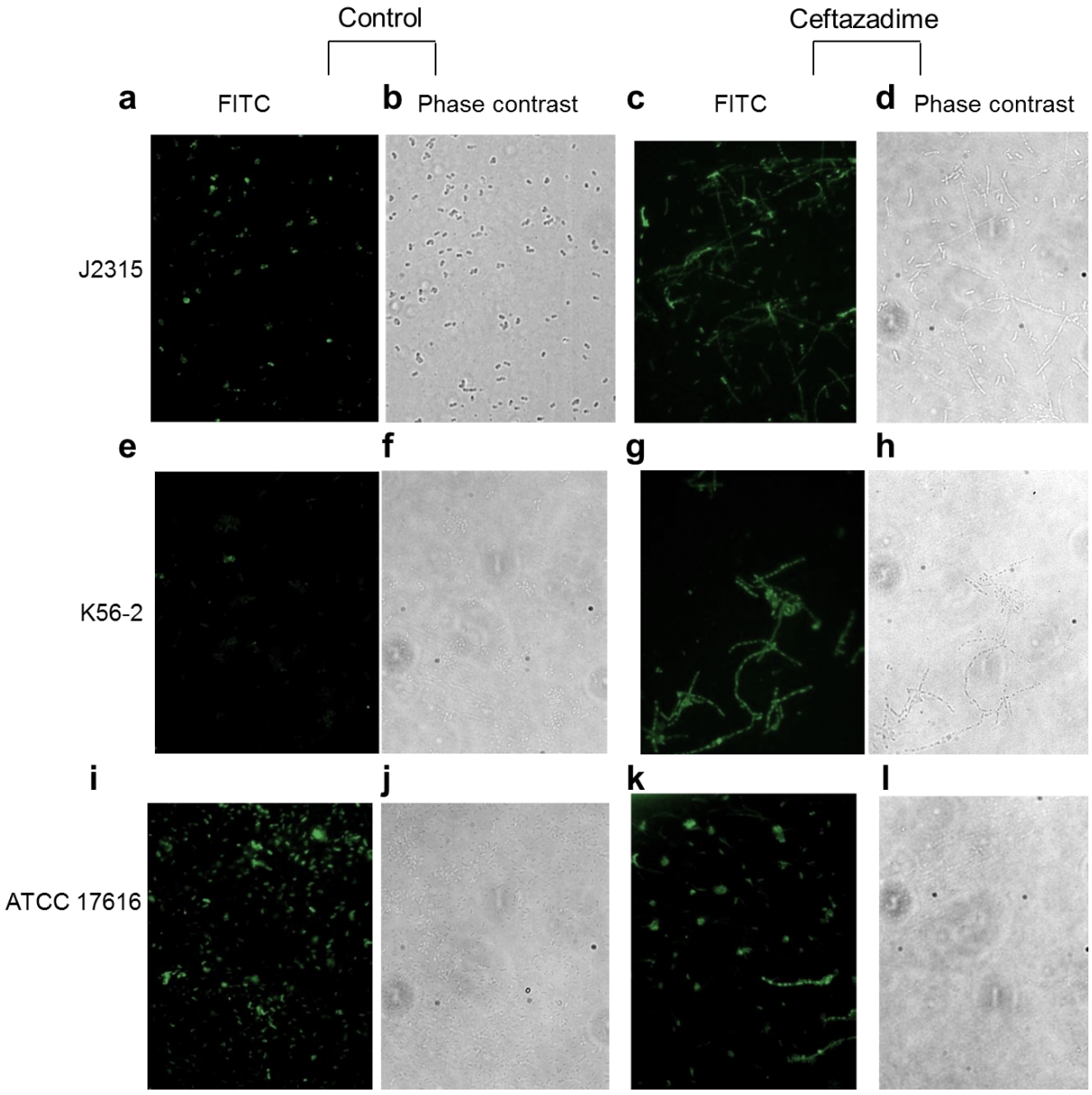

Figure 8.5. Insulin exposed control or ceftazidime-derived persister cells at 100x oil immersion magnification. Insulin exposed control or ceftazidime-derived persister cells, 100x oil immersion magnification. Images are representative of 6 fields of view. (a-b) Phase contrast FITC B. cenocepacia J2315 (untreated), (c-d) phase contrast and FITC *B. cenocepacia* J2315 ceftazidime-derived persister cells, (e-f), phase contrast and FITC *B. cenocepacia* K56-2 (untreated), (g-h) phase contrast and FITC *B. cenocepacia* K56-2 ceftazidime-derived persister cells, (i-j) phase contrast and FITC *B. multivorans* ATCC 17616 (untreated), (k-l) phase contrast and FITC *B. multivorans* ATCC 17616 ceftazidime-derived persister cells.

Based on the images in Figure 8.5, *B. cenocepacia* K56-2 persister cells appear enhanced for insulin binding compared to non-persister, insulin-exposed controls (Figure 8.5 (e-h)). *B. cenocepacia* J2315 appears moderately enhanced for insulin binding in persister cells compared to untreated controls

(Figure 8.5 (a-d)). *B. multivorans* ceftazidime-derived persister cells are not enriched for insulin binding (Figure 8.5 (i-l)).

Whilst microscopy was useful for the study of ceftazidime-derived persister cells, the elongated phenotype of *B. cenocepacia* and *B. multivorans* made insulin binding difficult to quantify. Ceftazidime was not an ideal candidate for FCM and FACS-based analyses. Laser detectors would not have accurately visualised the chains or elongated cells as individual particles (single cells). An antibiotic which did not induce the elongation phenotype would enable quantification between untreated cells and persister cells exposed to insulin. Consequently, the following study utilised ciprofloxacin-derived persister cells.

8.3.4.2 Ciprofloxacin-derived persister cells and FCM

In order to quantify insulin-bound persister cells by FCM and FACS, ciprofloxacin was used to reveal persister cells of *B. cenocepacia*. Ciprofloxacin, a fluoroquinolone antibiotic, did not induce the elongated cell phenotype at high concentrations. However, ciprofloxacin does not cause lysis of the bacterial cell, resulting persister cell populations were a mix of persister cells and dead cells (still intact but not removed during washing steps). Consequently, the red fluorescent dye propidium iodide (PI) was used, which is only taken up by cells with damaged membranes; cells with intact membranes (live or persister cells) would not be stained. PI is normally used as part of a live/dead stain kit in FACS analysis, with SYTOX Green used to partition live cells. However, due to FITC and SYTOX green emission having similar wavelengths, SYTOX Green was not included, and selection for ‘live’ cells in untreated and persister cell populations was based on lack of PI uptake.

Prior to beginning persister cell and FACS analysis, the ciprofloxacin MIC was determined for two strains of *B. cenocepacia*; the clinical isolate J2315 (used in previous studies in this chapter) and the environmental isolate MC0-3. Previous studies within the lab suggested MC0-3 had a higher persister cell frequency than other *B. cenocepacia* isolates. The MIC was determined using E-test strips for each strain and 100x the MICs were found to be 25 µg/ml for MC0-3 and 200 µg/ml for J2315.

For the ciprofloxacin persister assay, 100x was used to calculate ciprofloxacin-persister cell frequency. J2315 formed ciprofloxacin persister cells at a lower frequency of 0.002 %, while MC0-3 formed persister cells at a frequency of 0.0106 %. MC0-3 was used for subsequent insulin studies using FACS due to its higher persister cell frequency as the assessment of insulin binding by persister cells would likely be more robust.

FACS analysis profiling of ciprofloxacin-derived persister cells of *B. cenocepacia* MC0-3 entailed the use of two dyes for insulin-bound and live/dead population separation. By selection of particles based on their emission in the FITC/GFP and PI emission wavelengths, quantification of live insulin bound persister was possible (Figure 8.6). Results in Figure 8.6(a) indicate the majority of cells seen by FACS analysis of persister cells were classified as ‘dead’, based on PI staining (695/40-A on x-axis). Dead cells are depicted by the broad peak in the right hand side of the graph in Figure 8.6 (a). The y-axis depicts counts (or total cells seen by FACS) versus the x-axis, PI (‘dead’ cells stain) emission. Only a small population of cells had little or no staining by PI. This is in accordance with 24 hours of antibiotic treatment at 100x the MIC for ciprofloxacin resulting in ~ 99.9 % cell death, with the persister cell frequency for MC0-3 being 0.0106% of the total population.

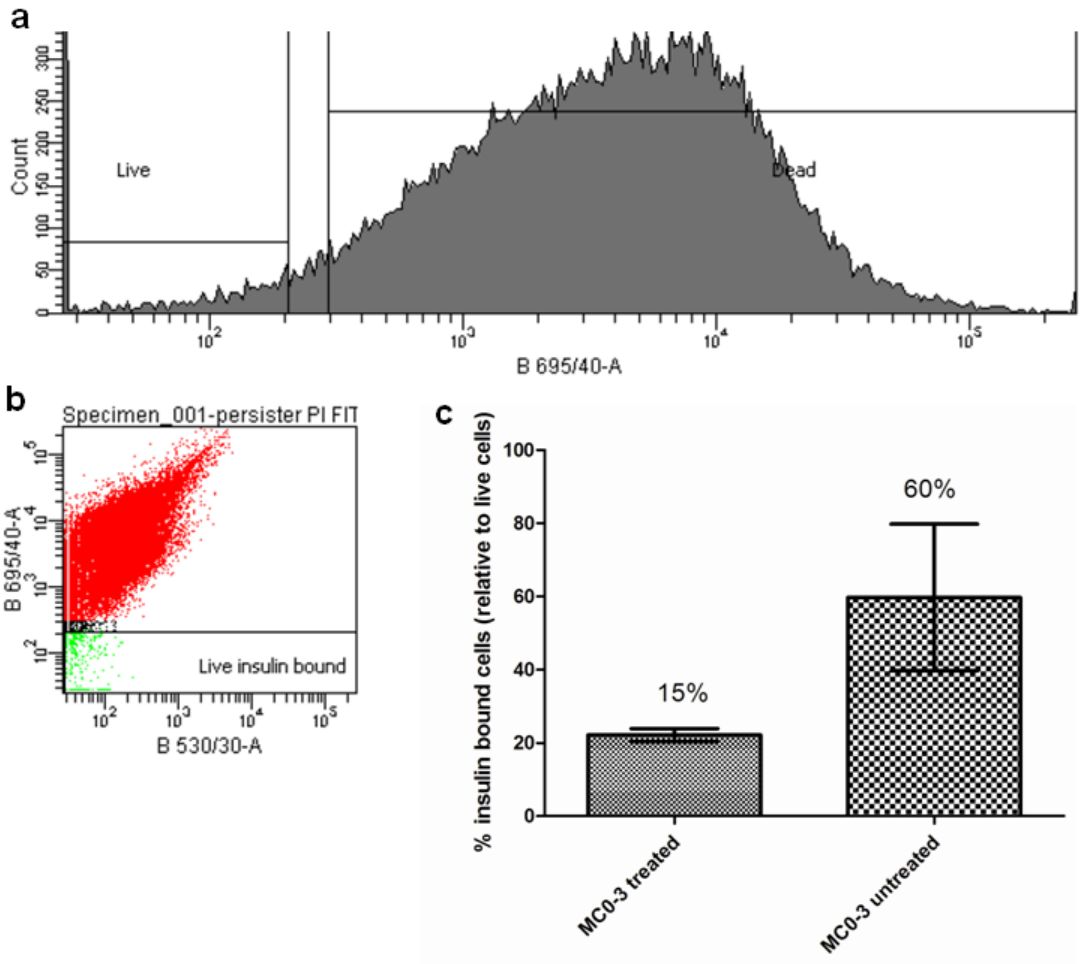

Figure 8.6. FACS analysis profiling of insulin-exposed B. cenocepacia MC0-3 ciprofloxacin-derived persister cells. (a) *B. cenocepacia* MC0-3 counts (number of total particles (cells) detected (y-axis)) versus 695/40-A nm (x-axis) propidium iodide (PI). (b) MC0-3 cells PI vs. FITC (B530/30-A) emissions indicate insulin-bound live/persister cells (green population) amidst dead cells (red population). (c) Ciprofloxacin MC0-3 persisters exposed to FITC-insulin and PI staining for cell viability. Bars show percentage insulin-bound cells (relative to live cells). N=3, error bars are standard error (SEM).

Only cells with low or no red fluorescence due to lack of uptake of PI were selected as live. Within the group deemed live (persisters) (Figure 8.6 (b) on previous page) the insulin bound FITC-bright cells were quantified, as depicted by the green population in the bottom of Figure 8.6 (b). The bar graph in Figure 8.6 (c) showed a difference between live insulin binding MC0-3 persister cells and untreated MC0-3, but this difference was not statistically

significant. These data did not indicate that ciprofloxacin-derived persister cells were enriched for insulin binding. This observation was repeated three times on separate days and data presented in Figure 8.6 (c) is cumulative of three individual biological replicates, whilst panels (a) and (b) of the same figure are representative data of single biological replicates.

Difficulties with the FACS ciprofloxacin-derived persister cell/insulin binding assay included live cells taking up propidium iodide stain, gauged by the observation that some untreated/non-persister cells exposed to PI stained positive with the dye, indicating PI was entering healthy cells to some extent. As a result, time in the presence of PI prior to FCM analysis was minimised. Attempts made to optimise this experiment included initially staining persisters with PI, isolating 'live' persister cells, and then exposing them to insulin and a second round of FACS. However, the low number of persister cells in a population and the time taken to sort sufficient persister cells, created too long of processing time. The data summarised in Figure 8.6 was generated using a streamlined process, with PI staining directly after insulin exposure and immediately prior to FACS analysis to avoid uptake of the stain by any weakly intact persister or healthy cell membranes. Stringent gating selections were used to ensure live and insulin-bound cells (calculated relative to the live population) were not skewed.

8.4 Discussion

Previous reports in literature demonstrated insulin binding capabilities of members of the Bcc and *B. pseudomallei*. Insulin binding was not observed in *P. aeruginosa* (96). Bcc cause respiratory disease in CF patients, of which CFRD is a common comorbidity. A major risk factor for *B. pseudomallei* (causative agent of melioidosis) is diabetes (227). Whether CFRD patients may be equally susceptible to *B. pseudomallei* (or Bcc) infection is unknown. Alternatively, Nisr *et al.* suggested that microorganisms such as *B. cenocepacia* and *B. multivorans* could contribute to the onset of CFRD by mimicking human insulin receptors and binding insulin (141). Spurred on by these and previous observations of insulin binding in the Bcc, the present study assessed insulin binding in a panel of 20 strains of *Burkholderia* (mainly representative members

of the Bcc), and *P. aeruginosa*. Using FITC-labelled insulin in conjunction with different methods of analysis, 10 out of 16 *Burkholderia* were confirmed to bind insulin, whilst the remaining strains were negative for insulin binding. All four *P. aeruginosa* isolates were found to be negative or ambiguous for insulin binding (summarised in Table 8.1 and depicted in Figures 8.1, 8.2). It is of note that in the present study, the *B. thailandensis* E264 was recorded as insulin-binding positive, whilst the same strain used in the Nisr *et al.* study was reported as non-insulin binding (141). This discrepancy could be accounted for by several factors, one of which being that the present study only assessed E264 binding by quantitative plate reader assay. It would have been useful to have checked the E264 strain by microscopy to ensure this deviation from the Nisr *et al.* result was consistent. It is also possible that the E264 isolates could be slightly different, depending on where the isolates were purchased or sourced, and for how many passages the bacteria had been grown on between going back to fresh plates from freezer stocks. Indeed, another possibility is that the length of incubation for strains used in the Nisr *et al.* method is not detailed. The strains used in the present study were all in late stationary phase, and grown in LB (5 g/l sodium chloride). If growth conditions differed even by a few hours incubation, it may have affected the insulin binding assay results.

The observation that *P. aeruginosa* ATCC 27853 does not bind insulin is in accordance with previous insulin binding studies by Kanai *et al.* and Nisr *et al.*, which used ATCC 27853 as a negative control. The present study additionally included three other *P. aeruginosa* strains, none of which definitively bound insulin. Factors for binding insulin in the Bcc are still undetermined, but Kanai *et al.* suggested factors responsible for insulin binding in *Burkholderia* are genus specific, further making *Burkholderia* distinct from *Pseudomonas*. Kanai *et al.* briefly assessed acid phosphatase activity of *B. pseudomallei* and *B. cepacia*. They identified a glycoprotein enzyme with phosphatase activity. The *B. pseudomallei* phosphatase was found to be more glycosylated than that of *B. cepacia*. The acid phosphatase of *P. aeruginosa* had much lower overall phosphatase activity. Differences such as these may explain inter- species variation, though often as shown in Table 8.1, a positive

and negative result was within a single species. Even *B. stabilis*, known for genomic stability, showed variation in insulin binding between two isolates assessed in this study. Fluorescence microscopy and FACS analysis of insulin-bound bacteria revealed insulin-binding was species- and even strain-specific. The present study went on to observe that insulin is bound by only a small number of cells within a given population. This is a novel observation, and one made consistently for insulin binding strains listed in Table 8.1. Interestingly, the Kanai *et al.* study found *B. pseudomallei* FITC-insulin exposure revealed ill-defined cells or cells in an aggregated mass. The present study utilised both the Kanai *et al.* and Nisr *et al.* protocols for insulin binding and fluorescent microscopy, and for both methods found insulin bound cells were distinct and brightly fluorescent relative to background and auto fluorescence as assessed by fluorescent microscopy. When high densities of insulin exposed cells were examined, insulin bound cells were still distinguishable.

Using *B. cenocepacia* J2315 as a model organism, FACS isolation and re-culturing of insulin bound cells did not enrich for insulin binding. This indicated insulin binding was not a stable phenotype within the total bacterial population. Insulin-binding proteins on the bacterial cell may be subject to phase variation (141). This study provides results that insulin binding is only maintained in a minority of the cell population, but there is need for further study to determine specific protein/hormone interactions that are required for binding insulin. Nisr *et al.* demonstrated a role for the outer A-layer of *Aeromonas salmonicida* in insulin binding. The same study used an insulin-ligand binding assay that identified two putative insulin-binding proteins (IBPs), one from *B. cenocepacia* and one from *B. multivorans*. This suggested that surface-exposed proteins in these two species play a role in mammalian hormone binding. This could correlate with different cells able to randomly express and expose different surface proteins (some insulin binding specific, some not) during growth. The phenomenon is called phase variation, a phenotypic adaption to diverse environments whereby bacterial fitness and survival is improved. Phase variants occur by genetic or epigenetic mutation. Often, phase variants revert back to wild-type phenotype so can be difficult to isolate and enrich. One

example is from *B. ambifaria* AMMD, where a phase variant was able to produce more EPS than the wild-type (215). Members of the Bcc are reported to utilised phase variation, and cases have been reported that support variation in favour of niche adaption. The phase variants produce proteins (or do not) by altering surface structures, or by making one or more antigenic forms of a protein related to virulence (204). Other proteins not immediately related to virulence are also varied. This could be a relevant adaption to sense and bind mammalian signalling hormones once within the host.

This study also examined insulin binding by ceftazidime- and ciprofloxacin-derived persister cells. In order to kill, many antibiotics require active targets, but persister cells evade killing by staying in a non-dividing, dormant, or decreased metabolic state (115). Based on the observation that a phenotypically distinct subpopulation of cells bound insulin, fluorescent microscopy of ceftazidime-derived persister cells (Figure 8.1) showed potential enrichment of insulin binding in *B. cenocepacia* K56-2. Phase variation could be at play during the insulin binding and persister cell assay. *B. multivorans* ATCC 17616 ceftazidime-derived persister cells were not enhanced for insulin binding compared to controls. *B. cenocepacia* J2315 ceftazidime-derived persister cells appeared to be enriched for insulin binding relative to untreated controls. Due to the elongated cells phenotype, ceftazidime persister cells could not be quantified by FACS analysis, thus the ability of *B. cenocepacia* MC0-3 ciprofloxacin-derived persister cells to bind insulin was quantified by FACS. No enhanced insulin binding was observed in persister cells compared to untreated controls (Figure 8.6). It could be reasoned that observations of potential enriched insulin binding in *B. cenocepacia* or *B. multivorans* ceftazidime-derived persister cells but not in *B. cenocepacia* ciprofloxacin-derived persister cells is possibly due to differences in the persister cells themselves. Ciprofloxacin-derived persister cells may be a different population compared to ceftazidime-derived persister cells due to inherent difference in the mode of action of these antibiotics.

The overall clinical significance of these studies is based around the observation that onset of diabetes or CFRD is often followed by an overall

clinical decline (137). There are undefined links between diabetes, pre-disposition to bacterial infection, and insulin. If bacteria from the soil environment synthesise binding or receptor proteins that mimic mammalian hormone binding proteins, this may be a way of sensing or signalling entrance to the mammalian host environment, enabling bacterial cells to signal and respond to the transition from the natural environment to mammalian host. Microorganisms in a mammalian host able to bind host insulin could potentially modulate levels of sugars in the host bloodstream and tissues. This may be a beneficial strategy for a bacterium in a nutrient deplete environment, however it is likely there are ample nutritional sources elsewhere in the CF host. Insulin binding may not benefit growth in Bcc species, but host hormone and bacterial interactions are not fully understood and could have ramifications for the pathogens phenotype and gene expression in the host environment. Nisr *et al.* suggested an auto-immune response role for insulin binding receptors, leading to the onset of diabetes. It is still not understood why diabetes predisposes individuals to contracting melioidosis, but CF patients harbouring Bcc strains able to bind insulin could contribute to the onset of diabetes or respiratory decline of CFRD.

CFRD still requires insulin treatment to improve body mass index and lung function, and treatment with insulin reduces sputum culture positivity of respiratory pathogens (144). Treatments in the clinic are intravenous insulin, however interest to develop inhaled insulin still continues (111). Currently inhaled insulin is approved in the US and EU for type I and II diabetes. Studies show that 1-3 mg inhaled insulin prior to meals is as effective at controlling glucose levels as sub-cutaneous injection of insulin. However, inhaled insulin in the case of CFRD is of concern due to a 1-1.5% reduction in FEV_1 in users (111). This decline in FEV_1 is reversed by halting treatment. The better adherence to treatment regimen than injection of inhaled insulin may outweigh this drawback, however if there are insulin-based influences on Bcc and other bacteria residing in the CF lung, surely inhaling insulin directly into the airways is noteworthy and warrants further investigation.

If *Burkholderia* and Bcc members were able to modulate insulin availability by binding host insulin, upon treatment with insulin, existing pathogens in the CFRD patients' respiratory tract might hinder improvement of weight and pulmonary function usually seen in CFRD patients after treatment, by binding the administered insulin. Our observations were inconclusive and strain-dependent as to whether persister cells are enriched for insulin binding. And even so, it is not clear if less than 1 % of the population binding insulin (as our studies report) could even be biologically significant.

The type of antibiotic administered to patients could select for different populations of persisters that bind insulin differently. Only two antibiotics were assessed in the present study. However, *Burkholderia* persistence has long been documented in melioidosis, and members of the Bcc cause chronic, difficult to eradicate infections in CF patients. Adaption to the human host and in the CF lung may or may not include the use of insulin binding proteins, but additional research is required to define the link between CFRD, clinical decline, and Bcc infection.

Potential avenues for future research include firstly identifying insulin-binding factors in the Bcc. Currently it has been suggested that there must be a specific binding motif or phospholipase activity (96,227). Secondly, identify what benefit binding insulin would be for the pathogen *in vivo* (if insulin is bound, host blood sugar rises potentially releasing more fuel for bacteria in tissues and blood stream of diabetics). Thirdly, what benefits would an environmental/soil dwelling organism gain if able to bind insulin. Insulin-binding may represent an acquired adaption by some members of *Burkholderia* to enhance pathogenicity in the human host.

8.5 Conclusions

1. Although insulin binding does occur in members of the Bcc it is a sub-population of the overall cell population that is able to bind insulin.

2. Insulin binding occurs in a stochastic (random) manner. Whilst the stochastic manner of insulin binding appears reminiscent of persister cell phenotypes, studies exploring the association between persister cell and insulin binding phenotypes were inconclusive, and could be dependent on strain-to-strain variation or the antibiotic used to reveal persister cells.

Chapter 9: Appendix

9.1 Primer sequences

Table 9.1. Primers used for insertional mutagenesis. Crude knockout primers used for insertional inactivation with EcoRI/XbaI restriction sites to create crude knockout strains (CR).

Primer	Sequence
C1576 – *hecB* - XbaI	GTAGTTCTAGATGATGAAACGACGCACATTT
C1576 - *hecB* - EcoRI	GTAGTGAATTCCGATGAATACGTCCGTGATG
C1576 – *hecA* - XbaI	GTAGTTCTAGATCGAAAAACGACACGTTCAA
C1576 - *hecA*- EcoRI	GTAGTGAATTCGTCGCGATATTGTTCGAGGT
C1576 - *fim*- XbaI	GTAGTTCTAGATTACCGACGGCTCGATATTC
C1576 – *fim* - EcoRI	GTAGTGAATTCCCGTGAACAGGTTGCTGAAC
RSF1300 (71)	TAACGGTTGTGGACAACAAGCCAGGG
hecB-Fwd-Check	CATCACGGACGTATTCATCG
hecA-Fwd-Check	CGGCGTTTGACCATAGTTG
fim-Fwd-check	GGTGTCGACCTACGTGCAG

Table 9.2. Primer sequences used for complementation of adhesin mutants. Strains fim CR, hecB CR were complemented to make strains fim CO and hecB CO. pDA17 primers were used to confirm insertion of inserts into vector.

Primer	Sequence
Bmul-*fim*-NdeI-F	GTACCATATGCGCAAGTCAATCAAGTC
Bmul-*fim*-XbaI-R	GTACTCTAGATTGCGAAATTTCCTTCGTGG
Bmul-*hecB*-NdeI-F	GTACCATATGAAACGACGCACATTTCG
Bmul-*hecB*-XbaI-R	GTACTCTAGAGTAGTTCCAGTTCATTGTCG
pDA17-Fwd	TTGTTGTTGGGTAGGCAGTC
pDA17-Rev	ACCGCTTCTGCGTTCTGAT

Table 9.3. Primers used RT-PCR and qRT-PCR transcriptome validation. Housekeeping genes (not listed) were Bcc MLST primers for genes gapA and gyrA.

Primer	Sequence
bceB-qPCR-Fwd	cgtgacgccggtcggccggttc
bceB-qPCR-Rev	ggatttggtcaagggctaca
hecB-qPCR-Fwd	tgatgaaacgacgcacattt
hecB-qPCR-Rev	ggtggctgctccaactgac
hecA-qPCR-Fwd	gcaacaatctgaccgcaac
hecA-qPCR-REV	aggctcttgacgctaccttg
fim-qPCR-Fwd	agcagccatctgttcgtc
fim-qPCR-REV	gtagcccgcatccttgtg

9.2 Bacterial strains and plasmids used in this study

Table 9.4. Bacterial strains used for insulin studies. Bcc strains*, Burkholderia thailandensis* and *P. aeruginosa* isolates used in insulin binding studies.

Species	Strain ID
B. ambifaria	AMMD
B. anthina	W92
B. cenocepacia	J2315
B. cenocepacia	MC0-3
B. cenocepacia	ATCC 17765
B. cenocepacia	K56-2
B. cepacia	ATCC 17759
B. cepacia	ATCC 25416
B. dolosa	E12
B. multivoran	C1576
B. multivorans	ATCC 17616
B. pyrrocinia	ATCC 15958
B. stabilis	C7322
B. stabilis	LMG 14294
B. thailandensis	E246
B. vietnamiensis	PC 259
B. vietnamiensis	LMG 16232
P. aeruginosa	PA01
P. aeruginosa	H129
P. aeruginosa	C3425
P. aeruginosa	ATCC 27853

Table 9.5 Summary table of Bcc isolates used in adhesin dot-blot hybridisation. Strains are listed including their source, MLST assignment where known (ST), country of origin, and presence/absence of genes encoding the HecA-like, HecB-like and fimbrial usher (fim) proteins. Isolates belonging to the ST-27 outbreak strain are highlighted in bold. ENV, environmental isolate; CF, clinical isolate (CF); Non-CF, clinical isolate (non-CF). Where no MLST sequence type (ST) is defined, that isolate does not match an existing ST within the Bcc MLST database. [a] The inclusion of *B. ambifaria* MC40-6 provides an indication of the stringency of the hybridisation and washing procedure, as the sequence of the C1576-derived *hecB*-specific probe displays 83% nucleotide identity to the comparable sequence in *B. ambifaria* MC40-6 (gene BamMC406_6761).

Isolate ID	Species	Source	ST	Location	*hecA*	*hecB*	*fim*
BCC0384	*B. multivorans*	CF	15	UK	-	-	-
BCC0710	*B. multivorans*	CF	15	UK	-	-	-
BCC0553	*B. multivorans*	CF	16	Canada	-	-	-
BCC0300	*B. multivorans*	CF	16	France	-	-	-
BCC0065	*B. multivorans*	Non-CF	16	USA	-	-	-
E2667	*B. multivorans*	CF	18	UK	-	-	+
BCC1369	*B. multivorans*	CF	25	USA	+	+	+
BCC1378	*B. multivorans*	CF	25	USA	-	+	+
BCC1379	*B. multivorans*	CF	25	USA	-	-	+
C1574	*B. multivorans*	**CF**	**27**	**UK**	**+**	**+**	**+**
C1576	*B. multivorans*	**CF**	**27**	**UK**	**+**	**+**	**+**
C1578	*B. multivorans*	**CF**	**27**	**UK**	**+**	**+**	**+**
C1579	*B. multivorans*	**CF**	**27**	**UK**	**+**	**+**	**+**
C1581	*B. multivorans*	**CF**	**27**	**UK**	**+**	**+**	**+**
C1582	*B. multivorans*	**CF**	**27**	**UK**	**+**	**+**	**+**
C1591	*B. multivorans*	**CF**	**27**	**UK**	**+**	**+**	**+**
C1593	*B. multivorans*	**CF**	**27**	**UK**	**+**	**+**	**+**

C1606	*B. multivorans*	**CF**	**27**	**UK**	**+**	**+**	**+**
C1607	*B. multivorans*	**CF**	**27**	**UK**	**+**	**+**	**+**
C1608	*B. multivorans*	**CF**	**27**	**UK**	**+**	**+**	**+**
C1610	*B. multivorans*	**CF**	**27**	**UK**	**+**	**+**	**+**
C1636	*B. multivorans*	**CF**	**27**	**UK**	**+**	**+**	**+**
C1670	*B. multivorans*	**CF**	**27**	**UK**	**+**	**+**	**+**
C1703	*B. multivorans*	**CF**	**27**	**UK**	**+**	**+**	**+**
C1958	*B. multivorans*	**CF**	**27**	**UK**	**+**	**+**	**+**
C1978	*B. multivorans*	**CF**	**27**	**UK**	**+**	**+**	**+**
C2012	*B. multivorans*	**CF**	**27**	**UK**	**+**	**+**	**+**
E3491	*B. multivorans*	**CF**	**27**	**UK**	**+**	**+**	**+**
E3637	*B. multivorans*	**CF**	**27**	**UK**	**+**	**+**	**+**
C1629	*B. multivorans*	**CF**	**27**	**UK**	**+**	**+**	**+**
E2737	*B. multivorans*	**CF**	**27**	**UK**	**+**	**+**	**+**
E247	*B. multivorans*	**CF**	**27**	**UK**	**+**	**+**	**+**
E68	*B. multivorans*	**CF**	**27**	**UK**	**+**	**+**	**+**
E88	*B. multivorans*	**CF**	**27**	**UK**	**+**	**+**	**+**
E4555	*B. multivorans*	**CF**	**27**	**UK**	**+**	**+**	**+**
BCC1376	*B. multivorans*	CF	179	USA	+	+	+
BCC1368	*B. multivorans*	CF	179	USA	-	-	+
BCC1370	*B. multivorans*	CF	179	USA	-	-	+
BCC0962	*B. multivorans*	CF	180	Czech R.	-	-	+
BCC0915	*B. multivorans*	CF	180	Czech R.	-	-	+
BCC0904	*B. multivorans*	Non-CF	180	Czech R.	-	-	+
BCC0208	*B. multivorans*	CF	189	Canada	-	-	+
E3814	*B. multivorans*	CF	191	UK	-	-	+
BCC0087	*B. multivorans*	CF	199	Canada	-	-	-

BCC1149	*B. multivorans*	CF	199	Canada	-	-	-
BCC1188	*B. multivorans*	CF	199	Canada	-	-	-
E3902	*B. multivorans*	CF	287	UK	-	-	+
E2791	*B. multivorans*	CF		UK	+	+	+
E3961	*B. multivorans*	CF		UK	+	+	+
E1788	*B. multivorans*	CF		UK	-	-	+
E277	*B. multivorans*	CF		UK	-	-	+
E2441	*B. multivorans*	CF		UK	-	-	+
E2525	*B. multivorans*	CF		Ireland	-	-	-
E2972	*B. multivorans*	CF		UK	-	-	+
E3002	*B. multivorans*	CF		UK	-	-	+
E3218	*B. multivorans*	CF		UK	-	-	+
E3318	*B. multivorans*	CF		UK	-	-	+
E3355	*B. multivorans*	CF		UK	-	-	+
E3362	*B. multivorans*	CF		UK	-	-	+
E3481	*B. multivorans*	CF		UK	-	-	+
E3571	*B. multivorans*	CF		UK	-	-	+
E3641	*B. multivorans*	CF		UK	-	-	+
E3675	*B. multivorans*	CF		UK	-	-	+
E3756	*B. multivorans*	CF		UK	-	-	+
E3762	*B. multivorans*	CF		UK	-	-	+
E3913	*B. multivorans*	CF		UK	-	-	+
E3919	*B. multivorans*	CF		UK	-	-	+
E4030	*B. multivorans*	CF		UK	-	-	+
E4039	*B. multivorans*	CF		UK	-	-	+
E4048	*B. multivorans*	CF		UK	-	-	+
E4075	*B. multivorans*	CF		UK	-	-	+

E4079	*B. multivorans*	CF		UK	-	-	+
E4100	*B. multivorans*	CF		UK	-	-	+
E4326	*B. multivorans*	CF		UK	-	-	+
E4331	*B. multivorans*	CF		UK	-	-	+
E4569	*B. multivorans*	CF		UK	-	-	+
E4626	*B. multivorans*	CF		UK	-	-	+
E4721	*B. multivorans*	CF		UK	-	-	+
E4730	*B. multivorans*	CF		UK	-	-	+
E4731	*B. multivorans*	CF		UK	-	-	+
E4748	*B. multivorans*	CF		UK	-	-	+
E4778	*B. multivorans*	CF		UK	-	-	-
J3336	*B. multivorans*	CF		UK	-	-	+
BCC0321	*B. multivorans*	ENV	20	UK	-	-	+
ATCC 17616	*B. multivorans*	ENV	21	USA	-	-	-
BCC0317	*B. multivorans*	ENV	22	Canada	-	-	+
BCC0401	*B. multivorans*	ENV	416	USA	-	-	-
BCC0487	*B. multivorans*	ENV	416	USA	-	-	-
BCC0050	*B. multivorans*	ENV	439	UK	-	-	+
AMMD	*B. ambifaria*	ENV	77	USA	-	-	-
MC40-6 [a]	*B. ambifaria*	ENV	136	USA	-	-	-
W92	*B. anthina*	ENV	421	USA	-	-	-
K56-2	*B. cenocepacia*	CF	30	Canada	-	-	-
ATCC 25416	*B. cepacia*	ENV	10	USA	-	-	-
E12	*B. dolosa*	CF		UK	-	-	-
C7322	*B. stabilis*	CF		Canada	-	-	-
LMG20358	*B. ubonensis*	ENV	299	Thailand	-	-	-

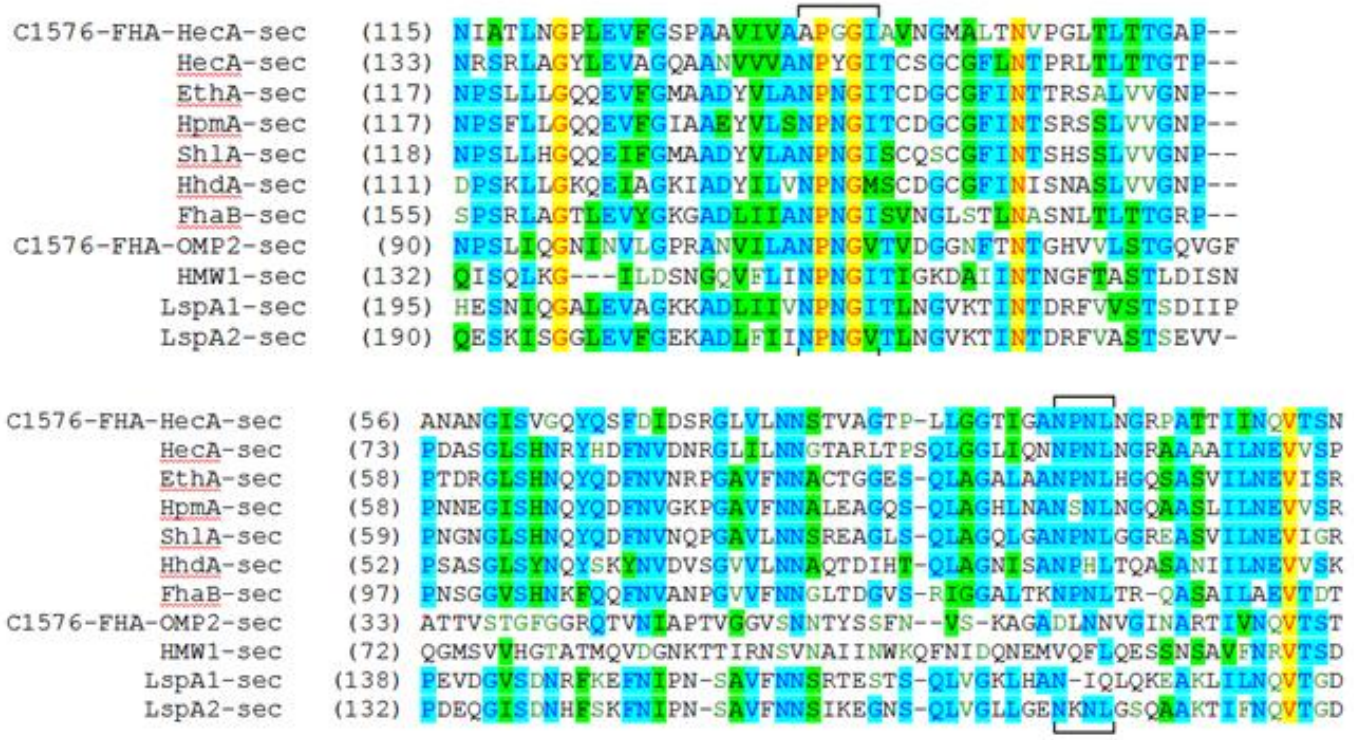

Figure 9.1. Alignment of the putative secretion domain ('sec') of the predicted FHA outer membrane proteins of B. multivorans C1576 (FHA HecA-like & OMP 2). Outer membrane proteins from C1576 with the comparable secretion domain of known TpsA family proteins as described by Jacob-Dubuisson *et al.* (91). Conserved NPNL and NPNGI motifs are indicated by brackets above and below the alignment. The NPNL motif is conserved within the C1576 FHA HecA-like protein, whilst the NPNGI motif is conserved within the C1576 FHA OMP 2 protein. HecA, *Erwinia chrysanthemi* (AAN38708); FhaB, *Bordetella pertussis* Tohama I (NP_880571); HhdA, *Haemophilus ducreyi* (AAC43538); HpmA, *Proteus mirabilis* (P16466); ShlA, *Serratia marcescens* (P15320); HMW1, *Haemophilus influenzae* (AAS77299); EthA, *Edwardsiella tarda* (BAA21097); LspA1, *Haemophilus ducreyi* (NP_873911); LspA2, *Haemophilus ducreyi* (NP_873623). Numbers indicate the position relative to the starting methionine of the precursor protein. Alignment was generated using the AlignX tool of Vector NTI Advance 11.0 (Invitrogen).

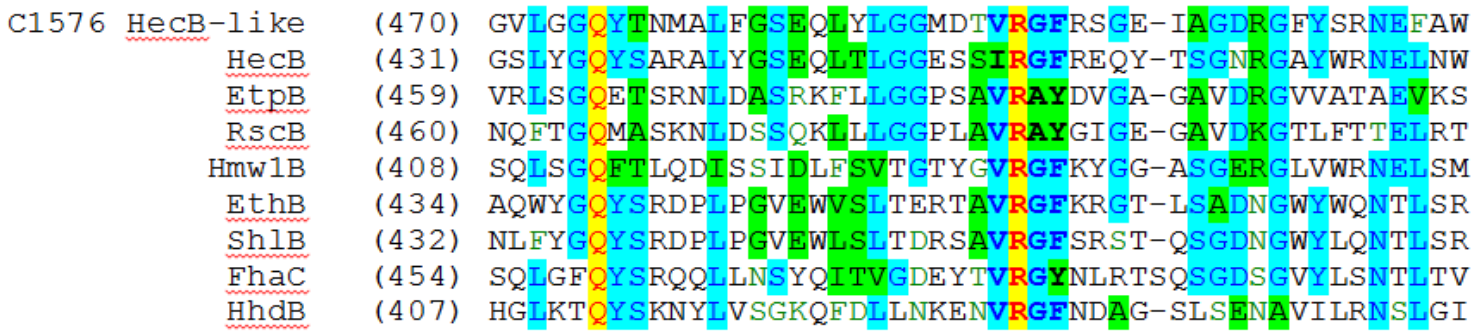

Figure 9.2. Sequence alignment of representative TpsB family proteins. The alignment is centred on the conserved VRGY/F tetrad (bold) described by Delattre *et al.* (60). Alongside the HecB-like protein of *B. multivorans* C1576, the alignment includes: HecB, *Erwinia chrysanthemi* (AAC31980); EtpB, *Escherichia coli* (AAX13508); RscB, *Yersinia enterocolitica* (AAK77859); Hmw1B, *Haemophilus influenzae* (YP_249394); EthB, *Edwardsiella tarda* (BAA21096); ShlB, *Serratia marcescens* (P15321); FhaC, *Bordetella pertussis* Tohama I (NP_880575); HhdB, *Haemophilus ducreyi* (AAC43537). Numbers indicate the position relative to the starting methionine of the protein. Alignment was generated using the AlignX tool of Vector NTI Advance 11.0 (Invitrogen).

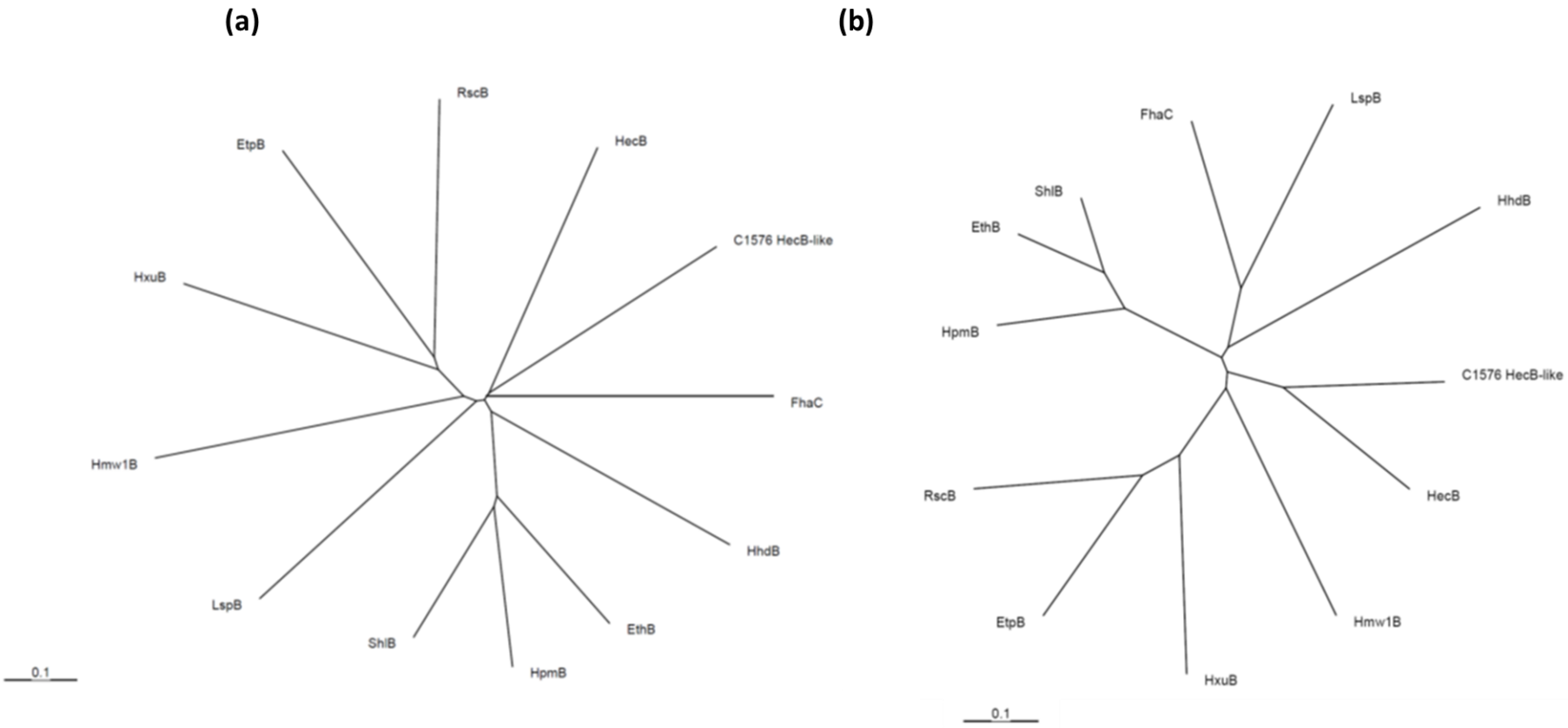

Figure 9.3. Dendrogram of representative TpsB family proteins, based either on full-length proteins (a), or on the conserved VRGY/F motif region depicted in Fig. 9.2 (b). Alignments and tree construction were performed using CLUSTAL and TREEVIEW respectively, revealing that the *B. multivorans* C1576 TpsB family protein is most closely related to the HecB protein of *Erwinia chrysanthemi*. LspB, *Haemophilus ducreyi* (NP_873622); HxuB, *Haemophilus influenzae* (P45356); HpmB, *Proteus mirabilis* (P16465). For details of other sequences, refer to legend of Fig. 9.2.

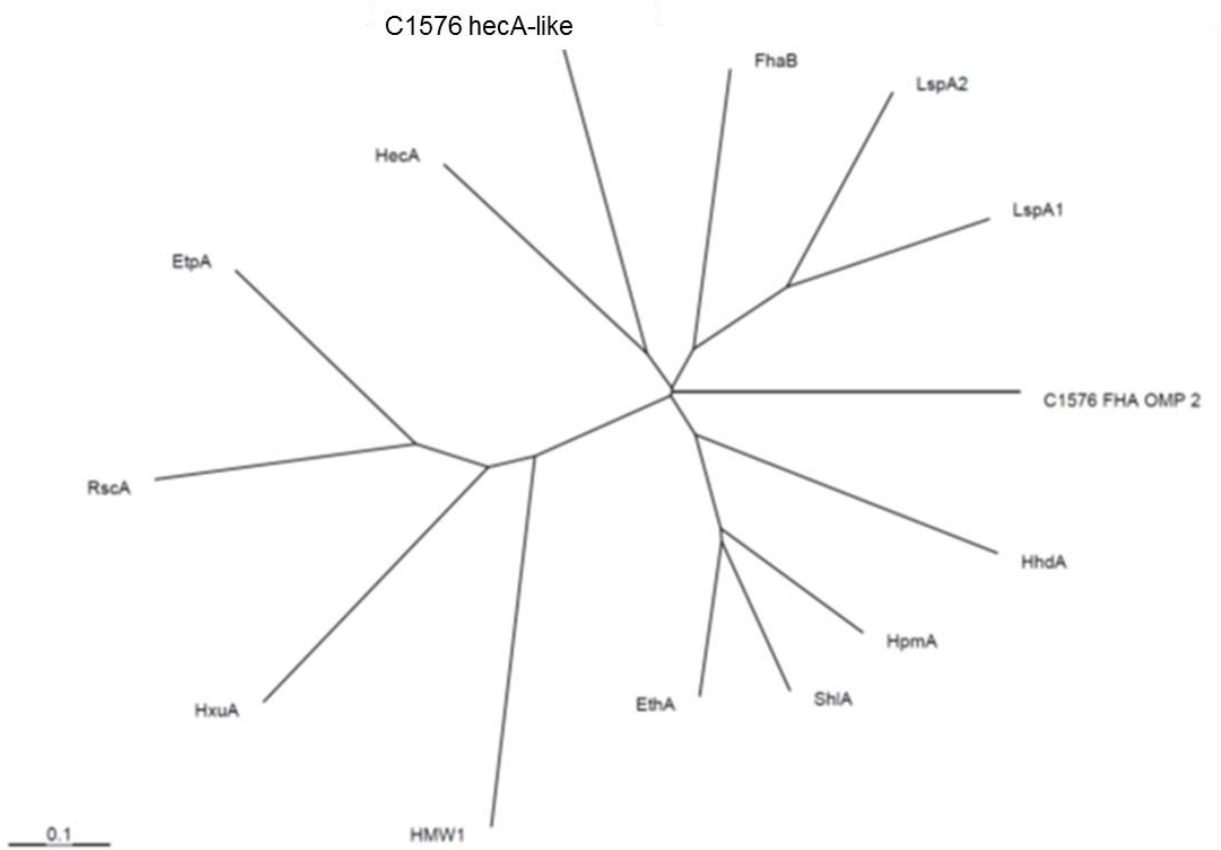

Figure 9.4. Dendrogram of the TPS domain of representative TpsA family proteins, as described by Mazar & Cotter (132) . Alignments and subsequent tree construction were performed using CLUSTAL and TREEVIEW respectively, revealing that the predicted 264 kDa TpsA family protein of *B. multivorans* C1576 ("C1576 HecA-like protein") is most closely related to the HecA protein of *Erwinia chrysanthemi*. The predicted 68 kDa FHA family protein of C1576 ("C1576 FHA OMP 2") is isolated. EtpA, *Escherichia coli* (YP_006203830); RscA, *Yersinia enterocolitica* (YP_001007402); HxuA, *Haemophilus influenzae* (NP_438433). For details of other sequences, refer to legend of Fig. 9.1.

9.3 Tables of differentially expressed genes from transcriptome profiling

The following tables present selected genes, fold-changes, and annotated function to significantly differentially expressed genes from the ATCC 17616 microarray and RNA-seq data set. Overall, there are less differentially regulated genes in the RNA-seq data because of sample quality issues, and only two samples per growth conditions were used for statistical analysis. Microarray data was analysed with 1-way ANOVA and RNA-seq was analysed with pairwise comparisons using Kals' test and Bonferroni post-test of FDR-adjusted p-values. In all tables of significantly differentially expressed genes, the fold-change indicates that the gene is up or downregulated in the first growth condition listed, relative to the second growth condition. The fold changes were deemed significant if > 1.5.

Table 9.6 Common differentially expressed genes from the mucoid microarray and RNA-seq YEM vs. YEO comparisons. Both *B. multivorans* ATCC 17616 and C1576 data sets are combined to assess commonalities between EPS-inducing conditions, mannitol dosage, and strain differences of genes differentially regulated in all these conditions.

ATCC 17616 and C1576		**Fold change observed in strain/growth condition**			
			ATCC 17616		**C1576**
Locus ID	**Function**	**YEF vs. YEO**	**YEM vs. YEO**	**0.25 % YEM vs. YEO**	**YEM vs. YEO**
Bmul_0305	Glutamate synthase (ferredoxin)	0.39	0.35	0.32	5.79
Bmul_0306	glutamate synthase subunit beta	2.45	2.18	2.17	10.38
Bmul_0321	toluene tolerance family protein	0.10	0.12	0.10	-2.99
Bmul_0682	protease Do	0.01	0.01	0.01	-152.85
Bmul_0683	hypothetical protein	0.06	0.07	0.07	-26.82
Bmul_0768	hypothetical protein	0.04	0.14	0.01	-49.15
Bmul_0888	hypothetical protein	0.00	0.00	0.01	-138.93
Bmul_0891	hypothetical protein	2.02	2.58	1.67	4.54
Bmul_0902	hypothetical protein	0.12	0.14	0.19	-8.67
Bmul_1098	histidine ammonia-lyase	0.20	0.39	0.26	-6.73
Bmul_1122	glutamine synthetase, type I	1.73	2.21	1.51	11.13
Bmul_1141	hypothetical protein	0.28	0.31	0.34	-19.78
Bmul_1213	hypothetical protein	0.04	0.05	0.04	-21.70
Bmul_1335	hypothetical protein	0.06	0.10	0.10	-9.38
Bmul_1391	PsiF repeat-containing protein	0.18	0.21	0.18	-5.20
Bmul_1533	hypothetical protein	0.14	0.19	0.14	-5.69
Bmul_1624	hypothetical protein	0.22	0.15	0.18	2.54
Bmul_2210	hypothetical protein	0.07	0.09	0.11	-7.99
Bmul_2361	hypothetical protein	0.10	0.25	0.08	-16.05
Bmul_2447	hypothetical protein	0.08	0.07	0.09	-3.48

Bmul_2737	ferric uptake regulator family protein	2.86	2.53	2.67	4.28
Bmul_3121	M48 family peptidase	1.54	1.50	4.04	18.44
Bmul_3593	hypothetical protein	0.03	0.12	0.01	-18.18
Bmul_3709	Hemolysin-type calcium-binding region	12.53	4.74	19.60	106.55
Bmul_3942	hypothetical protein	0.02	0.07	0.01	-6.29
Bmul_4183	alpha,alpha-trehalose-phosphate synthase (UDP-forming)	2.31	2.08	1.91	15.53
Bmul_4258	hypothetical protein	0.24	0.33	0.27	-16.06
Bmul_4377	hypothetical protein	4.67	4.83	4.99	7.72
Bmul_4390	Crp/FNR family transcriptional regulator	0.41	0.54	0.33	67.61
Bmul_4413	hypothetical protein	2.30	5.93	1.76	26.52
Bmul_4458	SH3 type 3 domain-containing protein	0.23	0.29	0.34	-10.31
Bmul_4459	hypothetical protein	0.05	0.06	0.08	-4.33
Bmul_4475	hypothetical protein	0.06	0.06	0.08	-63.63
Bmul_4675	hypothetical protein	0.28	0.39	0.13	-6.06
Bmul_4829	hypothetical protein	0.10	0.08	0.06	-28.08
Bmul_4896	glycoside hydrolase family 13 protein	5.06	4.05	5.18	10.38
Bmul_5297	Crp/FNR family transcriptional regulator	0.22	0.17	0.05	-10.67

Table 9.7. Differentially expressed EPS-related genes from B. multivorans C1576 RNA-seq data. Genes listed are biosynthetic genes known to be involved in Bcc EPS biosynthesis. As expected, bce cluster genes are upregulated in C1576 YEM relative to YEO, and in YEM relative to non-mucoid YEM and YEG. However, the most significant comparisons are between YEM vs. YEO, as it is the most robust comparison where only the sugar, not the concentration of YE, is varied.

C1576			Fold change observed in growth condition		
Locus ID	Gene name/orthologue	Function	YEM vs. YEO	YEM vs. non-mucoid YEM	YEM vs. YEG
Bmul_4377	BCAM1363	hypothetical protein	7.6		19.1
Bmul_4390	BCAM1348	Crp/FNR family transcriptional regulator	67.3		
Bmul_4413	BCAM1321	putative polyphosphate kinase	26.0		
Bmul_4605	*bceT*	UDP-glucose pyrophosphorylase	53.0	36.7	50.1
Bmul_4915	*bceF*	exopolysaccharide tyrosine-protein kinase	12.3		37.1
Bmul_4916	*bceE*	polysaccharide export protein	59.3		
Bmul_4918	*bceC*	undecaprenyl-phosphate glucose phosphotransferase	21.5		48.5
Bmul_4919	*bceB*	undecaprenyl-phosphate glucose phosphotransferase	28.8	25.2	42.4
Bmul_4920	*bceA*	mannose-1-phosphate guanylyltransferase	54.0	18.2	65.7

Table 9.8. Differentially expressed B. multivorans ATCC 17616 genes selected for putative or confirmed roles in Bcc EPS biosynthesis. Gene names, when available, are listed alongside locus ID.

ATCC 17616 Locus ID	Gene name/orthologue	Function	Fold change observed in growth condition: YEF vs. YEO	YEM vs. YEO	YEF vs. YEM
Bmul_4920	*bceA*	mannose-1-phosphate guanylyltransferase		2.44	3.0
Bmul_4919	*bceB*	undecaprenyl-phosphate glucose phosphotransferase			2.9
Bmul_4918	*bceC*	undecaprenyl-phosphate glucose phosphotransferase			4.1
Bmul_4917	*bceD*	protein tyrosine phosphatase	0.4		3.6
Bmul_4916	*bceE*	polysaccharide export protein	0.4		2.6
Bmul_4915	*bceF*	exopolysaccharide tyrosine-protein kinase	0.3		3.1
Bmul_4914	*bceG*	glycosyl transferase family protein	0.4		2.0
Bmul_4913	*bceH*	glycosyltransferase-like protein	0.2		4.9
Bmul_4912	*bceI*	hypothetical protein	0.4		2.5
Bmul_4911	*bceJ*	group 1 glycosyl transferase	0.3		4.5
Bmul_4910	*bceK*	group 1 glycosyl transferase	0.2		5.2
Bmul_4611	*bceO*	acyltransferase	0.5		3.6
Bmul_4609	*bceQ*	polysaccharide biosynthesis protein	-		5.1
Bmul_4608	*bceR*	group 1 glycosyl transferase	0.4		2.0
Bmul_2600	*wcbR*	beta-ketoacyl synthase	0.6		
Bmul_2608	*wzm*	ABC-2 type transporter	0.5		
Bmul_2610	*wcbD*	lipopolysaccharide biosynthesis protein	0.3		
Bmul_2616	*wcbA*	capsule polysaccharide biosynthesis protein	0.6		
Bmul_5217	BCAM0221	two component LuxR family transcriptional regulator	1.5	1.7	
Bmul_1956	BCAM1317	ABC transporter-like protein/		0.5	
Bmul_4413	BCAM1321	putative polyphosphate kinase	2.3	5.9	2.6
Bmul_4408	BCAM1331	putative tyrosine-protein kinase		1.8	

Bmul_4404	BCAM1335	group 1 glycosyl transferase	1.7	2.0
Bmul_4396	BCAM1342	sigma-54 dependent trancsriptional regulator	0.4	0.4
Bmul_4390	BCAM1348	Crp/FNR family transcriptional regulator	0.4	0.5
Bmul_4387	BCAM1351	TraR/DksA family transcriptional regulator	2.0	1.9
Bmul_4381	BCAM1357	gluconate 2-dehydrogenase (acceptor)	2.2	
Bmul_4379	BCAM1359	sodium/hydrogen exchanger	3.4	1.9
Bmul_4378	BCAM1362	peptidoglycan glycosyltransferase	2.2	
Bmul_4377	BCAM1363	hypothetical protein	4.7	4.8
Bmul_4375	*hpaR*	MarR family transcriptional regulator	1.9	2.0
Bmul_4373	*hpaG*	4-hydroxyphenylacetate degradation bifunctional isomerase/decarboxylase subunit HpaG2	0.3	

Table 9.9 Outer membrane proteins differentially regulated in the B. multivorans ATCC 17616 microarray data. Genes encoding for outer membrane proteins such as porins are general down-regulated in the mucoid vs. YEO conditions, with the exception of most notably two commonly upregulated genes, opcP and an outer membrane efflux encoding protein. OM = outer membrane.

ATCC 17616		Fold change observed in growth condition	
Locus ID	**Function**	**YEF vs. YEO**	**YEM vs. YEO**
Bmul_1937	porin		0.2
Bmul_2395	porin	0.5	0.4
Bmul_2963	porin	0.4	0.4
Bmul_3002	porin	0.5	0.5
Bmul_3268	OM porin		0.2
Bmul_3342	porin		8.4
Bmul_3463	porin		0.4
Bmul_3587	OM porin OpcP	1.6	1.6
Bmul_3710	OM efflux protein	12.7	5.7
Bmul_6034	porin		0.5
Bmul_6067	porin		0.4

Table 9.10 Outer membrane proteins differentially regulated in the B. multivorans C1576. OM = outer membrane. No other membrane protein-related genes were identified in C1576 growth condition comparisons of interest.

C1576		Fold-change in observed growth conditions
Locus ID	**Function**	**YEG vs. non-mucoid YEM**
Bmul_0157	aquaporin Z	-13.1
Bmul_0880	OM porin-like protein	-7.8
Bmul_4327	porin	-7.2

Table 9.11 Upregulated transcriptional regulator genes in B. multivorans ATCC 17616. Listed are the most significantly upregulated transcriptional regulators from the mucoid YEF and YEM vs. YEO ATCC 17616 microarray data sets. Note this list is not inclusive of every differentially expressed transcriptional regulator in the ATCC 17616 mucoid vs. YEO data sets, but the most upregulated for each condition and the regulators common to all mucoid vs. non-mucoid conditions. The Appendix CD contains the entire data set for each growth condition and differentially expressed transcriptional regulators are listed for. Asterisks (*) denotes regulator is common to all mucoid (including reduced YEM vs. YEO which is not shown) data sets.

ATCC 17616		Fold change observed under each growth condition	
Locus ID	Function	YEF vs. YEO	YEM vs. YEO
Bmul_0160	transcriptional activator FlhD		2.1
Bmul_0161	transcriptional activator FlhC		2.6
Bmul_2015	two component transcriptional regulator		5.7
Bmul_2557*	LysR family transcriptional regulator	1.7	1.9
Bmul_2962	LysR family transcriptional regulator	4.3	
Bmul_3022	anti-sigma-28 factor, FlgM		2.0
Bmul_3052	two component LuxR family transcriptional regulator	4.1	4.5
Bmul_3720	XRE family transcriptional regulator	5.7	
Bmul_3737	LuxR family transcriptional regulator		2.7
Bmul_3738	LuxR family transcriptional regulator	4.3	3.3
Bmul_4418	LysR family transcriptional regulator		4
Bmul_4658	ArsR family transcriptional regulator	4	
Bmul_4689*	TetR family transcriptional regulator	7.5	2.8
Bmul_4903	sigma-54 dependent trancsriptional regulator		3.2
Bmul_5074*	LysR family transcriptional regulator	5.8	5.4
Bmul_5903	two component LuxR family transcriptional regulator		3.2
Bmul_6032	IclR family transcriptional regulator	4.1	

Table 9.12 C1576 RNA-seq differentially regulated genes involved in signal transduction and transcriptional regulation. The genes listed in this table are the most significantly differentially expressed transcriptional regulators in the C1576 RNA-seq growth condition comparisons of interest.

C1576		Fold change observed in growth condition	
Locus ID	**Function**	**YEM vs. YEO**	**YEG vs. non-mucoid YEM**
Bmul_0192	AsnC family transcriptional regulator		-3.7
Bmul_0236	transcription antitermination protein NusG		-8.4
Bmul_0414	DNA-binding transcriptional activator GcvA		-14.5
Bmul_1005	TetR family transcriptional regulator		-5.9
Bmul_1791	XRE family transcriptional regulator		-4.1
Bmul_2177	RNA polymerase sigma factor RpoE		-5.8
Bmul_2442	transcription antitermination protein NusB	5.4	
Bmul_2962	LysR family transcriptional regulator		-27.7
Bmul_3031	putative transcriptional regulator		-10.1
Bmul_3128	LysR family transcriptional regulator	7.2	
Bmul_3128	LysR family transcriptional regulator		-10.7
Bmul_3545	AraC family transcriptional regulator	76.7	
Bmul_4270	AsnC family transcriptional regulator		-8.3
Bmul_4813	RNA polymerase sigma factor RpoD		-5.6

Table 9.13. B. multivorans ATCC 17616 differentially expressed motility genes. Genes related to the proteins responsible for flagella biosynthesis and chemotaxis pathways are the focus of this table. The flagella transcriptional regulators upregulated in YEM vs. YEO are listed in Table 9.10.

ATCC 17616			**Fold change observed in growth condition**	
Locus ID	**Gene name**	**Function**	**YEF vs. YEO**	**YEM vs. YEO**
Bmul_0038	*fliR*	flagellar biosynthesis protein FliR		2.6
Bmul_0040	*fliP*	flagellar biosynthesis protein FliP		10.1
Bmul_0041	*fliO*	flagellar biosynthesis protein FliO	0.6	
Bmul_0042	*fliN*	flagellar motor switch protein FliN	2	4.2
Bmul_0043	*fliM*	flagellar motor switch protein FliM		2.5
Bmul_0044	*fliL*	flagellar basal body-associated protein FliL	3.1	7.2
Bmul_0150	*fliD*	flagellar hook-associated 2 domain-containing protein	3.6	10.3
Bmul_0151	*fliC*	flagellin domain-containing protein	2.6	10
Bmul_0162	*motA*	flagellar motor protein MotA	3.3	9.3
Bmul_0163	*motB*	flagellar motor protein MotB		2.1
Bmul_0164		response regulator receiver protein		3.7
Bmul_0166	*cheW*	CheW protein	2.1	5.2
Bmul_0167		methyl-accepting chemotaxis sensory transducer	3.8	10
Bmul_0168		MCP methyltransferase, CheR-type		8.5
Bmul_0170		chemotaxis-specific methylesterase		4.2
Bmul_0171		response regulator receiver protein		2.2
Bmul_0172	*cheZ*	chemotaxis regulator CheZ		1.6
Bmul_0173		hypothetical protein		1.6
Bmul_0174		hypothetical protein	3	2.9
Bmul_0176	*flhA*	flagellar biosynthesis protein FlhA	4.1	4.4
Bmul_0178	*flhG*	flagellar biosynthesis protein, FlhG	2.4	2.1
Bmul_0179		flagellar biosynthesis sigma factor		7

Bmul_1733	*cpaB*	Flp pilus assembly protein CpaB	2	1.7
Bmul_1736		Flp/Fap pilin component		2.6
Bmul_3012		flagellar rod assembly protein/muramidase FlgJ		2.4
Bmul_3014		flagellar basal body L-ring protein		5.2
Bmul_3015	*flgG*	flagellar basal body rod protein FlgG	2.5	4
Bmul_3017	*flgE*	flagellar hook protein FlgE		4.3
Bmul_3018		flagellar basal body rod modification protein	2.5	5.3
Bmul_3019	*flgC*	flagellar basal body rod protein FlgC	5.3	14.9
Bmul_3059	*fliS*	flagellar protein FliS		1.9
Bmul_3060	*fliE*	flagellar hook-basal body complex subunit FliE	0.6	
Bmul_3062		flagellar motor switch protein G		2.7
Bmul_3063		flagellar assembly protein H		5
Bmul_3065	*fliJ*	flagellar export protein FliJ		7.2
Bmul_4997		methyl-accepting chemotaxis sensory transducer		0.5
Bmul_4998		OmpA/MotB domain-containing protein		0.3
Bmul_4999		MotA/TolQ/ExbB proton channel		0.4

Table 9.14 Motility-related genes differentially expressed in the B. multivorans C1576 RNA-seq.

C1576 Locus ID	Gene name	Function	Fold change observed in growth condition YEG vs. non-mucoid YEM
Bmul_0162	*motA*	flagellar motor protein MotA	-11.9
Bmul_0163	*motB*	flagellar motor protein MotB	-14.2
Bmul_3010	*flgK*	flagellar hook-associated protein FlgK	-11.0
Bmul_3362		methyl-accepting chemotaxis sensory transducer with Pas/Pac sensor	-14.6

Table 9.15 B. multivorans ATCC 17616 microarray gene expression data related to nitrogen metabolism.

ATCC 17616		Fold change observed in growth condition
Locus ID	**Function**	**YEF vs. YEO**
Bmul_4113	aerobic-type carbon monoxide dehydrogenase large subunit	0.5
Bmul_4143	ABC-type nitrate/sulfonate/bicarbonate transport systems	0.6
Bmul_4148	nitrite reductase (NAD(P)H), small subunit	2.3
Bmul_4784	ABC-type nitrate/sulfonate/bicarbonate transport systems	0.5
Bmul_5383	nitrate reductase, alpha subunit (NarG)	2.6
Bmul_5384	nitrate reductase, beta subunit (NarH)	3.2

Table 9.16 C1576 RNA-seq data set genes involved in nitrogen metabolism. Genes involved in anaerobic respiration and nitrogen assimilation are listed below.

C1576		Fold change observed in growth condition
Locus ID	**Function**	**YEM vs. YEO**
Bmul_1212	cytochrome o ubiquinol oxidase subunit IV	-14.6
Bmul_4149	molybdopterin oxidoreductase	566.2

Table 9.17 Secretion-related genes differentially expressed in B. multivorans C1576 RNA-seq data. C1576 genes differentially expressed in growth conditions of interest were sorted based on putative involvement intracellular trafficking and secretion-related genes.

C1576 Locus ID	Function	Fold change observed in growth condition YEG vs. non-mucoid YEM
Bmul_0235	preprotein translocase subunit SecE	-5.5
Bmul_0269	preprotein translocase subunit SecY	-6.4
Bmul_0449	preprotein translocase subunit SecB	-8.9
Bmul_2665	preprotein translocase subunit SecY	-23.9
Bmul_2827	preprotein translocase subunit SecA	-6.0

Table 9.18 Secretion-related genes differentially regulated in ATCC 17616. These genes were selected based on involvement with intracellular trafficking and secretion-related genes.

ATCC 17616		Fold change observed for growth condition	
Locus ID	**Function**	**YEF vs. YEO**	**YEM vs. YEO**
Bmul_0352	type VI secretion system Vgr family protein	1.8	1.7
Bmul_1728	type II secretion system protein	1.6	
Bmul_1729	type II secretion system protein	1.8	
Bmul_1730	type II secretion system protein E	1.5	
Bmul_1869	secretion protein HlyD family protein	0.1	0.2
Bmul_2545	transport-associated protein	0.7	
Bmul_2585	protein TolR		0.7
Bmul_2587	translocation protein TolB	0.5	
Bmul_2930	type VI secretion protein	1.6	1.5
Bmul_3711	type I secretion system ATPase	13.6	5.9
Bmul_3750	type III secretion exporter	4.5	1.9
Bmul_3903	type VI secretion protein		1.8
Bmul_3913	type VI secretion protein	4.9	
Bmul_4244	transport-associated protein	0.6	
Bmul_5730	type VI secretion system Vgr family protein	0.5	
Bmul_5888	secretion protein HlyD family protein		2.2

Table 9.19 B. multivorans ATCC 17616 microarray data shows genes related to antibiotic-resistance and multidrug efflux pumps.

ATCC 17616		Fold change observed in growth condition	
Locus ID	**Function**	**YEF vs. YEO**	**YEM vs. YEO**
Bmul_0051	RND efflux system outer membrane lipoprotein	0.4	0.4
Bmul_0194	beta-lactamase domain-containing protein		2.2
Bmul_0312	ABC transporter	0.5	0.5
Bmul_1294	ABC transporter related	0.3	0.4
Bmul_1356	ABC transporter related	1.7	
Bmul_1642	ABC transporter	2.3	
Bmul_1750	RND efflux system outer membrane lipoprotein	0.6	0.6
Bmul_1751	efflux pump membrane protein	0.6	
Bmul_1768	Antibiotic biosynthesis monooxygenase	3.1	
Bmul_1866	RND efflux system outer membrane lipoprotein	0.3	0.5
Bmul_1956	ABC transporter related		0.5
Bmul_2104	RND family efflux transporter MFP subunit	0.2	0.2
Bmul_2427	ABC transporter related	0.4	
Bmul_2711	ABC transporter related	1.7	
Bmul_3313	beta-lactamase domain-containing protein		0.6
Bmul_4048	Beta-lactamase		0.6
Bmul_4052	ABC transporter related	0.4	0.4
Bmul_4219	Antibiotic biosynthesis monooxygenase		0.5
Bmul_4303	beta-lactamase domain-containing protein		2.4
Bmul_4313	RND family efflux transporter MFP subunit		0.7
Bmul_4356	RND family efflux transporter MFP subunit	2	1.7
Bmul_4684	RND efflux system outer membrane lipoprotein	0.3	
Bmul_4887	ABC transporter related	2.4	
Bmul_5001	ABC transporter related	0.3	0.4

Bmul_5647	Antibiotic biosynthesis monooxygenase		0.5
Bmul_5749	ABC-2 type transporter	2.2	
Bmul_5962	ABC transporter related	0.5	0.5
Bmul_6151	RND efflux system outer membrane lipoprotein	0.6	

Table 9.20 B. multivorans ATCC 17616 microarray data related to carbohydrate transport and metabolism.

ATCC 17616		Fold change observed in growth condition	
Locus ID	**Function**	**YEF vs. YEO**	**YEM vs. YEO**
Bmul_0712	mannitol dehydrogenase domain-containing protein	3.5	
Bmul_2432	6-phosphogluconolactonase	4.3	
Bmul_2433	Glucokinase	0.5	
Bmul_3206	Monosaccharide-transporting ATPase	0.4	0.5
Bmul_3245	carbon starvation protein CstA	3.6	
Bmul_3354	glucose-6-phosphate 1-dehydrogenase	2.1	
Bmul_5837	succinate dehydrogenase iron-sulfur subunit	1.9	
Bmul_5839	succinate dehydrogenase, hydrophobic membrane anchor protein	1.8	
Bmul_5840	succinate dehydrogenase, cytochrome b556 subunit	2.2	
Bmul_5961	Monosaccharide-transporting ATPase	0.3	

Table 9.21 RNA-seq C1576 data summary of genes differentially expressed related to carbohydrate transport and metabolism.

C1576 Locus ID	Function	Fold-change in observed growth condition	
		YEM vs. YEO	YEG vs. non-mucoid YEM
Bmul_0482	PTS system N-acetylglucosamine-specific transporter subunit IIBC		-17.7
Bmul_0647	general substrate transporter		-26.1
Bmul_0699	sorbitol dehydrogenase	14.7	
Bmul_0712	mannitol dehydrogenase domain-containing protein		-45.4
Bmul_1163	phosphopyruvate hydratase		-6
Bmul_1711	ABC transporter-like protein		-11.5
Bmul_1712	monosaccharide-transporting ATPase		-15.8
Bmul_1713	periplasmic binding protein/LacI transcriptional regulator		-9.9
Bmul_2038	general substrate transporter		-26.4
Bmul_2428	binding-protein-dependent transport systems inner membrane component		-8.6
Bmul_2429	binding-protein-dependent transport system inner membrane protein		-5.5
Bmul_2430	extracellular solute-binding protein		-7.8
Bmul_2722	2-dehydro-3-deoxyphosphogluconate aldolase		-8.5
Bmul_2747	glyceraldehyde-3-phosphate dehydrogenase, type I		-7.4
Bmul_2784	ribokinase-like domain-containing protein		-5.4
Bmul_2968	N-acylglucosamine 2-epimerase		-10.7
Bmul_4153	major facilitator transporter		-21.2
Bmul_4154	mannonate dehydratase		-48.4
Bmul_4168	major facilitator transporter		-20.5

Table 9.22 B. multivorans ATCC 17616 microarray data that lists potential virulence factors. These include genes encoding for haemagglutinin-related proteins, phosphatases, lipases, lipoproteins, superoxide dismutases, adhesins, and phage-related genes. Motility and chemotaxis genes, as well as secretion-system related proteins are listed elsewhere but are also considered potential virulence factors.

ATCC 17616		Fold change observed in growth condition	
Locus ID	**Function**	**YEF vs. YEO**	**YEM vs. YEO**
Bmul_0576	phospholipase D/Transphosphatidylase		1.9
Bmul_0753	Superoxide dismutase	2.9	2.7
Bmul_0860	superoxide dismutase copper/zinc binding	1.7	1.6
Bmul_1151	17 kDa surface antigen	0.1	0.1
Bmul_1806	putative bacteriophage protein		1.7
Bmul_1815	putative bacteriophage protein	0.6	0.7
Bmul_1914	acid phosphatase	2.0	9.3
Bmul_1997	putative hemolysin-like protein		3.0
Bmul_2139	phospholipase C, phosphocholine-specific		10.1
Bmul_2410	lipopolysaccharide heptosyltransferase I	0.3	
Bmul_2496	lipopolysaccharide heptosyltransferase I		2.1
Bmul_2610	lipopolysaccharide biosynthesis protein	0.3	
Bmul_2951	phospholipase C, phosphocholine-specific		17.2
Bmul_3223	17 kDa surface antigen		0.3
Bmul_3271	phospholipase C, phosphocholine-specific	0.2	
Bmul_3329	17 kDa surface antigen	0.3	
Bmul_3343	YaeC family lipoprotein	1.5	1.8
Bmul_3376	toxin ChpB		0.5
Bmul_3447	phospholipase D/transphosphatidylase		7.9
Bmul_3477	hemagluttinin domain-containing protein	0.1	0.2

Bmul_3522	hemagluttinin domain-containing protein	0.2	0.3
Bmul_3709	Hemolysin-type calcium-binding region	12.5	4.7
Bmul_4479	fimbrial biogenesis outer membrane usher protein		0.2
Bmul_4511	phospholipase/Carboxylesterase	1.7	1.6
Bmul_4837	P2 family phage major capsid protein	2.0	4.0
Bmul_4852	phage tail protein I	0.4	0.4
Bmul_4860	putative phage-related tail transmembrane protein	0.3	0.4
Bmul_4871	putative phage-encoded membrane protein	2.7	2.4
Bmul_6272	integrase family protein	2.1	
Bmul_6273	hypothetical protein	2.7	
Bmul_6274	site-specific recombinase, phage integrase family protein	3.1	

Table 9.23 B. multivorans C1576 RNA-seq data related to potential virulence factors. These include haemagglutinin-related proteins, phosphatases, lipases, lipoproteins, and adhesins. Motility and chemotaxis genes, as well as secretion-system related proteins are listed elsewhere but are also potential virulence factors. Including in this list are the novel adhesins discussed and characterised in Chapter 5, and screened for in the panel of isolates listed in Appendix Table 9.5. These adhesins are identified by bold script. Due to their absence in the genome of the environmental isolate *B. multivorans* ATCC 17616, adhesins were mapped to *B. multivorans* CGD1 isolate and *B. ambifaria* MC0-40, based on NCBI BLAST searches for highest amino acid identify.

C1576		**Fold change observed in growth condition**	
Locus ID	**Function**	**YEM vs. YEO**	**YEG vs. non-mucoid YEM**
Bmul_0195	rare lipoprotein A		-10.9
Bmul_0682	protease Do	8.1	
Bmul_3252	hopanoid biosynthesis associated radical SAM protein HpnH		-6.9
Bmul_3709	hemolysin-type calcium-binding region	106.5	
BURMUCGD1_3349	Fimbrial protein (1)	3.7	
BURMUCGD1_3350	FimC	13.3	
BURMUCGD1_3351	Fimbrial usher	7.0	
BURMUCGD1_3352	Fimbrial protein (2)	4.6	
BURMUCGD1_3353	Fimbrial protein (3)	2.5	
MC406_6760	PPIase	1.7	
MC406_6761	HecB-like	1.3	
MC406_6763	FHA OMP (2)	1.7	
MC406_6766	FHA OMP (1)	1.5	

Table 9.24. Genes common to the Silva et al. data set. The table is not an exhaustive comparison but highlights key similarities and clusters of genes in common with the *B. multivorans* transcriptome study by Silva *et al*. (178). The data shown in the far right column compares differential gene expression of two clonal isolates, one mucoid one non-mucoid. The data presented in this table from Silva *et al.* simplified their findings to signify 'D' for gene decreased in expression or 'U' upregulated or enhanced in expression in their mucoid vs. non-mucoid isolate data. In this way, comparison between the mucoid vs. non-mucoid growth conditions explored in the present study and observations between the significant overlap between the two data sets can be made.

			ATCC 17616		C1576	Silva *et al.*
Locus	Gene name	Function	YEF vs. YEO	YEM vs. YEO	YEM vs. YEO	Mucoid vs. non-mucoid
Bmul_0042	*fliN*	flagellar motor switch protein FliN	2.0			U
Bmul_0044	*fliL*	flagellar basal body-associated protein FliL	3.1			U
Bmul_0159		glycosyl transferase group 1	0.4	0.5		D
Bmul_0160		transcriptional activator FlhD		2.1		U
Bmul_0161		transcriptional activator FlhC		2.6		U
Bmul_0162	*motA*	flagellar motor protein MotA	3.3			U
Bmul_0166	*cheW*	CheW protein	2.1			U
Bmul_0167		methyl-accepting chemotaxis sensory transducer	3.8			U
Bmul_0174		hypothetical protein	3.0			U
Bmul_0176	*flhA*	flagellar biosynthesis protein FlhA	2.4			U
Bmul_0305	*gltB*	Glutamate synthase (ferredoxin)		0.3	5.8	U
Bmul_0306	*gltD*	glutamate synthase subunit beta	2.5	2.2	10.4	U
Bmul_0682	*degP*	protease Do	0.01	0.01	-152.8	U
Bmul_0712	*mtlK*	mannitol dehydrogenase domain-containing protein	3.5			U
Bmul_1320	*papA*	phage shock protein A, PspA	0.1	0.2		D
Bmul_2395		porin	0.5	0.4		U
Bmul_2557		LysR family transcriptional regulator	1.7	1.9		U
Bmul_2585	*tolR*	*protein TolR*		0.7		D
Bmul_2930	*bcsL*	type VI secretion protein	1.6	1.5		U

Bmul_3015	*flgG*	flagellar basal body rod protein FlgG	2.5			U
Bmul_3018		flagellar basal body rod modification protein	2.5			U
Bmul_3019	*flgC*	flagellar basal body rod protein FlgC	5.3			U
Bmul_3060	*fliE*	flagellar hook-basal body complex subunit FliE	0.6			U
Bmul_4598	*fdh*	molybdopterin oxidoreductase Fe4S4 region	1.5			D
Bmul_4605	*bceT*	UDP-glucose pyrophosphorylase			4.3	U
Bmul_4915	*bceF*	exopolysaccharide tyrosine-protein kinase	0.3		12.3	U
Bmul_4916	*bceE*	polysaccharide export protein			59.3	U
Bmul_4917	*bceD*	protein tyrosine phosphatase	0.4			U
Bmul_4918	*bceC*	undecaprenyl-phosphate glucose phosphotransferase			21.5	U
Bmul_4919	*bceB*	undecaprenyl-phosphate glucose phosphotransferase			28.8	U
Bmul_4920	*bceA*	mannose-1-phosphate guanylyltransferase		2.4	54.0	U

Chapter 10: General conclusions and future work

10.1 Aims

The purpose of this final chapter is to present general conclusions of each main body of work with respect to the main aims of the thesis and potential avenues for future work.

10.2 Summary

The incidence of cystic fibrosis related diabetes (CFRD) is on the rise as patient life expectancy continues to improve. Sugars elevated in diabetics include glucose, fructose, and mannose. These sugars, in addition to mannitol (recently approved as an inhaled osmolyte for patients with cystic fibrosis) were the basis for this study, aimed at assessing the impact these clinically relevant sugars have on virulence in *Burkholderia multivorans*. Of these sugars, both mannitol and fructose induce exopolysaccharide (EPS) production, a putative virulence factor attributed to members of the *Burkholderia cepacia* complex (Bcc). *B. multivorans* is a member of the Bcc, and recent shifts in the epidemiology of the Bcc place *B. multivorans* as the dominant species in Bcc respiratory infections in patients with cystic fibrosis (CF). In contrast to *B. cenocepacia*, very little is known about the mechanisms of virulence in *B. multivorans.*

Using an EPS-deficient knockout, Chapter 3 presented studies that first identified EPS-dependent and -independent virulence relevant phenotypes associated with growth on mannitol (mucoid) and mannose (non-mucoid). These phenotypes included mannitol enhanced invasion of alveolar epithelial cells, attenuation in the *Galleria mellonella* model of infection, increased biofilm formation and motility, and strain dependent enhanced adhesion to mucin. Crucially, including the EPS-deficient knockouts alongside *B. multivorans* wild-types enabled differentiation between EPS phenotypes or those attributed to a broader sugar effect.

In addition to phenotypic analysis of the *B. multivorans* sugar response, transcriptomic profiling was undertaken by microarray and RNA-seq to investigate the genetic basis for EPS production in two representative strains of *B. multivorans*. These studies were aimed to determine the genome-wide response of *B. multivorans* to relevant sugars. This has allowed correlation of gene expression changes (presented in Chapter 4) with some of the results from phenotypic studies (from Chapters 3 and 5) and provided insight into strain variation between the *B. multivorans* isolates in response to different sugars.

It was observed in both phenotypic studies and transcriptomic data that *B. multivorans* ATCC 17616 (an environmental strain) grown in mannitol resulted in enhanced motility relative to fructose or mannose grown cultures, in an EPS-independent manner. Microarray data confirmed the mannitol and fructose upregulated the flagella assembly and chemotaxis pathways (more so in mannitol than in fructose). In addition, *B. multivorans* C1576 (CF isolate) revealed the upregulation of the *bce* EPS cluster during growth on mannitol – thus confirming that although this strain is reported to produce more than one type of EPS (compared to ATCC 17616 which reportedly only produces cepacian). Interestingly, this was not the case from mannitol-or fructose-grown ATCC 17616, which did not enhance expression of key EPS biosynthesis genes following growth on these sugars.

In Chapter 5, an observation from phenotypic studies in Chapter 3, which indicated the role for EPS in adherence to mucin was strain dependent, was further explored. EPS production positively correlated with the ability of ATCC 17616 to adhere to mucin. The ability of the CF isolate C1576 to adhere to mucin was EPS independent. Whole genome sequencing of C1576 identified putative adhesins that were absent from ATCC 17616, namely a fimbrial locus and two distinct adhesins of the filamentous haemagglutinin (FHA) family. In Chapter 5 the present study went on to hypothesise that the presence of these putative adhesins in C1576 could explain the observed strain variation in adhesion, and went on to characterise these adhesins and assess the distribution within other clinical and environmental isolates of *B. multivorans* and the Bcc. Results indicated that the FHA locus was restricted to clinical *B. multivorans* isolates, and found almost exclusively in outbreak related isolates, whilst the fimbrial locus was widely distributed amongst clinical and environmental isolates. These adhesins (the first to be identified and described for *B. multivorans*) played a role in biofilm formation, adhesion to A549 human lung epithelial cells, and mucin. The RNA-seq dataset using mannitol-grown C1576 confirmed the upregulation of the three adhesins by mannitol, explaining the enhanced adhesion in the clinical isolate independent of EPS production.

Additional studies presented in Chapters 6 and 7 of this dissertation assessed the impact of growth on different sugars and sugar alcohols on the composition and biological activity of *B. multivorans* EPS. To carry out composition analysis mass spectrometry was used to compare composition of sugars known to be found in the Bcc cepacian repeat unit, to EPS extracts from ATCC 17616 and C1576 grown on mannitol or fructose. Due to technical difficulties with reproducibility, these composition analysis studies did not show any significantly altered EPS composition between strains or carbon sources.

In Chapter 7, characterising biological activity of *B. multivorans* EPS was discussed. In iron toxicity, scavenging of reactive oxygen species (ROS) and desiccation protection assays, mannitol- and fructose-derived EPS resulted in strain-to-strain differences and variations between fructose- and mannitol-derived EPS for both the clinical and environmental isolates. This variation in biological activity indicated the impact of different carbon sources on the biological activity of the EPS.

Still relevant to CFRD, Chapter 8 assessed the ability of some members of the Bcc to bind insulin using fluorescent microscopy and fluorescent plate reader assays. Studies also showed using flow cytometry cell sorting and fluorescence microscopy that it is a small number of cells within a given population that bind insulin. Following fluorescence- activated cell sorting, insulin bound cells in repeated subculture were not enriched for insulin binding, and therefore these studies indicated that insulin binding occurs in a random subset of cells.

Phenotypic studies have shed light on the role of EPS in virulence-relevant assays, and linked this by transcriptomic study to highlight that sugars of clinical significance can alter bacterial behaviour significantly *in vitro.* Due to technical issues with reproducibility, it is inconclusive whether altering the carbon source that induces EPS production impacted on EPS composition, but it did influence biological activity of *B. multivorans* EPS.

In all, this programme of study has added to the sparse knowledge base of *B. multivorans* virulence factors, including improving understanding of the

consequence and biological significance of EPS, identification and characterisation of the first adhesins described in *B. multivorans.* These adhesins were upregulated by mannitol and played a role in adhesion and biofilm formation, and creation of an improved method for carrying out EPS phenotypic studies by using an EPS deficient mutant alongside the wild-type strain to eliminate confusion between sugar effects versus EPS-dependent phenotypes.

10.3 Future work

With regards to future work leading on from studies presented in Chapter 3, of great interest is the improvement of the macrophage assay by the creation of aminoglycoside-sensitive *B. multivorans* strains, using the elegant mutagenesis method described by Hamad *et al.* (86). Use of these antibiotic sensitive strains would mean fewer antibiotics (and much lower concentrations) required to kill off extracellular bacteria, and assurance that extracellular bacteria are entirely killed off. Although efforts were made to construct gentamicin sensitive *B. multivorans* in the present study, attempts were unsuccessful. Preliminary trials using GFP-labelled *B. multivorans* and confocal microscopy were not carried on without gentamicin sensitive mutants. Another observation of interest for follow-up from data presented in Chapter 3 is the mannitol-enhanced survival of tobramycin-exposed biofilms. It would be interesting to extend this experiment to clinical isolates of *B. multivorans*, other aminoglycosides, and even other classes of antibiotics. The biofilm system used in Chapter 3 is a good *in vitro* model for studying these effects and with further work could define any connection between mannitol and biofilm aminoglycoside resistance, which could inform on antibiotics chosen to treat CF patients receiving mannitol therapy.

In Chapter 4 the transcriptome profiles of two *B. multivorans* isolates indicated strain variation exists with regards to the impact of different sugar on the induction of EPS. Indeed, strains apparently varied in the pathways used in EPS production. The transcriptome studies enabled EPS regulation to be

assessed as well as broader impacts of different sugars on virulence relevant genes. Several transcriptional regulators common to both strains were upregulated in mucoid growth conditions would be excellent candidates for future mutagenesis studies to decipher EPS-regulation pathways. Study of such regulators would also include establishing how many of the EPS-independent genes or phenotypes are also controlled by these transcriptional regulators, and thus co-ordinately regulated in conjunction with EPS production. The identification and characterisation of transcriptional regulators upregulated in mucoid conditions would help explain the extensive overlap between the data set presented in Chapter 4 and mucoid/non-mucoid comparisons of *B. multivorans* clonal isolates such as those described by Silva *et al.* (178).

Although the composition analysis of EPS from different carbon sources discussed in Chapter 6 requires different or improved methodologies to draw any definitive conclusions, in Chapter 7 studies of the impact of carbon source on EPS biological activity suggested that carbon source did impact on several phenotypes associated with stress survival. Thus it is clear further means to explore differences in the mannitol and fructose EPS composition would be worthwhile, using such technology as NMR to detect structural differences or polysaccharides other than cepacian that could influence the interaction between polysaccharides and host environment.

Overall these responses to sugar and sugar alcohols are important to understand as they have potential influence on the course of a *B. multivorans* CF respiratory infection. As Bcc infected patients are notoriously varied in infection outcome, it is important to inform researchers and clinicians alike of the varied sugar response and significance of EPS in *B. multivorans* virulence.

Chapter 11: References

References

1. **Acord, J., J. Maskell, and A. Sefton**. 2005. A rapid microplate method for quantifying inhibition of bacterial adhesion to eukaryotic cells. J.Microbiol.Methods **60**:55-62.

2. **Adi, H., P. M. Young, H. K. Chan, H. Agus, and D. Traini**. 2010. Co-spray-dried mannitol-ciprofloxacin dry powder inhaler formulation for cystic fibrosis and chronic obstructive pulmonary disease. Eur.J.Pharm.Sci. **40**:239-247.

3. **Aitken, M. L., G. Bellon, B. K. De, P. A. Flume, H. G. Fox, D. E. Geller, E. G. Haarman, H. U. Hebestreit, A. Lapey, I. M. Schou, J. B. Zuckerman, and B. Charlton**. 2012. Long-term inhaled dry powder mannitol in cystic fibrosis: an international randomized study. Am.J Respir.Crit Care Med. **185**:645-652.

4. **Alba-Loureiro, T. C., C. D. Munhoz, J. O. Martins, G. A. Cerchiaro, C. Scavone, R. Curi, and P. Sannomiya**. 2007. Neutrophil function and metabolism in individuals with diabetes mellitus. Braz.J.Med.Biol.Res. **40**:1037-1044.

5. **Allison, D. G. and M. J. Goldsbrough**. 1994. Polysaccharide production in *Pseudomonas cepacia*. J.Basic Microbiol. **34**:3-10.

6. **Allison, K. R., M. P. Brynildsen, and J. J. Collins**. 2011. Metabolite-enabled eradication of bacterial persisters by aminoglycosides. Nature. **473(7346)**:216-220.

7. **Alves, C. A., R. A. Aguiar, A. C. Alves, and M. A. Santana**. 2007. Diabetes mellitus in patients with cystic fibrosis. J.Bras.Pneumol. **33**:213-221.

8. **Ammendolia, M. G., L. Bertuccini, F. Iosi, F. Minelli, F. Berlutti, P. Valenti, and F. Superti**. 2010. Bovine lactoferrin interacts with cable pili of *Burkholderia cenocepacia*. Biometals **23**:531-542.

9. **Armbruster, C. E., B. Pang, K. Murrah, R. A. Juneau, A. C. Perez, K. E. Weimer, and W. E. Swords**. 2011. RbsB (NTHI_0632) mediates quorum signal uptake in nontypeable *Haemophilus influenzae* strain 86-028NP. Mol.Microbiol. **82(4)**:836-850.

10. **Aronoff, S. C.** 1988. Outer membrane permeability in *Pseudomonas cepacia*: diminished porin content in a beta-lactam-resistant mutant and in resistant cystic fibrosis isolates. Antimicrob.Agents Chemother. **32**:1636-1639.

11. **Asiah, K., Y. A. Hanifah, M. Z. Norzila, L. Hasniah, and A. Rusanida**. 2006. Unrecognised infection in a cystic fibrosis patient. J.Paediatr.Child Health **42**:217-218.

12. **Baker, E. H., N. Clark, A. L. Brennan, D. A. Fisher, K. M. Gyi, M. E. Hodson, B. J. Philips, D. L. Baines, and D. M. Wood**. 2007. Hyperglycemia and cystic fibrosis alter respiratory fluid glucose concentrations estimated by breath condensate analysis. J.Appl.Physiol **102**:1969-1975.

13. **Balder, R., S. Lipski, J. J. Lazarus, W. Grose, R. M. Wooten, R. J. Hogan, D. E. Woods, and E. R. Lafontaine**. 2010. Identification of *Burkholderia mallei* and *Burkholderia pseudomallei* adhesins for human respiratory epithelial cells. BMC.Microbiol. **10**:250.

14. **Baldwin, A., E. Mahenthiralingam, P. Drevinek, C. Pope, D. J. Waine, D. A. Henry, D. P. Speert, P. Carter, P. Vandamme, J. J. LiPuma, and C. G. Dowson**. 2008. Elucidating the global epidemiology of *Burkholderia multivorans* in cystic fibrosis by multilocus sequence typing. J Clin.Microbiol. **46**:290-295.

15. **Baldwin, A., P. A. Sokol, J. Parkhill, and E. Mahenthiralingam**. 2004. The *Burkholderia cepacia* epidemic strain marker is part of a novel genomic island encoding both virulence and metabolism-associated genes in *Burkholderia cenocepacia*. Infect.Immun. **72**:1537-1547.

16. **Baran, D., V. P. de, and H. A. Ooms**. 1990. Concentration of tobramycin given by aerosol in the fluid obtained by bronchoalveolar lavage. Respir Med. **84**:203-204.

17. **Bartholdson, S. J., A. R. Brown, B. R. Mewburn, D. J. Clarke, S. C. Fry, D. J. Campopiano, and J. R. Govan**. 2008. Plant host and sugar alcohol induced exopolysaccharide biosynthesis in the *Burkholderia cepacia* complex. Microbiology **154**:2513-2521.

18. **Baumann, U., S. Wu, K. M. Flaherty, and D. B. McKay**. 1993. Three-dimensional structure of the alkaline protease of *Pseudomonas aeruginosa*: a two-domain protein with a calcium binding parallel beta roll motif. EMBO J. **12(9)**:3357-3364.

19. **Bazzini, S., C. Udine, A. Sass, M. R. Pasca, F. Longo, G. Emiliani, M. Fondi, E. Perrin, F. Decorosi, C. Viti, L. Giovannetti, L. Leoni, R. Fani, G. Riccardi, E. Mahenthiralingam, and S. Buroni**. 2011. Deciphering the role of RND efflux transporters in *Burkholderia cenocepacia*. PLoS.ONE. **19;6(4)**:e18902.

20. **Bernier, S. P., L. Silo-Suh, D. E. Woods, D. E. Ohman, and P. A. Sokol**. 2003. Comparative analysis of plant and animal models for characterization of *Burkholderia cepacia* virulence. Infect.Immun. **71**:5306-5313.

21. **Bevivino, A., C. Dalmastri, S. Tabacchioni, L. Chiarini, M. L. Belli, S. Piana, A. Materazzo, P. Vandamme, and G. Manno**. 2002. *Burkholderia cepacia* complex bacteria from clinical and environmental sources in Italy: genomovar status and distribution of traits related to virulence and transmissibility. J.Clin.Microbiol. **40(3)**:846-851.

22. **Biddick, R., T. Spilker, A. Martin, and J. J. LiPuma**. 2003. Evidence of transmission of *Burkholderia cepacia*, *Burkholderia multivorans* and *Burkholderia dolosa* among persons with cystic fibrosis. FEMS Microbiol.Lett. **228**:57-62.

23. **Bilton, D., P. Robinson, P. Cooper, C. G. Gallagher, J. Kolbe, H. Fox, A. Jaques, and B. Charlton**. 2011. Inhaled dry powder mannitol in cystic fibrosis: an efficacy and safety study. Eur.Respir.J **38**:1071-1080.

24. **Bishop, J. L. and B. B. Finlay**. 2006. Friend or foe? Antimicrobial peptides trigger pathogen virulence. Trends Mol.Med. **12**:3-6.

25. **Bobadilla, J. L., M. Macek, Jr., J. P. Fine, and P. M. Farrell**. 2002. Cystic fibrosis: a worldwide analysis of CFTR mutations--correlation with incidence data and application to screening. Hum.Mutat. **19**:575-606.

26. **Boucher, R. C.** 2007. Evidence for airway surface dehydration as the initiating event in CF airway disease. J.Intern.Med. **261(1)**:5-16.

27. **Brackman, G., P. Cos, L. Maes, H. J. Nelis, and T. Coenye**. 2011. Quorum sensing inhibitors increase the susceptibility of bacterial biofilms to antibiotics in vitro and in vivo. Antimicrob.Agents Chemother. **55**:2655-2661.

28. **Brennan, A. L., D. M. Geddes, K. M. Gyi, and E. H. Baker**. 2004. Clinical importance of cystic fibrosis-related diabetes. J.Cyst.Fibros. **3**:209-222.

29. **Brennan, A. L., K. M. Gyi, D. M. Wood, J. Johnson, R. Holliman, D. L. Baines, B. J. Philips, D. M. Geddes, M. E. Hodson, and E. H. Baker**. 2007. Airway glucose concentrations and effect on growth of respiratory pathogens in cystic fibrosis. J.Cyst.Fibros. **6**:101-109.

30. **Brisse, S., C. Cordevant, P. Vandamme, P. Bidet, C. Loukil, G. Chabanon, M. Lange, and E. Bingen**. 2004. Species distribution and ribotype diversity of *Burkholderia cepacia* complex isolates from French patients with cystic fibrosis. J.Clin.Microbiol. **42**:4824-4827.

31. **Burns, J. L., R. L. Gibson, S. McNamara, D. Yim, J. Emerson, M. Rosenfeld, P. Hiatt, K. McCoy, R. Castile, A. L. Smith, and B. W. Ramsey**. 2001. Longitudinal assessment of *Pseudomonas aeruginosa* in young children with cystic fibrosis. J.Infect.Dis. **183**:444-452.

32. **Burns, J. L., M. Jonas, E. Y. Chi, D. K. Clark, A. Berger, and A. Griffith**. 1996. Invasion of respiratory epithelial cells by *Burkholderia (Pseudomonas) cepacia*. Infect.Immun. **64**:4054-4059.

33. **Bylund, J., L. A. Burgess, P. Cescutti, R. K. Ernst, and D. P. Speert**. 2006. Exopolysaccharides from *Burkholderia cenocepacia* inhibit neutrophil chemotaxis and scavenge reactive oxygen species. J.Biol.Chem. **281**:2526-2532.

34. **Caraher, E., C. Duff, T. Mullen, K. S. Mc, P. Murphy, M. Callaghan, and S. McClean**. 2007. Invasion and biofilm formation of *Burkholderia dolosa* is comparable with *Burkholderia cenocepacia* and *Burkholderia multivorans*. J.Cyst.Fibros. **6(1)**:49-56.

35. **Cardona, S. T., J. Wopperer, L. Eberl, and M. A. Valvano**. 2005. Diverse pathogenicity of *Burkholderia cepacia* complex strains in the *Caenorhabditis elegans* host model. FEMS Microbiol.Lett. **250**:97-104.

36. **Cerantola, S., J. Bounery, C. Segonds, N. Marty, and H. Montrozier**. 2000. Exopolysaccharide production by mucoid and non-mucoid strains of *Burkholderia cepacia*. FEMS Microbiol.Lett. **185**:243-246.

37. **Cerantola, S., N. Marty, and H. Montrozier**. 1996. Structural studies of the acidic exopolysaccharide produced by a mucoid strain of *Burkholderia cepacia*, isolated from cystic fibrosis. Carbohydr.Res. **285**:59-67.

38. **Cescutti, P., M. Bosco, F. Picotti, G. Impallomeni, J. H. Leitao, J. A. Richau, and I. Sa-Correia**. 2000. Structural study of the exopolysaccharide produced by a clinical isolate of *Burkholderia cepacia*. Biochem.Biophys.Res.Commun. **273**:1088-1094.

39. **Cescutti, P., M. Foschiatti, L. Furlanis, C. Lagatolla, and R. Rizzo**. 2010. Isolation and characterisation of the biological repeating unit of cepacian, the exopolysaccharide produced by bacteria of the *Burkholderia cepacia* complex. Carbohydr.Res. **345**:1455-1460.

40. **Chaowagul, W., N. J. White, D. A. Dance, Y. Wattanagoon, P. Naigowit, T. M. Davis, S. Looareesuwan, and N. Pitakwatchara**. 1989. Melioidosis: a major cause of community-acquired septicemia in northeastern Thailand. J.Infect.Dis. **159**:890-899.

41. **Chen, K., G. W. Sun, K. L. Chua, and Y. H. Gan**. 2005. Modified virulence of antibiotic-induced *Burkholderia pseudomallei* filaments. Antimicrob.Agents Chemother. **49**:1002-1009.

42. **Chernish, R. N. and S. D. Aaron**. 2003. Approach to resistant gram-negative bacterial pulmonary infections in patients with cystic fibrosis. Curr.Opin.Pulm.Med. **9(6)**:509-515.

43. **Chieng, S., L. Carreto, and S. Nathan**. 2012. *Burkholderia pseudomallei* transcriptional adaptation in macrophages. BMC.Genomics. **13**:328-13.

44. **Christenson, J. C., D. F. Welch, G. Mukwaya, M. J. Muszynski, R. E. Weaver, and D. J. Brenner**. 1989. Recovery of *Pseudomonas gladioli* from respiratory tract specimens of patients with cystic fibrosis. J.Clin.Microbiol. **27**:270-273.

45. **Chung, J. W. and D. P. Speert**. 2007. Proteomic identification and characterization of bacterial factors associated with *Burkholderia cenocepacia* survival in a murine host. Microbiology. **153**:206-214.

46. **Clode, F. E., M. E. Kaufmann, H. Malnick, and T. L. Pitt**. 2000. Distribution of genes encoding putative transmissibility factors among epidemic and nonepidemic strains of *Burkholderia cepacia* from cystic fibrosis patients in the United Kingdom. J Clin.Microbiol. **38**:1763-1766.

47. **Coakley, R. D., B. R. Grubb, A. M. Paradiso, J. T. Gatzy, L. G. Johnson, S. M. Kreda, W. K. O'Neal, and R. C. Boucher**. 2003. Abnormal surface liquid pH regulation by cultured cystic fibrosis bronchial epithelium. Proc.Natl.Acad.Sci.U.S.A. **100**:16083-16088.

48. **Coenye, T., J. J. LiPuma, D. Henry, B. Hoste, K. Vandemeulebroecke, M. Gillis, D. P. Speert, and P. Vandamme**. 2001. *Burkholderia cepacia* genomovar VI, a new member of the *Burkholderia cepacia* complex isolated from cystic fibrosis patients. Int.J.Syst.Evol.Microbiol. **51(Pt 2)**:271-279.

49. **Coenye, T., E. Mahenthiralingam, D. Henry, J. J. LiPuma, S. Laevens, M. Gillis, D. P. Speert, and P. Vandamme**. 2001. *Burkholderia ambifaria* sp. nov., a novel member of the *Burkholderia cepacia* complex including biocontrol and cystic fibrosis-related isolates. Int.J.Syst.Evol.Microbiol. **51**:1481-1490.

50. **Coenye, T. and P. Vandamme**. 2003. Diversity and significance of *Burkholderia* species occupying diverse ecological niches. Environ.Microbiol. **5**:719-729.

51. **Conway, B. A., K. K. Chu, J. Bylund, E. Altman, and D. P. Speert**. 2004. Production of exopolysaccharide by *Burkholderia cenocepacia* results in altered cell-surface interactions and altered bacterial clearance in mice. J.Infect.Dis. **190**:957-966.

52. **Conway, B. A., V. Venu, and D. P. Speert**. 2002. Biofilm formation and acyl homoserine lactone production in the *Burkholderia cepacia* complex. J Bacteriol. **184**:5678-5685.

53. **Corbett, C. R., M. N. Burtnick, C. Kooi, D. E. Woods, and P. A. Sokol**. 2003. An extracellular zinc metalloprotease gene of *Burkholderia cepacia*. Microbiology **149**:2263-2271.

54. **Crapo, J. D., B. E. Barry, P. Gehr, M. Bachofen, and E. R. Weibel**. 1982. Cell number and cell characteristics of the normal human lung. Am.Rev.Respir.Dis. **126(2)**:332-337.

55. **Cunha, M. V., J. H. Leitao, E. Mahenthiralingam, P. Vandamme, L. Lito, C. Barreto, M. J. Salgado, and I. Sa-Correia**. 2003. Molecular analysis of *Burkholderia cepacia* complex isolates from a Portuguese cystic fibrosis center: a 7-year study. J.Clin.Microbiol. **41**:4113-4120.

56. **Cunha, M. V., S. A. Sousa, J. H. Leitao, L. M. Moreira, P. A. Videira, and I. Sa-Correia**. 2004. Studies on the involvement of the exopolysaccharide produced by cystic fibrosis-associated isolates of the *Burkholderia cepacia* complex in biofilm formation and in persistence of respiratory infections. J.Clin.Microbiol. **42**:3052-3058.

57. **Davidson, D. J., J. R. Dorin, G. McLachlan, V. Ranaldi, D. Lamb, C. Doherty, J. Govan, and D. J. Porteous**. 1995. Lung disease in the cystic fibrosis mouse exposed to bacterial pathogens. Nat.Genet. **9**:351-357.

58. **Daviskas, E., S. D. Anderson, A. Jaques, and B. Charlton**. 2010. Inhaled mannitol improves the hydration and surface properties of sputum in patients with cystic fibrosis. Chest **137**:861-868.

59. **Daviskas, E., S. D. Anderson, A. Jaques, and B. Charlton**. 2010. Inhaled mannitol improves the hydration and surface properties of sputum in patients with cystic fibrosis. Chest **137**:861-868.

60. **Delattre, A. S., B. Clantin, N. Saint, C. Locht, V. Villeret, and F. Jacob-Dubuisson**. 2010. Functional importance of a conserved sequence motif in FhaC, a prototypic member of the TpsB/Omp85 superfamily. FEBS J **277**:4755-4765.

61. **Denman, C. C. and A. R. Brown**. 2013. Mannitol promotes adherence of an outbreak strain of *Burkholderia multivorans* via an exopolysaccharide-independent mechanism that is associated with upregulation of newly-identified fimbrial and afimbrial adhesins. Microbiology. **159**:771-781.

62. **Di, A., M. E. Brown, L. V. Deriy, C. Li, F. L. Szeto, Y. Chen, P. Huang, J. Tong, A. P. Naren, V. Bindokas, H. C. Palfrey, and D. J. Nelson**. 2006. CFTR regulates phagosome acidification in macrophages and alters bactericidal activity. Nat.Cell Biol. **8**:933-944.

63. **Dodge, J. A., P. A. Lewis, M. Stanton, and J. Wilsher**. 2007. Cystic fibrosis mortality and survival in the UK: 1947-2003. Eur.Respir.J. **29**:522-526.

64. **Drabick, J. A., E. J. Gracely, G. J. Heidecker, and J. J. LiPuma**. 1996. Survival of *Burkholderia cepacia* on environmental surfaces. J.Hosp.Infect. **32(4)**:267-276.

65. **Dubey, A. K., C. S. Baker, K. Suzuki, A. D. Jones, P. Pandit, T. Romeo, and P. Babitzke**. 2003. CsrA regulates translation of the *Escherichia coli* carbon starvation gene, cstA, by blocking ribosome access to the cstA transcript. J.Bacteriol. **185(15)**:4450-4460.

66. **Dubois, M., K. Gilles, J. K. Hamilton, P. A. Rebers, and F. Smith**. 1951. A colorimetric method for the determination of sugars. Nature. **168(4265)**:167.

67. **Evans, S. E., Y. Xu, M. J. Tuvim, and B. F. Dickey**. 2010. Inducible innate resistance of lung epithelium to infection. Annu.Rev.Physiol. **72**:413-435.

68. **Ferreira, A. S., J. H. Leitao, I. N. Silva, P. F. Pinheiro, S. A. Sousa, C. G. Ramos, and L. M. Moreira**. 2009. Distribution of cepacian biosynthesis genes among environmental and clinical *Burkholderia* strains and role of cepacian exopolysaccharide in resistance to stress conditions. Appl.Environ.Microbiol. **76**:441-450.

69. **Ferreira, A. S., J. H. Leitao, I. N. Silva, P. F. Pinheiro, S. A. Sousa, C. G. Ramos, and L. M. Moreira**. 2010. Distribution of cepacian biosynthesis genes among environmental and clinical *Burkholderia* strains and role of cepacian exopolysaccharide in resistance to stress conditions. Appl.Environ.Microbiol. **76(2)**:441-450.

70. **Figurski, D. H. and D. R. Helinski**. 1979. Replication of an origin-containing derivative of plasmid RK2 dependent on a plasmid function provided in trans. Proc.Natl.Acad.Sci.U.S.A **76**:1648-1652.

71. **Flannagan, R. S., D. Aubert, C. Kooi, P. A. Sokol, and M. A. Valvano**. 2007. *Burkholderia cenocepacia* requires a periplasmic HtrA protease for growth under thermal and osmotic stress and for survival in vivo. Infect.Immun. **75**:1679-1689.

72. **Flannagan, R. S., T. Linn, and M. A. Valvano**. 2008. A system for the construction of targeted unmarked gene deletions in the genus *Burkholderia*. Environ.Microbiol. **10**:1652-1660.

73. **Fones, H. and G. M. Preston**. 2012. The impact of transition metals on bacterial plant disease. FEMS Microbiol.Rev.10-6976.

74. **Ghio, A. J., V. L. Roggli, J. M. Soukup, J. H. Richards, S. H. Randell, and M. S. Muhlebach**. 2012. Iron accumulates in the lavage and explanted lungs of cystic fibrosis patients. J.Cyst.Fibros.S1569-S1993.

75. **Giard, D. J., S. A. Aaronson, G. J. Todaro, P. Arnstein, J. H. Kersey, H. Dosik, and W. P. Parks**. 1973. In vitro cultivation of human tumors: establishment of cell lines derived from a series of solid tumors. J.Natl.Cancer Inst. **51**:1417-1423.

76. **Glendinning, K. J., Y. N. Parsons, K. Duangsonk, B. A. Hales, D. Humphreys, C. A. Hart, and C. Winstanley**. 2004. Sequence divergence in type III secretion gene clusters of the *Burkholderia cepacia* complex. FEMS Microbiol.Lett. **235**:229-235.

77. **Goldberg, J. B., S. Ganesan, A. T. Comstock, Y. Zhao, and U. S. Sajjan**. 2011. Cable pili and the associated 22 kDa adhesin contribute to *Burkholderia cenocepacia* persistence in vivo. PLoS.ONE. **6**:e22435.

78. **Goldman, M. J., G. M. Anderson, E. D. Stolzenberg, U. P. Kari, M. Zasloff, and J. M. Wilson**. 1997. Human beta-defensin-1 is a salt-sensitive antibiotic in lung that is inactivated in cystic fibrosis. Cell. **88(4)**:553-560.

79. **Govan, J. R.** 2000. Infection control in cystic fibrosis: methicillin-resistant *Staphylococcus aureus*, *Pseudomonas aeruginosa* and the *Burkholderia cepacia* complex. J.R.Soc.Med. **93 Suppl 38:40-5.**:40-45.

80. **Govan, J. R., A. R. Brown, and A. M. Jones**. 2007. Evolving epidemiology of *Pseudomonas aeruginosa* and the *Burkholderia cepacia* complex in cystic fibrosis lung infection. Future.Microbiol. **2**:153-164.

81. **Govan, J. R. and V. Deretic**. 1996. Microbial pathogenesis in cystic fibrosis: mucoid *Pseudomonas aeruginosa* and *Burkholderia cepacia*. Microbiol.Rev. **60**:539-574.

82. **Govan, J. R. and J. W. Nelson**. 1992. Microbiology of lung infection in cystic fibrosis. Br.Med.Bull. **48**:912-930.

83. **Govan, R. W.** 2009. Sugar sweet and deadly: authors' response. Microbiology **155**:666.

84. **Gray, R. D., A. Duncan, D. Noble, M. Imrie, D. S. O'Reilly, J. A. Innes, D. J. Porteous, A. P. Greening, and A. C. Boyd**. 2010. Sputum trace metals are biomarkers of inflammatory and suppurative lung disease. Chest **137**:635-641.

85. **Hales, B. A., J. A. Morgan, C. A. Hart, and C. Winstanley**. 1998. Variation in flagellin genes and proteins of *Burkholderia cepacia*. J.Bacteriol. **180(5)**:1110-1118.

86. **Hamad, M. A., A. M. Skeldon, and M. A. Valvano**. 2010. Construction of aminoglycoside-sensitive *Burkholderia cenocepacia* strains for use in studies of

intracellular bacteria with the gentamicin protection assay. Appl.Environ.Microbiol. **76**:3170-3176.

87. **Hansen, C. R., T. Pressler, and N. Hoiby**. 2008. Early aggressive eradication therapy for intermittent *Pseudomonas aeruginosa* airway colonization in cystic fibrosis patients: 15 years experience. J.Cyst.Fibros. **7**:523-530.

88. **Herasimenka, Y., P. Cescutti, G. Impallomeni, S. Campana, G. Taccetti, N. Ravenni, F. Zanetti, and R. Rizzo**. 2007. Exopolysaccharides produced by clinical strains belonging to the *Burkholderia cepacia* complex. J.Cyst.Fibros. **6**:145-152.

89. **Hodak, H., A. Wohlkonig, C. Smet-Nocca, H. Drobecq, J. M. Wieruszeski, M. Senechal, I. Landrieu, C. Locht, M. Jamin, and F. Jacob-Dubuisson**. 2008. The peptidyl-prolyl isomerase and chaperone Par27 of *Bordetella pertussis* as the prototype for a new group of parvulins. J Mol.Biol. **376**:414-426.

90. **Inatsuka, C. S., S. M. Julio, and P. A. Cotter**. 2005. *Bordetella* filamentous hemagglutinin plays a critical role in immunomodulation, suggesting a mechanism for host specificity. Proc.Natl.Acad.Sci.U.S.A **102**:18578-18583.

91. **Jacob-Dubuisson, F., C. Locht, and R. Antoine**. 2001. Two-partner secretion in Gram-negative bacteria: a thrifty, specific pathway for large virulence proteins. Mol.Microbiol. **40**:306-313.

92. **Janczarek, M.** 2011. Environmental signals and regulatory pathways that influence exopolysaccharide production in rhizobia. Int.J.Mol.Sci. **12(11)**:7898-7933.

93. **Jaques, A., E. Daviskas, J. A. Turton, K. McKay, P. Cooper, R. G. Stirling, C. F. Robertson, P. T. Bye, P. N. Lesouef, B. Shadbolt, S. D. Anderson, and B. Charlton**. 2008. Inhaled mannitol improves lung function in cystic fibrosis. Chest **133**:1388-1396.

94. **Jones, A. M., M. E. Dodd, J. R. Govan, V. Barcus, C. J. Doherty, J. Morris, and A. K. Webb**. 2004. *Burkholderia cenocepacia* and *Burkholderia multivorans*: influence on survival in cystic fibrosis. Thorax. **59**:948-951.

95. **Kalish, L. A., D. A. Waltz, M. Dovey, G. Potter-Bynoe, A. J. McAdam, J. J. LiPuma, C. Gerard, and D. Goldmann**. 2006. Impact of *Burkholderia dolosa* on lung function and survival in cystic fibrosis. Am.J.Respir.Crit Care Med. **173**:421-425.

96. **Kanai, K., E. Kondo, and T. Kurata**. 1996. Affinity and response of *Burkholderia pseudomallei* and *Burkholderia cepacia* to insulin. Southeast Asian J.Trop.Med.Public Health **27**:584-591.

97. **Katsuwon, J. and A. J. Anderson**. 1989. Response of plant-colonizing pseudomonads to hydrogen peroxide. Appl.Environ.Microbiol. **55**:2985-2989.

98. **Kawasaki, T., H. Akanuma, and T. Yamanouchi**. 2002. Increased fructose concentrations in blood and urine in patients with diabetes. Diabetes Care. **25**:353-357.

99. **Keig, P. M., E. Ingham, and K. G. Kerr**. 2001. Invasion of human type II pneumocytes by *Burkholderia cepacia*. Microb.Pathog. **30**:167-170.

100. **Kerem, B., J. M. Rommens, J. A. Buchanan, D. Markiewicz, T. K. Cox, A. Chakravarti, M. Buchwald, and L. C. Tsui**. 1989. Identification of the cystic fibrosis gene: genetic analysis. Science **245**:1073-1080.

101. **Kieninger, E., F. Singer, C. Tapparel, M. P. Alves, P. Latzin, H. L. Tan, C. Bossley, C. Casaulta, A. Bush, J. C. Davies, L. Kaiser, and N. Regamey**. 2013. High rhinovirus burden in lower airways of children with cystic fibrosis. Chest. **143(3)**:782-790.

102. **Kim, J. F., J. H. Ham, D. W. Bauer, A. Collmer, and S. V. Beer**. 1998. The hrpC and hrpN operons of *Erwinia chrysanthemi* EC16 are flanked by plcA and homologs of hemolysin/adhesin genes and accompanying activator/transporter genes. Mol.Plant Microbe Interact. **11**:563-567.

103. **Knowles, M. R., J. M. Robinson, R. E. Wood, C. A. Pue, W. M. Mentz, G. C. Wager, J. T. Gatzy, and R. C. Boucher**. 1997. Ion composition of airway surface liquid of patients with cystic fibrosis as compared with normal and disease-control subjects. J.Clin.Invest. **100(10)**:2588-2595.

104. **Koch, C., M. Rainisio, U. Madessani, H. K. Harms, M. E. Hodson, G. Mastella, S. G. McKenzie, J. Navarro, and B. Strandvik**. 2001. Presence of cystic fibrosis-related diabetes mellitus is tightly linked to poor lung function in patients with cystic fibrosis: data from the European Epidemiologic Registry of Cystic Fibrosis. Pediatr.Pulmonol. **32**:343-350.

105. **Kopito, L. E. and H. Shwachman**. 1976. The pancreas in cystic fibrosis: chemical composition and comparative morphology. Pediatr Res. **10**:742-749.

106. **Kuehn, M., K. Lent, J. Haas, J. Hagenzieker, M. Cervin, and A. L. Smith**. 1992. Fimbriation of *Pseudomonas cepacia*. Infect.Immun. **60**:2002-2007.

107. **Lagatolla, C., S. Skerlavaj, L. Dolzani, E. A. Tonin, B. C. Monti, M. Bosco, R. Rizzo, L. Giglio, and P. Cescutti**. 2002. Microbiological characterisation of *Burkholderia cepacia* isolates from cystic fibrosis patients: investigation of the exopolysaccharides produced. FEMS Microbiol.Lett. **209**:99-106.

108. **Lambiase, A., M. R. Catania, and F. Rossano**. 2010. Anaerobic bacteria infection in cystic fibrosis airway disease. New Microbiol. **33**:185-194.

109. **Lamothe, J., K. K. Huynh, S. Grinstein, and M. A. Valvano**. 2007. Intracellular survival of *Burkholderia cenocepacia* in macrophages is associated with a delay in the maturation of bacteria-containing vacuoles. Cell Microbiol. **9**:40-53.

110. **Lanng, S., B. Thorsteinsson, J. Nerup, and C. Koch**. 1994. Diabetes mellitus in cystic fibrosis: effect of insulin therapy on lung function and infections. Acta Paediatr. **83**:849-853.

111. **Laube, B. L.** 2001. Treating diabetes with aerosolized insulin. Chest. **120(3 Suppl)**:99S-106S.

112. **Lefebre, M. and M. Valvano**. 2001. In vitro resistance of *Burkholderia cepacia* complex isolates to reactive oxygen species in relation to catalase and superoxide dismutase production. Microbiology. **147**:97-109.

113. **Lek, N. and C. L. Acerini**. 2010. Cystic fibrosis related diabetes mellitus - diagnostic and management challenges. Curr Diabetes Rev. **6**:9-16.

114. **Lessie, T. G., W. Hendrickson, B. D. Manning, and R. Devereux**. 1996. Genomic complexity and plasticity of *Burkholderia cepacia*. FEMS Microbiol.Lett. **144(2-3)**:117-128.

115. **Lewis, K.** 2010. Persister cells. Annu.Rev.Microbiol. **64**:357-372.

116. **Lieberman, T. D., J. B. Michel, M. Aingaran, G. Potter-Bynoe, D. Roux, M. R. Davis, Jr., D. Skurnik, N. Leiby, J. J. LiPuma, J. B. Goldberg, A. J. McAdam, G. P. Priebe, and R. Kishony**. 2011. Parallel bacterial evolution within multiple patients identifies candidate pathogenicity genes. Nat.Genet. **43(12)**:1275-1280.

117. **Linker, A., L. R. Evans, and G. Impallomeni**. 2001. The structure of a polysaccharide from infectious strains of *Burkholderia cepacia*. Carbohydr.Res. **335**:45-54.

118. **Liou, T. G., F. R. Adler, S. C. Fitzsimmons, B. C. Cahill, J. R. Hibbs, and B. C. Marshall**. 2001. Predictive 5-year survivorship model of cystic fibrosis. Am.J.Epidemiol. **153**:345-352.

119. **LiPuma, J. J.** 2010. The changing microbial epidemiology in cystic fibrosis. Clin.Microbiol.Rev. **23**:299-323.

120. **LiPuma, J. J., T. Spilker, T. Coenye, and C. F. Gonzalez**. 2002. An epidemic *Burkholderia cepacia* complex strain identified in soil. Lancet. **359**:2002-2003.

121. **Livak, K. J. and T. D. Schmittgen**. 2001. Analysis of relative gene expression data using real-time quantitative PCR and the 2(-Delta Delta C(T)) Method. Methods **25**:402-408.

122. **Loutet, S. A. and M. A. Valvano**. 2010. A decade of *Burkholderia cenocepacia* virulence determinant research. Infect.Immun. **78**:4088-4100.

123. **Ludwig, A., T. Jarchau, R. Benz, and W. Goebel**. 1988. The repeat domain of *Escherichia coli* haemolysin (HlyA) is responsible for its Ca2+-dependent binding to erythrocytes. Mol.Gen.Genet. **214(3)**:553-561.

124. **Magalhaes, M., M. C. de Britto, and P. Vandamme**. 2002. *Burkholderia cepacia* genomovar III and *Burkholderia vietnamiensis* double infection in a cystic fibrosis child. J.Cyst.Fibros. **1(4)**:292-294.

125. **Mahenthiralingam, E., A. Baldwin, and P. Vandamme**. 2002. *Burkholderia cepacia* complex infection in patients with cystic fibrosis. J.Med.Microbiol. **51**:533-538.

126. **Mahenthiralingam, E., M. E. Campbell, J. Foster, J. S. Lam, and D. P. Speert**. 1996. Random amplified polymorphic DNA typing of *Pseudomonas*

aeruginosa isolates recovered from patients with cystic fibrosis. J.Clin.Microbiol. **34(5)**:1129-1135.

127. **Mahenthiralingam, E., T. Coenye, J. W. Chung, D. P. Speert, J. R. Govan, P. Taylor, and P. Vandamme**. 2000. Diagnostically and experimentally useful panel of strains from the *Burkholderia cepacia* complex. J.Clin.Microbiol. **38**:910-913.

128. **Mahenthiralingam, E., P. Vandamme, M. E. Campbell, D. A. Henry, A. M. Gravelle, L. T. Wong, A. G. Davidson, P. G. Wilcox, B. Nakielna, and D. P. Speert**. 2001. Infection with *Burkholderia cepacia* complex genomovars in patients with cystic fibrosis: virulent transmissible strains of genomovar III can replace *Burkholderia multivorans*. Clin.Infect.Dis. **33(9)**:1469-1475.

129. **Maillard, J. Y. and P. Hartemann**. 2012. Silver as an antimicrobial: Facts and gaps in knowledge. Crit Rev.Microbiol.

130. **Martin, D. W. and C. D. Mohr**. 2000. Invasion and intracellular survival of *Burkholderia cepacia*. Infect.Immun. **68**:24-29.

131. **Masoud-Landgraf, L., A. Badura, E. Eber, G. Feierl, E. Marth, and W. Buzina**. 2013. Modified culture method detects a high diversity of fungal species in cystic fibrosis patients. Med.Mycol.

132. **Mazar, J. and P. A. Cotter**. 2007. New insight into the molecular mechanisms of two-partner secretion. Trends Microbiol. **15**:508-515.

133. **McGowan, S. E., J. J. Murray, and M. G. Parrish**. 1986. Iron binding, internalization, and fate in human alveolar macrophages. J.Lab Clin.Med. **108(6)**:587-595.

134. **Mil-Homens, D., E. P. Rocha, and A. M. Fialho**. 2010. Genome-wide analysis of DNA repeats in *Burkholderia cenocepacia* J2315 identifies a novel adhesin-like gene unique to epidemic-associated strains of the ET-12 lineage. Microbiology **156**:1084-1096.

135. **Millar-Jones, L., H. C. Ryley, A. Paull, and M. C. Goodchild**. 1998. Transmission and prevalence of *Burkholderia cepacia* in Welsh cystic fibrosis patients. Respir.Med. **92(2)**:178-183.

136. **Minasian, C. C., C. Wallis, and A. Bush**. 2007. Mannitol as a mucolytic in cystic fibrosis. J R.Soc.Med. **100 Suppl 47**:53-56.

137. **Moran, A., D. Hardin, D. Rodman, H. F. Allen, R. J. Beall, D. Borowitz, C. Brunzell, P. W. Campbell, III, S. E. Chesrown, C. Duchow, R. J. Fink, S. C. Fitzsimmons, N. Hamilton, I. Hirsch, M. S. Howenstine, D. J. Klein, Z. Madhun, P. B. Pencharz, A. L. Quittner, M. K. Robbins, T. Schindler, K. Schissel, S. J. Schwarzenberg, V. A. Stallings, W. B. Zipf, and .** 1999. Diagnosis, screening and management of cystic fibrosis related diabetes mellitus: a consensus conference report. Diabetes Res.Clin.Pract. **45(1)**:61-73.

138. **Moreira, L. M.** Personal communication. 13.

139. **Moreira, L. M., P. A. Videira, S. A. Sousa, J. H. Leitao, M. V. Cunha, and I. Sa-Correia**. 2003. Identification and physical organization of the gene cluster involved in the biosynthesis of *Burkholderia cepacia* complex exopolysaccharide. Biochem.Biophys.Res.Commun. **312**:323-333.

140. **Mullen, T., K. Markey, P. Murphy, S. McClean, and M. Callaghan**. 2007. Role of lipase in *Burkholderia cepacia* complex (Bcc) invasion of lung epithelial cells. Eur.J Clin.Microbiol.Infect.Dis. **26**:869-877.

141. **Nisr, R. B., A. J. Moody, and M. L. Gilpin**. 2012. Screening microorganisms for insulin binding reveals binding by *Burkholderia multivorans* and *Burkholderia cenocepacia* and novel attachment of insulin to *Aeromonas salmonicida* via the A-layer. FEMS Microbiol.Lett. **328**:93-99.

142. **Nogueira, C. E., J. R. Ruggiero, P. Sist, P. Cescutti, R. Urbani, and R. Rizzo**. 2005. Conformational features of cepacian: the exopolysaccharide produced by clinical strains of *Burkholderia cepacia*. Carbohydr.Res. **340**:1025-1037.

143. **Norskov-Lauritsen, N., H. K. Johansen, M. G. Fenger, X. C. Nielsen, T. Pressler, H. V. Olesen, and N. Hoiby**. 2010. Unusual distribution of *Burkholderia cepacia* complex species in Danish cystic fibrosis clinics may stem from restricted transmission between patients. J.Clin.Microbiol. **48**:2981-2983.

144. **Nousia-Arvanitakis, S., A. Galli-Tsinopoulou, and M. Karamouzis**. 2001. Insulin improves clinical status of patients with cystic-fibrosis-related diabetes mellitus. Acta Paediatr. **90**:515-519.

145. **Nzula, S., P. Vandamme, and J. R. Govan**. 2002. Influence of taxonomic status on the in vitro antimicrobial susceptibility of the *Burkholderia cepacia* complex. J.Antimicrob.Chemother. **50**:265-269.

146. **O'Gorman, J. and H. Humphreys**. 2012. Application of copper to prevent and control infection. Where are we now? J.Hosp.Infect. **81(4)**:217-223.

147. **Painter, R. G., V. G. Valentine, N. A. Lanson, Jr., K. Leidal, Q. Zhang, G. Lombard, C. Thompson, A. Viswanathan, W. M. Nauseef, G. Wang, and G. Wang**. 2006. CFTR Expression in human neutrophils and the phagolysosomal chlorination defect in cystic fibrosis. Biochemistry. **45**:10260-10269.

148. **Paisley, D., M. Gosling, and H. Danahay**. 2010. Regulation of airway mucosal hydration. Expert.Rev.Clin.Pharmacol. **3(3)**:361-369.

149. **Palmer, K. L., L. M. Aye, and M. Whiteley**. 2007. Nutritional cues control *Pseudomonas aeruginosa* multicellular behavior in cystic fibrosis sputum. J Bacteriol. **189**:8079-8087.

150. **Parke, J. L. and D. Gurian-Sherman**. 2001. Diversity of the *Burkholderia cepacia* complex and implications for risk assessment of biological control strains. Annu.Rev.Phytopathol. **39**:225-258.

151. **Peckham, D.** 2009. Routine screening for cystic fibrosis-related diabetes. J.R.Soc.Med. **102 Suppl 1**:36-39.

152. **Pezzulo, A. A., X. X. Tang, M. J. Hoegger, M. H. Alaiwa, S. Ramachandran, T. O. Moninger, P. H. Karp, C. L. Wohlford-Lenane, H. P. Haagsman, E. M. van, B. Banfi, A. R. Horswill, D. A. Stoltz, P. B. McCray, Jr., M. J. Welsh, and J. Zabner**. 2012. Reduced airway surface pH impairs bacterial killing in the porcine cystic fibrosis lung. Nature **487**:109-113.

153. **Pitkanen, E.** 1996. Mannose, mannitol, fructose and 1,5-anhydroglucitol concentrations measured by gas chromatography/mass spectrometry in blood plasma of diabetic patients. Clin.Chim.Acta **251**:91-103.

154. **Potts, M.** 1994. Desiccation tolerance of prokaryotes. Microbiol.Rev. **58(4)**:755-805.

155. **Pugh, C., V. Hathwar, J. H. Richards, J. Stonehuerner, and A. J. Ghio**. 2005. Disruption of iron homeostasis in the lungs of transplant patients. J Heart Lung Transplant. **24**:1821-1827.

156. **Puthucheary, S. D. and S. A. Nathan**. 2008. Comparison of serum F2 isoprostane levels in diabetic patients and diabetic patients infected with *Burkholderia pseudomallei*. Singapore Med.J. **49**:117-120.

157. **Quon, B. S., J. D. Reid, P. Wong, P. G. Wilcox, A. Javer, J. M. Wilson, and R. D. Levy**. 2011. *Burkholderia gladioli* - a predictor of poor outcome in cystic fibrosis patients who receive lung transplants? A case of locally invasive rhinosinusitis and persistent bacteremia in a 36-year-old lung transplant recipient with cystic fibrosis. Can.Respir.J. **18(4)**:e64-e65.

158. **Ralph, P. and I. Nakoinz**. 1975. Phagocytosis and cytolysis by a macrophage tumour and its cloned cell line. Nature **257**:393-394.

159. **Reid, D. W. and S. C. Bell**. 2009. Sugar sweet and deadly? Microbiology **155**:665-666.

160. **Riordan, J. R., J. M. Rommens, B. Kerem, N. Alon, R. Rozmahel, Z. Grzelczak, J. Zielenski, S. Lok, N. Plavsic, J. L. Chou, and .** 1989. Identification of the cystic fibrosis gene: cloning and characterization of complementary DNA. Science **245**:1066-1073.

161. **Robinson, M., E. Daviskas, S. Eberl, J. Baker, H. K. Chan, S. D. Anderson, and P. T. Bye**. 1999. The effect of inhaled mannitol on bronchial mucus clearance in cystic fibrosis patients: a pilot study. Eur.Respir.J **14**:678-685.

162. **Rojas, C. M., J. H. Ham, W. L. Deng, J. J. Doyle, and A. Collmer**. 2002. HecA, a member of a class of adhesins produced by diverse pathogenic bacteria, contributes to the attachment, aggregation, epidermal cell killing, and virulence phenotypes of *Erwinia chrysanthemi* EC16 on *Nicotiana clevelandii* seedlings. Proc.Natl.Acad.Sci.U.S.A **99**:13142-13147.

163. **Rommens, J. M., M. C. Iannuzzi, B. Kerem, M. L. Drumm, G. Melmer, M. Dean, R. Rozmahel, J. L. Cole, D. Kennedy, N. Hidaka, and .** 1989. Identification of the cystic fibrosis gene: chromosome walking and jumping. Science **245**:1059-1065.

164. **Rosales-Reyes, R., D. F. Aubert, J. S. Tolman, A. O. Amer, and M. A. Valvano**. 2012. *Burkholderia cenocepacia* type VI secretion system mediates escape of type II secreted proteins into the cytoplasm of infected macrophages. PLoS.ONE. **7(7)**:e41726.

165. **Rubin, B. K.** 2007. Mucolytics, expectorants, and mucokinetic medications. Respir.Care **52**:859-865.

166. **Sage, A., A. Linker, D. J. Evans, and T. G. Lessie**. 1990. Hexose phosphate metabolism and exopolysaccharide formation in *Pseudomonas cepacia*. Current Microbiology **20**:191-198.

167. **Sajjan, S. U., L. A. Carmody, C. F. Gonzalez, and J. J. LiPuma**. 2008. A type IV secretion system contributes to intracellular survival and replication of *Burkholderia cenocepacia*. Infect.Immun. **76**:5447-5455.

168. **Sajjan, S. U. and J. F. Forstner**. 1992. Identification of the mucin-binding adhesin of *Pseudomonas cepacia* isolated from patients with cystic fibrosis. Infect Immun. **60**:1434-1440.

169. **Santo, C. E., D. Quaranta, and G. Grass**. 2012. Antimicrobial metallic copper surfaces kill *Staphylococcus haemolyticus* via membrane damage. Microbiologyopen. **1(1)**:46-52.

170. **Sass, A., A. Marchbank, and E. Mahenthiralingam**. 2009. Gene expression changes in *Burkholderia cenocepacia*: the global transcriptomic response to different growth conditions encountered in the cystic fibrosis lung. Pediatr.Pulmonol. **(Abstracts of the North American Cystic Fibrosis Conference) Suppl 32**:311 (Abstract 382).

171. **Sass, A., A. Marchbank, E. Tullis, J. J. LiPuma, and E. Mahenthiralingam**. 2011. Spontaneous and evolutionary changes in the antibiotic resistance of *Burkholderia cenocepacia* observed by global gene expression analysis. BMC.Genomics. **12**:373-12.

172. **Schmerk, C. L. and M. A. Valvano**. 2013. *Burkholderia multivorans* survival and trafficking within macrophages. J.Med.Microbiol. **62(Pt 2)**:173-184.

173. **Schmidt, S., J. F. Blom, J. Pernthaler, G. Berg, A. Baldwin, E. Mahenthiralingam, and L. Eberl**. 2009. Production of the antifungal compound pyrrolnitrin is quorum sensing-regulated in members of the *Burkholderia cepacia* complex. Environ.Microbiol. **11(6)**:1422-1437.

174. **Schultz, J. E. and A. Matin**. 1991. Molecular and functional characterization of a carbon starvation gene of *Escherichia coli*. J.Mol.Biol. **218(1)**:129-140.

175. **Seed, K. D. and J. J. Dennis**. 2008. Development of *Galleria mellonella* as an alternative infection model for the *Burkholderia cepacia* complex. Infect.Immun. **76**:1267-1275.

176. **Segonds, C., T. Heulin, N. Marty, and G. Chabanon**. 1999. Differentiation of *Burkholderia* species by PCR-restriction fragment length polymorphism analysis of the 16S rRNA gene and application to cystic fibrosis isolates. J.Clin.Microbiol. **37**:2201-2208.

177. **Sibley, C. D., H. Rabin, and M. G. Surette**. 2006. Cystic fibrosis: a polymicrobial infectious disease. Future.Microbiol. **1:53-61.**:53-61.

178. **Silva, I. N., A. S. Ferreira, J. D. Becker, J. E. Zlosnik, D. P. Speert, J. He, D. Mil-Homens, and L. M. Moreira**. 2011. Mucoid morphotype variation of *Burkholderia multivorans* during chronic cystic fibrosis lung infection is correlated with changes in metabolism, motility, biofilm formation and virulence. Microbiology **157**:3124-3137.

179. **Sim, S. H., Y. Yu, C. H. Lin, R. K. Karuturi, V. Wuthiekanun, A. Tuanyok, H. H. Chua, C. Ong, S. S. Paramalingam, G. Tan, L. Tang, G. Lau, E. E. Ooi, D. Woods, E. Feil, S. J. Peacock, and P. Tan**. 2008. The core and accessory genomes of *Burkholderia pseudomallei*: implications for human melioidosis. PLoS.Pathog. **4**:e1000178.

180. **Simpson, J. A., S. E. Smith, and R. T. Dean**. 1989. Scavenging by alginate of free radicals released by macrophages. Free Radic.Biol.Med. **6**:347-353.

181. **Singh, P. K., B. F. Tack, P. B. McCray, Jr., and M. J. Welsh**. 2000. Synergistic and additive killing by antimicrobial factors found in human airway surface liquid. Am.J Physiol Lung Cell Mol.Physiol **279**:L799-L805.

182. **Smith, J. J., S. M. Travis, E. P. Greenberg, and M. J. Welsh**. 1996. Cystic fibrosis airway epithelia fail to kill bacteria because of abnormal airway surface fluid. Cell. **%19;85(2)**:229-236.

183. **Snouwaert, J. N., K. K. Brigman, A. M. Latour, N. N. Malouf, R. C. Boucher, O. Smithies, and B. H. Koller**. 1992. An animal model for cystic fibrosis made by gene targeting. Science. **257(5073)**:1083-1088.

184. **Sokol, P. A., U. Sajjan, M. B. Visser, S. Gingues, J. Forstner, and C. Kooi**. 2003. The CepIR quorum-sensing system contributes to the virulence of *Burkholderia cenocepacia* respiratory infections. Microbiology **149**:3649-3658.

185. **Sokurenko, E. V., V. Chesnokova, D. E. Dykhuizen, I. Ofek, X. R. Wu, K. A. Krogfelt, C. Struve, M. A. Schembri, and D. L. Hasty**. 1998. Pathogenic adaptation of *Escherichia coli* by natural variation of the FimH adhesin. Proc.Natl.Acad.Sci.U.S.A **95**:8922-8926.

186. **Speert, D. P., M. Bond, R. C. Woodman, and J. T. Curnutte**. 1994. Infection with *Pseudomonas cepacia* in chronic granulomatous disease: role of nonoxidative killing by neutrophils in host defense. J Infect.Dis. **170**:1524-1531.

187. **Speert, D. P., D. Henry, P. Vandamme, M. Corey, and E. Mahenthiralingam**. 2002. Epidemiology of Burkholderia cepacia complex in patients with cystic fibrosis, Canada. Emerg.Infect.Dis. **8**:181-187.

188. **Stutman, H. R. and M. I. Marks**. 1987. Pulmonary infections in children with cystic fibrosis. Semin Respir Infect **2**:166-176.

189. **Sullivan, C. and C. H. Kim**. 2008. Zebrafish as a model for infectious disease and immune function. Fish.Shellfish.Immunol. **25**:341-350.

190. **Sutherland, I. W.** 1985. Biosynthesis and composition of gram-negative bacterial extracellular and wall polysaccharides. Annu.Rev.Microbiol. **39**:243-270.

191. **Tan, K., S. Clancy, M. Borovilos, M. Zhou, S. Horer, S. Moy, L. L. Volkart, J. Sassoon, U. Baumann, and A. Joachimiak**. 2009. The mannitol operon repressor MtlR belongs to a new class of transcription regulators in bacteria. J Biol.Chem. **284**:36670-36679.

192. **Taylor, J. B., L. A. Hogue, J. J. LiPuma, M. J. Walter, S. L. Brody, and C. L. Cannon**. 2009. Entry of *Burkholderia* organisms into respiratory epithelium: CFTR, microfilament and microtubule dependence. Journal of Cystic Fibrosis **9**:36-43.

193. **Teper, A., A. Jaques, and B. Charlton**. 2011. Inhaled mannitol in patients with cystic fibrosis: A randomised open-label dose response trial. J Cyst.Fibros. **10**:1-8.

194. **Terheggen-Lagro, S. W., G. T. Rijkers, and C. K. van der Ent**. 2005. The role of airway epithelium and blood neutrophils in the inflammatory response in cystic fibrosis. J.Cyst.Fibros. **4 Suppl 2:15-23.**:15-23.

195. **Thomas, M. S.** 2007. Iron acquisition mechanisms of the Burkholderia cepacia complex. Biometals. **20**:431-452.

196. **Thomas, R. and T. Brooks**. 2004. Common oligosaccharide moieties inhibit the adherence of typical and atypical respiratory pathogens. J.Med.Microbiol. **53**:833-840.

197. **Tietze, F., G. E. Mortimore, and N. R. Lomax**. 1962. Preparation and properties of fluorescent insulin derivatives. Biochim.Biophys.Acta **59**:336-346.

198. **Tomich, M., A. Griffith, C. A. Herfst, J. L. Burns, and C. D. Mohr**. 2003. Attenuated virulence of a *Burkholderia cepacia* type III secretion mutant in a murine model of infection. Infect.Immun. **71**:1405-1415.

199. **Tomich, M. and C. D. Mohr**. 2004. Transcriptional and posttranscriptional control of cable pilus gene expression in Burkholderia cenocepacia. J Bacteriol. **186**:1009-1020.

200. **Turi, J. L., F. Yang, M. D. Garrick, C. A. Piantadosi, and A. J. Ghio**. 2004. The iron cycle and oxidative stress in the lung. Free Radic.Biol.Med. **36(7)**:850-857.

201. **Urban, T. A., J. B. Goldberg, J. F. Forstner, and U. S. Sajjan**. 2005. Cable pili and the 22-kilodalton adhesin are required for *Burkholderia cenocepacia* binding to and transmigration across the squamous epithelium. Infect.Immun. **73**:5426-5437.

202. **Urban, T. A., A. Griffith, A. M. Torok, M. E. Smolkin, J. L. Burns, and J. B. Goldberg**. 2004. Contribution of Burkholderia cenocepacia flagella to infectivity and inflammation. Infect.Immun. **72(9)**:5126-5134.

203. **van der Sar, A. M., B. J. Appelmelk, C. M. Vandenbroucke-Grauls, and W. Bitter**. 2004. A star with stripes: zebrafish as an infection model. Trends Microbiol. **12**:451-457.

204. **van der Woude, M. W. and A. J. Baumler**. 2004. Phase and antigenic variation in bacteria. Clin.Microbiol.Rev. **17(3)**:581-611.

205. **Van, A. H., A. Sass, S. Bazzini, R. K. De, C. Udine, T. Messiaen, G. Riccardi, N. Boon, H. J. Nelis, E. Mahenthiralingam, and T. Coenye**. 2013. Biofilm-grown Burkholderia cepacia complex cells survive antibiotic treatment by avoiding production of reactive oxygen species. PLoS.ONE. **8(3)**:e58943.

206. **Vandamme, P., D. Henry, T. Coenye, S. Nzula, M. Vancanneyt, J. J. LiPuma, D. P. Speert, J. R. Govan, and E. Mahenthiralingam**. 2002. *Burkholderia anthina* sp. nov. and *Burkholderia pyrrocinia*, two additional *Burkholderia cepacia* complex bacteria, may confound results of new molecular diagnostic tools. FEMS Immunol.Med.Microbiol. **33**:143-149.

207. **Vandamme, P., B. Holmes, M. Vancanneyt, T. Coenye, B. Hoste, R. Coopman, H. Revets, S. Lauwers, M. Gillis, K. Kersters, and J. R. Govan**. 1997. Occurrence of multiple genomovars of Burkholderia cepacia in cystic fibrosis patients and proposal of Burkholderia multivorans sp. nov. Int.J.Syst.Bacteriol. **47**:1188-1200.

208. **Vandamme, P., E. Mahenthiralingam, B. Holmes, T. Coenye, B. Hoste, P. De Vos, D. Henry, and D. P. Speert**. 2000. Identification and population structure of Burkholderia stabilis sp. nov. (formerly Burkholderia cepacia genomovar IV). J.Clin.Microbiol. **38**:1042-1047.

209. **Vanlaere, E., A. Baldwin, D. Gevers, D. Henry, B. E. De, J. J. LiPuma, E. Mahenthiralingam, D. P. Speert, C. Dowson, and P. Vandamme**. 2009. Taxon K, a complex within the *Burkholderia cepacia* complex, comprises at least two novel species, *Burkholderia contaminans* sp. nov. and *Burkholderia lata* sp. nov. Int.J.Syst.Evol.Microbiol. **59(Pt 1)**:102-111.

210. **Vanlaere, E., J. J. LiPuma, A. Baldwin, D. Henry, B. E. De, E. Mahenthiralingam, D. Speert, C. Dowson, and P. Vandamme**. 2008. *Burkholderia latens* sp. nov., *Burkholderia diffusa* sp. nov., *Burkholderia arboris* sp. nov., *Burkholderia seminalis* sp. nov. and *Burkholderia metallica* sp. nov., novel species within the *Burkholderia cepacia* complex. Int.J.Syst.Evol.Microbiol. **58(Pt 7)**:1580-1590.

211. **Varga, J. J., L. Losada, A. M. Zelazny, L. Brinkac, D. Harkins, D. Radune, J. Hostetler, E. P. Sampaio, C. M. Ronning, W. C. Nierman, D. E. Greenberg, S. M. Holland, and J. B. Goldberg**. 2012. Draft Genome Sequence Determination for Cystic Fibrosis and Chronic Granulomatous Disease *Burkholderia multivorans* Isolates. J Bacteriol. **194**:6356-6357.

212. **Venturi, V., A. Friscina, I. Bertani, G. Devescovi, and C. Aguilar**. 2004. Quorum sensing in the *Burkholderia cepacia* complex. Res.Microbiol. **155**:238-244.

213. **Vermis, K., T. Coenye, J. J. LiPuma, E. Mahenthiralingam, H. J. Nelis, and P. Vandamme**. 2004. Proposal to accommodate *Burkholderia cepacia* genomovar VI as *Burkholderia dolosa* sp. nov. Int.J.Syst.Evol.Microbiol. **54(Pt 3)**:689-691.

214. **Vermis, K., T. Coenye, E. Mahenthiralingam, H. J. Nelis, and P. Vandamme**. 2002. Evaluation of species-specific recA-based PCR tests for genomovar level identification within the *Burkholderia cepacia* complex. J.Med.Microbiol. **51**:937-940.

215. **Vial, L., M. C. Groleau, M. G. Lamarche, G. Filion, J. Castonguay-Vanier, V. Dekimpe, F. Daigle, S. J. Charette, and E. Deziel**. 2010. Phase variation has a role in *Burkholderia ambifaria* niche adaptation. ISME.J. **4(1)**:49-60.

216. **Videira, P. A., A. P. Garcia, and I. Sa-Correia**. 2005. Functional and topological analysis of the *Burkholderia cenocepacia* priming glucosyltransferase BceB, involved in the biosynthesis of the cepacian exopolysaccharide. J Bacteriol. **187**:5013-5018.

217. **Vinion-Dubiel, A. D. and J. B. Goldberg**. 2003. Lipopolysaccharide of *Burkholderia cepacia* complex. J.Endotoxin.Res. **9**:201-213.

218. **Visser, M. B., S. Majumdar, E. Hani, and P. A. Sokol**. 2004. Importance of the ornibactin and pyochelin siderophore transport systems in *Burkholderia cenocepacia* lung infections. Infect.Immun. **72**:2850-2857.

219. **Vranes, J., Z. Zagar, and S. Kurbel**. 1996. Influence of subinhibitory concentrations of ceftazidime, ciprofloxacin and azithromycin on the morphology and adherence of P-fimbriated *escherichia coli*. J Chemother. **8**:254-260.

220. **Vriezen, J. A., F. J. de Bruijn, and K. Nusslein**. 2006. Desiccation responses and survival of *Sinorhizobium meliloti* USDA 1021 in relation to growth phase, temperature, chloride and sulfate availability. Lett.Appl.Microbiol. **42(2)**:172-178.

221. **Wheeler, G. L.** 2000. P.h.D. thesis. Exeter University, College of Life and Environmental Studies.

222. **Whiteford, M. L., J. D. Wilkinson, J. H. McColl, F. M. Conlon, J. R. Michie, T. J. Evans, and J. Y. Paton**. 1995. Outcome of *Burkholderia* (*Pseudomonas*) *cepacia* colonisation in children with cystic fibrosis following a hospital outbreak. Thorax. **50**:1194-1198.

223. **Wilsher, M. L., J. Kolbe, A. J. Morris, and D. F. Welch**. 1997. Nosocomial acquisition of Burkholderia gladioli in patients with cystic fibrosis. Am.J.Respir.Crit Care Med. **155**:1436-1440.

224. **Wine, J. J.** 1999. The genesis of cystic fibrosis lung disease. J Clin.Invest **103**:309-312.

225. **Winsor, G. L., B. Khaira, R. T. Van, R. Lo, M. D. Whiteside, and F. S. Brinkman**. 2008. The *Burkholderia* Genome Database: facilitating flexible queries and comparative analyses. Bioinformatics. **24**:2803-2804.

226. **Witko-Sarsat, V.** 2013. Neutrophils in the Innate Immunity Conundrum of Cystic Fibrosis: A CFTR-Related Matter? J.Innate.Immun. **5(3)**:195-196.

227. **Woods, D. E., A. L. Jones, and P. J. Hill**. 1993. Interaction of insulin with *Pseudomonas pseudomallei*. Infect.Immun. **61**:4045-4050.

228. **Yabuuchi, E., Y. Kawamura, T. Ezaki, M. Ikedo, S. Dejsirilert, N. Fujiwara, T. Naka, and K. Kobayashi**. 2000. *Burkholderia uboniae* sp. nov., L-arabinose-assimilating but different from *Burkholderia thailandensis* and *Burkholderia vietnamiensis*. Microbiol.Immunol. **44(4)**:307-317.

229. **Zabner, J., M. P. Seiler, J. L. Launspach, P. H. Karp, W. R. Kearney, D. C. Look, J. J. Smith, and M. J. Welsh**. 2000. The osmolyte xylitol reduces the salt concentration of airway surface liquid and may enhance bacterial killing. Proc.Natl.Acad.Sci.U.S.A. **97(21)**:11614-11619.

230. **Zahariadis, G., M. H. Levy, and J. L. Burns**. 2003. Cepacia-like syndrome caused by *Burkholderia multivorans*. Can.J Infect.Dis. **14**:123-125.

231. **Zhou, Y., K. Song, R. G. Painter, M. Aiken, J. Reiser, B. A. Stanton, W. M. Nauseef, and G. Wang**. 2013. Cystic fibrosis transmembrane conductance regulator recruitment to phagosomes in neutrophils. J.Innate.Immun. **5(3)**:219-230.

232. **Zirbes, J. and C. E. Milla**. 2009. Cystic fibrosis related diabetes. Paediatr.Respir.Rev. **10**:118-123.

233. **Zlosnik, J. E., P. S. Costa, R. Brant, P. Y. Mori, T. J. Hird, M. C. Fraenkel, P. G. Wilcox, A. G. Davidson, and D. P. Speert**. 2011. Mucoid and nonmucoid *Burkholderia cepacia* complex bacteria in cystic fibrosis infections. Am.J Respir.Crit Care Med. **183**:67-72.

234. **Zlosnik, J. E., T. J. Hird, M. C. Fraenkel, L. M. Moreira, D. A. Henry, and D. P. Speert**. 2008. Differential mucoid exopolysaccharide production by members of the *Burkholderia cepacia* complex. J.Clin.Microbiol. **46**:1470-1473.

235. **Zughaier, S. M., H. C. Ryley, and S. K. Jackson**. 1999. A melanin pigment purified from an epidemic strain of *Burkholderia cepacia* attenuates monocyte respiratory burst activity by scavenging superoxide anion. Infect.Immun. **67(2)**:908-913.